

# Development of Low-valent Manganese Complexes for the Catalytic Applications in Hydrosilylation Reactions

By

RAKESH RANJAN BEHERA

CHEM11201804020

National Institute of Science Education and Research,  
Bhubaneswar, Odisha

*A thesis submitted to the  
Board of Studies in Chemical Sciences  
In partial fulfilment of requirements  
for the Degree of*

**DOCTOR OF PHILOSOPHY**

*Of*

**HOMI BHABHA NATIONAL INSTITUTE**



May, 2023

# Homi Bhabha National Institute<sup>1</sup>

## Recommendations of the Viva Voce Committee

As members of the Viva Voce Committee, we certify that we have read the dissertation prepared by **Rakesh Ranjan Behera** entitled **Development of Low-valent Manganese Complexes for the Catalytic Applications in Hydrosilylation Reactions** and recommend that it may be accepted as fulfilling the thesis requirement for the award of Degree of Doctor of Philosophy.

Chairman - Dr. Sudip Barman	<i>Sudip Barman</i>	Date: 16.10.2023
Guide / Convener - Dr. Bidraha Bagh	<i>Bidraha Bagh</i>	Date: 16.10.2023
Examiner - Dr. Sundargopal Ghosh	<i>Sundargopal Ghosh</i>	Date: 16 Oct 2023
Member 1- Dr. Prasenjit Mal	<i>Prasenjit Mal</i>	Date: 16.10.2023
Member 2- Dr. Sanjib Kar	<i>Sanjib Kar</i>	Date: 16.10.2023
Member 3- Dr. Shantanu Pal	<i>Shantanu Pal</i>	Date: 16.10.2023

Final approval and acceptance of this thesis is contingent upon the candidate's submission of the final copies of the thesis to HBNI.

I/We hereby certify that I/we have read this thesis prepared under my/our direction and recommend that it may be accepted as fulfilling the thesis requirement.

Date:

Place:

*Bidraha Bagh*  
(Dr. Bidraha Bagh)

Guide

<sup>1</sup> This page is to be included only for final submission after successful completion of viva voce.

## STATEMENT BY AUTHOR

This dissertation has been submitted in partial fulfilment of requirements for an advanced degree at Homi Bhabha National Institute (HBNI) and is deposited in the library to be made available to borrowers under the rules of the HBNI.

Brief quotations from this dissertation are allowable without special permission, provided that accurate acknowledgment of the source is made. Requests for permission for extended quotation from or reproduction of this manuscript in whole or in part may be granted by the Competent Authority of HBNI when in his or her judgment the proposed use of the material is in the interests of scholarship. In all other instances, however, permission must be obtained from the author.



**Rakesh Ranjan Behera**

## DECLARATION

I, hereby declare that the investigation presented in the thesis has been carried out by me. The work is original and has not been submitted earlier as a whole or in part for a degree/ diploma at this or any other Institution / University.

A handwritten signature in blue ink that reads "Rakesh Ranjan Behera". The signature is written in a cursive style and is enclosed within a thin, light-colored rectangular border.

**Rakesh Ranjan Behera**

## List of Publications arising from the thesis

### Journals

1. #**Behera, R. R.**; Ghosh, R.; Panda, S.; Khamari, S.; Bagh, B. Hydrosilylation of Esters Catalyzed by Bisphosphine Manganese (I) Complex: Selective Transformation of Esters to Alcohols. *Org. Lett.* **2020**, *22*, 3642-3648.
2. #**Behera, R. R.**; Panda, S.; Ghosh, R.; Kumar, A. A.; Bagh, B. Manganese-Catalyzed Chemoselective Hydrosilylation of Nitroarenes: Sustainable Route to Aromatic Amines. *Org. Lett.* **2022**, *24*, 9179–9183.
3. #**Behera, R. R.**; Saha, R.; Ghosh, R.; Kumar, A. A.; Sethi, S.; Jana, N., C.; Bagh, B. Hydrosilylation of Terminal Alkynes Catalyzed by Air-stable Manganese-NHC Complex. (Accepted)
4. Ghosh, R.; **Behera, R. R.**; Panda, S.; Behera, S. K.; Jana, N. C.; Bagh, B. Catalytic Transfer Hydrogenation of Lignocellulosic Biomass Model Compounds Furfural and Vanillin with Ethanol by an Air-stable Iron (II) Complex. *ChemCatChem* **2022**, e202201062.
5. Sethi, S.; Jana, N. C.; Behera, S.; **Behera, R. R.**; Bagh, B. Azide–Alkyne Cycloaddition Catalyzed by Copper (I) Coordination Polymers in PPM Levels Using Deep Eutectic Solvents as Reusable Reaction Media: A Waste-Minimized Sustainable Approach. *ACS omega* **2023** *8*, 868-878.
6. Panda, S.; Nanda, A.; **Behera, R. R.**; Ghosh, R.; Bagh, B. Cobalt Catalyzed Chemoselective Reduction of Nitroarenes: Hydrosilylation under Thermal and Photochemical Reaction Conditions. *Chem. Comm.* **2023**, published Online.

# List of publications pertaining to the thesis.

## Conferences

1. “Hydrosilylation of Esters Catalyzed by Bisphosphine Manganese(I) Complex: Selective Transformation of Ester to Alcohol” **Rakesh Ranjan Behera** and Dr. Bidraha Bagh\*, “Recent Advances in Material Chemistry.” (RAMC 2021), National Conference held on 8-9<sup>th</sup> March, 2021, Utkal University, Bhubaneswar. **(Oral Presentation, Online)**”
2. Hydrosilylation of Esters Catalyzed by Bisphosphine Manganese(I) Complex: A Selective Transformation of Ester to Alcohol” **Rakesh Ranjan Behera** and Dr. Bidraha Bagh\*, International e-Conference on “Developments in Chemical, Biological and Environmental Sciences” (DCBES 2021) held on 28-30<sup>th</sup> June, 2021, GITAM School of Science, Hyderabad & GITAM Institute of Science, Visakhapatnam. **(Oral Presentation, Online)**
3. "Manganese Catalyzed Chemoselective Hydrosilylation of Nitroarenes: Sustainable Route to Aromatic Amines." **Rakesh Ranjan Behera** and Dr. Bidraha Bagh\*, International E-Conference on “Materials Science for Sustainable Environment” (ICMSSE-2022) held on 23-24<sup>th</sup> August 2022, School of Physical Sciences, Holy Cross College (Autonomous), Tiruchirappalli- 620 002, Tamil Nadu. **(Oral Presentation, Online)**

*Dedicated to....*

*My Family  
and  
Dr. Bidraha Bagh*

## ACKNOWLEDGEMENTS

This is a very small way to show my heartfelt gratitude through the expression of thankfulness by words written through each corner of my heart and mind for those who were my companions throughout this whole long journey.

I am grateful to the **Almighty** for beholding me and blessings me giving strength at each step of my life.

The struggles of my **parents** for helping me to grow to this level were much more tedious than my own path of hurdles for which I bow my head for them. The unconditional love, blessings and inspiration from my **family** was more than what one would expect which has strengthened me to face all the hurdles in my journey of life.

I would like to express my gratitude and respect to my supervisor, **Dr. Bidraha Bagh**, NISER, for continuous support and kind-heartedness. He gave full freedom for free thinking and work out the problems, which helped me a lot in my research career. His constant support throughout the entire phase of my PhD will be remembered life-long.

I am thankful to the Director, **Prof. S. Panda**, NISER, for providing the laboratory facilities, which help me to complete my research work.

I thank my Doctoral committee members, Chairman **Dr. P. Mal, Dr. S. Barman, Dr. S. Kar and Dr. S. Pal** and all other faculties in SCS NISER, especially scientific officer **Dr. Arun Kumar** for his support on numerous occasions.

I sincerely thank **Dr. Mriganka, Mr. Deepak, Mr. Amit, Mr. Prakash, and Mr. Sanjaya** NISER for performing characterization of my samples.

I am immensely obliged to **all my teachers** of school, graduation and post-graduation who inculcated knowledge, discipline and inspiration for Chemistry.

It gives me enormous pleasure to thank all those seniors, friends and juniors who made my life at NISER certainly gratifying and memorable. Special mention must be made of my lab mates,

and special thanks to my labmates **Surajit Panda, Ratnakr Saha, Subrat Sethi, Rahul Ghosh and Dr. Narayan Chandra Jana** for their help, support and guidance. No words are enough for my pillar of strength during my Ph.D tenure, my bosom friends **Panisha Nayak, Manisha Nayak** and **Prajnashree Panda**. Thanks a million! My sincere thanks to all my hostel mate, in particular **Shakti Ranjan Mohanty** his friendship and support in all deeds. My special thanks to **Dr. Kasturi Sahoo, Dr. Tanmayee Nanda and Dr. Bedadyuti Vedvyas Pati** who helped me in most of the experimental related problems. Also, I would like to acknowledge my special friend **Subhasis Mohanty** and **Subhrajit Mohanty** for their support. Their company will be remembered forever.

I am greatly thankful to all of my family members, particularly my father **Dhirendra Behera** and my mother **Mrs. Jyostnamayee Behera** and my elder brother **Dinesh Ranjan Behera** for their support, suggestions and care.

I am privileged to stay strongly bonded to my beloved brother **Nikesh Ranjan Behera and Abhisek Behera**, who cared and stood with me whenever I got stuck in any kind of snags.

Finally, I would like to express my earnest gratitude to everyone who contributed for the accomplishment of my course and I express my apology for those whom I could not mention here.



**Rakesh Ranjan Behera**

## CONTENTS

	Page No.
<b>Synopsis</b>	<b>11</b>
<b>List of Tables</b>	<b>20</b>
<b>List of Schemes</b>	<b>21</b>
<b>List of Figures</b>	<b>24</b>
<b>List of Abbreviations</b>	<b>29</b>
<b>Chapter 1</b>	<b>30</b>
<b>Chapter 2</b>	<b>74</b>
<b>Chapter 3</b>	<b>115</b>
<b>Chapter 4</b>	<b>176</b>
<b>Summary</b>	<b>251</b>

## SYNOPSIS

### **Introduction**

Catalyst use is a key element of the movement toward greener, more sustainable synthesis. To attain sustainable production, chemists must focus on resource efficiency through highly atom-economic and selective processes.<sup>1</sup> Hydrosilylation is a suitable response in this context. It is a totally and utterly atom economic strategy to the formation of carbon–heteroatom, carbon–carbon bonds and heteroatom-heteroatom bonds. Organosilanes are mostly environmentally benign, and when compared to the poisonous heavier elements of Group 4 (lead and tin), silicon compounds are considered relatively non-toxic. Organosilanes are also useful hydride source in the synthesis process.

Finding the sustainable and step-economic strategies for the synthesis and functionalization of organic compounds has recently become an important topic of research in synthetic organic chemistry. To achieve environmentally benign methods, chemists have rendered unremitting efforts to replace toxic metal hydride reagents and harsh reaction conditions with mild and metal-free reagents. One of the most important transformations in synthetic chemistry is the reduction of carbon-carbon multiple bonds (e.g., olefines, alkynes), carbon-heteroatom (e.g., carbonyls, imines, nitriles, amides, carboxylic acids, and esters) and heteroatom-heteroatom (e.g., NO<sub>2</sub>, N<sub>2</sub>). The traditional approach of using an equimolar amount of active hydride species like LiAlH<sub>4</sub>, LiBH<sub>4</sub>, NaBH<sub>4</sub>, and DIBALH is efficient yet difficult. Furthermore, the creation of a stoichiometric ratio of byproducts is undesirable. As a result, catalytic hydrogenation is often desired. Catalytic hydrosilylation is an advantageous hydrogenation alternative that avoids the use of highly flammable molecular hydrogen and the need for appropriate pressure equipment.<sup>2</sup> Liquid hydrosilanes are an appealing alternative to H<sub>2</sub> because of their mild nature and ease of handling. Furthermore, hydrosilylation processes are

often carried out under mild circumstances and tolerate a wide range of functional groups. The use of precious metal catalysts has dominated the field of hydrosilylation to date.<sup>4,5</sup>

The creation of novel catalysts based on earth-abundant first-row transition metals is now an emerging field in homogeneous catalysis that has shown remarkable progress in the past decade. A compound of transition metals as a pre-catalyst,  $ML_n$  ( $L = \text{ligand}$ ), particularly an electron-rich complex of a late transition metal such as  $\text{Co(I)}$ ,  $\text{Ru(I)}$ ,  $\text{Ni(0)}$ ,  $\text{Pd(0)}$ , and  $\text{Pt(0)}$ , activates both  $\text{HSiR}_3$  and a variety of substrates. While progress in manganese, iron, cobalt and nickel has been significant in this field.<sup>6,7</sup> The fundamental purpose of this report is to investigate the use of well-defined Mn complexes in hydrosilylation procedures to reduce various functional groups. Manganese is the earth's 12th most abundant element. Manganese has resurfaced in the twenty-first century as a result of its abundance, lack of toxicity, and renewability in light of green and sustainable chemical needs. Both manganese and its efficiency in catalysis have been thrust into the spotlight as a result of a growing interest in developing more sustainable chemistry in the future. Despite these achievements, utilization of manganese base metal in catalysis has gotten less attention than other first-row transition metals, especially in hot-topic research fields like hydrosilylation. Recently low valent manganese complexes are gaining considerable attention in the field of homogeneous catalysis and mostly carbene, phosphine and nitrogen based bidentate and pincer ligands are utilized. In addition, cooperative ligands have received attention as versatile donor. Our aim is to utilize structurally different ligand frameworks for the synthesis of low valent manganese complexes. The steric and electronic properties of the ligand architectures will be tuned in such a way that the manganese complexes can be used as effective catalysts in the reduction of various unsaturated bonds.

Herein we present homogeneous manganese catalysts capable of hydrosilylation of carbonyl-containing compounds such as aldehydes, ketones, esters, amides, and carboxylic acids, as well

as alkenes, alkynes, nitriles, and nitro compounds.<sup>6</sup> The work we have done on (i) selective hydrosilylation of esters catalyzed by bisphosphine manganese complex, (ii) manganese-catalyzed chemoselective hydrosilylation of nitroarenes and (iii) hydrosilylation of terminal alkynes catalyzed by air-stable manganese-NHC complex. A challenging reduction of ester transformation into alcohol has also been studied. A large variety of aromatic, aliphatic, and cyclic esters bearing different functional groups were selectively converted into the corresponding alcohols in good yields. Valuable fatty alcohols were also achieved under much milder reaction conditions from fatty esters. For the 1<sup>st</sup> time the manganese catalysed hydrosilylation of nitroarenes has been achieved. It was most challenging substrate to reduce. The potential utility of this catalytic protocol has been demonstrated by the preparation of commercial drug molecules. Further, Manganese-NHC complex has been utilized as an effective catalyst for the hydrosilylation of terminal alkynes with good selectivity towards the less thermodynamically stable  $\beta$ -(Z)-vinylsilanes.

### **Scope and Organization of the Present Thesis**

In this thesis, mild and sustainable methodologies have been introduced for homogeneous catalysis using manganese as base metal catalysts with different ligand framework like mostly, phosphine, nitrogen and carbene based ligands. The reduction of esters, nitroarenes and alkynes using hydrosilylation method by utilizing those manganese metal-based catalysts. In addition, the synthesis of various fatty alcohol from fatty esters, the synthesis of drug molecules from nitro compounds have also been discussed. Scope of the reactions, detailed mechanistic studies, and post-synthetic applications of each protocol are shown in the corresponding chapters. This current thesis includes four chapters with the following contents. Chapter-wise discussions are given below.

## **CHAPTER 1**

### **Introduction to Manganese Catalysed Hydrosilylation Reactions**

This chapter highlights the basic introduction to low-valent manganese complexes, its activity, and its synthetic utility. Manganese complex-mediated applications in various hydrosilylation reactions such as aldehydes, ketones, esters, amides, and carboxylic acids, as well as alkenes, alkynes, nitriles, and nitro compounds are summarized. Finally, the chapter is closed with a brief outline of the research focus of the current thesis.

## CHAPTER 2

**Hydrosilylation of Esters Catalyzed by Bisphosphine Manganese(I) Complex: Selective Transformation of Esters to Alcohols** (Behera, R. R.; Ghosh, R.; Panda, S.; Khamari, S.; Bagh, B. *Org. Lett.* **2020**, *22*, 3642.).

The reduction of carboxylic acids and esters to the corresponding alcohols is one of the most important transformations in synthetic chemistry. The conventional method of using a stoichiometric amount of reactive hydrides such as  $\text{LiAlH}_4$ ,  $\text{LiBH}_4$ , and DIBALH is an efficient but tricky reaction. In addition, the formation of a stoichiometric amount of byproducts is detrimental. Therefore, catalytic hydrogenation is often desirable. However, hydrogenation of esters by molecular hydrogen suffers from poor selectivity, and drastic reaction conditions (high temperature and high hydrogen pressure) are required. Although the utilization of earth-abundant, nonprecious TMs as catalysts is sustainable and thus desirable, the reports on the catalytic hydrosilylation of esters by base metals are extremely limited. The use of manganese catalysts for the hydrosilylation of carbonyls is well established. Only a few reports have described the hydrosilylation of carboxyl substrates. In the last 8–10 years, Mn(I) complexes have gained immense interest for their catalytic applications in a variety of chemical transformations. Selective and efficient hydrosilylations of esters to alcohols by a well-defined manganese(I) complex with a commercially available bisphosphine ligand are described. These reactions are easy alternatives for stoichiometric hydride reduction or hydrogenation, and employing cheap, abundant, and nonprecious metal is attractive. The hydrosilylations were

performed at 100 °C under solvent-free conditions with low catalyst loading. A large variety of aromatic, aliphatic, and cyclic esters bearing different functional groups were selectively converted into the corresponding alcohols in good yields. This protocol includes relatively unreactive substrates such as fatty esters and polyesters. We targeted polyester as a potential substrate relevant to polymer recycling. The number of homogeneous catalysts for this purpose is very scarce. We choose the industrial sample dynacoll-7360, or poly(1,6-hexamethylene adipate), which is produced by the condensation polymerization of 1,6-hexanediol and adipic acid. Another advantage of this catalytic protocol is the solvent-free hydrosilylation. Further investigations will involve the utilization of this catalyst for the hydrosilylation of various other substrates.



**Figure 1.** Hydrosilylation of Various Esters to Alcohols Catalyzed by manganese complex under solvent-free condition.

### CHAPTER 3

**Manganese Catalyzed Chemoselective Hydrosilylation of Nitroarenes: Sustainable Route to Aromatic Amines** (Behera, R. R.; Panda, S.; Ghosh, R.; Kumar, A. A.; Bagh, B. *Org. Lett.* **2022**, *24*, 9179.)

Amine-group containing organic compounds are important synthetic blocks in synthetic chemistry. They furnish a wide array of potential applications in the areas fields of agrochemicals, pharmaceutical, dyes, and biologically active compounds, and so forth. So due to salient applications of nitro aryl moieties, the study of catalytic hydrosilylation of nitro arene has become an important topic over a century. Nitroarenes can be transformed into aniline derivatives by a number of well known noncatalytic methods such as Bechamp' reduction or the use of sulfide reagents. The major drawbacks of Bechamp' reduction involve the

requirement of corrosive HCl and excess amounts of iron with a large amount of waste production. Various other reducing agents such as CO/H<sub>2</sub>O, hydroiodic acid, sodium hydrosulfite, tin(II) chloride, hydrazine, and ammonia borane have been utilized for the same purpose. However, heterogeneous catalysts often encounter poor chemoselectivity and also produce (toxic) byproducts. In this context, homogeneous catalysts are gaining momentum because high chemoselectivity can be achieved. Although the utilization of earth-abundant nonprecious-transition metal catalysts is desirable, reports on base-metal-catalyzed hydrosilylation of nitroarenes are limited. Surprisingly, manganese-mediated hydrosilylation of nitroarenes has not been reported previously. Herein we report efficient catalytic hydrosilylations of nitroarenes to form the corresponding aromatic amines using a well-defined manganese(II)–NNO pincer complex with a low catalyst loading (1 mol %) under solvent-free conditions. This base-metal-catalyzed hydrosilylation is an easy and sustainable alternative to classical hydrogenation. A large variety of nitroarenes bearing various functionalities were selectively transformed into the corresponding aromatic amines in good yields. With different electron-donating and -withdrawing functionalities nitroarenes were effectively reduced to the corresponding amines. Several reducible functionalities such as ester, cyano, amide, and alkene were tolerated. The potential utility of the present catalytic protocol was demonstrated by the preparation of commercial drug molecules. Based on previous reports and supported by experimental evidence, we propose a catalytic path that involves reduction of manganese(II) to manganese(0) followed by oxidative addition of the silane. Further investigation will involve the use of the present catalytic protocol for the reduction of unsaturated substrates in different hydrofunctionalizations.

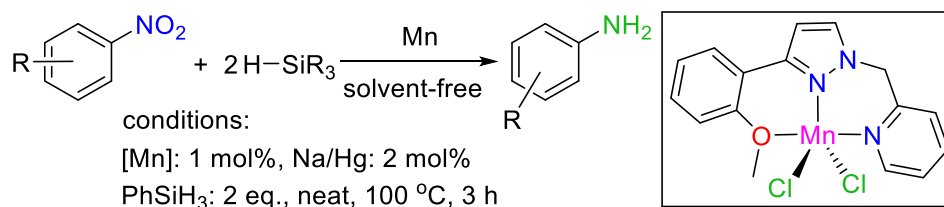


**Figure 2.** Hydrosilylation of Various Nitroarenes to aromatic amine by manganese(II) complex.

## CHAPTER 4

### Hydrosilylation of Terminal Alkynes Catalyzed by Air-stable Manganese-NHC Complex

(Behera, R. R.; Saha, R.; Kumar, A. A.; Sethi, S.; Jana, N.C.; Bagh, B. <https://doi.org/10.1021/acs.joc.3c00127>)

Vinylsilanes are widely used as versatile synthetic key components in organic synthesis and have widespread application in life sciences and material chemistry due to their excellent stability, low toxicity, and simplicity of handling. The most simple and atom-efficient way to produce synthetically useful vinylsilanes is catalytic hydrosilylation of alkynes using transition metal complexes. Controlling the regio- and stereoselectivity is a principal issue in hydrosilylation of alkynes, as this technique may result in a mixture of regio- and stereoisomers such as  $\alpha$ -,  $\beta$ -(Z)-, and  $\beta$ -(E)-vinylsilanes (Scheme 1a).  $\beta$ -(Z)-, and  $\beta$ -(E)-isomers are the results of anti-Markovnikov addition of Si-H bond to the alkyne moiety. Since the first report of homogeneous metal-catalyzed hydrosilylation of unsaturated C-C bond published in late 1950s, researchers have investigated this chemical transformation in a variety of ways to develop new metal catalysts that lead to the regio- and stereoselective production of vinylsilanes. Over the last few decades, transition metal catalyzed hydrosilylations of various unsaturated moieties have been advanced immensely. Parallely, various transition metal catalysts particularly with noble metals such as Ru, Rh, Ir, Pd and Pt have been developed for the hydrosilylation of alkynes. Many noble metal-catalyzed alkyne hydrosilylations yielded  $\beta$ -(E)-vinylsilanes with remarkable selectivity. The synthesis of the thermodynamically unfavorable  $\beta$ -(Z)-isomer is thought to be more difficult than the selective synthesis of  $\beta$ -(E)-vinylsilanes. Furthermore, some catalysts have been reported to produce competitive dehydrogenative silylation products, such as alkynylsilane and the corresponding alkene. The use of earth-abundant and inexpensive base metal catalysts is important for sustainable and economical chemical transformations and in recent years, many efforts have been directed to the use of base metal catalysts which can catalyze hydrosilylation of alkenes and alkynes effectively. In recent years, catalysis with base metal manganese has received a significant

amount of interest. Catalysis with manganese complexes having N-heterocyclic carbenes (NHCs) is relatively underdeveloped in comparison to the extensively investigated manganese catalysts possessing pincer ligands (particularly phosphine-based ligands). Herein, we describe the synthesis of two imidazolium salts decorated with picolyl arms ( $L_1$  and  $L_2$ ) as NHC precursors. Facile coordination of  $L_1$  and  $L_2$  with  $MnBr(CO)_5$  in presence of base resulted in the formation manganese(I)-NHC complexes (1 and 2) as an air-stable solid in good isolated yield. Single crystal X-ray analysis revealed the structure of the cationic complexes  $[Mn(CO)_3(NHC)][PF_6]$  with tridentate N,C,N-binding of the NHC ligand in facile fashion. Along with a few known manganese(I) complexes, these Mn(I)-NHC complexes 1 and 2 were tested for the hydrosilylation of terminal alkynes. Complex 1 was proved to be an effective catalyst for the hydrosilylation of terminal alkynes with good selectivity towards the less thermodynamically stable  $\beta$ -(Z)- vinylsilanes. This method provided good regioselectivity (anti-Markovnikov addition) and stereoselectivity ( $\beta$ -(Z)-product). Experimental evidences suggested that present hydrosilylation pathway involved an organometallic mechanism with manganese(I)-silyl species as a possible reactive intermediate.

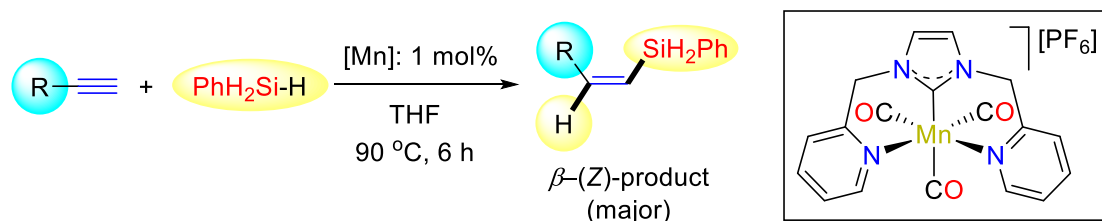


**Figure 3.** Hydrosilylation of various terminal alkyne by using Mn(I) NHC complex.

## References

- 1) A. R. Battersby, C. J. R. Fookes, G. W. J. Matcham, E. McDonald, *Nature* **1980**, 285, 17–21.
- 2) Yang, X.; Wang, C. Manganese-catalyzed hydrosilylation reactions. *Chem. - Asian J.* **2018**, 13, 2307-2315.
- 3) Oro, L. A., & Claver, C. *Iridium Complexes in Organic Synthesis*, Wiley, Germany, 2008.

- 4) Kettler, P. B. Platinum group metals in catalysis: fabrication of catalysts and catalyst precursors. *Org. Process Res. Dev.* **2003**, *7*, 342–354.
- 5) Ojima, I.; Li, Z.; Zhu, J. *The Chemistry of Organic Silicon Compounds*; Wiley: Avon, U.K., 1998; Chapter 29.
- 6) Van Putten, R.; Uslamin, E. A.; Garbe, M.; Liu, C.; Gonzalez-de-Castro, A.; Lutz, M.; Junge, K.; Hensen, E. J. M.; Beller, M.; Lefort, L.; Pidko, E. A. Non-Pincer-Type Manganese Complexes as Efficient Catalysts for the Hydrogenation of Esters. *Angew. Chem., Int. Ed.* **2017**, *56*, 7531–7534.
- 7) Du, X.; Huang, Z. Advances in base-metal-catalyzed alkene hydrosilylation. *ACS Catal.*, **2017**, *7*, 1227-1243.
- 8) Behera, R. R.; Ghosh, R.; Panda, S.; Khamari, S.; Bagh, B. Hydrosilylation of esters catalyzed by bisphosphine manganese (I) complex: selective transformation of esters to alcohols. *Organic letters*, **2020**, *22*, 3642-3648.
- 9) Behera, R. R.; Panda, S.; Ghosh, R.; Kumar, A. A.; Bagh, B. Manganese-Catalyzed Chemoselective Hydrosilylation of Nitroarenes: Sustainable Route to Aromatic Amines. *Org. Lett.* **2022**, *24*, 9179.
- 10) Behera, R. R.; Saha, R.; Kumar, A. A.; Sethi, S.; Jana, N.C.; Bagh, B. Hydrosilylation of Terminal Alkynes Catalyzed by Air-stable Manganese-NHC Complex. <https://doi.org/10.1021/acs.joc.3c00127>

### List of Tables

<b>Table 2.1</b> Performance of complex <b>2.1</b> for the hydrosilylation of benzyl benzoate under different reaction conditions.	80
<b>Table 3.1</b> Catalytic performance of complex <b>3.1</b> for the hydrosilylation of nitrobenzene.	122
<b>Table 4.1</b> Catalytic performance of <b>4.1</b> for the hydrosilylation of terminal alkynes.	186

## List of Schemes

<b>Scheme 1.1</b> Formation of $(\text{CO})_4\text{MnCH}(\text{O}[\text{Si}]\text{C}_6\text{H}_5$ from either A) a manganese silyl precursor or B) manganese acyl precursor.	37
<b>Scheme 1.2</b> Hydrosilylation of ketones and esters catalysed by manganese-acyl complex.	38
<b>Scheme 1.3</b> Manganese-catalyzed hydrosilylation of acetone.	38
<b>Scheme 1.4</b> Reduction of carbonyl functionalities by sub-stoichiometric manganese compounds A) Reduction of ketones and B) Reduction of esters to ethers.	39
<b>Scheme 1.5</b> Hydrosilylation of aldehydes and ketones catalyzed by NHC–Mn complex.	40
<b>Scheme 1.6</b> Hydrosilylation of ketones catalyzed co-ordinatively unsaturated manganese species.	40
<b>Scheme 1.7</b> Hydrosilylation of ketones catalyzed by the Salen-Mn complex.	42
<b>Scheme 1.8</b> Hydrosilylation of ketones catalyzed by bis(imino)pyridine complex.	43
<b>Scheme 1.9</b> Proposed mechanisms for the PDI–Mn-catalyzed hydrosilylation.	44
<b>Scheme 1.10</b> Hydrosilylation of carbonyls employing NHC Mn complexes.	45
<b>Scheme 1.11</b> Asymmetric hydrosilylation of aryl ketones by PDI-Mn(II) complex.	46
<b>Scheme 1.12</b> Mn Catalyzed hydrosilylation of carboxylic acids to aldehydes.	47
<b>Scheme 1.13</b> Mn-Catalyzed hydrosilylation of carboxylic acids to alcohols.	48
<b>Scheme 1.14</b> Mechanism for hydrosilylation of carboxylic acids employing $\text{Mn}(\text{CO})_5\text{Br}$ .	49
<b>Scheme 1.15</b> Manganese complexes used in hydrosilylation of ester.	50

<b>Scheme 1.16</b> Mechanism for ester hydrosilylation by employing manganese complex <b>1.16</b> .	51
<b>Scheme 1.17</b> Mechanism for the hydrosilylation of esters employing <b>1.38</b> .	52
<b>Scheme 1.18</b> Mn-Catalyzed hydrosilylation of ester to aldehyde.	52
<b>Scheme 1.19</b> Mn-Catalyzed hydrosilylation of amides.	53
<b>Scheme 1.20</b> Manganese pincer complex catalyzed hydrosilylation of carbon dioxide.	54
<b>Scheme 1.21</b> Manganese catalyzed hydrosilylation of nitriles to amines.	55
<b>Scheme 1.22</b> Manganese-catalyzed hydrosilylation of alkenes.	56
<b>Scheme 1.23</b> Mn-Catalyzed hydrosilylation of alkenes.	58
<b>Scheme 1.24</b> Mechanisms for the hydrosilylation of alkenes employing $Mn_2(CO)_{10}$ .	59
<b>Scheme 1.25</b> Hydrosilylation of alkynes employing Mn catalysts.	60
<b>Scheme 1.26</b> Different pathways for E- and Z- selective alkene employing manganese complex.	61
<b>Scheme 2.1</b> Hydrosilylation of esters by Mn(I) catalysts.	76
<b>Scheme 2.2</b> Synthesis of fac-[Mn(xantphos)(CO) <sub>3</sub> Br] ( <b>2.1</b> ) with the molecular structure of <b>2.1</b> showing 50% ellipsoid (hydrogen atoms are omitted for clarity).	78
<b>Scheme 2.3</b> Hydrosilylation of various esters to alcohols catalyzed by complex <b>2.1</b> .	81
<b>Scheme 2.4</b> Catalytic hydrosilylation of esters with practical implications.	84
<b>Scheme 3.1</b> Reduction (hydrosilylation and hydrogenation) of esters by base metal catalysts.	119
<b>Scheme 3.2</b> Synthesis of complex <b>3.1</b> with the molecular structure of <b>1</b> showing 50% ellipsoids.	121
<b>Scheme 3.3</b> Selective hydrosilylation of nitroarenes with various functionalities catalyzed by complex <b>3.1</b> .	124
<b>Scheme 3.4</b> Syntheses of drug molecules a) dapsone, b) benzocaine, c) butamben, d) lidocaine and e) tetracaine by utilizing present hydrosilylation protocol.	126

<b>Scheme 3.5</b> Plausible catalytic path for the hydrosilylation of nitroarene and control experiments.	129
<b>Scheme 4.1</b> Transition metal catalyzed hydrosilylation of alkynes.	179
<b>Scheme 4.2</b> Synthesis of manganese complexes <b>4.1</b> and <b>4.2</b> with the molecular structure, using 50% probability ellipsoids.	183
<b>Scheme 4.3</b> Substrate scope for terminal alkyne hydrosilylation.	188
<b>Scheme 4.4</b> Control experiments.	191
<b>Scheme 4.5</b> Plausible Reaction Path for Complex 1-Catalyzed Alkyne Hydrosilylation.	192

## List of Figures

<b>Figure 1.1</b>	Catalytic hydrosilylation using various metal catalysts.	32
<b>Figure 1.2</b>	Manganese presents a step forward towards sustainable catalysis.	35
<b>Figure 1.3</b>	Two manganese complexes used in hydrosilylation reaction and ring flipping.	41
<b>Figure 1.4</b>	Manganese complexes used in hydrosilylation reaction of carbonyl compounds.	46
<b>Figure 1.5</b>	Manganese complexes used in hydrosilylation of carbonyl compounds.	47
<b>Figure 2.1</b>	$^1\text{H}$ NMR (400 MHz) spectrum of complex <b>1</b> in $\text{CDCl}_3$ at r.t.	95
<b>Figure 2.2</b>	$^{31}\text{P}\{^1\text{H}\}$ NMR (162 MHz) spectrum of complex <b>1</b> in $\text{CDCl}_3$ at r.t.	95
<b>Figure 2.3</b>	$^{13}\text{C}\{^1\text{H}\}$ NMR (101 MHz) spectrum of complex <b>1</b> in $\text{CDCl}_3$ at r.t..	96
<b>Figure 2.4</b>	$^1\text{H}$ NMR (400 MHz) spectrum of benzyl alcohol ( <b>1a'</b> / <b>4a'</b> / <b>7a'</b> ) in $\text{CDCl}_3$ at r.t.	96
<b>Figure 2.5</b>	$^{13}\text{C}$ NMR (101 MHz) spectrum of benzyl alcohol ( <b>1a'</b> / <b>4a'</b> / <b>7a'</b> ) in $\text{CDCl}_3$ at r.t..	97
<b>Figure 2.6</b>	$^1\text{H}$ NMR (400 MHz) spectrum of 4-methoxybenzyl alcohol ( <b>1b'</b> / <b>7b'</b> ) in $\text{CDCl}_3$ at r.t.	97
<b>Figure 2.7</b>	$^{13}\text{C}$ NMR (101 MHz) spectrum of 4-methoxybenzyl alcohol ( <b>1b'</b> / <b>7b'</b> ) in $\text{CDCl}_3$ at r.t.	98
<b>Figure 2.8</b>	$^1\text{H}$ NMR (400 MHz) spectrum of 2-methylbenzyl alcohol ( <b>2a'</b> ) in $\text{CDCl}_3$ at r.t.	98
<b>Figure 2.9</b>	$^{13}\text{C}$ NMR (101 MHz) spectrum of 2-methylbenzyl alcohol ( <b>2a'</b> ) in $\text{CDCl}_3$ at r.t.	99

<b>Figure 2.10</b>	$^1\text{H}$ NMR (400 MHz) spectrum of 2-methoxybenzyl alcohol ( <b>2b'</b> ) in $\text{CDCl}_3$ at r.t.	99
<b>Figure 2.11</b>	$^{13}\text{C}$ NMR (101 MHz) spectrum of 2-methoxybenzyl alcohol ( <b>2b'</b> ) in $\text{CDCl}_3$ at r.t.	100
<b>Figure 2.12</b>	$^1\text{H}$ NMR (400 MHz) spectrum of 3-chlorobenzyl alcohol ( <b>3'</b> ) in $\text{CDCl}_3$ at r.t.	100
<b>Figure 2.13</b>	$^{13}\text{C}$ NMR (101 MHz) spectrum of 3-chlorobenzyl alcohol ( <b>3'</b> ) in $\text{CDCl}_3$ at r.t..	101
<b>Figure 2.14</b>	$^1\text{H}$ NMR (400 MHz) spectrum of 1,5-pentanediol ( <b>19'</b> ) in $\text{CDCl}_3$ at r.t.	101
<b>Figure 2.15</b>	$^{13}\text{C}$ NMR (101 MHz) spectrum of 1,5-pentanediol ( <b>19'</b> ) in $\text{CDCl}_3$ at r.t.	102
<b>Figure 2.16</b>	$^1\text{H}$ NMR (400 MHz) spectrum of 3-methyl-1,4-octanediol ( <b>21'</b> ) in $\text{CDCl}_3$ at r.t.	102
<b>Figure 2.17</b>	$^{13}\text{C}$ NMR (101 MHz) spectrum of 3-methyl-1,4-octanediol ( <b>21'</b> ) in $\text{CDCl}_3$ at r.t.	103
<b>Figure 3.1</b>	Representative GCMS spectrum of the crude reaction mixture from catalytic hydrosilylation of <i>p</i> -nitroanisole	135
<b>Figure 3.2</b>	$^1\text{H}$ NMR (400 MHz) spectrum of <i>p</i> -anisidine in $\text{CDCl}_3$ at r.t.	153
<b>Figure 3.3</b>	$^{13}\text{C}$ NMR (101 MHz) spectrum of <i>p</i> -anisidine in $\text{CDCl}_3$ at r.t..	153
<b>Figure 3.4</b>	$^1\text{H}$ NMR (400MHz) spectrum of methyl 4-aminobenzoate ( <b>A6a</b> ) in $\text{CDCl}_3$ at r.t.	154
<b>Figure 3.5</b>	$^{13}\text{C}$ NMR (101MHz) spectrum of methyl 4-aminobenzoate ( <b>A6a</b> ) in $\text{CDCl}_3$ at r.t.	154
<b>Figure 3.6</b>	$^1\text{H}$ NMR (400MHz) spectrum of 3-amino-2-chloropyridine ( <b>A19</b> ) in $\text{CDCl}_3$ at r.t.	155
<b>Figure 3.7</b>	$^{13}\text{C}$ NMR (101MHz) spectrum of 3-amino-2-chloropyridine ( <b>A19</b> ) in $\text{CDCl}_3$ at r.t..	155

<b>Figure 3.8</b>	$^1\text{H}$ NMR (400MHz) spectrum of 4,4'-sulfonyldianiline in $\text{CDCl}_3$ at r.t..	156
<b>Figure 3.9</b>	$^{13}\text{C}$ NMR (101MHz) spectrum of 4,4'-sulfonyldianiline in $\text{CDCl}_3$ at r.t.	156
<b>Figure 3.10</b>	$^1\text{H}$ NMR (400MHz) spectrum of butyl 4-aminobenzoate $\text{CDCl}_3$ at r.t.	157
<b>Figure 3.11</b>	$^{13}\text{C}$ NMR (101MHz) spectrum of butyl 4-aminobenzoate in $\text{CDCl}_3$ at r.t.	157
<b>Figure 3.12</b>	$^1\text{H}$ NMR (400MHz) spectrum of 2-(dimethylamino)ethyl 4-(butylamino) benzoate in $\text{CDCl}_3$ at r.t..	158
<b>Figure 3.13</b>	$^{13}\text{C}$ NMR (101MHz) spectrum of 2-(dimethylamino)ethyl 4-(butylamino) benzoate in $\text{CDCl}_3$ at r.t.	158
<b>Figure 4.1</b>	$^1\text{H}$ NMR (400 MHz, $\text{CDCl}_3$ ) of 1,3-bis(pyridin-2-ylmethyl)-1H-imidazolium chloride.	211
<b>Figure 4.2</b>	$^{13}\text{C}\{^1\text{H}\}$ NMR (101 MHz, $\text{CDCl}_3$ ) of 1,3-bis(pyridin-2-ylmethyl)-1H-imidazolium chloride.	211
<b>Figure 4.3</b>	$^1\text{H}$ NMR (400 MHz, $\text{CDCl}_3$ ) of 1,3-bis(pyridin-2-ylmethyl)-1H-imidazolium hexafluorophosphate ( <b>L</b> <sub>1</sub> ).	212
<b>Figure 4.4</b>	$^{13}\text{C}\{^1\text{H}\}$ NMR (101 MHz, $\text{CD}_3\text{CN}$ ) of 1,3-bis(pyridin-2-ylmethyl)-1H-imidazolium hexafluorophosphate ( <b>L</b> <sub>1</sub> ).	212
<b>Figure 4.5</b>	$^{31}\text{P}\{^1\text{H}\}$ NMR (162 MHz, $\text{CD}_3\text{CN}$ ) of 1,3-bis(pyridin-2-ylmethyl)-1H-imidazolium hexafluorophosphate ( <b>L</b> <sub>1</sub> ).	213
<b>Figure 4.6</b>	$^{19}\text{F}\{^1\text{H}\}$ NMR (377 MHz, $\text{CD}_3\text{CN}$ ) of 1,3-bis(pyridin-2-ylmethyl)-1H-imidazolium hexafluorophosphate ( <b>L</b> <sub>1</sub> ).	213
<b>Figure 4.7</b>	$^1\text{H}$ NMR (400 MHz, $\text{DMSO-d}_6$ ) of Complex <b>1</b> .	214
<b>Figure 4.8</b>	$^{31}\text{P}\{^1\text{H}\}$ NMR (162 MHz, $\text{DMSO-d}_6$ ) of Complex <b>1</b> ·THF.	214
<b>Figure 4.9</b>	$^{19}\text{F}\{^1\text{H}\}$ NMR (377 MHz, $\text{DMSO-d}_6$ ) of Complex <b>1</b> ·THF.	215
<b>Figure 4.10</b>	$^{13}\text{C}\{^1\text{H}\}$ NMR (101 MHz, $\text{DMSO-d}_6$ ) of Complex <b>1</b> .	215
<b>Figure 4.11</b>	IR spectrum of Complex <b>1</b> .	216

<b>Figure 4.12</b>	$^1\text{H}$ NMR (400 MHz, $\text{CDCl}_3$ ) of 5,6-dimethyl-1,3-bis(pyridin-2-ylmethyl)-1H-benzimidazole-3-mum chloride.	216
<b>Figure 4.13</b>	$^{13}\text{C}\{^1\text{H}\}$ NMR (101 MHz, $\text{CDCl}_3$ ) of 5,6-dimethyl-1,3-bis(pyridin-2-ylmethyl)-1H-benzimidazole-3-mum chloride.	217
<b>Figure 4.14</b>	$^1\text{H}$ NMR (400 MHz, $\text{CDCl}_3$ ) of 5,6-dimethyl-1,3-bis(pyridin-2-ylmethyl)-1H-benzimidazole-3-mum hexafluorophosphate ( <b>L</b> <sub>2</sub> ).	217
<b>Figure 4.15</b>	$^{31}\text{P}\{^1\text{H}\}$ NMR (162 MHz, $\text{CDCl}_3$ ) of 5,6-dimethyl-1,3-bis(pyridin-2-ylmethyl)-1H-benzimidazole-3-mum hexafluorophosphate ( <b>L</b> <sub>2</sub> ).	218
<b>Figure 4.16</b>	$^{13}\text{C}\{^1\text{H}\}$ NMR (101 MHz, $\text{CDCl}_3$ ) of 5,6-dimethyl-1,3-bis(pyridin-2-ylmethyl)-1H-benzimidazole-3-mum hexafluorophosphate ( <b>L</b> <sub>2</sub> ).	218
<b>Figure 4.17</b>	$^1\text{H}$ NMR (400 MHz, $\text{CD}_3\text{CN}$ ) of Complex <b>2</b> .	219
<b>Figure 4.18</b>	$^{31}\text{P}\{^1\text{H}\}$ NMR (162 MHz, $\text{DMSO-d}_6$ ) of Complex <b>2</b> .	219
<b>Figure 4.19</b>	$^{19}\text{F}\{^1\text{H}\}$ NMR (377 MHz, $\text{DMSO-d}_6$ ) of Complex <b>2</b> .	220
<b>Figure 4.20</b>	$^{13}\text{C}\{^1\text{H}\}$ NMR (101 MHz, $\text{DMSO-d}_6$ ) of Complex <b>2</b> .	220
<b>Figure 4.21</b>	IR spectrum of Complex <b>2</b> .	221
<b>Figure 4.22</b>	UV-Vis spectrum ( $\text{MeCN}$ , $10^{-4}$ M) of complexes <b>1</b> .	221
<b>Figure 4.23</b>	$^1\text{H}$ NMR (400 MHz) spectrum of ( <i>Z</i> )-phenyl(styryl)silane ( <b>P</b> <sub>1a</sub> ) in $\text{CDCl}_3$ at r.t.	222
<b>Figure 4.24</b>	$^{13}\text{C}\{^1\text{H}\}$ NMR (101 MHz) spectrum of ( <i>Z</i> )-phenyl(styryl)silane ( <b>P</b> <sub>1a</sub> ) in $\text{CDCl}_3$ at r.t.	222
<b>Figure 4.25</b>	$^1\text{H}$ NMR (400 MHz) spectrum of ( <i>Z</i> )-(4-methylstyryl)(phenyl)silane ( <b>P</b> <sub>2a</sub> ) in $\text{CDCl}_3$ at r.t.	223
<b>Figure 4.26</b>	$^1\text{H}$ NMR (400 MHz) spectrum of ( <i>Z</i> )-(4-methoxystyryl)(phenyl)silane ( <b>P</b> <sub>7a</sub> ) in $\text{CDCl}_3$ at r.t.	223

- Figure 4.27**  $^{13}\text{C}\{^1\text{H}\}$  NMR (101 MHz) spectrum of (Z)-(4-methoxystyryl)(phenyl)silane (**P7a**) in  $\text{CDCl}_3$  at r.t. 224
- Figure 4.28**  $^1\text{H}$  NMR (400 MHz) spectrum of (Z)-(3-methoxystyryl)(phenyl)silane (**P8a**) in  $\text{CDCl}_3$  at r.t. 224
- Figure 4.29**  $^{13}\text{C}\{^1\text{H}\}$  NMR (101 MHz) spectrum of (Z)-(3-methoxystyryl)(phenyl)silane (**P8a**) in  $\text{CDCl}_3$  at r.t. 225
- Figure 4.30**  $^1\text{H}$  NMR (400 MHz) spectrum of (Z)-3-(2-(phenylsilyl)vinyl)phenol (**P9a**) in  $\text{CDCl}_3$  at r.t. 225
- Figure 4.31**  $^{13}\text{C}\{^1\text{H}\}$  NMR (101 MHz) spectrum of (Z)-3-(2-(phenylsilyl)vinyl)phenol (**P9a**) in  $\text{CDCl}_3$  at r.t. 226
- Figure 4.32**  $^1\text{H}$  NMR (400 MHz) spectrum of (Z)-N,N-dimethyl-4-(2-(phenylsilyl)vinyl)aniline (**P10a**) in  $\text{CDCl}_3$  at r.t. 226
- Figure 4.33**  $^{13}\text{C}\{^1\text{H}\}$  NMR (101 MHz) spectrum of (Z)-N,N-dimethyl-4-(2-(phenylsilyl)vinyl)aniline (**P10a**) in  $\text{CDCl}_3$  at r.t. 227
- Figure 4.34**  $^1\text{H}$  NMR (400 MHz) spectrum of (Z)-phenyl(2-(thiophen-2-yl)vinyl)silane (**P20a**) in  $\text{CDCl}_3$  at r.t. 227
- Figure 4.35**  $^{13}\text{C}\{^1\text{H}\}$  NMR (101 MHz) spectrum of (Z)-phenyl(2-(thiophen-2-yl)vinyl)silane (**P20a**) in  $\text{CDCl}_3$  at r.t. 228
- Figure 4.36**  $^1\text{H}$  NMR (400 MHz) spectrum of (Z)-(2-cyclopentylvinyl)(phenyl)silane (**P23a**) in  $\text{CDCl}_3$  at r.t. 228
- Figure 4.37**  $^{13}\text{C}\{^1\text{H}\}$  NMR (101 MHz) spectrum of (Z)-(2-cyclopentylvinyl)(phenyl)silane (**P23a**) in  $\text{CDCl}_3$  at r.t. 229
- Figure 4.38**  $^1\text{H}$  NMR (400 MHz) spectrum of (Z)-hept-1-en-1-yl(phenyl)silane (**P25a**) in  $\text{CDCl}_3$  at r.t. 229
- Figure 4.38**  $^{13}\text{C}\{^1\text{H}\}$  NMR (101 MHz) spectrum of (Z)-hept-1-en-1-yl(phenyl)silane (**P25a**) in  $\text{CDCl}_3$  at r.t. 230

### List of Abbreviations

$^1\text{H}$ NMR	Proton Nuclear Magnetic Resonance
$^{13}\text{C}$ NMR	Carbon-13 Nuclear Magnetic Resonance
$^{19}\text{F}$ NMR	Fluorine-19 Nuclear Magnetic Resonance
UV-Vis	Ultraviolet–Visible
ESI	Electrospray Ionization
CCDC	Cambridge Crystallographic Data Centre
$\text{CH}_2\text{Cl}_2$	Dichloromethane
$\text{CHCl}_3$	Chloroform
EtOAc	Ethyl acetate
$\text{CH}_3\text{CN}$	Acetonitrile
$\text{CH}_3\text{OH}$	Methanol
THF	Tetrahydrofuran
CO	Carbon monoxide
HCl	Hydrogen chloride
$\text{K}'\text{OBu}$	Potassium tert-butoxide
$\text{CDCl}_3$	Deuterated chloroform
$\text{CD}_2\text{Cl}_2$	Dideuteromethylenechloride
$\text{CD}_3\text{CN}$	Deuterated acetonitrile
TLC	Thin Layer Chromatography
$\text{Na}_2\text{SO}_4$	Sodium sulphate
$\text{MnCl}_2$	Manganese(II) chloride
Anal.Calc	Analytically calculated
NHC	N-heterocyclic carbene
DMPO	5,5-Dimethyl-1-Pyrroline-N-Oxide
BHT	Butylated hydroxytoluene



---

# Introduction: Manganese Catalysed Hydrosilylation Reactions

---

## 1.1 Hydrosilylation

## 1.2 Why manganese metal complex

## 1.3 Manganese catalysed hydrosilylation

### 1.3.1 Manganese Catalyzed Hydrosilylation of carbonyls

### 1.3.2 Manganese Catalyzed Hydrosilylation of carboxylic acids

### 1.3.3 Manganese Catalyzed Hydrosilylation of esters

### 1.3.4 Manganese Catalyzed Hydrosilylation of amides

### 1.3.5 Manganese Catalyzed Hydrosilylation of carbon dioxide

### 1.3.6 Manganese Catalyzed Hydrosilylation of nitriles

### 1.3.7 Manganese Catalyzed Hydrosilylation of Alkenes

### 1.3.8 Manganese Catalyzed Hydrosilylation of Alkynes

## 1.1 HYDROSILYLATION

Catalyst use is a key element of the movement toward greener, more sustainable synthesis. To attain sustainable production, chemists must focus on resource efficiency through highly atom-economic and selective processes.<sup>1</sup> Hydrofunctionalisation is a suitable response in this context. It is a totally and utterly atom-economic strategy to the formation of carbon–heteroatom and carbon–carbon bonds (e.g., hydrosilylation). Hydrofunctionalisation has already been reported using a wide range of transition-metal catalysts, with platinum group metal catalysts being the most popularly used. The hydrofunctionalisation of olefins, in particular, is an extremely effective reaction because olefins are readily accessible, diversely functionalised, and the formation of carbon–carbon bonds is indeed highly valued<sup>2,3</sup>

Silicon chemistry has recently emerged as one of the most promising areas of chemistry research. Silicon is the eighth most plentiful element in the universe and the second most abundant in the earth's crust. The resemblance of silicon to carbon has driven scientists to explore the idea of replacing carbon with silicon to alter molecule biological and chemical activity.<sup>4</sup> Aside from the accessibility of silicon resources, organosilanes are mostly environmentally benign, and when compared to the poisonous heavier elements of Group 4 (lead and tin), silicon compounds are considered relatively non-toxic. Organosilanes are also useful intermediates in the synthesis process. Despite the fact that carbon-silicon bonds are relatively strong, there are few natural compounds that contain silicon-carbon bonds. The addition reaction of organic and inorganic silicon hydrides across multiple bonds, specifically carbon-carbon (such as C-C), carbon-heteroatom and (such as C-O and C-N) bonds, as well as heteroatom-heteroatom (such as N-N and N-O) bonds, is alluded to as hydrosilylation. 75 years ago (1947) Leo Sommer reported the first example of hydrosilylation,<sup>5</sup> based on the reaction between trichlorosilane and 1-octene in the presence of acetyl peroxide. However, John L. Speier's 1957 discovery of hexachloroplatinic acid as a very efficient precursor of the Pt-catalyst has become a strategic point for a wide applications.<sup>6</sup> This procedure will be widely used as a fundamental and elegant method for the laboratory and industrial synthesis of organosilicon molecular and macromolecular compounds, as well as various organic silyl derivatives that can be used directly in organic synthesis, over the next 50 years. Silicones (siloxanes) have a broad array of applications because of the discovery and development of organosilane polymers.<sup>7</sup> Organosilanes are also employed in a number of sectors, including pharmaceutical research,<sup>8</sup> biotoxins,<sup>9</sup> electronics, and photonics.<sup>7</sup> Asymmetric hydrosilylation, like other catalytic asymmetric processes, is accomplished by utilizing a chiral ligand on the metal catalyst.<sup>10</sup> The optically active hydrosilylation products are useful intermediates in organic synthesis, as they can be used in a variety of ways.<sup>11</sup>

One of the most important transformations in synthetic chemistry is the reduction of carbon-carbon multiple bonds (e.g., olefines, alkynes), carbon-heteroatom (e.g., carbonyls, imines, nitriles, amides, carboxylic acids, and esters) and heteroatom-heteroatom (e.g., NO<sub>2</sub>, N<sub>2</sub>).<sup>12</sup> The traditional approach of using an equimolar amount of active hydride species like LiAlH<sub>4</sub>, LiBH<sub>4</sub>, NaBH<sub>4</sub>, and DIBALH is efficient yet difficult.<sup>13</sup> Furthermore, the creation of a stoichiometric ratio of byproducts is undesirable. As a result, catalytic hydrogenation is often desired. Catalytic hydrosilylation is an advantageous hydrogenation alternative that avoids the use of highly flammable molecular hydrogen and the need for appropriate pressure equipment.<sup>14</sup> Liquid hydrosilanes are an appealing alternative to H<sub>2</sub> because of their mild nature and ease of handling. Furthermore, hydrosilylation processes are often carried out under mild circumstances and tolerate a wide range of functional groups. The use of precious metal catalysts has dominated the field of hydrosilylation to date.<sup>15</sup> These metals such as Pd, Ru, Ir, and Pt are the most stable and active catalysts in general, but they also raise environmental and safety problems. As a result, chemical synthesis and catalysis researchers are looking for more environmentally friendly alternatives. The creation of novel catalysts based on earth-abundant first-row transition metals is now an emerging field in homogeneous catalysis that has shown remarkable progress in the recent decade.<sup>16</sup>

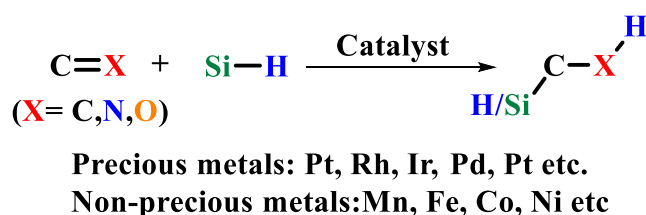


**Figure 1.1. Catalytic hydrosilylation using various metal catalysts.**

Early catalytic hydrosilylation research focused on platinum-catalyzed reactions involving a variety of hydrosilanes. In the hydrosilylation field, noble-metal catalysts, defined by Pt complexes, have held the lead so far. According to reports, the demand of Pt catalysts in the hydrosilylation of alkenes approaches 6 tonnes per year, and recycling them is difficult.<sup>17</sup>

A compound of transition metals as a pre-catalyst,  $ML_n$  ( $L = \text{ligand}$ ), particularly an electron-rich complex of a late transition metal such as Pd, Ru, Ir, and Pt, activates both  $HSiR_3$  and a variety of substrates.<sup>18</sup> The progresses in first-row transition metals, particularly iron and cobalt has been significant and have been widely used for various organic transformations, while hydrosilylation mediated by Mn has been growing interest in this field.<sup>16a, 19</sup> As a result, the hydrosilylation by iron complexes are divided into multiple subsections, each devoted to a particular type of ligand such as monodentate, bidentate, pincer-type and pentadentate ligand.<sup>20</sup> New catalysts for hydrosilylation have been developed, primarily homogeneous and immobilized late and early TM-complexes have been reported.<sup>21, 22, 23</sup> These catalysts provide a variety of convenient synthesis approaches to molecular organosilicon reagents, including enhanced yield, selectivity, and turnover rate. The catalytic mechanism is determined by the catalyst used, and the logical construction of unique catalytic systems is widely studied.

## 1.2. Why manganese metal complex

Transition metal complexes are popular in today's synthetic chemistry, with uses ranging from mediating catalysis to serving as precursors in chemical vapour deposition of materials.<sup>24</sup> Metal-containing compounds were utilised as basic colours for paints and pigments early on,<sup>25</sup> but it wasn't until the late 1800s that the structure of these coordination complexes was recognised, thanks in large part to Alfred Werner's pioneering work.<sup>26</sup> Naturally, the scope of metal complexes has expanded throughout time, from simple homoleptic coordination compounds naturally occurring ligands like CO, halides,  $NH_3$ , and  $H_2O$  (e.g.  $[Co(NH_3)_6]Cl_3$ ) to species containing designer ligands.<sup>27</sup> Use of such precious metal catalysts has dominated the field of hydrosilylation to date.<sup>15</sup> These metals are the most stable and active catalysts in general, but they also raise environmental and safety issues. As a result, chemical synthesis and catalysis researchers are looking for more environmentally friendly alternatives. The creation

of novel catalysts based on earth-abundant first-row transition metals is now an emerging field in homogeneous catalysis that has shown remarkable progress in the past decade.

The fundamental purpose of this report is to investigate the use of well-defined Mn complexes in hydrosilylation procedures to reduce various functional groups. Manganese is the earth's 12th most abundant element<sup>28</sup>, and it is now produced at a rate of 18.5 million metric tonnes per year (2020).<sup>29</sup> Manganese has several uses, the most important of which are in the steel and iron industries.<sup>30</sup> Manganese also has several applications in metallurgy, electronics, and the chemical industry, to name a few.<sup>31</sup> Manganese has a lot of potential in chemical synthesis because of its different oxidation states (-3 to +7). This enables it to serve critical functions in chemical synthesis support. Manganese is found in a variety of enzymes that are essential to life on Earth, the most noteworthy of which being its position in the core of oxygen-evolving complexes, which help plants split water to make oxygen.<sup>32</sup> Traditional oxidation reactions have relied heavily on high-valence manganese compounds, such as  $\text{KMnO}_4$ .<sup>31b</sup> Manganese is also gaining popularity as a catalyst for alkene epoxidation processes, such as Jacobsen's catalyst.<sup>33</sup> Manganese-catalyzed radical cyclization reactions<sup>34</sup> and C–H activation reactions<sup>35</sup>, to mention a few, illustrate the chemical reactivity of this group 7 transition metal in the lab, in addition to oxidation reactions. Manganese has resurfaced in the twenty-first century as a result of its abundance, lack of toxicity, and renewability in light of green and sustainable chemical needs. Both manganese and its efficiency in catalysis have been thrust into the spotlight as a result of a growing interest in developing more sustainable chemistry in the future. Manganese complexes have been frequently employed in (de)hydrogenation<sup>36</sup> and hydrosilylation processes.<sup>31a</sup> Organosilicon compounds are very desirable cornerstones in organic synthesis and industry, as the starting ingredients for emulsifying agent, softeners, lubricants, silicone rubber, and other products, because to their stability, non-toxicity, simplicity of handling, and diverse transformations.<sup>37</sup> Many studies have

focused on base-metal catalysts (Mn, Fe, Co, etc.) in recent decades due to their cheaper cost, reduced toxicity, and long-term benefits.<sup>31b</sup> Due to their non-toxicity and environmental friendliness, two elements in the first-row transition metals are showing promise candidates as palladium alternatives. Iron is well-known; however, manganese has been comparatively less explored.<sup>31b</sup>

Organic molecule reduction is a useful chemical method for creating new high-value compounds as well as bulk raw molecules. Hydrogen's ability to utilize carbon dioxide in the construction of a methanol-based economy has sparked increased interest in the latter.<sup>38</sup> The advancement of manganese-mediated hydrosilylation process has lagged behind that of the well-studied Fe,<sup>21</sup> Co,<sup>22</sup> or Ni<sup>23</sup> catalysts. Manganese-catalyzed hydrosilylation processes, on the other hand, are receiving increasing attention.<sup>31b</sup> We will concentrate on homogeneous manganese catalysts capable of hydrosilylation of carbonyl-containing compounds such as aldehydes, ketones, esters, amides, and carboxylic acids, as well as alkenes, alkynes, nitriles, and nitro compounds, in this report.



**Figure 1.2. Manganese presents a step forward towards sustainable catalysis.**

Silanes, which are weak hydride sources, are used in hydrosilylation processes.<sup>39</sup> Under mild reaction conditions, the activation of these easily available precursors in the presence of a catalyst yields the silylated species. These functionalized compounds are excellent precursors for Suzuki<sup>40</sup> and Hiyama cross-coupling reactions.<sup>41</sup>

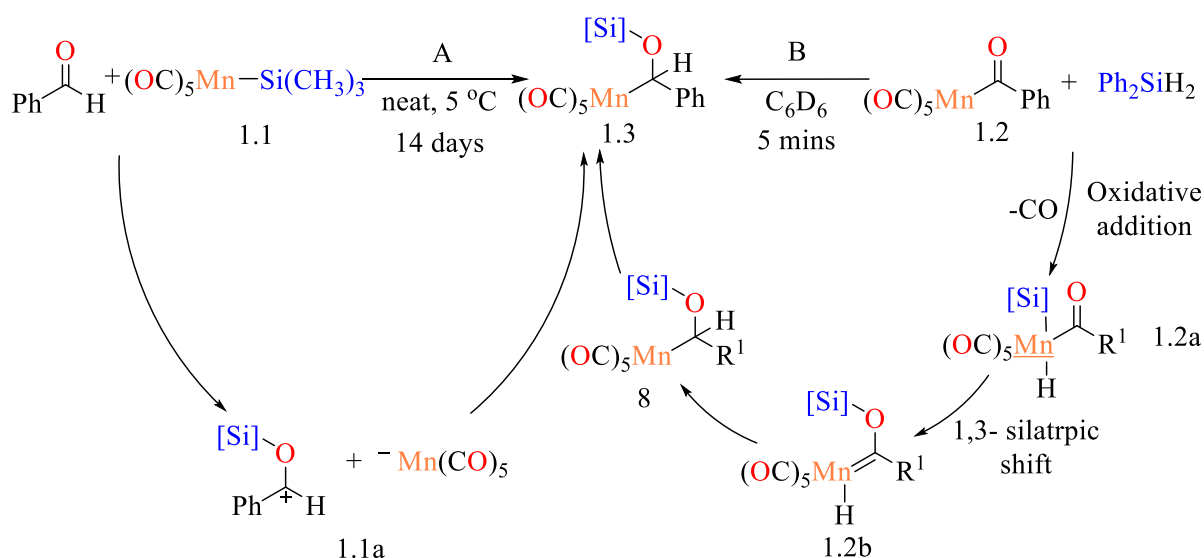
**1.3. Manganese catalysed hydrosilylation**

Despite these achievements, manganese catalysis has gotten less attention than other first-row transition metals, especially in hot-topic research fields like cross-coupling, hydrogenation, and hydrofunctionalization.<sup>42</sup> However, considerable breakthroughs in manganese catalysis, particularly in hydrofunctionalization processes, have been made since 2016.<sup>42</sup> The oldest known reduction processes discussed in this report are manganese-catalyzed hydrosilylation reactions. Faltynek *et al.* demonstrated in 1983 that a silylpentacarbonylmanganese(I) complex may convert terminal alkenes to their corresponding alkylsiloxane via thermal or photochemical activation with heptamethylcyclotetrasiloxane (HMCTS).<sup>43</sup> While the photochemical reaction produced the target product cleanly, the thermally activated system produced an unselective mixture of products. It was also revealed that manganese was not the catalytically active component; rather, the Mn–Si link was homolytically broken to produce the active silyl radical. Hilal's group employed decacarbonyldimanganese(0) in addition with silanes to form an active Mn(I) hydride, which they used to reduce hexene at substantially lower temperatures.<sup>44</sup> A decade later Cutler utilised a Mn(I) acetyl complex to reduce esters to ethers by deoxygenative reduction, and to reduce ketones to secondary alcohols a year later via hydrosilylation method.<sup>45</sup> These early instances from Cutler's lab revealed the potential of low-valent manganese catalysts having loadings of 2.4 mol percent, allowing acetophenone reduction in under 4 minutes. With  $\text{PhMe}_2\text{SiH}$  in  $\text{C}_6\text{D}_6$ ,

yields of many ketone molecules such as acetone and cyclohexanone were 90%. Meanwhile, the reaction might take place in a solvent-free environment with a reduced catalyst loading.

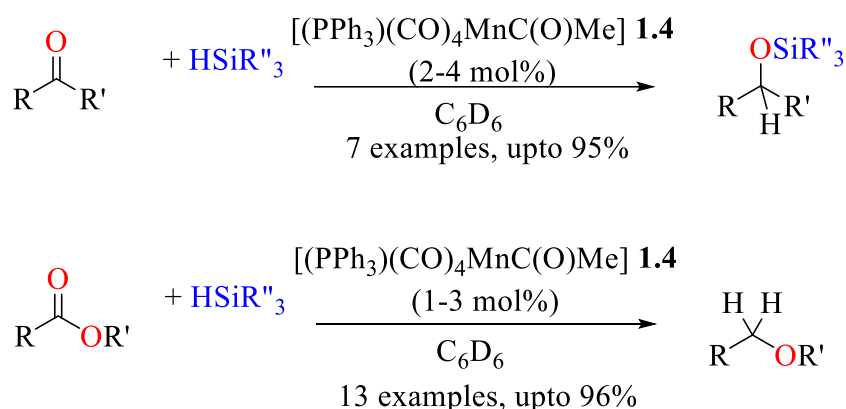
### 1.3.1. Manganese Catalyzed Hydrosilylation of carbonyls

The utilisation of stoichiometric proportions of a manganese-silyl or manganese-acyl species was the focus of the earliest reports of carbonyl hydrosilylation assisted by a manganese species.<sup>43</sup> Gladysz stated that benzaldehyde was inserted into the manganese-silyl link of  $(\text{CO})_5\text{MnSiMe}_3$  (Scheme 1.1).<sup>46</sup> This reaction took over two weeks. Cutler and coworkers described a similar reaction of both a manganese-acyl species **1.2** and a hydrosilane.<sup>45</sup> (Scheme 1.1). Despite the fact that they produce the same product **1.3**, the reactions are mechanistically different. It was suggested that the benzaldehyde oxygen would first add to the silyl group in a nucleophilic method before adding the manganese centre to the acyl carbon when employing the manganese silyl complex **1.1**. It was proposed that the creation of an intermediate ion pair **1.1a**. Manganese(III) hydride **1.2a** was formed by oxidative addition of the hydrosilane, followed by a 1,3-silatropic shift to provide alkenyl manganese species **1.2b**, and finally a 1,2-hydride shift to generate the hydrosilylation product **1.3**.



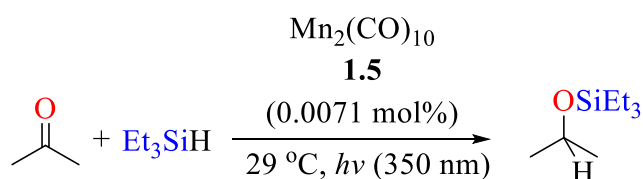
**Scheme 1.1** Formation of  $(\text{CO})_4\text{MnCH(O[Si]C}_6\text{H}_5$  from either A) a manganese silyl precursor or B) manganese acyl precursor.

The hydrosilylation of simple ketones and esters was also accomplished using this catalytic system (Scheme 1.2).<sup>45b</sup> For the hydrosilylation of acetone with PhMe<sub>2</sub>SiH, the catalytic efficiency of **1.4** was substantially better than that of [Rh(PPh<sub>3</sub>)<sub>3</sub>Cl]. Pre-treating catalyst **1.4** in silane for 20 minutes significantly expedited the reaction, reducing the reaction time to less than four minutes from 45 minutes. In addition, **1.4** was a highly efficient catalyst for the hydrosilylation–deoxygenation pathway's reduction of ester to ether.<sup>47</sup>



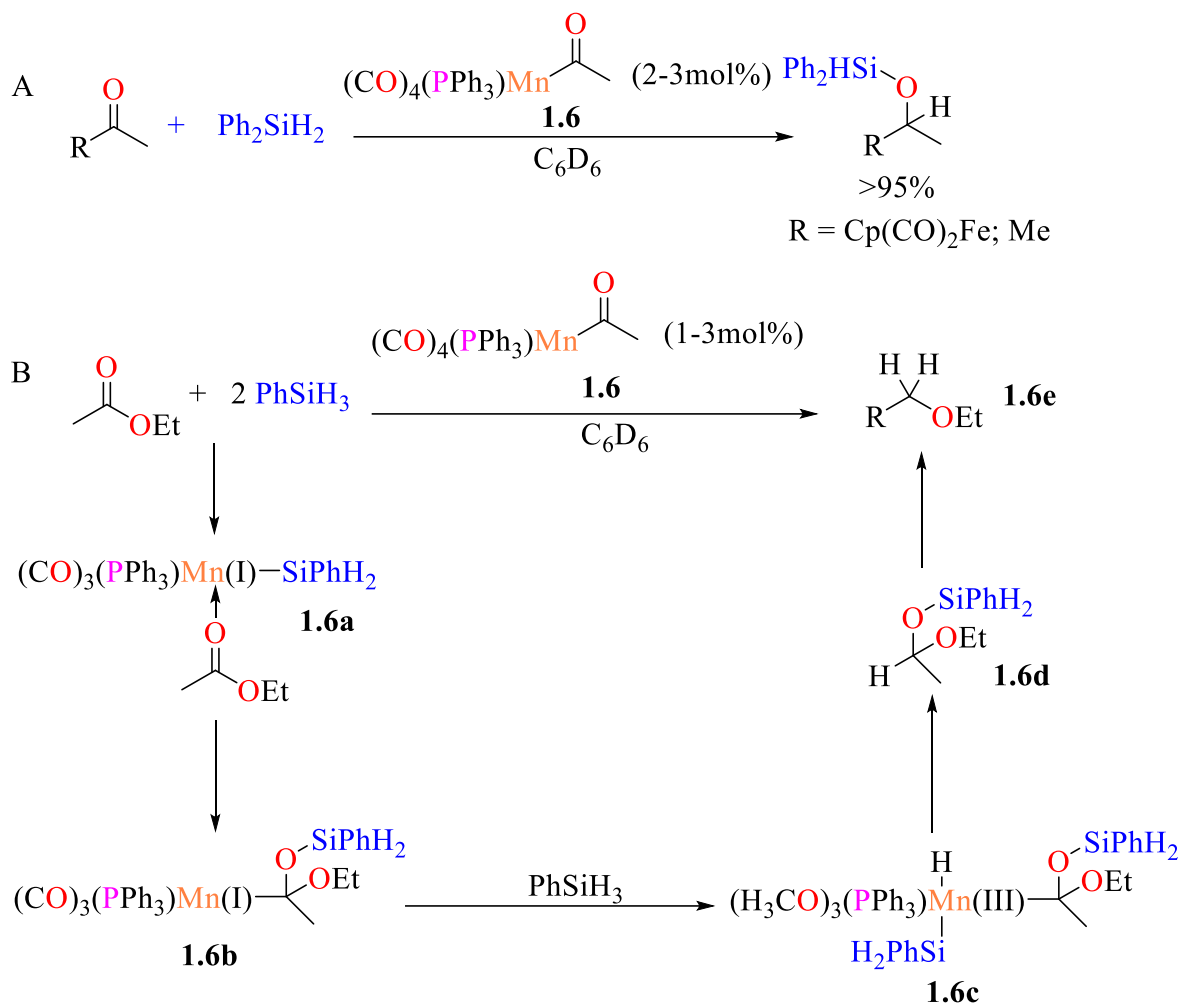
**Scheme 1.2 Hydrosilylation of ketones and esters catalysed by manganese-acyl complex.**

Yates published the first manganese-catalyzed hydrosilylation of ketones under UV irradiation in 1982. (Scheme 1.3).<sup>48</sup> However, only 5% of the anticipated hydrosilylation product yield was appeared.



**Scheme 1.3 Manganese-catalyzed hydrosilylation of acetone.**

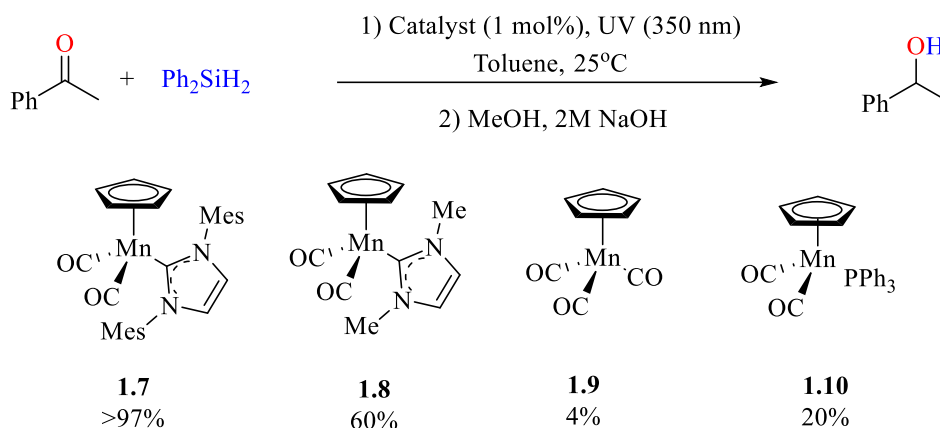
When a non-labile organometallic acyl group or an organic carbonyl was added to sub-stoichiometric amounts of manganese acyl species **1.6**, the reaction proceeded to provide high yields of silyl ether products (Scheme 1.4 A).<sup>49</sup> The active catalyst was thought to be PPh<sub>3</sub>(CO)<sub>3</sub>MnSiR<sub>3</sub> **1.6a**, which was formed by adding excess hydrosilane to the pre-catalyst.



**Scheme 1.4 Reduction of carbonyl functionalities by sub-stoichiometric manganese compounds A) Reduction of ketones and B) Reduction of esters to ethers.**

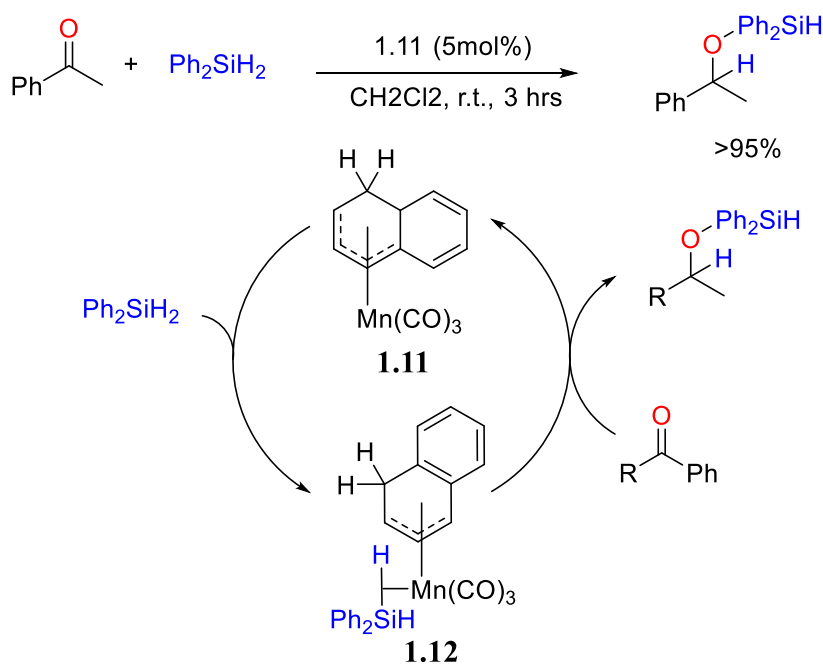
When compared to other donor ligands, the usage of triphenylphosphine as a ligand resulted in higher reaction rates.<sup>49</sup> By a method similar to that of ketone reduction, the same pre-catalyst might be employed to catalyse the hydrosilylation of esters to generate the ether and silyl acetate products (**Scheme 1.4B**).<sup>49</sup>

Under UV irradiation, Lavigne et al. discovered that N-heterocyclic carbene (NHC) manganese carbonyl complexes (**1.7** and **1.8**) catalysed the reduction of aldehydes and ketones (**Scheme 1.5**).<sup>50</sup> The usage of the similar cymantrene compound **1.9**, as well as weak  $\sigma$ -donor type ligands such triphenylphosphine **1.10**, had no effect.



### Scheme 1.5 Hydrosilylation of aldehydes and ketones catalyzed by NHC–Mn complex.

Chung and coworkers took a novel technique to the production of a co-ordinately unsaturated manganese species (Scheme 1.6).<sup>51</sup> The adoption of a 5-1-hydronaphthalene ligand facilitated a haptotropic shift between the 5- (**1.11**) and 3- coordination states (**1.12**). This enables for manganese-catalyzed diphenylsilane hydrosilylation of ketones.



### Scheme 1.6 Hydrosilylation of ketones catalyzed co-ordinately unsaturated manganese species.

The  $\eta^6$ -coordinated cationic complex **1.13** had stronger catalytic reactivity than the  $\eta^5$ -coordinated neutral complex **1.14**, and it could be employed with both secondary and tertiary

silanes. Ring slippage ( $\eta^5$  to  $\eta^3$ ,  $\eta^6$  to  $\eta^4$ ) was thought to be an important element in catalysis because it supplied coordination sites in the reaction for silanes and/or ketones.<sup>51b</sup>

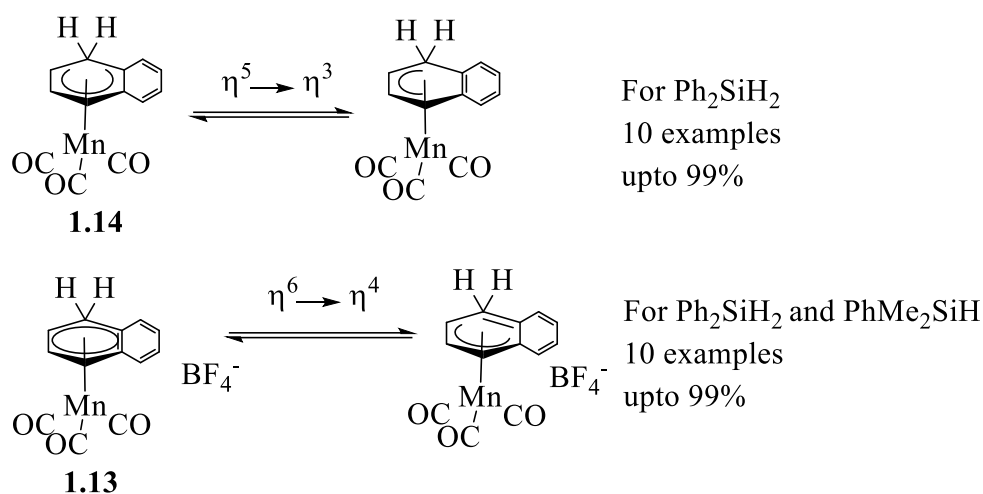
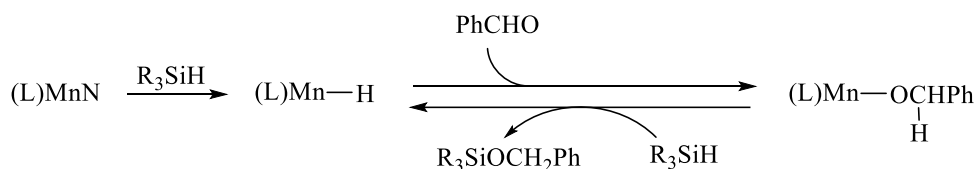
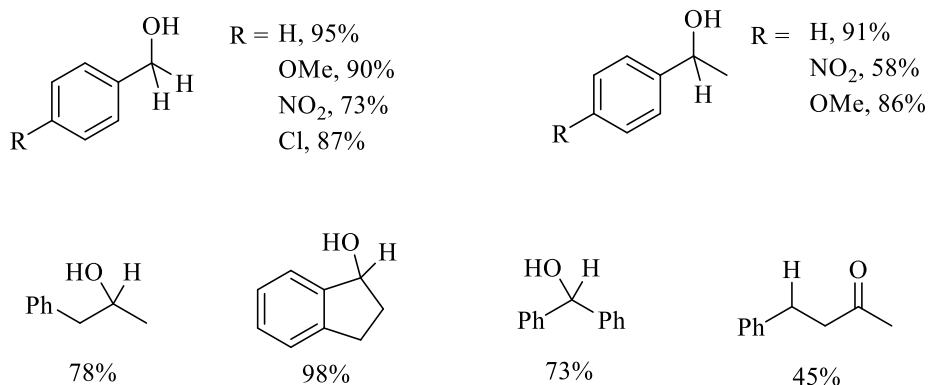
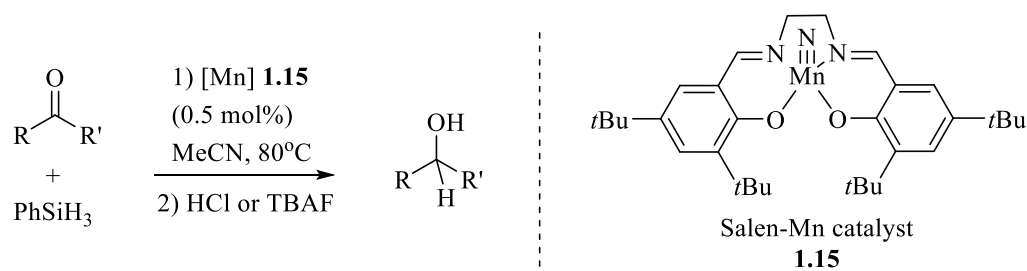


**Figure 1.3** Two manganese complexes used in hydrosilylation reaction and ring flipping.

Du group reported a novel Salen–Mn(V) complex **1.15** mediates the hydrosilylation of ketones and aldehydes, high catalytic performance and strong functional-group tolerance (Scheme 1.7).<sup>53</sup> The addition of a Salen type ligand framework gave tuning locations for additional catalyst changes.

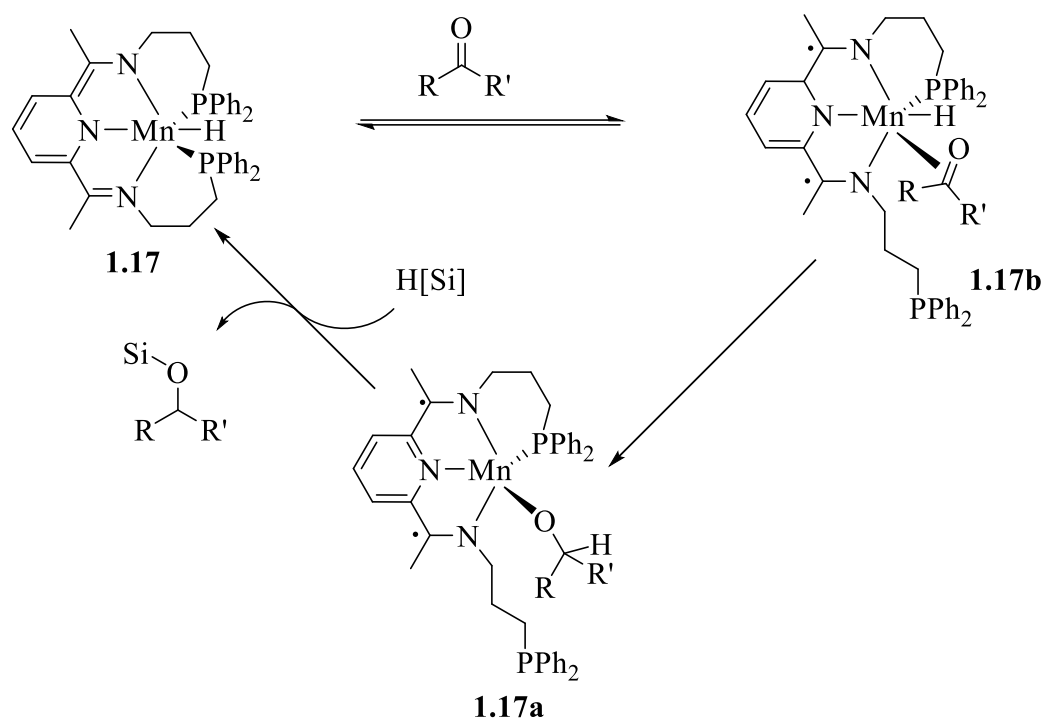


### Scheme 1.7 Hydroxylation of ketones catalyzed by the Salen-Mn complex.

It's worth noting that the catalyst's highest turnover frequency (TOF) was 11760 h<sup>-1</sup>. The reduction of catalyst **1.17** yielded manganese(III) hydride, that performed C=O bond insertion and silyl transfer to yield the final alcohol product following hydrolysis.

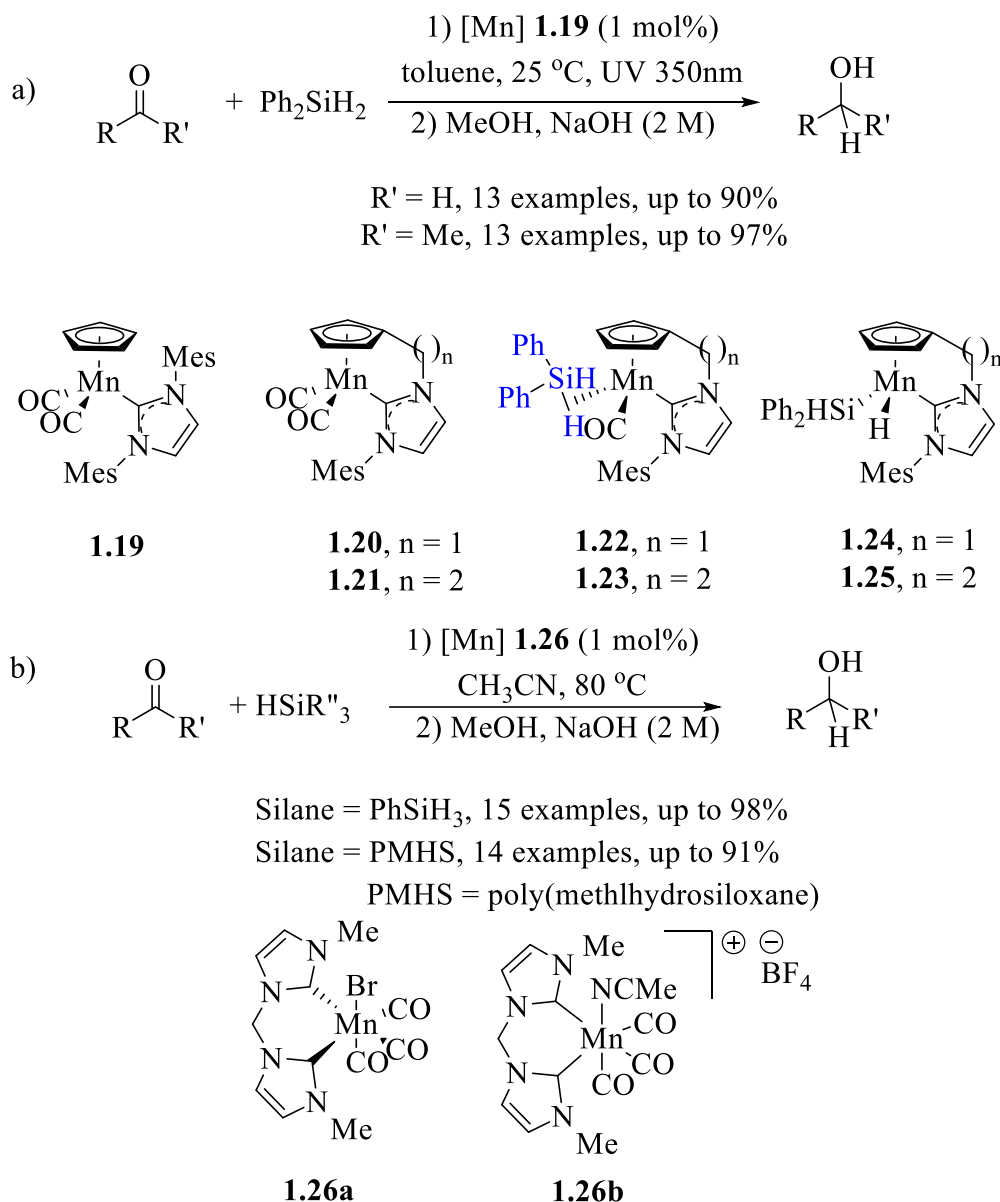
Trovitch *et al.* observed that a pentadentate bis(imino)pyridine complex having pendant -donor phosphine groups **1.16** catalysed the hydrosilylation of aldehydes, ketones, esters, and formates (Scheme 1.18a).<sup>54</sup> For the hydrosilylation of ketones, Complex **1.16** has a TOF of 76,800 h<sup>-1</sup>, which is higher than other first-row transition metals. A modified Ojima process was reported for hydrosilylation employing **1.16**, in which a hydrosilane undergoes oxidative addition at the manganese centre and produced the intermediate **1.16a**. (Scheme 1.8b).<sup>54b</sup> The carbonyl would next be hydrometallated before being reductively eliminated to generate the O-Si bond. It was proposed a hexacoordinate manganese hydride species **1.17**, that a modified





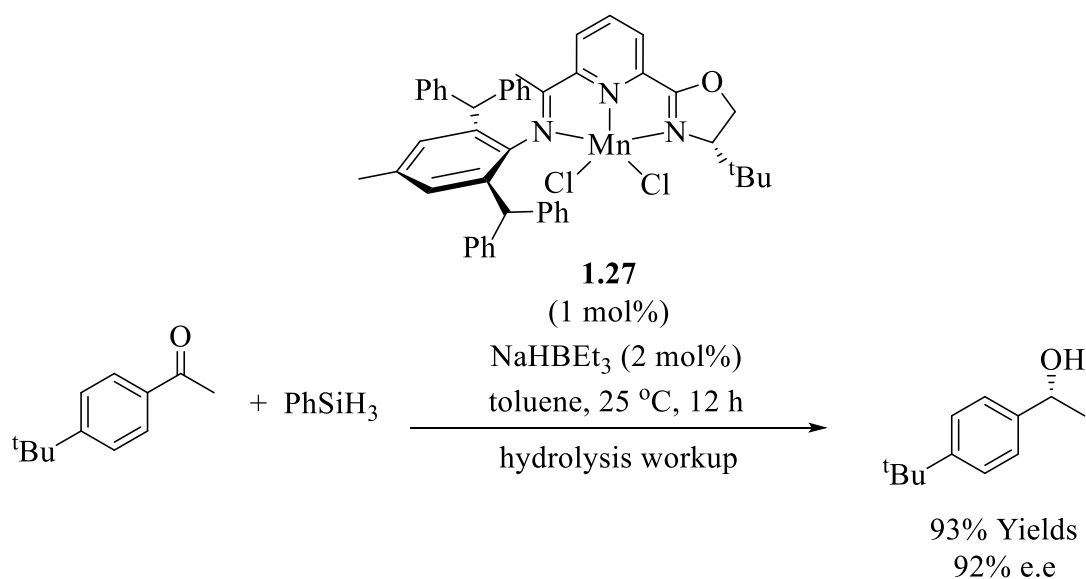
**Scheme 1.9** Proposed mechanisms for the PDI-Mn-catalyzed hydrosilylation.

NHC-Mn complexes **1.19–1.20** were also developed for the irradiation-induced hydrosilylation of aldehydes and ketones (**Scheme 6a**).<sup>55</sup> The reactivity of two anchored complexes **1.19** and **1.21** was comparatively low compared to the initial half-sandwich complex **1.20**, allowing the manganese-silane  $\sigma$ -complexes complexes **1.22** and **1.23** to be separated successfully. The authors postulated a typical Ojima mechanism for the reaction based on the mechanistic investigation, with the production of active noncarbonyl Mn (III) **1.24** and **1.25** as the crucial step.<sup>56</sup> The Royo group discovered manganese complexes with bis-NHC ligands **1.26a** and **1.26b**, which have been demonstrated to be excellent catalysts for the hydrosilylation of a wide range of aldehydes and ketones (**Scheme 6b**).<sup>57</sup>



### Scheme 1.10. Hydrosilylation of carbonyls employing NHC Mn complexes.

In 2017, Huang and colleagues published the first report of asymmetric hydrosilylation of aryl ketones with a manganese catalyst (**Scheme 1.21**).<sup>58</sup> The reduction of ketones was achieved with an enantiomeric excess (e.e.) of up to 92 percent using a manganese complex containing chiral iminopyridine oxazoline ligand which is in one specific enantioisomeric form. The activator NaEt<sub>3</sub>BH was used in catalytic amount. The reaction time was somewhat longer than Trovitch's PDI-Mn(II) complexes for similar reactions and a maximum TON of 99 was achieved.



**Scheme 1.11** Asymmetric hydrosilylation of aryl ketones by PDI-Mn(II) complex.

Similar activity for hydrosilylation of carbonyl compounds were observed with Royo and Turculet's bis-NHC Mn(I)-complex **1.28**,<sup>57</sup> and PN-chelated Mn(II)-complex Mn **1.29**<sup>60</sup> respectively. Complex **1.28** required a longer reaction time and higher temperature despite having a wide scope. The phenyl cyclopropyl ketone radical clock experiment shows that **1.28** involves a radical mechanism.

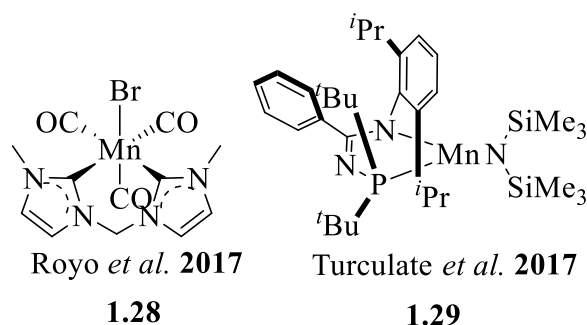


**Figure 1.4** Manganese complexes used in hydrosilylation reaction of carbonyl compounds.

With a TON of up to 396 in 2019, Leitner used the bidentate NN-iminotriazole-based Mn(I)-complex Mn **1.29** for hydrosilylation of ketone.<sup>61</sup> The Mn(I)  $\alpha$ -diimine complex **1.30** that Madrahimov synthesized in 2020 provided a TON of up to 900 for the same process.<sup>61</sup> Sunada utilized Mn(hmnds)<sub>2</sub>(THF)<sub>2</sub> complex **1.31** that was capable of catalyzing the carbonyl

hydrosilylation process without the use of an external ligand.<sup>62</sup> Recent research by Kundu demonstrated that Mn(I)-complex Mn **1.32** also performed well in the hydrosilylation procedure, though with a somewhat higher reaction temperature.<sup>63</sup>

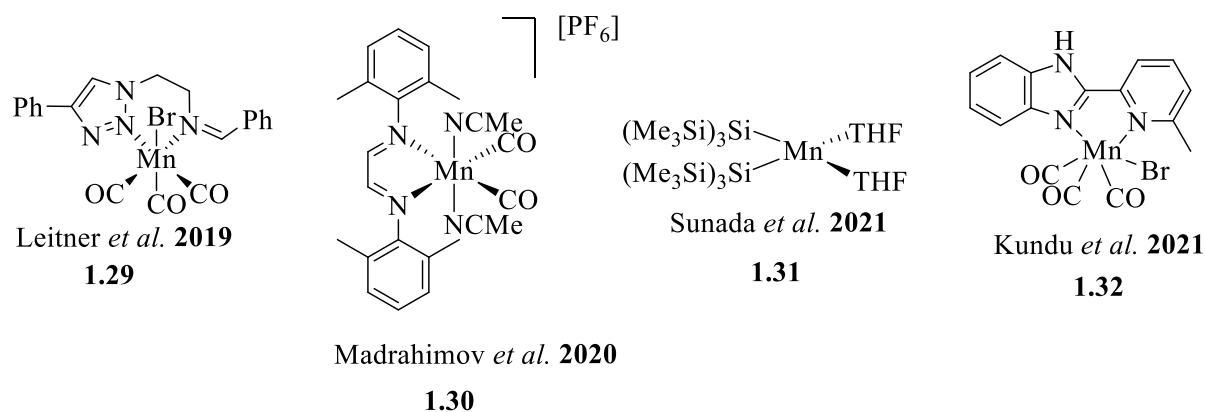
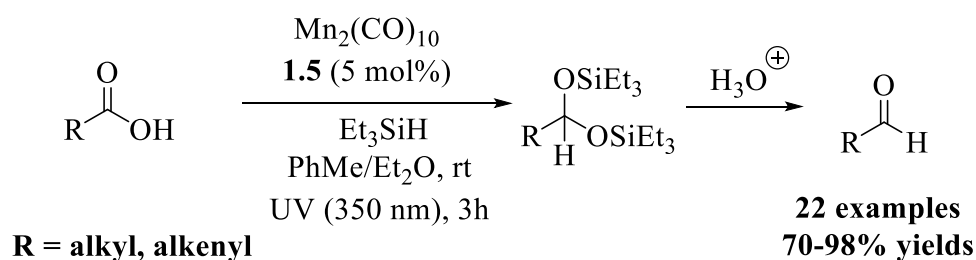


**Figure 1.5** Manganese complexes used in hydrosilylation of carbonyl compounds.

### 1.3.2. Manganese Catalyzed Hydrosilylation of carboxylic acids

A long-standing focus is the search for appropriate catalytic systems for the hydrosilylation of difficult carboxylic acids. Darcel and Sortais made a significant contribution in this approach by demonstrating that the decacarbonyl manganese complex **1.5** enhanced the hydrosilylative reduction of carboxylic acids with silanes to aldehydes under photocatalytic conditions.<sup>64</sup> In this methodology, steric crowding close to the reaction centre had a significant

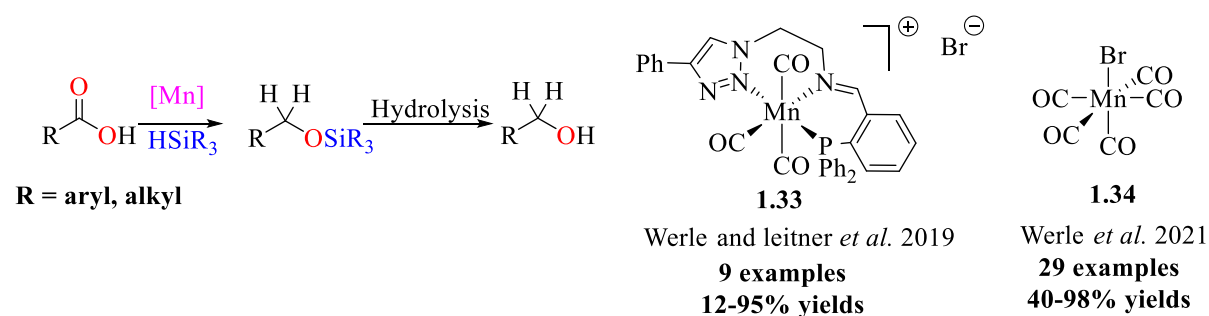


**Scheme 1.12** Mn Catalyzed hydrosilylation of carboxylic acids to aldehydes.

impact on the outcome of the reaction. For mono-hydridic silanes like  $\text{Et}_3\text{SiH}$ ,  $\text{PhMe}_2\text{SiH}$ , and  $\text{Ph}_2\text{MeSiH}$ , the major product of the acidic hydrolysis was the aldehyde. On the other hand,

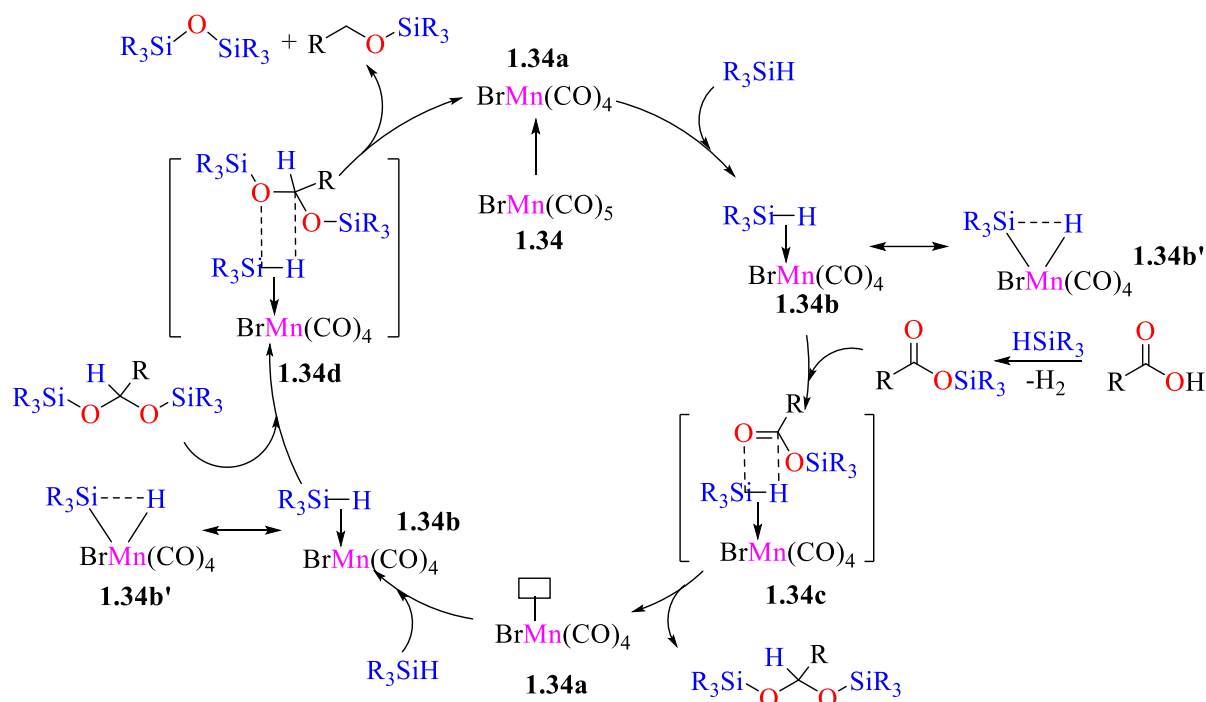
alcohol was generated as the main byproduct in the case of secondary silanes like  $\text{Ph}_2\text{SiH}_2$  and  $\text{Et}_2\text{SiH}_2$ . To the silanes used, this approach was chemodivergent.

Werle' and Leitner developed a tridentate NNP-Mn(I) complex **1.33** that facilitated the hydrosilylative route for the reduction of carboxylic acids to alcohols later in 2019.<sup>61</sup> However, a few carboxylic acids with aryl and aliphatic groups were covered in the study. The same group has recently shown that only  $\text{Mn}(\text{CO})_5\text{Br}$  can catalyse the reaction with a wide range of aliphatic carboxylic acids.<sup>65</sup> Some aromatic carboxylic acids,



### Scheme 1.13 Mn-Catalyzed hydrosilylation of carboxylic acids to alcohols.

however, are still inert under these circumstances. When the reaction first started, there was a lot of gas evolution, which meant that silyl carboxylic acid was forming (Scheme 1.23). By removing one CO, the coordinatively unsaturated pentacoordinate species  $\text{Mn}(\text{CO})_4\text{Br}$  **1.34a** are formed, which initiates the catalytic cycle. The latter then uses a redox neutral route to activate the Si-H bond to create the intermediate **1.34b**. **1.34a** and disilylether are both regenerated together with the outer-sphere transfer of hydride to the carbonyl carbon of the silyl ester of carboxylic acid. The same series of actions are performed with intermediate disilyl ether until silyl ether of reduced alcohol is produced.

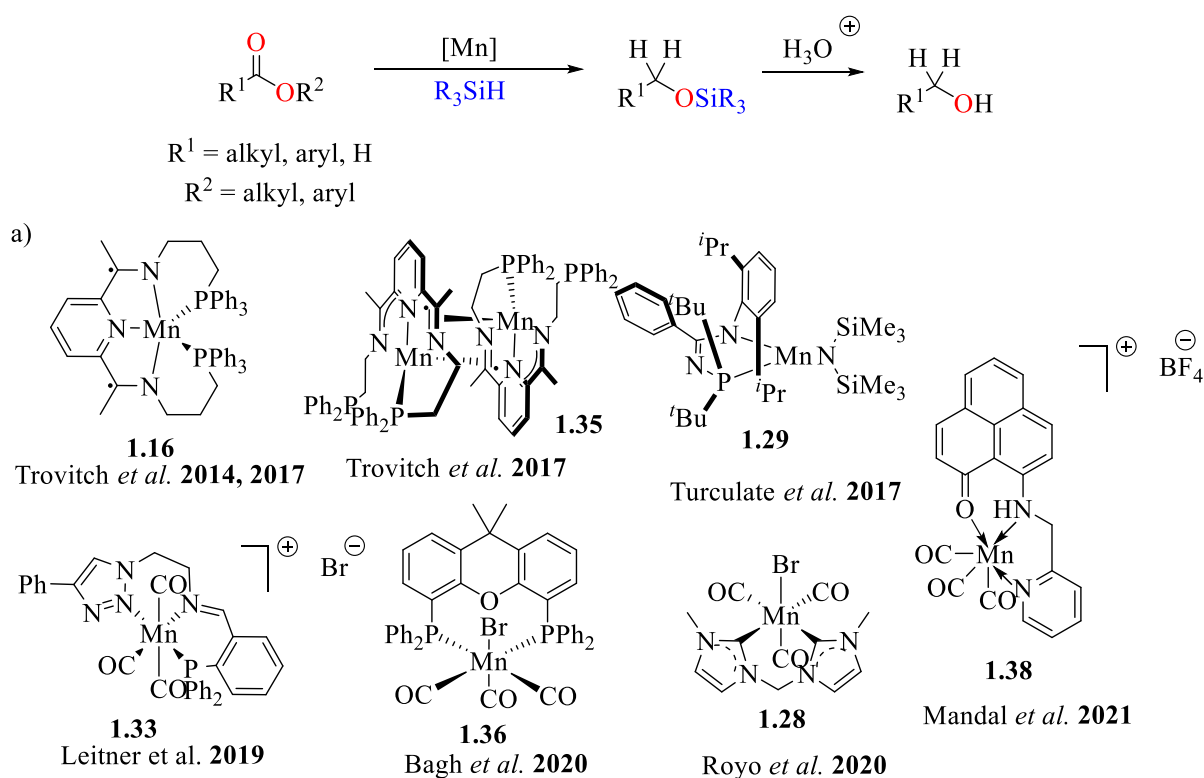


**Scheme 1.14** Mechanism for hydrosilylation of carboxylic acids employing  $\text{Mn(CO)}_5\text{Br}$ .

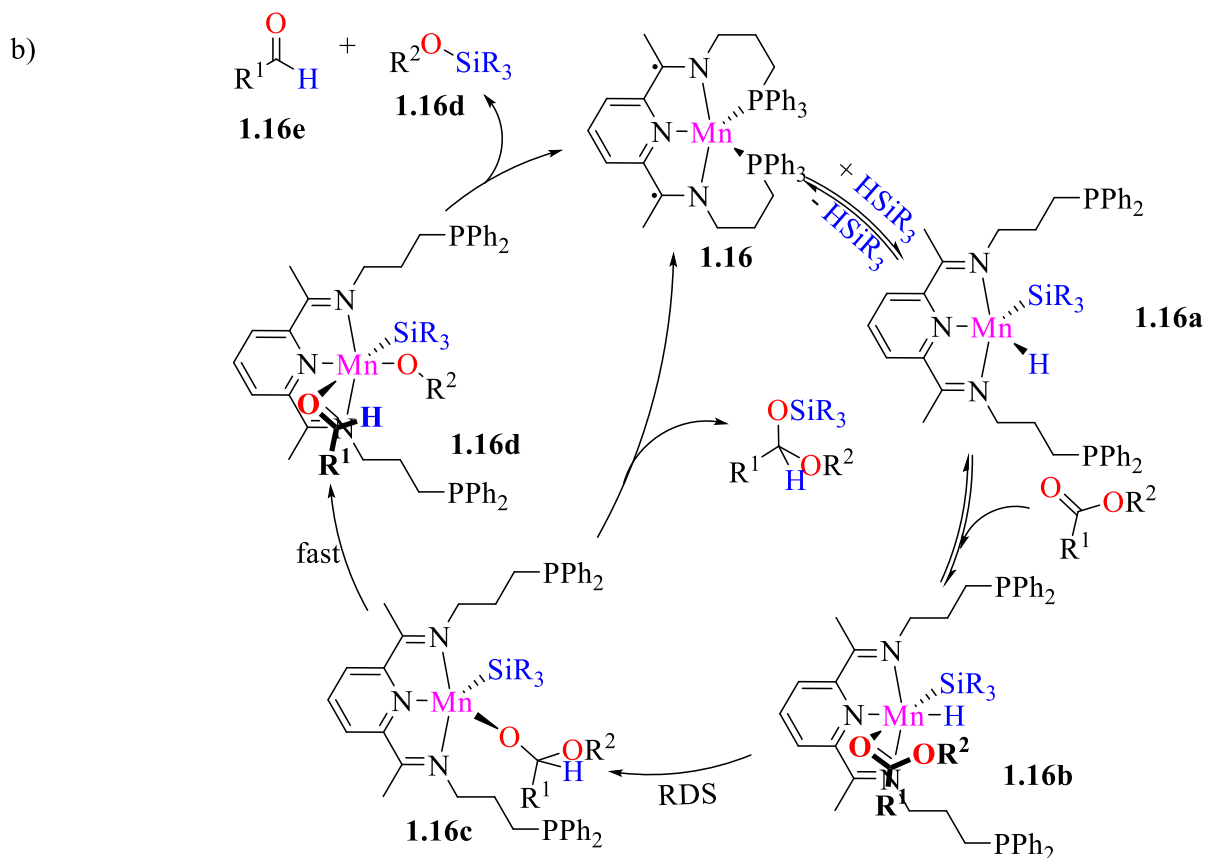
### 1.3.3. Manganese Catalyzed Hydrosilylation of esters

One of the earliest methods developed during the initial reports on alkene hydrosilylation is the hydrosilylation of esters.<sup>43</sup> In 1995, the deoxygenative reduction of esters to silyl ethers of alcohols was successfully accomplished by Cutler using a  $[(\text{PPh}_3)(\text{CO})_4\text{Mn}(\text{COCH}_3)]$  complex.<sup>47</sup> The active form of the precatalyst that was proposed was the coordinative unsaturated  $[(\text{PPh}_3)\text{Mn}(\text{CO})_3(\text{SiR}_3)]$ . Trovitch *et al.* made this transformation using their PDI ligand based Mn(II)-complexes **1.16**, which were previously used for the hydrosilylative reduction of aldehydes and ketones (Scheme 1.26a).<sup>53c</sup> Initial research using **1.16** suggested that over a protracted reaction time of up to 10 days, the transformation may be accomplished with a small number of acetate esters.<sup>53a</sup> Complex **1.16** exhibited excellent catalytic activity with formate esters, with a TON of up to 4400 and a TOF of  $330 \text{ min}^{-1}$ .<sup>53b</sup> Similar reactivity was also demonstrated by the dimeric complex **1.35** at a slightly slower pace.<sup>53</sup> A mechanism akin to Ojima mechanism was suggested (Scheme 1.26b).<sup>53c</sup> Here, alkoxide elimination moves more quickly than reductive elimination.

Turculet then utilised the PN-chelate Mn(II)-complex **1.29**, which has an amide arm, to hydrosilylation of methyl esters to the corresponding alcohol.<sup>58</sup> Only five substrates were used. Leitner performed the hydrosilylation of ester procedure in 2019 using the neutral tridentate NNP-Mn(I) complex **1.33**, though at a higher temperature.<sup>59</sup> Very recently, our group disclosed using the Mn(I)-complex **1.36** having xantphos ligand for the similar reaction.<sup>66</sup> Royo then utilised bis-NHC Mn(I)-complex **1.28** for ester hydrosilylation under analogous circumstances.<sup>67</sup> The ability of **1.36** to tolerate the heterocyclic backbone and C-C multiple bonds was by far its biggest benefit over **1.28**, despite the fact that their activities were relatively similar.

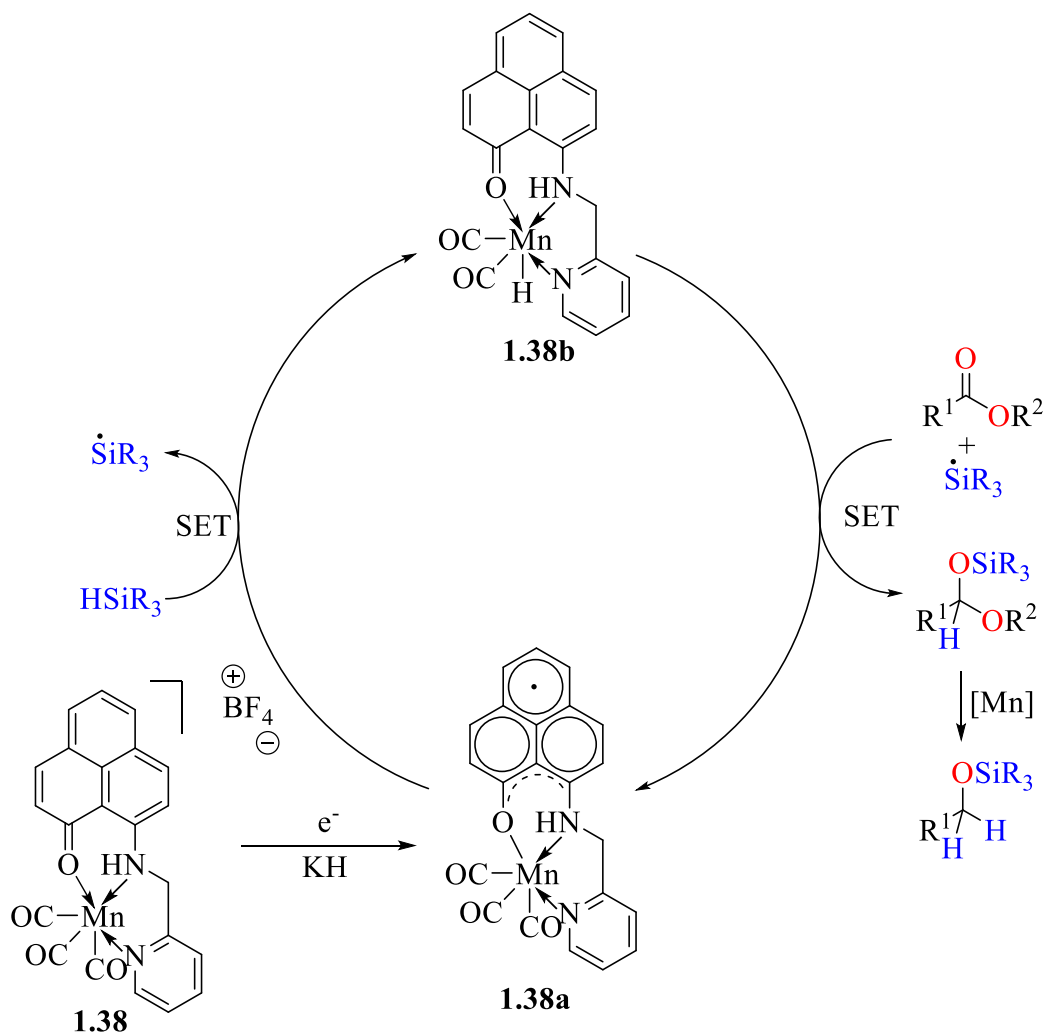


**Scheme 1.15** Manganese complexes used in hydrosilylation of ester.



**Scheme 1.16** Mechanism for ester hydrosilylation by employing manganese complex **1.16**.

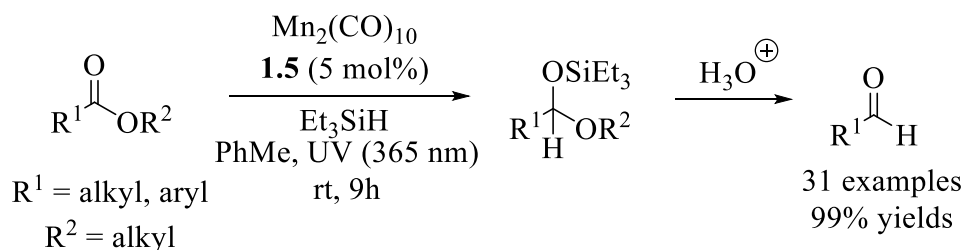
Mandal recently developed phenalenyl core-based Mn(I)-complex **1.38** to hydrosilylate esters. As the catalyst's activator, KH was required.<sup>68</sup> Notably, the suggested technique was tolerant to conjugated double bonds and heteroaryl moieties. In the introduction of TEMPO to the catalytic system, the reaction produced less favourable results. This suggested a route that was radical-mediated. KH treatment of the precatalyst produced an EPR active species. Here, the ligand backbone performs the role of a redox-active ligand. The reduction of **1.38** by KH to produce **1.38a** initiates the catalytic cycle. One electron is occupied by the ligand core. The Mn-hydride species **1.38b** subsequently activates the Si-H bond through SET to the  $\sigma$ -antibonding orbital, producing the silyl radical  $\text{R}_3\text{Si}$  and the Mn-hydride species **1.38b**. The regeneration of **1.38b** occurs when the hydride from **1.38b** is transferred to an ester group, where it recombines with a silyl radical to produce the intermediate silyl ether. Intermediate generates alkyl silyl ether as it enters a new cycle.



**Scheme 1.17 Mechanism for the hydrosilylation of esters employing 1.38.**

Sortais published the sole instance of the manganese-catalyzed hydrosilylation of esters into aldehydes in 2020. (Scheme 1.28).<sup>69</sup> Here the catalyst was manganese decacarbonyl.

Under the illumination of 365 nm light, the reaction was carried out at ambient

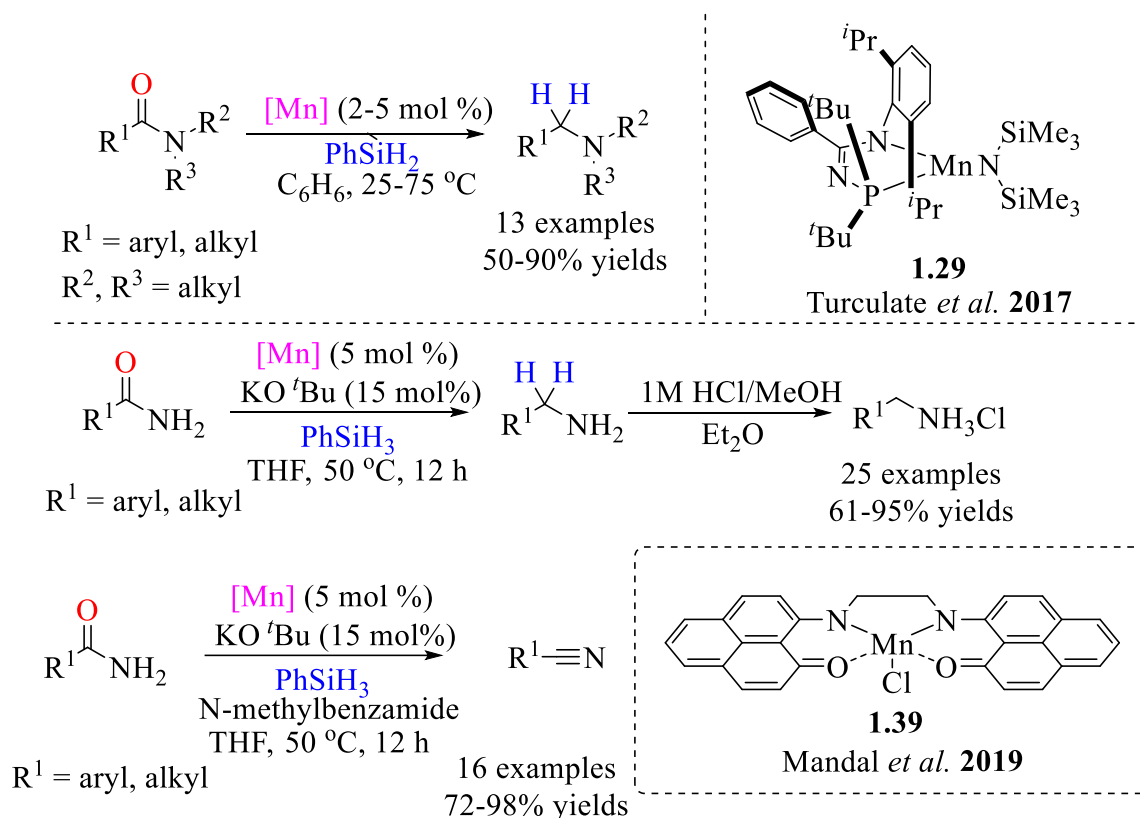


**Scheme 1.18 Mn-Catalyzed hydrosilylation of ester to aldehyde.**

temperature. One equivalent of silane was used in the hydrosilylation process to create silyl ether, which when hydrolyzed yields aldehyde.

### 1.3.4. Manganese Catalyzed Hydrosilylation of amides.

Fuchikami published their important research on the reductive hydrosilylation of N-acetylpiperidine to N-ethyl piperidine in 2001.<sup>70</sup> In 2017, Turculet disclosed the **1.29** complex-catalyzed hydrosilylation of amides, which marked a significant progress in this research (Scheme 1.29).<sup>58</sup> However, with a larger range of substrates and a lower catalyst loading, the reaction could be carried out. The group concentrated on amide hydrosilylation, which was difficult. Several tertiary amides were deoxygenatively reduced during the course of an overnight period at room temperature using catalyst **1.29** (2 mol%). However, only tertiary amides were included in the study. Later in 2019, Mandal used the phenalenyl-derived Mn(III)-complex **1.39** to produce primary amines and nitriles by the chemodivergent hydrosilylation of amides (Scheme 1.29).<sup>71</sup> A coordinatively labile complex [LMn-THF]<sup>+</sup> (L = phenalenyl

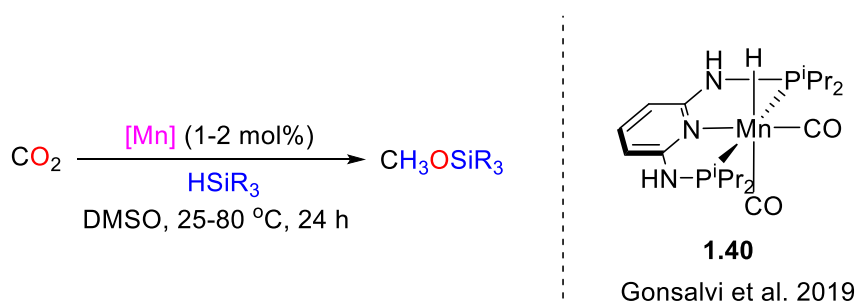


Scheme 1.19 Mn-Catalyzed hydrosilylation of amides.

ligand) and an active silane [ $\text{PhH}_3\text{Si}(\text{O}^t\text{Bu})$ ] are formed from this complex when it is treated with  $\text{KO}^t\text{Bu}$  and then reacts with silane.. A nitrile intermediate is produced by the initial hydride transfer to amide; two subsequent hydride additions then result in the production of amine.

### 1.3.5. Manganese Catalyzed Hydrosilylation of carbon dioxide

In 2019, Gonsalvi used the  $(\text{PN}_3\text{P})\text{Mn}(\text{I})$ -complex **1.40** to perform reductive hydrosilylate carbon dioxide into methyl silyl ether (**Scheme 1.30**).<sup>72</sup> According on the type of silane employed, the reaction was discovered to be selective. Monohydrosilanes like  $\text{PhMe}_2\text{SiH}$  and  $\text{Ph}_3\text{SiH}$  solely produced silyl formate  $\text{Si}(\text{O}_2\text{CH})$ , however with a poor yield. In contrast, the switch to dihydro or trihydrosilanes resulted in the formation of highly selective methoxy silyl derivatives at  $80\text{ }^\circ\text{C}$ . Fortunately, after 24 hours,  $\text{PhSiH}_3$  completely converted to methoxy silane. Without changing the outcome of the reaction, the catalyst loading might be reduced

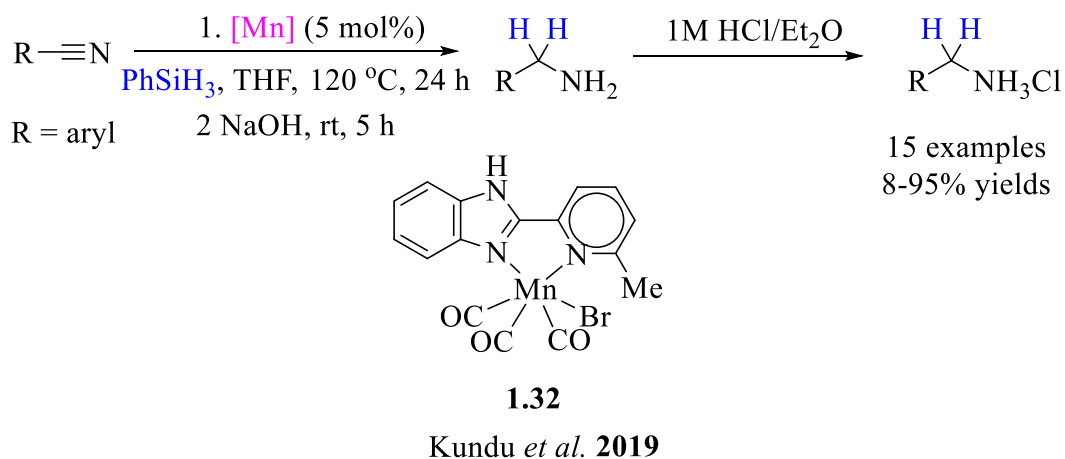


### Scheme 1.20 Manganese pincer complex catalyzed hydrosilylation of carbon dioxide.

further. It was suggested that the catalytic cycle would continue through a coordinated formate intermediate, such as was previously predicted for  $\text{CO}_2$  hydrogenation.

### 1.3.6. Manganese Catalyzed Hydrosilylation of nitriles

Using  $\text{N,N}$ -chelate  $\text{Mn}(\text{I})$ -complex **1.32**, Kundu performed the reductive hydrosilylation of nitriles in 2020. (**Scheme 1.31**).<sup>62</sup> The previously mentioned ketone hydrosilylation procedure

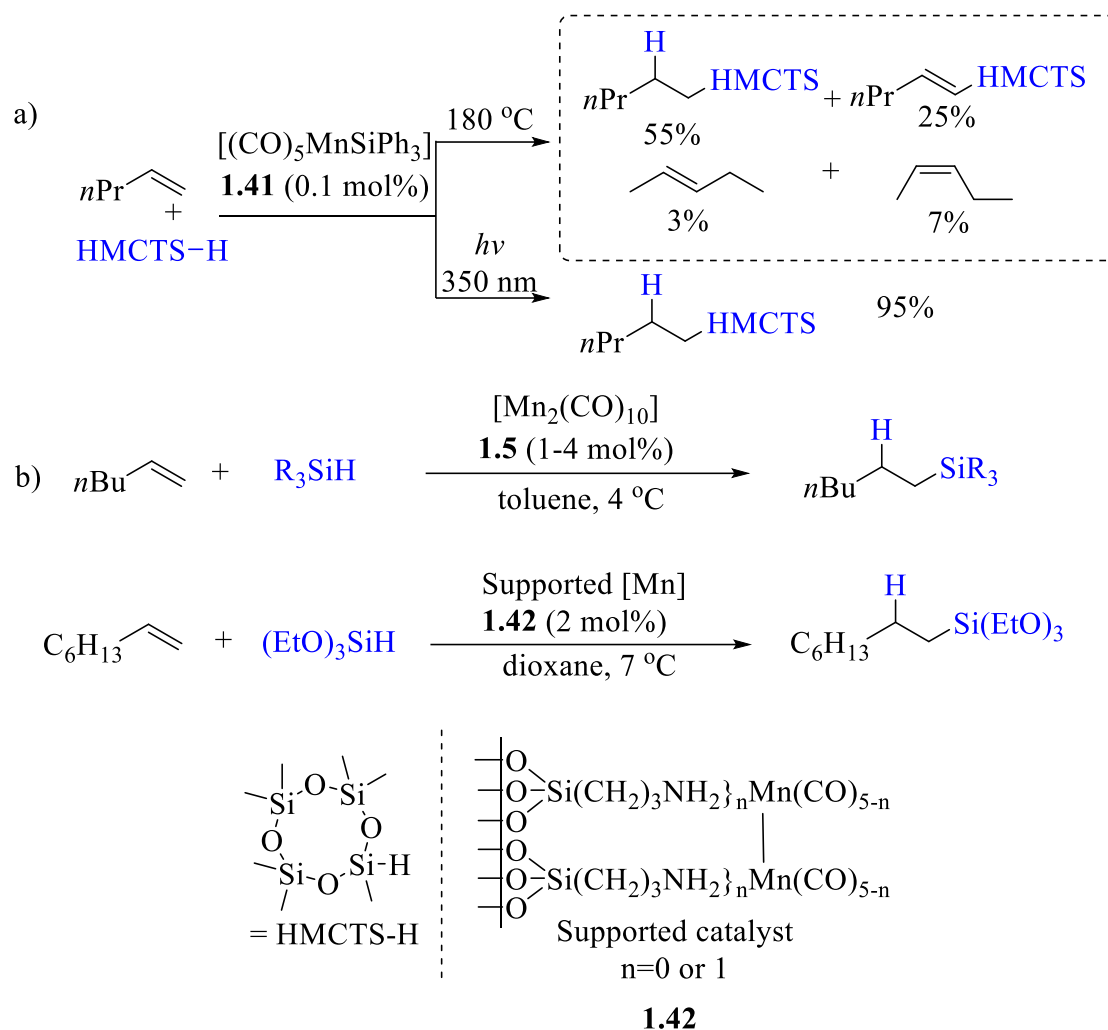


### Scheme 1.21 Manganese catalyzed hydrosilylation of nitriles to amines.

has also been carried out using the complex. It's interesting to note that the reaction was tolerant of a heterocyclic moiety, and good yields of the chloride salt of amines were obtained.

### 1.3.7. Manganese Catalyzed Hydrosilylation of Alkenes

Faltynek made the first contribution to Mn-catalyzed alkene hydrosilylation in 1983. (Scheme 1.32a).<sup>43</sup> Under UV or heating conditions,  $[(\text{CO})_5\text{MnSiPh}_3]$  **1.41** was used as a catalyst to hydrosilylate 1-pentene with a cyclic silane (HMCTS-H) having eight members ring. At 180 °C, produced a number of products, including the anticipated hydrosilylation, alkene isomerization, and dehydrogenative silylation. On the other hand, a single hydrosilylation product was obtained in high yield when photoirradiation was used. Hilal demonstrated the  $[\text{Mn}_2(\text{CO})_{10}]$ -catalyzed hydrosilylation of 1-hexene using  $\text{Et}_3\text{SiH}$  and  $(\text{EtO})_3\text{SiH}$  in 1987, but the process produced a small amount of product. (Scheme 1.32b).<sup>73</sup> The same group

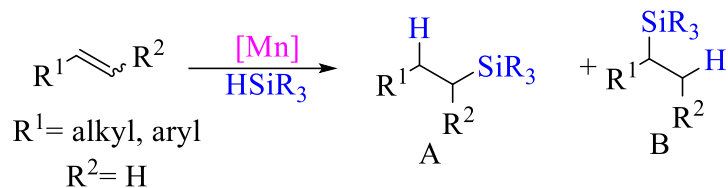


### Scheme 1.22 Manganese-catalyzed hydrosilylation of alkenes.

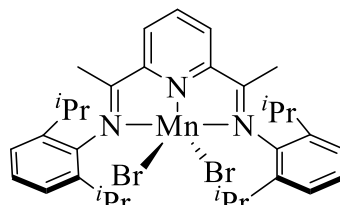
revealed another instance of the hydrosilylation of terminal olefin after more than a decade.<sup>74</sup> Utilizing a dimeric manganese complex **1.42** supported by poly(siloxane), the hydrosilylation product was produced in good yield with no evidence of olefin isomerization.

In 2000, it was found that  $\text{Mn}(\text{dpm})_3$  (dpm = dipivaloylmethanato) **1.43** served as the catalyst for the catalytic hydrosilylative reduction of  $\alpha,\beta$ -unsaturated ketones to saturated ketones.<sup>75</sup>  $\text{PhSiH}_3$  was used as the reductant and the reaction was carried out in an isopropanol solvent. It was suggested that the actual reducing agent was the in situ-formed  ${}^i\text{PrOSiH}_2\text{Ph}$ . Thomas used the regioselective anti-Markovnikov hydrosilylation of inactive alkenes using the bis(imino)pyridine ligand based Mn(II)-complex **1.44** in 2017 (scheme 1.33).<sup>76</sup> The authors demonstrated that  $\text{NaOtBu}$  might facilitate the hydrosilylation of olefin to produce product in

a reasonable yield at ambient temperatures. In accordance with more research on the subject, aliphatic alkenes exclusively produced the product with anti-Markovnikov selectivity, but aromatic alkenes resulted in some deterioration of selectivity. The outcome of the reaction was unaffected by the inclusion of the radical scavenger TEMPO. However, the yields were reduced by the presence of trityl cation ( $\text{Ph}_3\text{C}^+$ ). As a result, the involvement of a Mn-hydride species as an active reaction intermediate was suggested. The species' true nature, however, was unknown. In 2018, Trovitch carried out the same transformation using  $\beta$ -diketimine Mn-complex **1.45** (scheme 1.33).<sup>77</sup> It's interesting to note that whereas aromatic alkenes produced the Markovnikov-selective product, aliphatic alkenes led to anti-Markovnikov selectivity. Wang demonstrated in the same year that alkenes could also be converted to linear higher alkylsilanes using the commercially available  $\text{Mn}(\text{CO})_5\text{Br}$  (scheme 1.33).<sup>78</sup> This approach could only be used in a wider range at a lower temperature and in less time.



Mn(dpm)<sub>3</sub>  
Magnus *et al.* 2000  
**1.43**  
8 examples  
25-100% yields

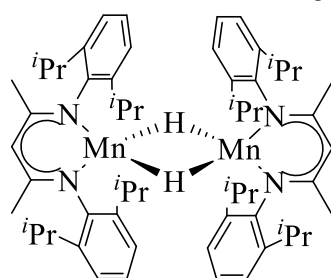


Thomas *et al.* 2017

**1.44**

16 examples  
35->95% yields

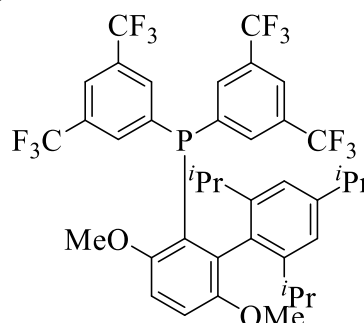
MnBr(CO)<sub>5</sub>  
Wang *et al.* 2018  
**1.34**  
26 examples  
61-95% yields



Trovitch *et al.* 2018

**1.45**

20 examples  
19->99% yields



+ Mn<sub>2</sub>(CO)<sub>10</sub>  
Xie *et al.* 2021

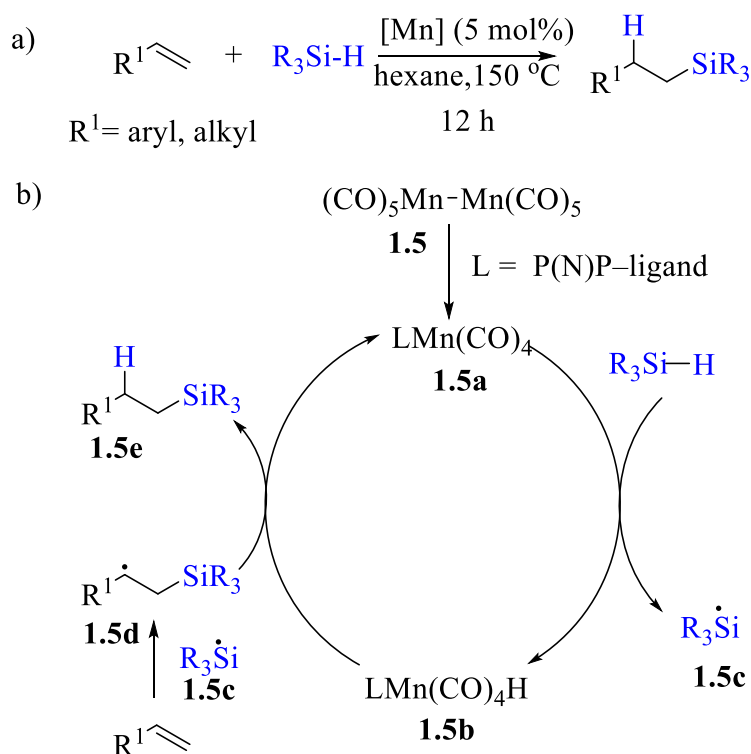
**1.46**

13 examples  
72-89% yields

### Scheme 1.23 Mn-Catalyzed hydrosilylation of alkenes.

Recently, the same reaction was carried out by Xie and colleagues using Mn<sub>2</sub>(CO)<sub>10</sub> in the presence of a large monodentate phosphine ligand (scheme 1.34a).<sup>79</sup> The results of the experimental investigations suggested that a radical process was involved. The reduced yield after TEMPO addition serves as clear evidence of this. It was proposed that the ligand aids in the thermal dissociation of Mn<sub>2</sub>(CO)<sub>10</sub> to produce radical manganese-centered **1.5a** (Scheme 1.34b). A silyl radical and the Mn-hydride species **1.5b** are produced when silane transfers a hydrogen atom. Following a second hydrogen atom transfer from Mn-hydride, the radical **1.5d** with a carbon centre undergoes addition to the alkene double bond to produce the alkylsilane

product. The last HAT is carried out via the trans disposition of the large ligand and Mn-hydride reduces steric crowding for the alkyl radical approach.

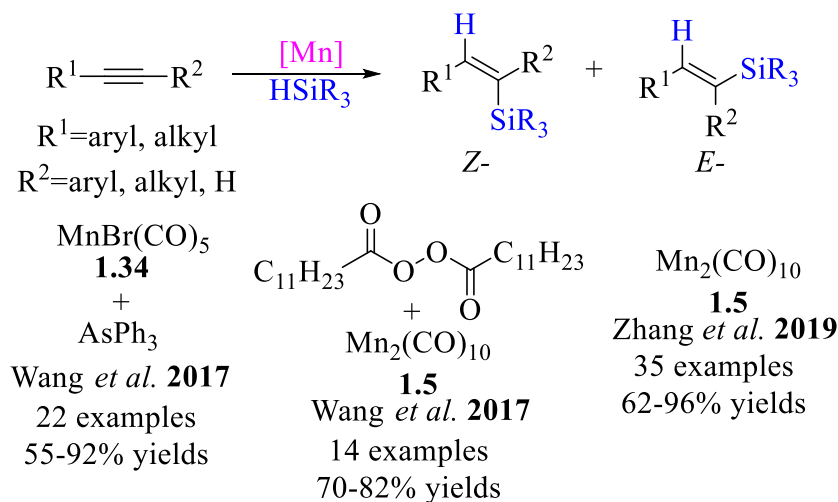


**Scheme 1.24** Mechanisms for the hydrosilylation of alkenes employing  $\text{Mn}_2(\text{CO})_{10}$ .

### 1.3.8. Manganese Catalyzed Hydrosilylation of Alkynes

In 2017, Wang showed that alkynes can be hydrosilylated stereodivergently to produce both *E*- and *Z*-alkenes under two distinct catalytic conditions (Scheme 1.35), respectively.<sup>80</sup> To optimise the reaction conditions, they initially used diphenylacetylene and diphenylsilane as the model substrates. Low yields of the intended products were produced in the presence of  $[\text{Mn}(\text{CO})_5\text{Br}]$ , along with appreciable amounts of hydrogenative byproducts. Surprisingly, adding the arsenic ligand  $\text{AsPh}_3$  demonstrated remarkable selectivity for the production of the *E*-product at 150 °C in the toluene solvent (Scheme 1.35). However, the selectivity suffers when bulky aliphatic substituents are present. In contrast, the reaction was skewed towards the synthesis of *Z*-alkenes without the need for a ligand at 120 °C in the decalin solvent when the exogenous radical initiator dilauroyl peroxide (LPO) was present (Scheme

1.35). This procedure was also effectively used to aryl alkyl alkynes, showing strong stereo- and regioselectivities.



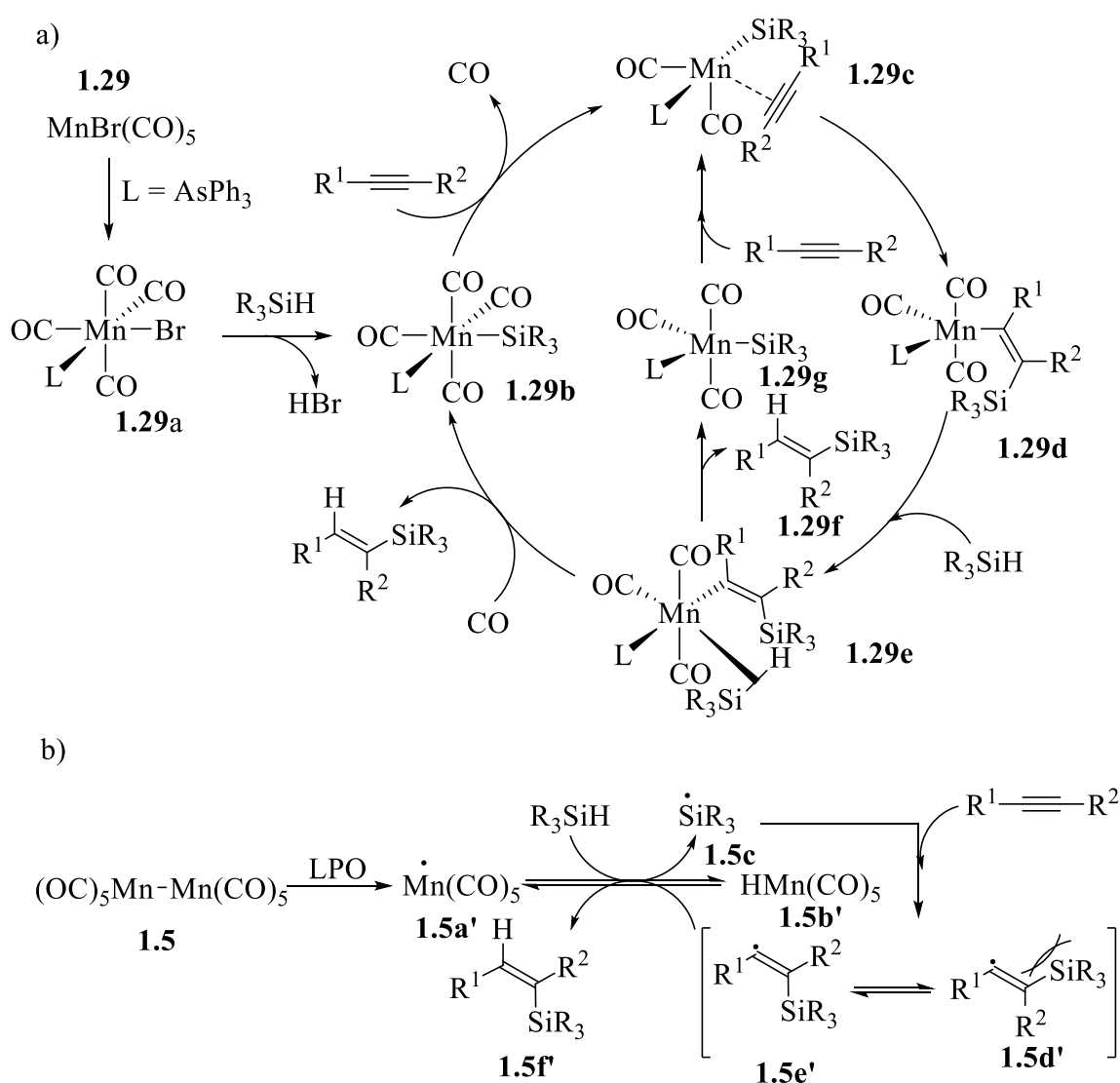
### Scheme 1.25 Hydrosilylation of alkynes employing Mn catalysts.

A hypothesised catalytic cycle of the  $[\text{Mn}(\text{CO})_5\text{Br}]$  in presence of  $\text{AsPh}_3$ -catalyzed *E*-selective hydrosilylation of alkynes is depicted in (Scheme 1.36a) and is based on in-depth mechanistic research. By substituting  $\text{AsPh}_3$  for CO as the ligand and reacting the resultant molecule **1.29a** with silane in an  $\sigma$ -metathesis process, the important manganese-silyl intermediate **1.29b** was produced. To form the alkenyl-manganese intermediate **1.29d**, complex **1.29b** underwent coordination, followed by the insertion of the alkyne's  $\text{C}\equiv\text{C}$  bond. The catalytic cycle was closed by the ligation **1.29e** and  $\sigma$ -metathesis reaction of silane, which produced the desired product **1.29f** and regenerated **1.29c**. Alternately, the desired product might be immediately liberated from species **1.29e**, which would then regenerate species **1.29b**, which would then go through coordination of an alkyne to produce intermediate **1.29c**.

In contrast, the *E/Z* selectivity in the hydrosilylation of alkynes was inverted when the dinuclear complex  $[\text{Mn}_2(\text{CO})_{10}]$  and dilauroyl peroxide (LPO) were used (Scheme 1.36b). The homolysis of  $[\text{Mn}_2(\text{CO})_{10}]$  was the initial step in the reaction, producing manganese radical species **1.5a'**, which then took hydrogen from silane to produce silyl radical **1.5c** and manganese hydride **1.5b'**. The alkenyl radicals **1.5d'** and/or **1.5e'** were then produced when the silyl radical **1.5c**

attacked the alkyne's triple bond. The Z-configured radical **1.5e'**, which interacted with manganese hydride **1.5b'** to produce the intended product **1.5f'**, was preferred because of steric hindrance.

Zhang demonstrated in 2019 that manganese decacarbonyl alone was capable of catalysing the hydrosilylation of both terminal and internal alkynes with almost quantifiable yields and good Z-selectivity without the need for a ligand.<sup>81</sup> There was a comparable radical-induced process put forth.



**Scheme 1.26** Different pathways for E- and Z- selective alkene employing manganese complex.

### References

1. Anastas, P. T.; Warner, J. C. Principles of green chemistry. *Green chemistry: Theory and practice* **1998**, 29-56.
2. Johansson Seechurn, C. C. C.; DeAngelis, A.; Colacot, T. J. Chapter 1. Introduction to New Trends in Cross-Coupling. In *New Trends in Cross-Coupling: Theory and Applications*; Royal Society of Chemistry, 2014; pp 1–19. Suzuki, A.; Heck, R. F.; Negishi, E. The nobel prize in chemistry 2010.
3. Tacke, R.; Wannagat, U. *Bioactive Organo-Silicon Compounds*; Springer: Berlin, Heidelberg, 1979.
4. Sommer, L. H.; Pietrusza, E. W.; Whitmore, F. C. Peroxide-Catalyzed Addition of Trichlorosilane to 1-Octene. *J. Am. Chem. Soc.* **1947**, *69*, 188–188, DOI: 10.1021/ja01193a508
5. Speier, J. L.; Webster, J. A.; Barnes, G. H. The addition of silicon hydrides to olefinic double bonds. Part II. The use of group VIII metal catalysts. *J. Am. Chem. Soc.*, **1957**, *79*, 974-979.
6. Miller, R. D.; Michl, J. Polysilane high polymers. *Chem. Rev.* **1989**, *89*, 1359–1410.
7. Sieburth, S. McN.; Nittoli, T.; Mutahi, A. M.; Guo, L. Silanediols: A new class of potent protease inhibitors. *Angew. Chem., Int. Ed.* **1998**, *37*, 812–814.
8. Franz, A. K.; Wilson, S. O. Organosilicon Molecules with Medicinal Applications. *J. Med. Chem.* **2013**, *56*, 388–405.
9. a) Noyori, R. *Asymmetric Catalysis in Organic Synthesis*; Wiley: New York, 1994. b) Noyori, R.; Ohkuma, T. Asymmetric Catalysis by Architectural and Functional Molecular Engineering: Practical Chemo- and Stereoselective Hydrogenation of Ketones. *Angew. Chem., Int. Ed.* **2001**, *40*, 40–73.

10. Weissman, S. A.; Rossen, K.; Reider, P. J. Stereoselective Synthesis of Styrene Oxides via a Mitsunobu Cyclodehydration. *Org. Lett.* **2001**, *3*, 2513–2515.
11. Das, K.; Waiba, S.; Jana, A.; Maji, B. Manganese-Catalyzed Hydrogenation, Dehydrogenation, and Hydroelementation Reactions. *Chem. Soc. Rev.* **2022**, *51*, 4386–4464.
12. Ege, S. N. *Organic Chemistry*; D. C. Heath Company: Lexington, MA, 1989; p 596.
13. Marciniak, B. Hydrosilylation of carbon—carbon multiple bonds in organic synthesis. *Hydrosilylation*: Dordrecht: Springer Netherlands; **2009**:87–123.
14. Ojima, I.; Kogure, T. Reduction of carbonyl compounds via hydrosilylation. 4. Highly regioselective reductions of  $\alpha,\beta$ -unsaturated carbonyl compounds. *Organometallics* **1982**, *1*, 1390–1399.
15. a) Bullock, R. M. *Catalysis Without Precious Metals*; John Wiley & Sons, 2011. b) Bullock, R. M.; Chen, J. G.; Gagliardi, L.; Chirik, P. J.; Farha, O. K.; Hendon, C. H.; Jones, C. W.; Keith, J. A.; Klosin, J.; Minter, S. D.; Morris, R. H.; Radosevich, A. T.; Rauchfuss, T. B.; Strotman, N. A.; Vojvodic, A.; Ward, T. R.; Yang, J. Y.; Surendranath, Y. Using Nature's Blueprint to Expand Catalysis with Earth-Abundant Metals. *Science* **2020**, *369*, eabc3183, DOI: 10.1126/science.abc3183.
16. Holwell, A. J. Optimised Technologies are Emerging which Reduce Platinum Usage in Silicone Curing. *Platinum Met. Rev.* **2008**, *52*, 243–246.
17. Ojima, I. In *The Chemistry of Organic Silicon Compounds*, Vol. 1; Patai, S., Rappoport, Z., Eds.; Wiley: Chichester, U.K., 1989; Chapter 25.
18. Mukherjee, A.; Milstein, D. Homogeneous Catalysis by Cobalt and Manganese Pincer Complexes. *ACS Catal.* **2018**, *8*, 11435–11469.
19. a) Wei, D.; Darcel, C. Iron catalysis in reduction and hydrometalation reactions. *Chem. Rev.* **2019**, *119*, 2550–2610. b) Lopes, R.; Royo, B. Iron N-heterocyclic carbenes in reduction reactions. *Isr J Chem.* **2017**, *57*, 1151–1159. c) Gaillard, S.; Renaud, J. L. Iron-

- Catalyzed Hydrogenation, Hydride Transfer, and Hydrosilylation: An Alternative to Precious-Metal Complexes?. *ChemSusChem* **2008**, *1*, 505–509. d) Zhou, S.; Junge, K.; Addis, D.; Das, S.; Beller, M. A Convenient and General Iron-Catalyzed Reduction of Amides to Amines. *Angew. Chem., Int. Ed.* **2009**, *48*, 9507–9510.
20. For selected reviews, see: a) Greenhalgh, M. D.; Jones, A. S.; Thomas, S. P. Iron-Catalysed Hydrofunctionalisation of Alkenes and Alkynes. *ChemCatChem* **2015**, *7*, 190–222. b) Du, X.; Huang, Z. Advances in Base-Metal Catalyzed Alkene Hydrosilylation. *ACS Catal.* **2017**, *7*, 1227–1243. c) Tondreau, A. M.; Atienza, C. C. H.; Weller, K. J.; Nye, S. A.; Lewis, K. M.; Delis, J. G. P.; Chirik, P. J. Iron Catalysts for Selective Anti-Markovnikov Alkene Hydrosilylation Using Tertiary Silanes. *Science* **2012**, *335*, 567–570. d) Belger, C.; Plietker, B. Aryl–aryl interactions as directing motifs in the stereodivergent iron-catalyzed hydrosilylation of internal alkynes. *Chem. Commun.* **2012**, *48*, 5419–5421. e) Greenhalgh, M. D.; Frank, D. J.; Thomas, S. P. Iron-catalysed chemo-, regio-, and stereoselective hydrosilylation of alkenes and alkynes using a bench-stable iron (II) pre-catalyst. *Adv. Synth. Catal.* **2014**, *356*, 584–590. f) Challinor, A. J.; Calin, M.; Nichol, G. S.; Carter, N. B.; Thomas, S. P. Amine-Activated Iron Catalysis: Air- and Moisture-Stable Alkene and Alkyne Hydrofunctionalization. *Adv. Synth. Catal.* **2016**, *358*, 2404–2409.
21. For selected reviews and examples, see: a) Sun, J.; Deng, L. Cobalt complex-catalyzed hydrosilylation of alkenes and alkynes. *ACS Catal.* **2016**, *6*, 290–300. b) Mo, Z.; Xiao, J.; Gao, Y.; Deng, L. Regio- and stereoselective hydrosilylation of alkynes catalyzed by three-coordinate cobalt (I) alkyl and silyl complexes. *J. Am. Chem. Soc.* **2014**, *136*, 17414–17417. c) Chen, C.; Hecht, M. B.; Kavara, A.; Brennessel, W. W.; Mercado, B. Q.; Weix, D. J.; Holland, P. L. Rapid, regioconvergent, solvent-free alkene hydrosilylation with a cobalt catalyst. *J. Am. Chem. Soc.* **2015**, *137*, 13244–13247. d)

- Rivera-Hernandez, A.; Fallon, B. J.; Ventre, S.; Simon, C.; Tremblay, M. H.; Gontard, G.; Derat, E.; Amatore, M.; Aubert, C.; Petit, M. Regio- and Stereoselective Hydrosilylation of Unsymmetrical Alkynes Catalyzed by a Well-Defined, Low-Valent Cobalt Catalyst. *Org. Lett.* **2016**, *18*, 4242–4245. e) Guo, J.; Lu, Z. Highly Chemo-, Regio-, and Stereoselective Cobalt-Catalyzed Markovnikov Hydrosilylation of Alkynes. *Angew. Chem., Int. Ed.* **2016**, *55*, 10835–10838. f) Zuo, Z.; Yang, J.; Huang, Z. Cobalt-catalyzed alkyne hydrosilylation and sequential vinylsilane hydroboration with Markovnikov selectivity. *Angew. Chem., Int. Ed.* **2016**, *55*, 10839–10843. g) Teo, W. J.; Wang, C.; Tan, Y. W.; Ge, S. Cobalt-Catalyzed Z-Selective Hydrosilylation of Terminal Alkynes. *Angew. Chem., Int. Ed.* **2017**, *56*, 4328–4332.
22. a) Buslov, I.; Becouse, J.; Mazza, S.; Montandon-Clerc, M.; Hu, X. *Angew. Chem., Int. Ed.* **2015**, *54*, 14523–14526. b) Buslov, I.; Keller, S. C.; Hu, X. Alkoxy hydrosilanes as surrogates of gaseous silanes for hydrosilylation of alkenes. *Org. Lett.* **2016**, *18*, 1928–1931.
23. Tedstone, A. A.; Lewis, D. J.; O'Brien, P. Synthesis, Properties, and Applications of Doped Layered Transition Metal Dichalcogenides. *Chem. Mater.* **2016**, *28*, 1965–1974.
24. Wen, L.; Shi, G.; Sun, Y.; Cui, Y.; Zhang, S.; Chen, X.; Xin, B. Rapid and efficient extraction of Zn from wasted Zn-rich paint residue by indirect bioleaching and successive production of high-purity ZnCO<sub>3</sub>/ZnO by precipitation. *J. Environ. Mana.* **2023**, *342*, 118294.
25. Li, C.; Pang, Y.; Xu, Y.; Lu, M.; Tu, L.; Li, Q.; Sun, Y. Near-infrared metal agents assisting precision medicine: from strategic design to bioimaging and therapeutic applications. *Chem. Soc. Rev.*, **2023**, *52*, 4392–4442.
26. Marinetti, A.; Voituriez, A. *Enantioselective Phosphine Organocatalysis*; Synlett, 2010; Vol. 2010; pp 174–194.

27. Haynes, W. M. *Handbook of Chemistry and Physics*, 96th ed., Haynes, W. M.; Bruno, T. J.; Lide, D. R., Eds.; CRC Press: Boca Raton, FL, 2015.
28. U.S. Geological Survey Publications;  
<https://pubs.usgs.gov/periodicals/mcs2021/mcs2021-manganese.pdf> Last accessed: 17/11/2021.
29. Cannon, W. F. In Fact Sheet; U.S. Geological Survey: Reston, VA, 2014, p. 2;  
<http://pubs.er.usgs.gov/publication/fs20143087> DOI: 10.3133/fs20143087.
30. a) Novák, P.; Benediktova, D.; Mestek, S.; Tsepeleva, A.; Kopeček, J. Aluminum alloys with natural ratio of alloying elements manufactured by powder metallurgy. *J. Alloys Compd.*, **2023**, *931*, 167440. b) Yang, X.; Wang, C. Manganese-catalyzed hydrosilylation reactions. *Chem. - Asian J.* **2018**, *13*, 2307-2315.
31. Palucki, M.; Finney, N. S.; Pospisil, P. J.; Güler, M. L.; Ishida, T.; Jacobsen, E. N. The Mechanistic Basis for Electronic Effects on Enantioselectivity in the (Salen)Mn(III)-Catalyzed Epoxidation Reaction. *J. Am. Chem. Soc.* **1998**, *120*, 948–954.
32. a) Saisaha, P.; de Boer, J. W.; Browne, W. R. Mechanisms in Manganese Catalysed Oxidation of Alkenes with H<sub>2</sub>O<sub>2</sub>. *Chem. Soc. Rev.* **2013**, *42*, 2059–2074. b) Miao, L.; Wang, J.; Zhang, P. Review on manganese dioxide for catalytic oxidation of airborne formaldehyde. *Appl. Surf. Sci.* **2019**, *466*, 441–453. c) Kanady, J. S.; Tsui, E. Y.; Day, M. W.; Agapie, T. A synthetic model of the Mn<sub>3</sub>Ca subsite of the oxygen-evolving complex in photosystem II. *Science* **2011**, *333*, 733–736.
33. a) Snider, B. B. Manganese(III)-Based Oxidative Free-Radical Cyclizations. *Chem. Rev.* **1996**, *96*, 339–364. b) Davies, D. T.; Kapur, N.; Parsons, A. F. Preparation of N-heterocycles by radical cyclisation of enamides mediated by manganese (III) or copper (I). A comparison of cyclisation methods. *Tetrahedron* **2000**, *56*, 3941-3949.

34. a) Liu, W. P.; Ackermann, L. Manganese-Catalyzed C–H Activation. *ACS Catal.* **2016**, *6*, 3743–3752. b) Cano, R.; Mackey, K.; McGlacken, G. P. Recent Advances in Manganese-Catalysed C–H Activation: Scope and Mechanism. *Catal. Sci. Technol.* **2018**, *8*, 1251–1266. c) Hu, Y.; Zhou, B.; Wang, C. Inert C–H Bond Transformations Enabled by Organometallic Manganese Catalysis. *Acc. Chem. Res.* **2018**, *51*, 816–827.
35. a) Kallmeier, F.; Kempe, R. Manganese Complexes for (De)Hydrogenation Catalysis: A Comparison to Cobalt and Iron Catalysts. *Angew. Chem., Int. Ed.* **2018**, *57*, 46–60. b) Mukherjee, A.; Nerush, A.; Leitus, G.; Shimon, L. J. W.; Ben David, Y.; Espinosa Jalapa, N. A.; Milstein, D. Manganese-Catalyzed Environmentally Benign Dehydrogenative Coupling of Alcohols and Amines to Form Aldimines and H<sub>2</sub>: A Catalytic and Mechanistic Study. *J. Am. Chem. Soc.* **2016**, *138*, 4298–4301. c) Elangovan, S.; Topf, C.; Fischer, S.; Jiao, H.; Spannenberg, A.; Baumann, W.; Ludwig, R.; Junge, K.; Beller, M. Selective Catalytic Hydrogenations of Nitriles, Ketones, and Aldehydes by Well-Defined Manganese Pincer Complexes. *J. Am. Chem. Soc.* **2016**, *138*, 8809–8814. d) Elangovan, S.; Neumann, J.; Sortais, J. B.; Junge, K.; Darcel, C.; Beller, M. Efficient and selective N-alkylation of Amines with Alcohols Catalysed by Manganese Pincer Complexes. *Nat. Commun.* **2016**, *7*, 12641–12648. e) Kallmeier, F.; Irrgang, T.; Dietel, T.; Kempe, R. Highly Active and Selective Manganese C=O Bond Hydrogenation Catalysts: The Importance of the Multidentate Ligand, the Ancillary Ligands, and the Oxidation State. *Angew. Chem., Int. Ed.* **2016**, *55*, 11806–11809. f) Elangovan, S.; Garbe, M.; Jiao, H.; Spannenberg, A.; Junge, K.; Beller, M. Hydrogenation of Esters to Alcohols Catalyzed by Defined Manganese Pincer Complexes. *Angew. Chem., Int. Ed.* **2016**, *55*, 15364–15368. g) Mastalir, M.; Glatz, M.; Pittenauer, E.; Allmaier, G.; Kirchner, K. Sustainable Synthesis of Quinolines and Pyrimidines Catalyzed by Manganese PNP Pincer Complexes. *J. Am. Chem. Soc.* **2016**,

- 138, 15543–15546. h) Chakraborty, S.; Gellrich, U.; Diskin-Posner, Y.; Leitus, G.; Avram, L.; Milstein, D. Manganese-Catalyzed N-Formylation of Amines by Methanol Liberating H<sub>2</sub>: A Catalytic and Mechanistic Study. *Angew. Chem., Int. Ed.* **2017**, *56*, 4229–4233. i) Widegren, M. B.; Harkness, G. J.; Slawin, A. M. Z.; Cordes, D. B.; Clarke, M. L. A Highly Active Manganese Catalyst for Enantioselective Ketone and Ester Hydrogenation. *Angew. Chem., Int. Ed.* **2017**, *56*, 5825–5828. j) Kumar, A.; Espinosa-Jalapa, N. A.; Leitus, G.; Diskin-Posner, Y.; Avram, L.; Milstein, D. Direct Synthesis of Amides by Dehydrogenative Coupling of Amines with either Alcohols or Esters: Manganese Pincer Complex as Catalyst. *Angew. Chem., Int. Ed.* **2017**, *56*, 14992–14996. k) Fu, S.; Shao, Z.; Wang, Y.; Liu, Q. Manganese-Catalyzed Upgrading of Ethanol into 1-Butanol. *J. Am. Chem. Soc.* **2017**, *139*, 11941–11948.
36. a) Marciniak, B. G.; Gulinski, J.; Urbaniak, W.; Kornetka, Z. W. In *Comprehensive Handbook on Hydrosilylation*; Marciniak, B. G., Ed.; Pergamon: Oxford, U.K. 1992. b) Clarson, S. J. Hydrosilylation: A Comprehensive Review on Recent Advances. *Silicon* **2009**, *1*, 57–58.
37. Schuster, C. H.; Diao, T.; Pappas, I.; Chirik, P. J. BenchStable, Substrate-Activated Cobalt Carboxylate Pre-Catalysts for Alkene Hydrosilylation with Tertiary Silanes. *ACS Catal.* **2016**, *6*, 2632–2636.
38. Fontaine, F. G.; Courtemanche, M. A.; Légaré, M. A. Transition-Metal-Free Catalytic Reduction of Carbon Dioxide. *Chem. - Eur. J.* **2014**, *20*, 2990–2996.
39. Suzuki, A. Recent advances in the cross-coupling reactions of organoboron derivatives with organic electrophiles, 1995–1998. *J. Organomet. Chem.* **1999**, *576*, 147.
40. Foubelo, F.; Nájera, C.; Yus, M. The Hiyama Cross-Coupling Reaction: New Discoveries. *Chem. Rec.* **2016**, *16*, 2521–2533.

41. Schlichter, P.; Werlé, C. The Rise of Manganese-Catalyzed Reduction Reactions. *Synthesis* **2022**, *54*, 517-534.
42. Pratt, S. L.; Faltynek, R. A. Hydrosilylation Catalysis via Silylmanganese Carbonyl Complexes: Thermal vs. Photochemical Activation. *J. Organomet. Chem.* **1983**, *258*, C5–C8.
43. Hilal, H. S.; Abu-Eid, M.; Al-Subu, M.; Khalaf, S. Hydrosilylation Reactions Catalysed by Decacarbonyldimanganese(0). *J. Mol. Catal.* **1987**, *39*, 1–11.
44. DiBiase Cavanaugh, M.; Gregg, B. T.; Cutler, A. R. Manganese Carbonyl Complexes as Catalysts for the Hydrosilylation of Ketones: Comparison with  $\text{RhCl}(\text{PPh}_3)_3$ . *Organometallics* **1996**, *15*, 2764–2769.
45. Gladysz, J. A. New synthetic chemistry of transition metal trialkylsilane complexes. *Acc. Chem. Res.* **1984**, *17*, 326-332.
46. Mao, Z.; Gregg, B. T.; Cutler, A. R. Catalytic Hydrosilation of Organic Esters Using Manganese Carbonyl Acetyl Complexes,  $(\text{L})(\text{CO})_4\text{MnC}(\text{O})\text{CH}_3$  ( $\text{L} = \text{CO}, \text{PPh}_3$ ). *J. Am. Chem. Soc.* **1995**, *117*, 10139–10140.
47. Yates, R. L. Photoactivated homogeneous catalytic hydrosilylation of carbonyl compounds. *J. Catal.* **1982**, *78*, 111–115.
48. Gregg, B. T.; Hanna, P. K.; Crawford, E. J.; Cutler, A. R. Hydrosilation of manganese acyls  $(\text{CO})_5\text{MnCOR}$  ( $\text{R} = \text{CH}_3, \text{Ph}$ ). *J. Am. Chem. Soc.* **1991**, *113*, 384–385.
49. Zheng, J.; Elangovan, S.; Valyaev, D. A.; Brousses, R.; Cesar, V.; Sortais, J.-B.; Darcel, C.; Lugan, N.; Lavigne, G. Hydrosilylation of Aldehydes and Ketones Catalyzed by Half-Sandwich Manganese (I) N-Heterocyclic Carbene Complexes. *Adv. Synth. Catal.* **2014**, *356*, 1093 –1097.
50. a) Son, S. U.; Paik, S.-J.; Lee, I. S.; Lee, Y.-A.; Chung, Y. K.; Seok, W. K.; Lee, H. N. Chemistry of  $[(1H\text{-hydronaphthalene})\text{Mn}(\text{CO})_3]$ : The Role of Ring-Slippage in

- Substitution, Catalytic Hydrosilylation, and Molecular Crystal Structure of  $[(\eta^3\text{-C}_{10}\text{H}_9)\text{Mn}(\text{CO})_3\text{P}(\text{OMe})_3]$ . *Organometallics* **1999**, *18*, 4114–4118. b) Son, S. U.; Paik, S.-J.; Chung, Y. K. Hydrosilylation of ketones catalyzed by tricarbonyl(naphthalene) manganese cation. *J. Mol. Catal. A: Chem.* **2000**, *151*, 87–90.
51. Chidara, V. K.; Du, G. An Efficient Catalyst Based on Manganese Salen for Hydrosilylation of Carbonyl Compounds. *Organometallics* **2013**, *32*, 5034–5037.
52. (a) Mukhopadhyay, T. K.; Flores, M.; Groy, T. L.; Trovitch, R. J. A Highly Active Manganese Precatalyst for the Hydrosilylation of Ketones and Esters. *J. Am. Chem. Soc.* **2014**, *136*, 882–885. (b) Mukhopadhyay, T. K.; Rock, C. L.; Hong, M.; Ashley, D. C.; Groy, T. L.; Baik, M.-H.; Trovitch, R. J. Mechanistic Investigation of Bis(imino)pyridine Manganese Catalyzed Carbonyl and Carboxylate Hydrosilylation. *J. Am. Chem. Soc.* **2017**, *139*, 4901–4915. (c) Mukhopadhyay, T. K.; Ghosh, C.; Flores, M.; Groy, T. L.; Trovitch, R. J. Hydrosilylation of Aldehydes and Formates Using a Dimeric Manganese Precatalyst. *Organometallics* **2017**, *36*, 3477–3483.
53. Valyaev, D. A.; Wei, D.; Elangovan, S.; Cavailles, M.; Dorcet, V.; Sortais, J.-B.; Darcel, C.; Lugan, N. Half-Sandwich Manganese Complexes Bearing Cp Tethered N-Heterocyclic Carbene Ligands: Synthesis and Mechanistic Insights into the Catalytic Ketone Hydrosilylation. *Organometallics* **2016**, *35*, 4090–4098.
54. a) Ojima, I.; Nihonyanagi, M.; Kogure, T.; Kumagai, M.; Horiuchi, S.; Nakatsugawa, K.; Nagai, Y. Reduction of Carbonyl Compounds via Hydrosilylation: I. Hydrosilylation of carbonyl Compounds Catalyzed by Tris(triphenylphosphine)chlororhodium. *J. Organomet. Chem.* **1975**, *94*, 449-461. b) Riener, K.; Högerl, M. P.; Gigler, P.; Kühn, F. Rhodium-catalyzed hydrosilylation of ketones: Catalyst development and mechanistic insights. *ACS Catal.* **2012**, *2*, 613-621.

55. Pinto, M.; Friaes, S.; Franco, F.; Lloret-Fillol, J.; Royo, B. Manganese N-Heterocyclic Carbene Complexes for Catalytic Reduction of Ketones with Silanes. *ChemCatChem* **2018**, *10*, 2734–2740.
56. Ma, X.; Zuo, Z.; Liu, G.; Huang, Z. Manganese-Catalyzed Asymmetric Hydrosilylation of Aryl Ketones. *ACS Omega* **2017**, *2*, 4688–4692.
57. Kelly, C. M.; McDonald, R.; Sydora, O. L.; Stradiotto, M.; Turculet, L. A manganese pre-catalyst: mild reduction of amides, ketones, aldehydes, and esters. *Angew. Chem., Int. Ed.* **2017**, *56*, 15901–15904.
58. Martínez-Ferraté, O.; Chatterjee, B.; Werlé, C.; Leitner, W. Hydrosilylation of carbonyl and carboxyl groups catalysed by Mn(I) complexes bearing triazole ligands. *Catal. Sci. Technol.* **2019**, *9*, 6370–6378.
59. Yempally, V.; Shahbaz, A.; Fan, W. Y.; Madrahimov, S. T.; Bengali, A. A. Hydrosilylation of Aldehydes by a Manganese  $\alpha$ -Diimine Complex. *Inorganics* **2020**, *8*, 61.
60. Saito, K.; Ito, T.; Arata, S.; Sunada, Y. Four-Coordinated Manganese(II) Disilyl Complexes for the Hydrosilylation of Aldehydes and Ketones with 1,1,3,3-Tetramethyldisiloxane. *ChemCatChem* **2021**, *13*, 1152–1156.
61. Ganguli, K.; Mandal, A.; Sarkar, B.; Kundu, S. Benzimidazole fragment containing Mn-complex catalyzed hydrosilylation of ketones and nitriles. *Tetrahedron* **2020** *76*, 131439.
62. Zheng, J.; Chevance, S.; Darcel, C.; Sortais, J.-B. Selective reduction of carboxylic acids to aldehydes through manganese catalysed hydrosilylation. *Chem. Commun.* **2013**, *49*, 10010-10012.
63. Antico, E.; Schlichter, P.; Werle, C.; Leitner, W. Reduction of Carboxylic Acids to Alcohols via Manganese(I) Catalyzed Hydrosilylation. *JACS Au* **2021**, *1*, 742–749.

64. Mao, Z.; Gregg, B. T.; Cutler, A. R. Catalytic Hydrosilylation of Organic Esters Using Manganese Carbonyl Acetyl Complexes,  $(L)(CO)_4MnC(O)CH_3$  ( $L = CO, PPh_3$ ). *J. Am. Chem. Soc.* **1995**, *117*, 10139–10140.
65. Behera, R. R.; Ghosh, R.; Panda, S.; Khamari, S.; Bagh, B. Hydrosilylation of Esters Catalyzed by Bisphosphine Manganese(I) Complex: Selective Transformation of Esters to Alcohols. *Org. Lett.* **2020**, *22*, 3642–3648.
66. Sousa, S. C. A.; Realista, S.; Royo, B. Bench-Stable Manganese NHC Complexes for the Selective Reduction of Esters to Alcohols with Silanes. *Adv. Synth. Catal.* **2020**, *362*, 2437–2443.
67. Chakraborty, S.; Das, A.; Mandal, S. K. Redox-active ligand-based Mn(I)-catalyst for hydrosilylative ester reduction. *Chem. Commun.* **2021**, *57*, 12671–12674.
68. Wei, D.; Buhaibeh, R.; Canac, Y.; Sortais, J. B. Manganese and rheniumcatalyzed selective reduction of esters to aldehydes with hydrosilanes. *Chem. Commun.* **2020**, *56*, 11617–11620.
69. Igarashi, M.; Fuchikami, T. Transition-metal complex catalyzed reduction of amides with hydrosilanes: a facile transformation of amides to amines. *Tetrahedron Lett.* **2001**, *42*, 1945–1947.
70. Das, H. S.; Das, S.; Dey, K.; Singh, B.; K Haridasan, R. K.; Das, A.; Ahmed, J.; Mandal, S. K. Primary amides to amines or nitriles: a dual role by a single catalyst. *Chem. Commun.* **2019**, *55*, 11868–11871.
71. Bertini, F.; Glatz, M.; Stöger, B.; Peruzzini, M.; Veiros, L. F.; Kirchner, K.; Gonsalvi, L. Carbon Dioxide Reduction to Methanol Catalyzed by Mn(I) PNP Pincer Complexes under Mild Reaction Conditions. *ACS Catal.* **2019**, *9*, 632–639.
72. Hilal, H. S.; Abu-Eid, M.; Al-Subu, M.; Khalaf, S. Hydrosilylation Reactions Catalysed by Decacarbonyldimanganese(0). *J. Mol. Catal.* **1987**, *39*, 1–11.

73. Hilal, H. S.; Suleiman, M. A.; Jondi, W. J.; Khalaf, S.; Masoud, M. M. Poly(siloxane)-supported decacarbonyldimanganese(0) catalyst for terminal olefin hydrosilylation reactions: the effect of the support on the catalyst selectivity, activity and stability. *J. Mol. Catal. A: Chem.* **1999**, *144*, 47–59.
74. Magnus, P.; Waring, M. J.; Scott, D. A. Conjugate reduction of  $\alpha$ ,  $\beta$ -unsaturated ketones using an MnIII catalyst, phenylsilane and isopropyl alcohol. *Tetrahedron Lett.* **2000**, *41*, 9731.
75. Carney, J. R.; Dillon, B. R.; Campbell, L.; Thomas, S. P. Manganese-catalyzed hydrofunctionalization of alkenes. *Angew. Chem., Int. Ed.* **2018**, *57*, 10620.
76. Mukhopadhyay, T. K.; Flores, M.; Groy, T. L.; Trovitch, R. J. A  $\beta$ -diketiminato Manganese Catalyst for Alkene Hydrosilylation: Substrate Scope, Silicone Preparation, and Mechanistic Insight. *Chem. Sci.* **2018**, *9*, 7673–7680.
77. Yang, X.; Wang, C. Diverse Fates of  $\beta$ -Silyl Radical under Manganese Catalysis: Hydrosilylation and Dehydrogenative Silylation of Alkenes. *Chin. J. Chem.* **2018**, *36*, 1047–1051.
78. Dong, J.; Yuan, X.-A.; Yan, Z.; Mu, L.; Ma, J.; Zhu, C.; Xie, J. Manganese-catalyzed divergent silylation of alkenes. *Nat. Chem.* **2021**, *13*, 182–190.
79. Yang, X.; Wang, C. Dichotomy of manganese catalysis via organometallic or radical mechanism: stereodivergent hydrosilylation of alkynes. *Angew. Chem., Int. Ed.* **2018**, *57*, 923–940.
80. Liang, H.; Ji, Y. X.; Wang, R. H.; Zhang, Z. H.; Zhang, B. Visible-Light-Initiated Manganese-Catalyzed E-Selective Hydrosilylation and Hydrogermylation of Alkynes. *Org. Lett.* **2019**, *21*, 2750–2754.

---

# **Hydrosilylation of Esters Catalyzed by Bisphosphine Manganese(I) Complex: Selective Transformation of Esters to Alcohols**

---

**2.1 Abstract**

**2.2 Introduction**

**2.3 Result and Discussion**

**2.4 Conclusion**

**2.5 Experimental Section**

## 2.1 Abstract:

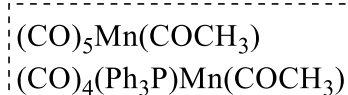
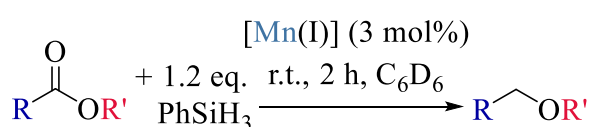
Selective and efficient hydrosilylations of esters to alcohols by a well-defined manganese(I) complex with commercially available bisphosphine ligand (xantphos) are described. These reactions are easy alternatives for stoichiometric hydride reduction or hydrogenation and employing cheap, abundant and nonprecious metal is attractive. The hydrosilylations were performed at 100 °C under solvent-free conditions with low (1 mol%) catalyst loading. A large variety of aromatic, aliphatic and cyclic esters bearing different functional groups were selectively converted into the corresponding alcohols in good to excellent isolated yields. This catalyst is also very efficient for the reduction of methyl laurate, methyl myristate and methyl caprate (major components of coconut and palm oil) to the corresponding fatty alcohols, which are important chemicals for consumer products. This catalyst is also capable of reducing polyester dynacoll-7360 to the starting diol and thus, this catalyst might be useful in recycling of polymer wastes.

## 2.2 Introduction:

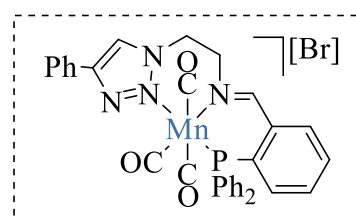
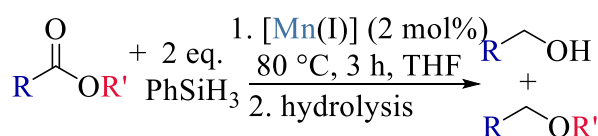
The reduction of carboxylic acids and esters to the corresponding alcohols is one of the most important transformations in synthetic chemistry. The conventional method of using stoichiometric amount of reactive hydride reagents such as  $\text{LiAlH}_4$ ,  $\text{LiBH}_4$ , DIBALH is efficient, but tricky reaction because of the pyrophoric nature of these reagents.<sup>1</sup> In addition, formation of stoichiometric amount of byproducts is detrimental. Therefore, catalytic hydrogenation is often desirable. However, hydrogenation of esters by molecular hydrogen suffers poor selectivity and drastic reaction conditions (high temperature and high hydrogen pressure).<sup>2</sup> To avoid the use of expensive high-pressure reactor for classical hydrogenation, transfer hydrogenation (TH) and hydrosilylation are gaining a lot of attention as easy alternatives. Though transition metal (TM) catalyzed transfer hydrogenations of aldehydes and ketones are abundant in literature,<sup>3</sup> the numbers of TM catalysts for transfer hydrogenation of esters are very rare. To the best of our knowledge, only three examples of TH of esters are

reported in the literature.<sup>4</sup> In 2015, two cationic half-sandwich ruthenium complexes  $[\text{Cp}(\text{P}i\text{Pr}_3)\text{Ru}(\text{CH}_3\text{CN})_2][\text{PF}_6]$  and  $[\text{Cp}^*(\text{phen})\text{Ru}(\text{CH}_3\text{CN})][\text{PF}_6]$  were reported as very efficient catalysts for the TH of esters with isopropanol as sacrificial hydrogen source.<sup>4a</sup> In the following year, Ru-SNS pincer complex was utilized for the reduction of ester using ethanol as an effective reductant.<sup>4b</sup> Very recently, Fe-PNP pincer complex was also effectively used.<sup>4c</sup> Besides TH, hydrosilylation of esters to the corresponding alcohols is an area of growing interest. In 1990s, titanocene dichloride and titanium alkoxides were reported as effective catalysts for the hydrosilylation of esters to alcohol.<sup>5</sup>  $\text{MoO}_2\text{Cl}_2$  was also utilized for the same purpose.<sup>6</sup> Besides early transition metals, noble metals such as rhodium, palladium, ruthenium were also reported for the reduction of esters. Wilkinson's catalyst  $[\text{RhCl}(\text{PPh}_3)_3]$  or  $[\text{RhCl}(\text{cod})]_2$  in presence of 4 eq. of  $\text{PPh}_3$  showed high activity for the hydrosilylation of esters to alcohols.<sup>7</sup> Partial reduction of 2-pyridinyl esters to the corresponding aldehydes was reported by palladium acetate in presence of excess  $\text{PPh}_3$ .<sup>8</sup> Hydrosilylation of esters by trinuclear ruthenium carbonyl clusters either selectively produced alkyl silyl acetal as partially reduced product [catalyst:  $\text{Ru}_3(\text{CO})_8$ ]<sup>9</sup> or gave a mixture of alcohol, aldehyde and ether [catalyst:  $\text{Ru}_3(\text{CO})_7(\text{acenaphthylene})$ ].<sup>10</sup>

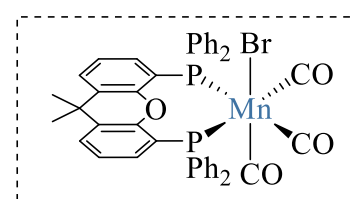
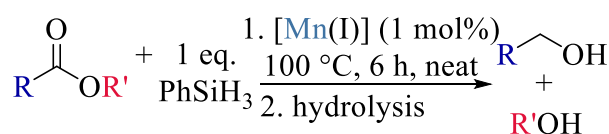
a) Previous work: catalyst by Cutler *et al.*



Previous work: catalyst by Werlé and Leitner *et al.*



b) **Present work:** selective reduction to alcohols



2.1

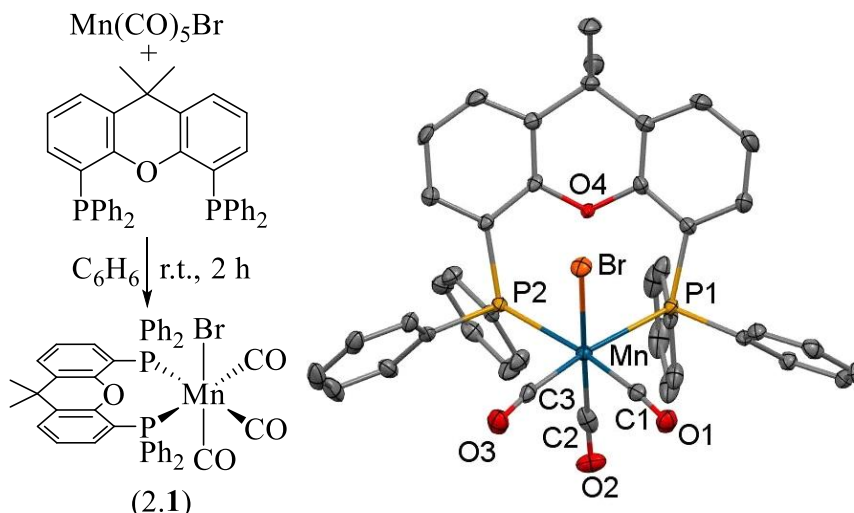
### Scheme 2.1 Hydrosilylation of esters by Mn(I) catalysts.

Although the utilization of earth-abundant, nonprecious TMs (iron, cobalt, nickel, copper or manganese) as catalysts is sustainable and thus desirable,<sup>11</sup> the reports on the catalytic hydrosilylation of esters by these metals are extremely limited. A cationic iron complex  $[\text{CpFe}(\text{CO})_2(\text{PCy}_3)][\text{BF}_4]$  showed good activity under visible light activation.<sup>12</sup> While the use of manganese catalysts for the hydrosilylation of carbonyls is well established,<sup>13</sup> there are only few reports on the hydrosilylation of carboxyl substrates. Reduction of carboxylic acids by  $\text{Mn}_2(\text{CO})_{10}$  yielded aldehydes rather than alcohols.<sup>14</sup> However, Mn(II) complexes with pentadentate redox-active bis(imino)pyridine based ligand<sup>15</sup> and N-phosphinoamidinate (potentially redox-active) ligand<sup>16</sup> were utilized as highly active catalysts for the reduction of ester to alcohol. To the best of our knowledge, there are only two reports on the hydrosilylation of esters catalyzed by Mn(I) complexes. In mid 1990s, hydrosilylation of esters to ethers were reported by using Mn(I) acetyl complexes,  $(\text{L})(\text{CO})_4\text{Mn}(\text{COCH}_3)$  ( $\text{L} = \text{CO}, \text{PPh}_3$ ) (Scheme 1).<sup>17</sup> Very recently, Mn(I) complexes with triazole based ligands were utilized for the hydrosilylation of esters yielding a mixture of alcohols and ethers (Scheme 1).<sup>18</sup> In last 8–10 years, Mn(I) complexes are gaining immense interest for their catalytic applications in varieties of chemical transformation.<sup>19, 20</sup> Herein, we address the use of a readily available Mn(I) complex with commercially available bisphosphine ligand as an effective catalyst for the hydrosilylation of a large variety of esters selectively to the corresponding alcohols under solvent-free conditions (Scheme 1). Several esters with commercial implication were also reduced to the corresponding alcohols in good to excellent isolated yields.

### 2.3 Result and Discussion

We selected Xantphos for the synthesis of the corresponding Mn(I) complex as it is readily available and it is one of the most used ligands for the development of a large variety of metal catalysts.<sup>21</sup> The neutral Mn(I) complex *fac*- $[\text{Mn}(\text{xantphos})(\text{CO})_3\text{Br}]$  (**2.1**) was synthesized in high isolated yield (95%) by reacting the commercially available precursor  $\text{Mn}(\text{CO})_5\text{Br}$  with

xantphos at r.t. (Scheme 2). The resulting yellow-orange complex **2.1** is diamagnetic and was characterized by  $^1\text{H}$ ,  $^{13}\text{C}$  and  $^{31}\text{P}$  NMR spectroscopy. The NMR spectra of complex **2.1** are consistent with overall  $C_s$  symmetry. The bisphosphine ligand framework was clearly seen in the  $^1\text{H}$  and  $^{13}\text{C}$  NMR spectra of complex **2.1**. A broad resonance at 26.14 ppm appears in the  $^{31}\text{P}$  NMR spectrum, which is down field shifted as compared to the free xantphos ligand (-17.97 ppm). Complex **2.1** was also characterized by IR spectroscopy. Three strong CO stretching vibrations at 2023, 1950 and 1909  $\text{cm}^{-1}$  were observed in the IR spectrum, which is consistent with the previously reported *fac*-isomer of similar bisphosphine-Mn(I) complexes.<sup>22</sup> Mass analysis of complex **2.1** shows the peak at 716.1161 corresponds to  $[\text{M}^+ - \text{Br}]$ . Complex **2.1** was further characterized by single-crystal X-ray analysis. The molecular structure with selected bond lengths and bond angles are depicted in Scheme 2. The geometry around manganese in complex **2.1** is distorted octahedral with two phosphorus atoms of bisphosphine moiety and two carbon atoms of two coordinated CO defining the equatorial plane and the bromine and a CO ligand occupying the axial position. The Mn-Br (2.4976(5) Å) and Mn-C(CO) (1.803(3), 1.821(4), 1.824(3) Å) bond distances in complex **2.1** are consistent with similar complexes (*fac*-[Mn(*i*Pr<sub>2</sub>P(CH<sub>2</sub>)<sub>2</sub>PiPr<sub>2</sub>)(CO)<sub>3</sub>Br]: 2.5378(12) and 1.878(10), 1.842(8), 1.844(8) Å;<sup>22b</sup> *fac*-[Mn(*n*Pr<sub>2</sub>P(CH<sub>2</sub>)<sub>2</sub>PnPr<sub>2</sub>)(CO)<sub>3</sub>Br]: 2.5593(6) and 1.776(4), 1.824(4), 1.829(8) Å<sup>22a</sup>). However, the Mn-P bond distances (2.4483(9), 2.4636(9) Å) in complex **2.1** are slightly longer as compared to the similar complexes (*fac*-[Mn(*i*Pr<sub>2</sub>P(CH<sub>2</sub>)<sub>2</sub>PiPr<sub>2</sub>)(CO)<sub>3</sub>Br]: 2.349(2), 2.365(2) Å;<sup>22b</sup> *fac*-[Mn(*n*Pr<sub>2</sub>P(CH<sub>2</sub>)<sub>2</sub>PnPr<sub>2</sub>)(CO)<sub>3</sub>Br]: 2.313(1), 2.314(1) Å<sup>22a</sup>). This is attributed to the much larger bite angle (100.48(3)°) of xantphos ligand compared to 1,2-bis(diisopropylphosphino)ethane in *fac*-[Mn(*i*Pr<sub>2</sub>P(CH<sub>2</sub>)<sub>2</sub>PiPr<sub>2</sub>)(CO)<sub>3</sub>Br] (83.85(7)°)<sup>22b</sup> and 1,2-bis(diisopropylphosphino)ethane in *fac*-[Mn(*n*Pr<sub>2</sub>P(CH<sub>2</sub>)<sub>2</sub>PnPr<sub>2</sub>)(CO)<sub>3</sub>Br] (83.60°).<sup>22a</sup>



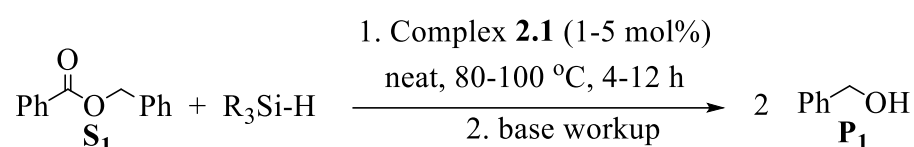
**Scheme 2.2 Synthesis of fac-[Mn(xantphos)(CO)<sub>3</sub>Br] (2.1) with the molecular structure of 2.1 showing 50% ellipsoid (hydrogen atoms are omitted for clarity)**

“Selected bond distances (Å) and angles (deg): Mn–Br 2.4976(5), Mn–P(1) 2.4483(9), Mn–P(2) 2.4636(9), Mn–C(1) 1.803(3), Mn–C(2) 1.821(4), Mn–C(3) 1.824(3), C(1)–O(1) 1.152(4), C(2)–O(2) 1.085(4), C(3)–O(3) 1.150(4), P(1)–Mn–P(2) 100.48(3), C(1)–Mn–C(3) 82.78(14), C(1)–Mn–P(1) 88.33(10), C(3)–Mn–P(2) 88.40(10), C(2)–Mn–Br 174.83(10), P(1)–Mn–Br 90.58(2), P(1)–Mn–C(2) 91.78(10), C(1)–Mn–Br 89.74(10), C(1)–Mn–C(2) 85.74(14).

We set out to examine the catalytic activity of complex **2.1** under various reaction conditions for the hydrosilylation of ester, using benzyl benzoate as standard substrate (Table 1). A blank test was performed (entry 1) and only starting ester was recovered. A complete conversion of benzyl benzoate (**S**<sub>1</sub>) to benzyl alcohol (**P**<sub>1</sub>) was observed when benzyl benzoate (0.5 mmol) was heated with 2 eq. of phenylsilane (1.0 mmol) at 100 °C for 6 h in presence of 5 mol% catalyst **2.1** (entry 2). Reducing the catalyst loading from 5 mol% to 2 mol% (entry 3) and 1 mol% (entry 4) led to the complete conversion of **S**<sub>1</sub> to **P**<sub>1</sub> in just 6 h at 100 °C with more than 90% isolated yield. Decreasing the reaction time to 4 h gave **P**<sub>1</sub> in 95% NMR yield (entry 6). We also tested various secondary and tertiary silanes such as diphenylsilane (entry 7), triphenylsilane (entry 8) and triethylsilane (entry 9) and we obtained **P**<sub>1</sub> in approximately 40–50% yield in 4 h. However, all of those tested silanes gave complete conversion of **S**<sub>1</sub> to **P**<sub>1</sub>, if

the hydrosilylations were carried out for 12 h. Therefore, phenylsilane proved to be the best one under the reaction conditions. Thereafter, the hydrosilylation of **S**<sub>1</sub> was tested at lower temperature. Lowering the temperature to 80 (entry 10) and 90 °C (entry 12), poorer yield (approximately 40-50%) of **P**<sub>1</sub> was obtained in 4 h. However, almost complete conversion of **S**<sub>1</sub> to **P**<sub>1</sub> was observed at 80 and 90 °C with prolonged heating for 12 h (entry 11 and 13). Thereafter, we varied the amount of silane used for the hydrosilylation of benzyl benzoate. Lowering the amount of phenylsilane from two to one equivalent, **P**<sub>1</sub> was obtained in 93% yield in 4 h (entry 16). The use of 1 eq. phenylsilane led to a complete conversion of **S**<sub>1</sub> to **P**<sub>1</sub> (92% isolated yield) in just 5 h at 100 °C with 1 mol% catalyst loading (entry 15).

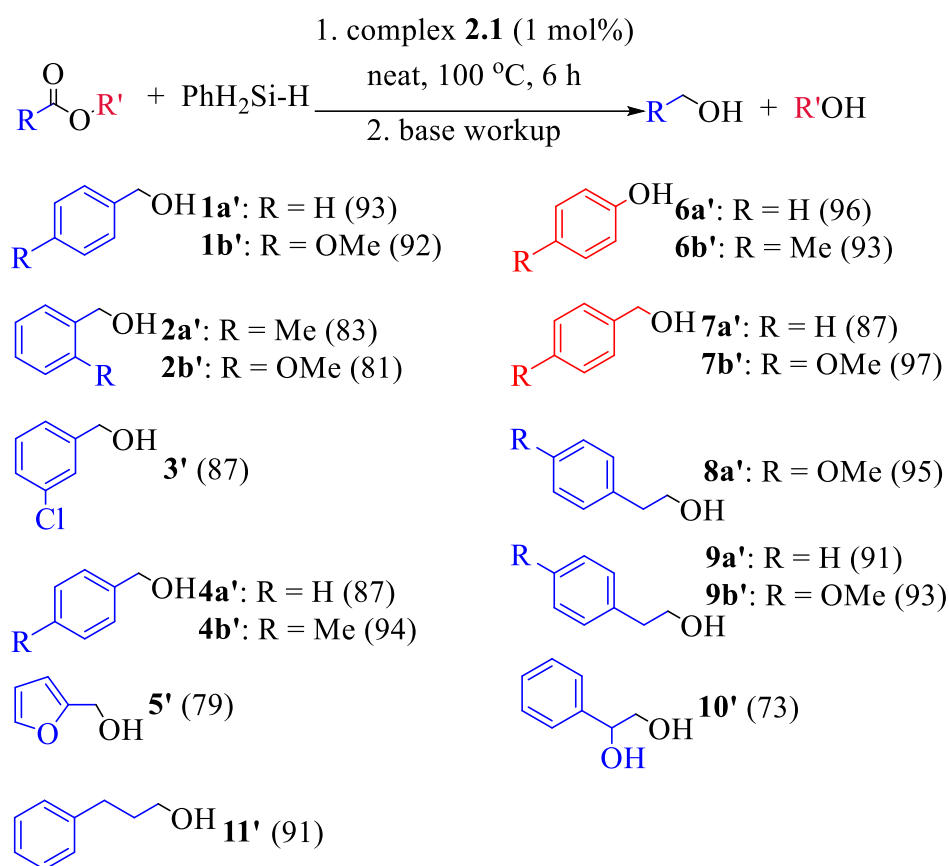
**Table 2.1. Performance of complex 2.1 for the hydrosilylation of benzyl benzoate under different reaction conditions<sup>a</sup>**



En.	<b>1</b> (Mol%)	<b>Silane</b> (Eq.)	<b>Temp.</b> (°C)	<b>Time</b> (H)	<b>Yield<sup>b</sup></b> (%)
<b>1</b>	no	PhSiH <sub>3</sub> (2)	100	6	0
<b>2</b>	<b>5</b>	PhSiH <sub>3</sub> (2)	100	6	>99
<b>3</b>	<b>2</b>	PhSiH <sub>3</sub> (2)	100	6	>99 (92) <sup>c</sup>
<b>4</b>	<b>1</b>	PhSiH <sub>3</sub> (2)	100	6	>99 (91) <sup>c</sup>
<b>5</b>	1	PhSiH <sub>3</sub> (2)	100	<b>5</b>	>99 (91) <sup>c</sup>
<b>6</b>	1	PhSiH <sub>3</sub> (2)	100	<b>4</b>	95
<b>7</b>	1	<b>Ph<sub>2</sub>SiH<sub>2</sub></b> (2)	100	4	51 (>99) <sup>d</sup>
<b>8</b>	1	<b>Ph<sub>3</sub>SiH</b> (2)	100	4	45 (>99) <sup>d</sup>
<b>9</b>	1	<b>Et<sub>3</sub>SiH</b> (2)	100	4	46 (>99) <sup>d</sup>
<b>10</b>	1	PhSiH <sub>3</sub> (2)	<b>80</b>	4	46
<b>11</b>	1	PhSiH <sub>3</sub> (2)	<b>80</b>	12	>99
<b>12</b>	1	PhSiH <sub>3</sub> (2)	<b>90</b>	4	53

<b>13</b>	1	PhSiH <sub>3</sub> (2)	<b>90</b>	4	>99
<b>14</b>	1	PhSiH <sub>2</sub> ( <b>1</b> )	100	6	>99
<b>15</b>	1	PhSiH <sub>2</sub> ( <b>1</b> )	100	5	>99 (92) <sup>c</sup>
<b>16</b>	1	PhSiH <sub>3</sub> ( <b>1</b> )	100	4	93

<sup>a</sup>Reactions conducted in pressure tube (10 mL) with 0.5 mmol **S1**, 0.5/ 1.0 mmol of silane and 1/ 2/ 5 mol% of complex **2.1**. <sup>b</sup>Yields of **P1** were determined by <sup>1</sup>H NMR spectroscopy using ferrocene (0.1 mmol) as external standard. <sup>c</sup>Isolated yields of **P1**. <sup>d</sup>NMR yields of **P1** for 12 h reaction. Then base workup was done using MeOH (15 mL) and 10 % aq. NaOH solution. Key parameters for each entry are indicated in bold.



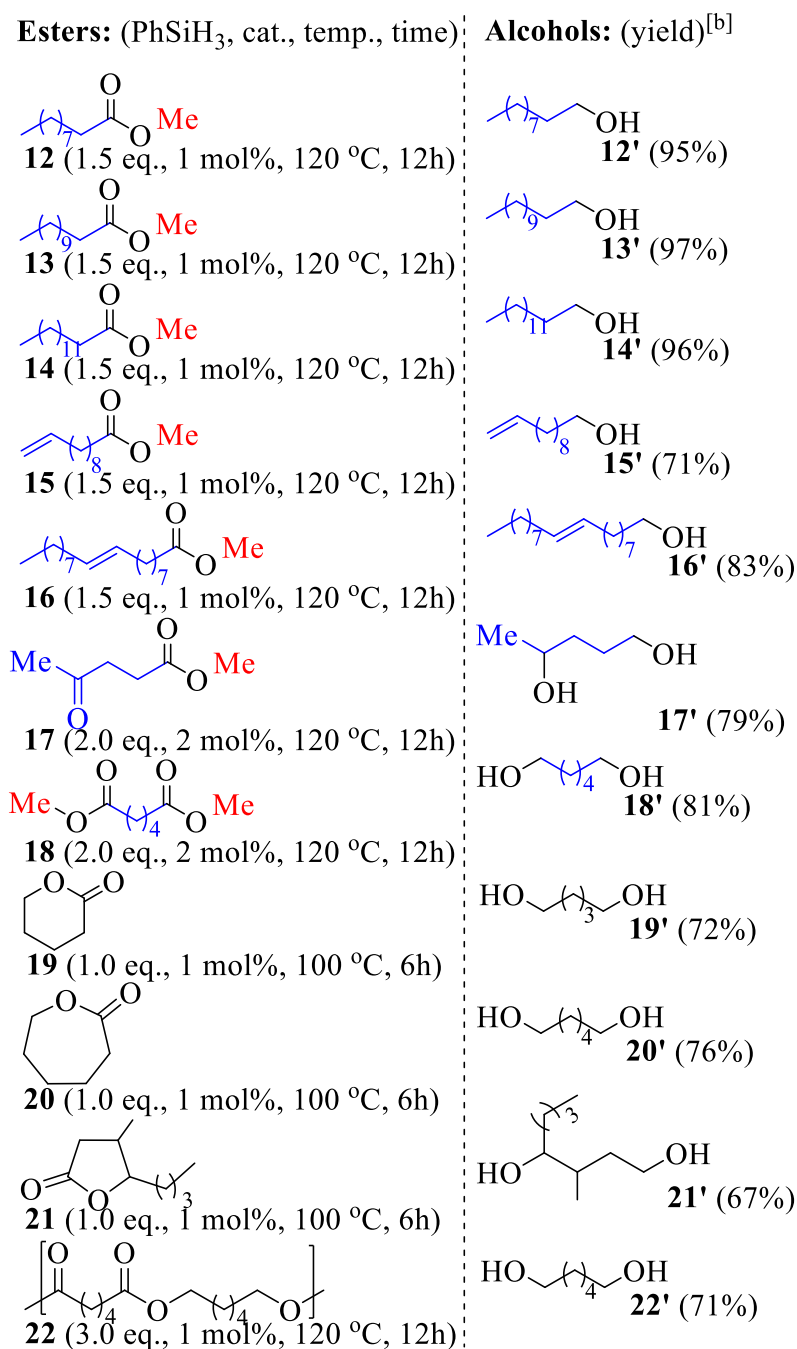
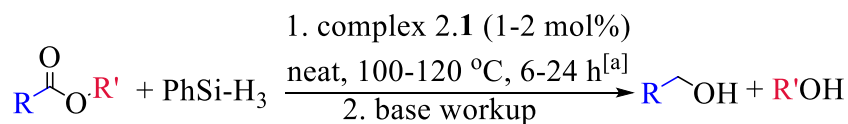
### Scheme 2.3 Hydrosilylation of various esters to alcohols catalyzed by complex **2.1**<sup>a</sup>

<sup>a</sup>Reactions conducted in pressure tube (10 mL) with 1.0 mmol of ester, 1.0 mmol of PhSiH<sub>3</sub> and 1 mol% of complex **2.1**. Isolated yields of alcohols in parentheses.

Thereafter, we explored various additional esters for the hydrosilylation of esters to alcohols based on the optimized reaction conditions (1 mol% catalyst loading, neat, 100 °C, 6 h) to expand the substrate scope (Scheme 2.3). First, we tested various aromatic esters. Methyl benzoate and substituted methyl benzoate (**1a**, **1b**, **2a**, **2b**, **3**) were reduced to benzyl alcohol and substituted benzyl alcohol in high isolated yields (**1a'**: 93%, **1b'**: 92%, **2a'**: 83%, **2b'**: 81%, **3'**: 87%). Very similarly, ethyl benzoate (**4a**) and substituted ethyl benzoate (**4b**) produced the corresponding alcohol (**4a'**: 87%, **4b'**: 94%) in excellent yields. Another aromatic ester, methyl 2-furoate (**5**) was also easily reduced to furfuryl alcohol (**5'**: 79%). This catalytic system is also very effective for the reduction of phenyl acetate or substituted phenyl acetate (**6a**, **6b**) to phenol or substituted phenols (**6a'**: 96%, **6b'**: 93%). Therefore, the catalytic system is compatible with both electron donating and electron withdrawing functionalities. Thereafter, more challenging aliphatic esters were tested. We were pleased to see that both benzyl acetate (**7a**) and 4-methoxy benzyl acetate (**7b**) were reduced to benzyl alcohol (**7a'**: 87%) and 4-methoxy benzyl alcohol (**7b'**: 97%) in excellent yields. This catalytic system is equally effective for methyl- and ethyl phenyl acetates (**8a**, **9a**, **9b**) to give corresponding 2-phenylethanols (**8a'**: 95%, **9a'**: 91%, **9b'**: 93%). Similarly, methyl 2-hydroxy-2-phenylacetate (**10**) gave 1-Phenyl-1,2-ethanediol (**10'**: 73%) in good yields. High yield was also obtained for the reduction of ethyl 3-phenylpropionate (**11**) to 3-phenyl-1-propanol (**11'**: 91%). To test the robustness of the present catalytic system, the hydrosilylation of methyl 4-methoxybenzoate (**1b**) and 4-methoxybenzyl acetate (**7b**) were scaled up 10 times and we obtained almost quantitative yields of 4-methoxybenzyl alcohol (96-97%) in both cases.

Reduction of esters for the production of alcohols is an extremely important process for the chemical industry. For example, long-chain fatty alcohols are widely utilized in consumer products such as lubricants, surfactants, plasticizers, flavorings and solvents for paints and the global demand are drastically increasing. Presently, a major portion of fatty alcohols are produced through hydrogenation of fatty esters derived from coconut and palm oil. For

example, CE-1270, an industrial sample obtained from coconut oil, contains mostly methyl laurate (~71-75%) and methyl myristate (~24-29%) with a small portion of methyl caprate (~1%). We set out to reduce those fatty esters by using complex **1** (Scheme 2.4). We were pleased to see that hydrosilylation of methyl caprate (**12**), methyl laurate (**13**) and methyl myristate (**14**) by complex **1** gave the corresponding fatty alcohols in almost quantitative yields (**12'**: 95%, **13'**: 97%, **14'**: 96%). Under identical reaction conditions, methyl 10-undecenoate (**15**) underwent reduction of only the ester moiety whereas the terminal alkene moiety remained intact (Scheme 2.4). The reduced product 10-undecen-1-ol (**15'**) was isolated in decent yield (71%). A gram-scale hydrosilylation of methyl laurate, **13** (10.0 mmol, 2.14 g) was also successfully accomplished (with almost quantitative yield) to test the robustness of the present catalytic system. Thereafter, we focused our attention to methyl oleate (**16**), methyl levulinate (**17**) and dimethyl adipate (**18**) for their relevance in biomass conversion and renewable chemistry (Scheme 2.4).<sup>23</sup> Similar to methyl 10-undecenoate (**15**), only the ester moiety of methyl oleate (**16**) was reduced while the alkene part was unaltered. The long chain fatty alcohol **16'** was isolated in good yield (83%). Thereafter, methyl levulinate (**17**) was subjected to hydrosilylation. It was not surprising to see that both keto and ester functionalities were reduced and the corresponding diol **17'** was obtained in good yield (79%). Similarly, dimethyl adipate (**18**) was cleanly reduced to the 1,6-hexanediol (**18'**: 81%). We also applied this hydrosilylation method for the reduction of lactones which can be derived from various natural sources (Scheme 2.4). The 6 and 7 membered lactones,  $\delta$ -valerolactone (**19**) and  $\epsilon$ -caprolactone (**20**) were reduced to the corresponding diols in good yields (**19'**: 72%, **20'**: 76%). Using the same protocol, Whiskey lactone (**21**) was also effectively reduced to the desired diol **21'** (77%).



**Scheme 2.4 Catalytic hydrosilylation of esters with practical implications.**

<sup>a</sup>Reactions conducted in pressure tube (10 mL) with 1.0 mmol of ester, 1.0-3.0 mmol of PhSiH<sub>3</sub> and 1-2 mol% of complex **2.1**. <sup>b</sup>Isolated yields of alcohols.

A major concern in our modern world is the polymer wastes and recycling of polymer wastes by converting them to their monomers is a huge challenge in the field of green chemistry. As the present catalytic system is very effective for the reduction of various esters, we targeted polyester as a potential substrate relevant to polymer recycling. The numbers of homogeneous catalysts for this purpose is very scarce.<sup>4c,24</sup> We choose an industrial sample dynacoll-7360 or poly(1,6-hexamethylene adipate) (**22**) which is produced by condensation polymerization of 1,6-hexanediol and adipic acid (Scheme 2.4). We were pleased to see that 1,6-hexanediol was obtained as recycled product in good yield (71%) if dynacoll-7360 was submitted to the present catalytic protocol.

## 2.5 Conclusion

In conclusion, we have developed a readily accessible base-metal catalyst which is very efficient for the hydrosilylation of esters selectively to alcohols under solvent-free conditions. Based on the well-established mechanism,<sup>5, 17, 18</sup> we propose a plausible pathway which involves the formation of alkyl/aryl silyl acetal intermediate. The substrate scope includes various aromatic and aliphatic esters and lactones. Industrially valuable fatty alcohols were also obtained under much milder reaction conditions from fatty esters which are the major components of coconut and palm oil. Typically, the hydrogenation of fatty esters is performed by using heterogeneous catalyst under harsh reaction conditions (250-300 °C and 2000-3000 psig of H<sub>2</sub> pressure).<sup>25</sup> Furthermore, the catalytic system is also applicable for important substrates relevant to renewable chemistry. Relevance in the present context, this base-metal catalyst might be a potential candidate for the hydrosilylation of polyesters which might be valuable for the recycling of plastic waste. Further investigations will involve the utilization of this catalytic system for the hydrosilylation of various other substrates and in different hydrofunctionalizations reactions such as hydrogenation and hydroboration.

## 2.6 Experimental Section

### 2.6.1 Materials

All air and moisture sensitive experiments such as synthesis and purification of complex 1 and catalytic hydrosilylations of esters were performed under dry nitrogen atmosphere using standard Schlenk or glovebox (MBraun) techniques. Hydrosilylations of esters were performed in Ace pressure tubes purchased from Sigma-Aldrich. Hydrolysis of the contents of hydrosilylations, analysis and purification of the hydrolysed products were carried out in air. For the air sensitive experiments, solvents (benzene, hexanes, pentane and THF) were distilled, degassed and stored over 3 Å molecular sieves. Solvents (benzene, hexanes, pentane, ethyl acetate, DCM, MeOH and THF) were purchased from Merck and Spectrochem. For recording NMR spectra of air and moisture sensitive samples, CDCl<sub>3</sub> was degassed and stored over 3 Å molecular sieves. CDCl<sub>3</sub> was purchased from Sigma Aldrich. Xantphos, Mn(CO)<sub>5</sub>Br, PhSiH<sub>3</sub>, Ph<sub>2</sub>SiH<sub>2</sub>, Ph<sub>3</sub>SiH, Et<sub>3</sub>SiH, ferrocene and all esters as substrates for hydrosilylations were purchased from Sigma Aldrich, Alfa Aesar and TCI Chemicals and used without further purification.

### 2.6.2 Physical Measurements

<sup>1</sup>H, <sup>13</sup>C and <sup>31</sup>P NMR spectra were recorded at Bruker AV-400 and JEOL-400 (<sup>1</sup>H at 400 MHz, <sup>13</sup>C at 101 MHz and <sup>31</sup>P at 162 MHz). <sup>1</sup>H NMR chemical shifts are referenced in parts per million (ppm) with respect to tetramethylsilane (δ 0.00 ppm), <sup>13</sup>C{<sup>1</sup>H} NMR chemical shifts are referenced in ppm with respect to CDCl<sub>3</sub> (δ 77.16 ppm) and <sup>31</sup>P{<sup>1</sup>H} chemical shifts are referenced in ppm with respect to 85% H<sub>3</sub>PO<sub>4</sub> in water (δ 0.00 ppm). The coupling constants (J) are reported in hertz (Hz). The following abbreviations are used to describe multiplicity: s = singlet, bs = broad signal, d = doublet, t = triplet, q = quadrate, m = multiplate. High resolution mass spectra were recorded on a Bruker micrOTOF-Q II Spectrometer. Elemental analysis was carried out on a EuroEA Elemental Analyser. Infrared (IR) spectra were recorded on a Perkin-Elmer FT-IR spectrophotometer

### 2.6.3 Crystal Structure Determination

A crystal of complex 2.1 (CCDC 1982008) was mounted in air at ambient conditions. All measurements were made on an Oxford Diffraction SuperNova area-detector diffractometer[S6] using mirror optics monochromated Mo K $\alpha$  radiation ( $\lambda = 0.71073 \text{ \AA}$ ) and Al filtered.[S7] The unit cell constants and an orientation matrix for data collection were obtained from a leastsquares refinement of the setting angles of reflections in the range  $2.1 < \theta < 26.4^\circ$ . A total of 1090 frames were collected using  $\omega$  scans, with 30+30 seconds exposure time, a rotation angle of  $1.0^\circ$  per frame, a crystal-detector distance of 65.0 mm, at  $T = 123(2)$  K. Data reduction was performed using the CrysAlisPro[S6] program. The intensities were corrected for Lorentz and polarization effects, and an absorption correction based on the multiscan method using SCALE3 ABSPACK in CrysAlisPro[S6] was applied. Data collection and refinement parameters are given in Table 1. The structure was solved by direct methods using SHELXT[S8], which revealed the positions of all non-hydrogen atoms of the title compound. The non-hydrogen atoms were refined anisotropically. All H-atoms were placed in geometrically calculated positions and refined using a riding model where each H-atom was assigned a fixed isotropic displacement parameter with a value equal to  $1.2U_{eq}$  of its parent atom. Refinement of the structure was carried out on F [S7] using full-matrix least-squares procedures, which minimized the function  $\sum w(F_o^2 - F_c^2)^2$  [S7]. The weighting scheme was based on counting statistics and included a factor to downweight the intense reflections. All calculations were performed using the SHELXL-2014/7[S9] program.

#### 2.6.4 Syntheses

##### Synthesis of complex 2.1:

Benzene (10 mL) was added to a solid mixture of  $\text{Mn}(\text{CO})_5\text{Br}$  (0.139 g, 0.50 mmol) and xantphos (0.332 g, 0.55 mmol). The reaction mixture was stirred at r.t. for 2 h resulting in a yellow-orange precipitate and pale-yellow solution. The liquid was syringed off and the solid was washed with hexanes (3 x 10 mL). The resulting yellow-orange solid was dried under high

vacuum to give complex 1 (0.375 g, 95%) as pure compound. Note: Single crystals suitable for X-ray structural analysis were obtained by slow diffusion of pentane into a solution of complex 1 in THF. Complex 1 is a new compound and was characterized by  $^1\text{H}$ ,  $^{13}\text{C}$  and  $^{31}\text{P}$  NMR spectroscopies, high resolution mass spectrometry, elemental analysis and single crystal X-ray analysis. Complex 1 displayed broad resonances in the  $^1\text{H}$  NMR spectrum which is consistent with similar bisphosphine manganese(I) complexes. [S1], [S2]  $^1\text{H}$  NMR (400 MHz,  $\text{CDCl}_3$ ):  $\delta$  1.12-1.62 (bs, 3H, Me), 1.63-2.13 (bs, 3H, Me), 6.65-6.98 (bs, 2H, Ar-H), 7.01-7.46 (bs, 18H, Ar-H), 7.50-7.84 (bs, 6H, Ar-H).  $^{13}\text{C}\{^1\text{H}\}$  NMR (101 MHz,  $\text{CDCl}_3$ ):  $\delta$  35.6, 124.2, 127.5, 128.2, 128.4, 129.8, 130.0, 131.5, 132.2, 133.3, 133.7, 153.9.  $^{31}\text{P}\{^1\text{H}\}$  NMR (162 MHz,  $\text{CDCl}_3$ ):  $\delta$  26.14. IR (KBr, pellet,  $\text{cm}^{-1}$ ): 2023, 1950, 1909 ( $\nu_{\text{CO}}$ ). HRMS (ESI)  $m/z$  for  $\text{C}_{42}\text{H}_{32}\text{MnO}_4\text{P}_2$ : 717.1156, found 717.1161 [ $\text{M}^+ - \text{Br}$ ]. Anal. Calcd for  $\text{C}_{42}\text{H}_{32}\text{BrMnO}_4\text{P}_2$  (797.50): C, 63.26; H, 4.04; N, 0.00. Found: C, 63.49; H, 4.03; N, 0.00.

Alternative synthetic procedures:

a) Complex 4.1 was also synthesized in very similar yield by using toluene instead of benzene as solvent.

b) THF was also used as solvent for the synthesis of complex 1 by following procedure. THF (5 mL) was added to a solid mixture of  $\text{Mn}(\text{CO})_5\text{Br}$  (0.138 g, 0.50 mmol) and xantphos (0.333 g, 0.50 mmol). The reaction mixture was stirred at 80 °C in an oil bath for 2 mins resulting in a yellow-orange yellow solution. The resulting solution was left at r.t. for 24 h followed by storing at -30 °C for 48 h. This resulted orange crystals. The crystals were dried under high vacuum to give complex 1 (0.355 g, 90%) as pure compound.

**Crystal data of complexes (2.1):**  $\text{C}_{42}\text{H}_{32}\text{BrMnO}_4\text{P}_2$ , yellow solid, Crystal size: 0.172 x 0.103 x 0.03  $\text{mm}^3$ ,  $M = 797.46$ , Triclinic with space group  $P -1$ ,  $a = 10.5431(5)$  Å,  $b = 10.6472(4)$  Å,  $c = 17.9264(6)$ ,  $\alpha = 89.841(3)^\circ$ ,  $\beta = 88.264(3)^\circ$ ,  $\gamma = 61.458(4)^\circ$ ,  $V = 1766.79(14)$  Å<sup>3</sup>,  $Z = 2$ ,  $F(000) = 812.0$ ,  $\mu - (\text{MoK}\alpha) = 1.638 \text{ mm}^{-1}$ , Theta range for data collection 2.178 to 27.271°, Density (calculated) 1.499  $\text{Mg/m}^3$ ,  $T = 100(2)\text{K}$ , min/max transmission factors =

1/0.738, 54540 Reflections collected, 26899 unique ( $R1 = 0.0607$ ),  $WR2 = 0.0869$  (all data). The structure has been deposited at the CCDC data center and can be retrieved using the deposit number 1982008.

### **General procedure for the hydrosilylation of esters**

**General condition for reaction optimization:** Benzyl benzoate (106 mg, 0.5 mmol), silane (1.0/ 0.5 mmol) and complex 1 (5/ 2/ 1 mol%) was transferred into a pressure tube fitted with a magnetic stir-bar. The reaction mixture was heated at appropriate temperature (80/ 90/ 100 °C) in an oil bath for appropriate time (4/ 5/ 6/ 12 h). Thereafter, the reaction mixture was cooled down to r.t. and MeOH (3 mL) and 10 % aq. NaOH solution (2 mL) was added. The resulting mixture was stirred overnight for complete hydrolysis. Ferrocene (18.6 mg, 0.1 mmol) as NMR standard was added to the solution. Organic compounds were extracted from the mixture with  $\text{CH}_2\text{Cl}_2$  (3 x 12 mL). The organic fraction was dried over  $\text{Na}_2\text{SO}_4$  and all volatiles were removed using rotary evaporator. The crude product was analysed by  $^1\text{H}$  NMR. Occasionally the crude product was purified by column chromatography using silica as stationary phase and a mixture of hexanes and ethylacetate as eluent.

**General condition for substrate screening:** Ester (1.0 mmol),  $\text{PhSiH}_3$  (108 mg, 1.0 mmol or 161 mg, 1.5 mmol) and complex 1 (4 mg, 1 mol%) was transferred into a pressure tube fitted with a magnetic stir-bar. The reaction mixture was heated at 100 °C (or 120 °C) in an oil bath for 6 h (or 24 h). Thereafter, the reaction mixture was cooled down to r.t. and MeOH (3 mL) and 10 % aq. NaOH solution (2 mL) was added. The resulting mixture was stirred overnight for complete hydrolysis. Organic compounds were extracted from the mixture with  $\text{CH}_2\text{Cl}_2$  (3 x 12 mL). The organic fraction was dried over  $\text{Na}_2\text{SO}_4$  and all volatiles were removed using rotary evaporator. The crude product was purified by column chromatography using silica as stationary phase and a mixture of hexanes and ethylacetate or hexanes and diethyl ether or DCM and MeOH as eluent (Note: For the separation of phenol or substituted phenols, triethylamine was used during column chromatography). General condition for gram-scale

hydrosilylation of esters: Esters [4-methoxybenzoate (1.66 g, 10.0 mmol)/ 4-methoxybenzyl acetate (1.80 g, 10.0 mmol)/ methyl laurate (2.14 g, 10.0 mmol)], PhSiH<sub>3</sub> (1.08 g, 10.0 mmol or 1.61 g, 15.0 mmol) and complex 1 (80 mg, 1 mol%) was transferred into a pressure tube fitted with a magnetic stir-bar. The reaction mixture was heated at 100 or 120 °C for 6 or 12 h) in an oil bath. Thereafter, the reaction mixture was cooled down to r.t. and MeOH (15 mL) and 10 % aq. NaOH solution (15 mL) was added. The resulting mixture was stirred overnight for complete hydrolysis. Organic compounds were extracted from the mixture with CH<sub>2</sub>Cl<sub>2</sub> (3 x 50 mL). The organic fraction was dried over Na<sub>2</sub>SO<sub>4</sub> and all volatiles were removed using rotary evaporator. The crude product was purified by column chromatography using silica as stationary phase and a mixture of hexanes and ethylacetate or hexanes and diethyl ether or DCM and MeOH as eluent. The product alcohols [4- methoxybenzyl alcohol (1.33 g, 96%)/4-methoxybenzyl alcohol (1.34 g, 97%)/dodecanol (1.86 g, 99%)] were obtained in almost quantitative yields.

#### NMR data of alcohols

Following alcohols (obtained by hydrosilylations of esters followed by column chromatography) are known compounds and they are characterized by <sup>1</sup>H and <sup>13</sup>C NMR spectroscopies.

**Benzyl alcohol (1a'/4a'/7a')**: A mixture of hexanes and ethyl acetate (3:2) was used as eluent for column chromatography. Isolated as a colorless liquid (1a': 101 mg, 93%; 4a': 94 mg, 87%; 7a': 94 mg, 87%). <sup>1</sup>H NMR (400 MHz, CDCl<sub>3</sub>): δ 1.98 (bs, 1H, OH), 4.68 (s, 2H, CH<sub>2</sub>), 7.20-7.45 (m, 5H, Ar-H). <sup>13</sup>C{<sup>1</sup>H} NMR (101 MHz, CDCl<sub>3</sub>): δ 65.4 (CH<sub>2</sub>), 127.1, 127.8, 128.7, 141.0 (Ar-C).

**4-Methoxybenzyl alcohol (1b'/7b')**: A mixture of hexanes and ethyl acetate (3:2) was used as eluent for column chromatography. Isolated as a colorless liquid (1b': 127 mg, 92%; 7b': 134 mg, 97%). <sup>1</sup>H NMR (400 MHz, CDCl<sub>3</sub>): δ 1.98 (bs, 1H, OH), 3.82 (s, 3H, OCH<sub>3</sub>), 4.61 (s, 2H,

CH<sub>2</sub>), 6.91 (d, 2H, Ar-H), 7.30 (d, 2H, Ar-H). <sup>13</sup>C{<sup>1</sup>H} NMR (101 MHz, CDCl<sub>3</sub>): δ 55.4 (OCH<sub>3</sub>), 65.0 (CH<sub>2</sub>), 114.0, 128.7, 133.2, 159.3 (Ar-C).

**2-Methylbenzyl alcohol (2a')**: A mixture of hexanes and ethyl acetate (3:2) was used as eluent for column chromatography. Isolated as a colorless liquid (2a': 101 mg, 83%). <sup>1</sup>H NMR (400 MHz, CDCl<sub>3</sub>): δ 2.37 (s, 3H, CH<sub>3</sub>), 2.82 (bs, 1H, OH), 4.64 (s, 2H, CH<sub>2</sub>), 7.15-7.31 (m, 3H, Ar-H), 7.33-7.44 (m, 1H, Ar-H). <sup>13</sup>C{<sup>1</sup>H} NMR (101 MHz, CDCl<sub>3</sub>): δ 18.7 (CH<sub>3</sub>), 63.2 (CH<sub>2</sub>), 126.0, 127.5, 127.7, 130.3, 136.1, 138.8 (Ar-C).

**2-Methoxybenzyl alcohol (2b')**: A mixture of hexanes and ethyl acetate (3:2) was used as eluent for column chromatography. Isolated as a colorless liquid (2b': 112 mg, 81%). <sup>1</sup>H NMR (400 MHz, CDCl<sub>3</sub>): δ 2.61 (bs, 1H, OH), 3.88 (s, 3H, OCH<sub>3</sub>), 4.71 (s, 2H, CH<sub>2</sub>), 6.91 (d, 1H, Ar-H), 6.98 (t, 1H, Ar-H), 7.25-7.36 (m, 2H, Ar-H). <sup>13</sup>C{<sup>1</sup>H} NMR (101 MHz, CDCl<sub>3</sub>): δ 56.3 (OCH<sub>3</sub>), 62.0 (CH<sub>2</sub>), 110.2, 120.7, 128.7, 128.9, 129.1, 157.4 (Ar-C).

**3-Chlorobenzyl alcohol (3')**: A mixture of hexanes and ethyl acetate (3:2) was used as eluent for column chromatography. Isolated as a colorless liquid (3': 124 mg, 87%). <sup>1</sup>H NMR (400 MHz, CDCl<sub>3</sub>): δ 2.25 (bs, 1H, OH), 4.67 (s, 2H, CH<sub>2</sub>), 7.10-7.50 (m, 5H, Ar-H). <sup>13</sup>C{<sup>1</sup>H} NMR (101 MHz, CDCl<sub>3</sub>): δ 64.6 (CH<sub>2</sub>), 125.0, 127.1, 127.8, 129.9, 134.5, 142.9 (Ar-C).

**4-Methylbenzyl alcohol (4b')**: A mixture of hexanes and ethyl acetate (3:2) was used as eluent for column chromatography. Isolated as a white solid (4b': 115 mg, 94%). <sup>1</sup>H NMR (400 MHz, CDCl<sub>3</sub>): δ 2.43 (s, 3H, CH<sub>3</sub>), 3.17 (bs, 1H, OH), 4.60 (s, 2H, CH<sub>2</sub>), 7.22 (d, 2H, Ar-H), 7.27 (d, 2H, Ar-H). <sup>13</sup>C{<sup>1</sup>H} NMR (101 MHz, CDCl<sub>3</sub>): δ 21.2 (CH<sub>3</sub>), 64.8 (CH<sub>2</sub>), 127.2, 129.2, 137.2, 138.1 (Ar-C).

**2-Furanmethanol (5')**: A mixture of hexanes and ethyl acetate (3:2) was used as eluent for column chromatography. Isolated as a colorless liquid (5': 78 mg, 79%). <sup>1</sup>H NMR (400 MHz, CDCl<sub>3</sub>): δ 3.15 (bs, 1H, OH), 4.54 (s, 2H, CH<sub>2</sub>), 6.20-6.36 (m, 2H, CH), 7.33-7.41 (m, 1H, CH). <sup>13</sup>C{<sup>1</sup>H} NMR (101 MHz, CDCl<sub>3</sub>): δ 57.2 (CH<sub>2</sub>), 107.7, 110.4, 142.5, 154.1 (CH).

**Phenol (6a')**: A mixture of hexanes and ethyl acetate (1:1) with  $\text{NEt}_3$  (10% by volume) was used as eluent for column chromatography. Isolated as a white solid (6a': 90 mg, 96%).  $^1\text{H}$  NMR (400 MHz,  $\text{CDCl}_3$ ):  $\delta$  5.35-5.95 (bs, 1H, OH), 6.75-6.98 (m, 3H, Ar-H), 7.09-7.27 (m, 2H, Ar-H).  $^{13}\text{C}\{^1\text{H}\}$  NMR (101 MHz,  $\text{CDCl}_3$ ):  $\delta$  115.7, 121.1, 130.0, 155.4 (Ar-C).

**4-Methylphenol (6b')**: A mixture of hexanes and ethyl acetate (1:1) with  $\text{NEt}_3$  (10% by volume) was used as eluent for column chromatography. Isolated as a white solid (6b': 101 mg, 93%).  $^1\text{H}$  NMR (400 MHz,  $\text{CDCl}_3$ ):  $\delta$  2.28 (s, 3H,  $\text{CH}_3$ ), 3.90 (bs, 1H, OH), 6.73 (d, 2H, Ar-H), 7.03 (d, 2H, Ar-H).  $^{13}\text{C}\{^1\text{H}\}$  NMR (101 MHz,  $\text{CDCl}_3$ ):  $\delta$  20.6 ( $\text{CH}_3$ ), 115.3, 129.9, 130.2, 153.7 (Ar-C).

**2-(4-Methoxyphenyl)ethanol (8a'/9b')**: A mixture of hexanes and ethyl acetate (3:2) was used as eluent for column chromatography. Isolated as a colorless liquid (8a': 145 mg, 95%; 9b': 142 mg, 93%).  $^1\text{H}$  NMR (400 MHz,  $\text{CDCl}_3$ ):  $\delta$  2.26 (bs, 1H, OH), 2.81 (t, 2H,  $\text{CH}_2$ ), 3.69-3.90 (m, 5H,  $\text{OCH}_2 + \text{OCH}_3$ ), 6.88 (d, 2H, Ar-H), 7.16 (d, 2H, Ar-H).  $^{13}\text{C}\{^1\text{H}\}$  NMR (101 MHz,  $\text{CDCl}_3$ ):  $\delta$  38.3 ( $\text{CH}_2$ ), 55.2 ( $\text{OCH}_3$ ), 63.7 ( $\text{OCH}_2$ ), 114.0, 130.0, 130.6, 158.2 (Ar-C).

**2-Phenylethanol (9a')**: A mixture of hexanes and ethyl acetate (3:2) was used as eluent for column chromatography. Isolated as a colorless liquid (9a': 111 mg, 91%).  $^1\text{H}$  NMR (400 MHz,  $\text{CDCl}_3$ ):  $\delta$  1.96 (bs, 1H, OH), 2.89 (t, 2H,  $\text{CH}_2$ ), 3.86 (t, 3H,  $\text{OCH}_2$ ), 7.15-7.30 (m, 3H, Ar-H), 7.31-7.40 (m, 2H, Ar-H).  $^{13}\text{C}\{^1\text{H}\}$  NMR (101 MHz,  $\text{CDCl}_3$ ):  $\delta$  39.2 ( $\text{CH}_2$ ), 63.7 ( $\text{OCH}_2$ ), 126.5, 128.6, 129.1, 138.6 (Ar-C).

**1-Phenyl-1,2-ethanediol (10')**: A mixture of DCM and MeOH (9:1) was used as eluent for column chromatography. Isolated as a white solid (10': 101 mg, 73%).  $^1\text{H}$  NMR (400 MHz,  $\text{CDCl}_3$ ):  $\delta$  2.82-3.56 (bs, 2H, OH), 3.57-3.82 (m, 2H,  $\text{CH}_2$ ), 4.72-4.89 (m, 1H, CH), 7.23-7.44 (m, 5H, Ar-H).  $^{13}\text{C}\{^1\text{H}\}$  NMR (101 MHz,  $\text{CDCl}_3$ ):  $\delta$  68.2 ( $\text{CH}_2$ ), 74.8 (CH), 126.2, 128.1, 128.6, 140.6 (Ar-C).

**3-Phenyl-1-propanol (11')**: A mixture of hexanes and ethyl acetate (3:2) was used as eluent for column chromatography. Isolated as a colorless liquid (11': 124 mg, 91%).  $^1\text{H}$  NMR (400 MHz,  $\text{CDCl}_3$ ):  $\delta$  1.93 (p, 2H,  $\text{CH}_2$ ), 2.17 (bs, 1H, OH), 2.75 (t, 2H,  $\text{CH}_2$ ), 3.70 (s, 2H,  $\text{CH}_2$ ), 7.13- 7.45 (m, 5H, Ar-H).  $^{13}\text{C}\{^1\text{H}\}$  NMR (101 MHz,  $\text{CDCl}_3$ ):  $\delta$  32.1, 34.3, 62.2 ( $\text{CH}_2$ ), 125.9, 128.5, 141.9 (Ar-C).

**1-Decanol (12')**: A mixture of hexanes and ethyl acetate (3:2) was used as eluent for column chromatography. Isolated as a faint yellow oil (12': 150 mg, 95%).  $^1\text{H}$  NMR (400 MHz,  $\text{CDCl}_3$ ):  $\delta$  0.88 (t, 3H,  $\text{CH}_3$ ) 1.15-1.42 (m, 14H,  $\text{CH}_2$ ), 1.48-1.62 (m, 2H,  $\text{CH}_2$ ), 2.00 (bs, 1H, OH), 3.61 (t, 2H,  $\text{CH}_2$ ).  $^{13}\text{C}\{^1\text{H}\}$  NMR (101 MHz,  $\text{CDCl}_3$ ):  $\delta$  14.2 ( $\text{CH}_3$ ), 22.8, 25.9, 29.4, 29.6, 29.7, 32.0, 32.9 ( $\text{CH}_2$ ), 63.0 ( $\text{OCH}_2$ ).

**1-Dodecanol (13')**: A mixture of hexanes and ethyl acetate (3:2) was used as eluent for column chromatography. Isolated as a faint yellow oil (13': 181 mg, 97%).  $^1\text{H}$  NMR (400 MHz,  $\text{CDCl}_3$ ):  $\delta$  0.87 (t, 3H,  $\text{CH}_3$ ), 1.22-1.39 (m, 18H,  $\text{CH}_2$ ), 1.51-1.63 (m, 2H,  $\text{CH}_2$ ), 2.02 (bs, 1H, OH), 3.62 (t, 2H,  $\text{CH}_2$ ).  $^{13}\text{C}\{^1\text{H}\}$  NMR (101 MHz,  $\text{CDCl}_3$ ):  $\delta$  14.2 ( $\text{CH}_3$ ), 22.8, 25.9, 29.5, 29.6, 29.7, 29.8, 32.1, 32.9 ( $\text{CH}_2$ ), 63.2 ( $\text{OCH}_2$ ).

**1-Tetradecanol (14')**: A mixture of hexanes and ethyl acetate (3:2) was used as eluent for column chromatography. Isolated as a white solid (14': 206 mg, 96%).  $^1\text{H}$  NMR (400 MHz,  $\text{CDCl}_3$ ):  $\delta$  0.87 (t, 3H,  $\text{CH}_3$ ), 1.19-1.39 (m, 22H,  $\text{CH}_2$ ), 1.45-1.61 (m, 2H,  $\text{CH}_2$ ), 2.60 (bs, 1H, OH), 3.59 (t, 2H,  $\text{CH}_2$ ).  $^{13}\text{C}\{^1\text{H}\}$  NMR (101 MHz,  $\text{CDCl}_3$ ):  $\delta$  14.2 ( $\text{CH}_3$ ), 22.8, 25.9, 29.6, 29.7, 29.8, 29.9, 32.0, 32.8 ( $\text{CH}_2$ ), 62.8 ( $\text{OCH}_2$ ).

**11-Hydroxy-1-undecene (15')**: A mixture of hexanes and diethyl ether (3:2) was used as eluent for column chromatography. Isolated as a colorless oil (15': 121 mg, 71%).  $^1\text{H}$  NMR (400 MHz,  $\text{CDCl}_3$ ):  $\delta$  1.18-1.47 (m, 13H,  $\text{CH}_2$  & OH), 1.49-1.65 (m, 2H,  $\text{CH}_2$ ), 1.96-2.13 (m, 2H,  $\text{CH}_2$ ), 3.55-3.73 (m, 2H,  $\text{CH}_2$ ), 4.86-5.08 (m, 2H,  $\text{CH}_2$ ), 5.71-5.92 (m, 1H, CH).  $^{13}\text{C}\{^1\text{H}\}$  NMR

(101 MHz, CDCl<sub>3</sub>):  $\delta$  25.9, 29.0, 29.2, 29.5, 29.7, 32.9, 33.9 (CH<sub>2</sub>), 63.2 (OCH<sub>2</sub>), 114.2, 139.3 (Calkene).

**9-Octadecen-1-ol (16')**: A mixture of hexanes and diethyl ether (3:2) was used as eluent for column chromatography. Isolated as a colorless oil (16': 222 mg, 83%). <sup>1</sup>H NMR (400 MHz, CDCl<sub>3</sub>):  $\delta$  0.89 (t, 3H, CH<sub>3</sub>), 1.21-1.43 (m, 23H, CH<sub>2</sub> & OH), 1.51-1.62 (m, 2H, CH<sub>2</sub>), 1.96-2.08 (m, 4H, CH<sub>2</sub>), 3.62 (t, 2H, CH<sub>2</sub>), 5.31-5.40 (m, 2H, CH). <sup>13</sup>C{<sup>1</sup>H} NMR (101 MHz, CDCl<sub>3</sub>):  $\delta$  14.2, 22.8, 25.9, 27.3, 29.4, 29.5, 29.6, 29.7, 29.9, 32.0, 32.9 (CH<sub>3</sub> & CH<sub>2</sub>), 63.0 (OCH<sub>2</sub>), 129.9 (CH).

**1,4-Pentanediol (17')**: A mixture of DCM and MeOH (9:1) was used as eluent for column chromatography. Isolated as a colorless oil (17': 82 mg, 79%). <sup>1</sup>H NMR (400 MHz, CDCl<sub>3</sub>):  $\delta$  1.19 (d, 3H, CH<sub>3</sub>), 1.42-1.73 (m, 4H, CH<sub>2</sub>), 2.80-3.30 (bs, 2H, OH), 3.56-3.71 (m, 2H, CH<sub>2</sub>), 3.76-3.87 (m, 1H, CH). <sup>13</sup>C{<sup>1</sup>H} NMR (101 MHz, CDCl<sub>3</sub>):  $\delta$  23.6 (CH<sub>3</sub>), 29.2, 36.4 (CH<sub>2</sub>), 62.9 (OCH<sub>2</sub>), 68.0 (OCH).

**1,6-Hexanediol (18'/20'/22')**: A mixture of DCM and MeOH (9:1) was used as eluent for column chromatography. Isolated as a white solid (18': 96 mg, 81%; 20': 90 mg, 76%; 22': 84 mg, 71%). <sup>1</sup>H NMR (400 MHz, CDCl<sub>3</sub>):  $\delta$  1.35-1.51 (m, 4H, CH<sub>2</sub>), 1.53-2.01 (m, 6H, CH<sub>2</sub> + OH), 3.68 (t, 4H, OCH<sub>2</sub>). <sup>13</sup>C{<sup>1</sup>H} NMR (101 MHz, CDCl<sub>3</sub>):  $\delta$  25.7, 32.8 (CH<sub>2</sub>), 63.0 (OCH<sub>2</sub>).

**1,5-pentanediol (19')**: A mixture of DCM and MeOH (9:1) was used as eluent for column chromatography. Isolated as a colorless oil (19': 75 mg, 72%). <sup>1</sup>H NMR (400 MHz, CDCl<sub>3</sub>):  $\delta$  1.40-1.51 (m, 2H, CH<sub>2</sub>), 1.52-1.65 (m, 4H, CH<sub>2</sub>), 2.36 (bs, 2H, OH), 3.66 (t, 4H, OCH<sub>2</sub>). <sup>13</sup>C{<sup>1</sup>H} NMR (101 MHz, CDCl<sub>3</sub>):  $\delta$  22.1, 32.3 (CH<sub>2</sub>), 62.7 (OCH<sub>2</sub>).

**3-Methyl-1,4-octanediol (21')**: A mixture of DCM and MeOH (9:1) was used as eluent for column chromatography. Isolated as a colorless oil (21': 107 mg, 67%). <sup>1</sup>H NMR (400 MHz, CDCl<sub>3</sub>):  $\delta$  0.85-1.04 (m, 6H, CH<sub>3</sub>), 1.22-1.58 (m, 7H, CH + CH<sub>2</sub>), 1.63-1.82 (m, 2H, CH<sub>2</sub>),

2.54-2.88 (bs, 2H, OH), 3.53-3.69 (m, 2H, OCH<sub>2</sub>), 3.72-3.82 (m, 1H, OCH). <sup>13</sup>C{<sup>1</sup>H} NMR (101 MHz, CDCl<sub>3</sub>): δ 14.0, 16.7, 22.9, 28.2, 34.3, 35.4, 36.1 (CH<sub>2</sub>), 60.6 (OCH<sub>2</sub>), 75.1 (OCH).

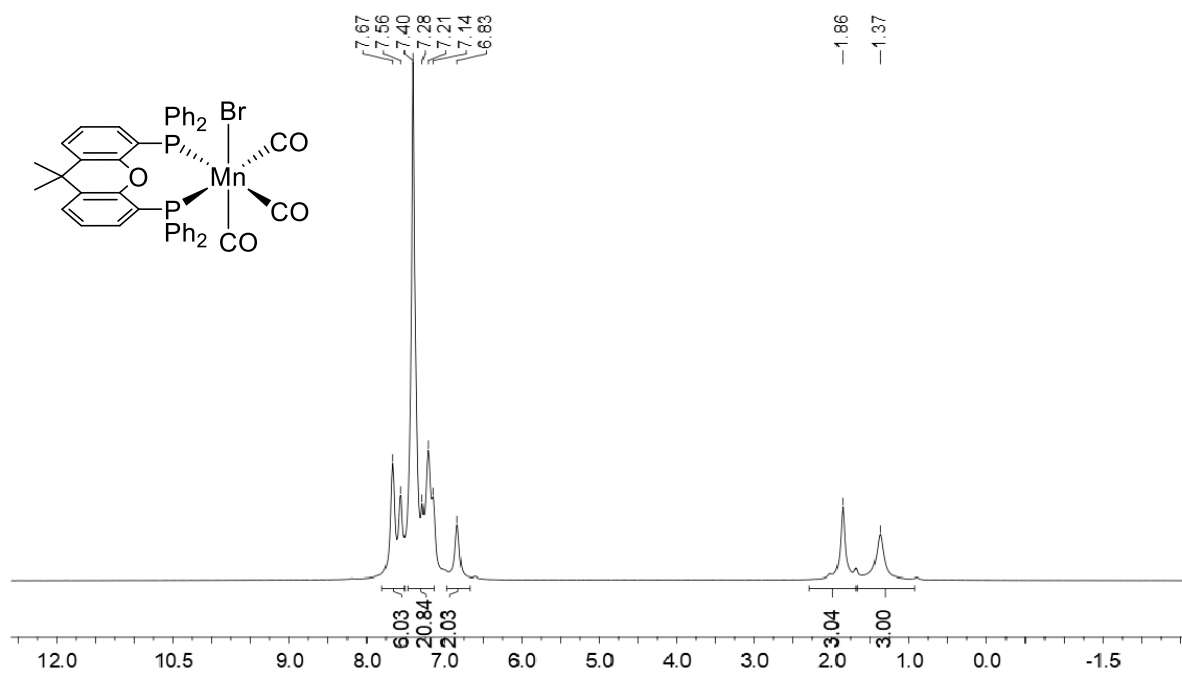


**Figure 2.1** <sup>1</sup>H NMR (400 MHz) spectrum of complex **1** in CDCl<sub>3</sub> at r.t.

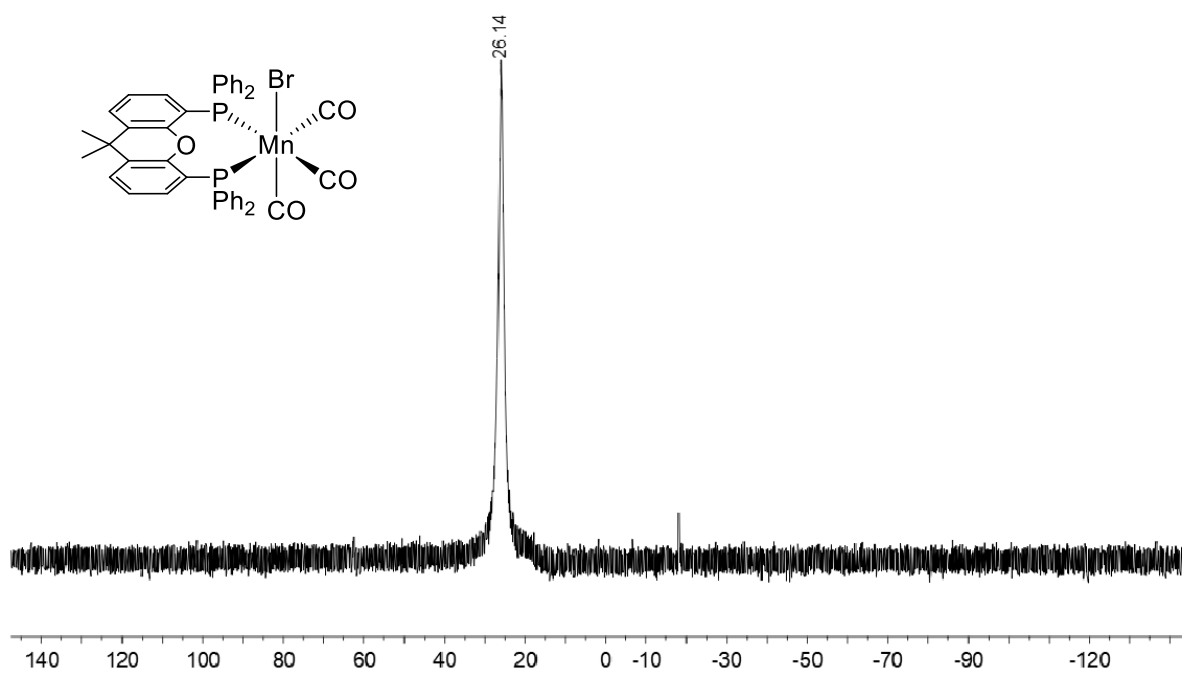


**Figure 2.2** <sup>31</sup>P{<sup>1</sup>H} NMR (162 MHz) spectrum of complex **1** in CDCl<sub>3</sub> at r.t.

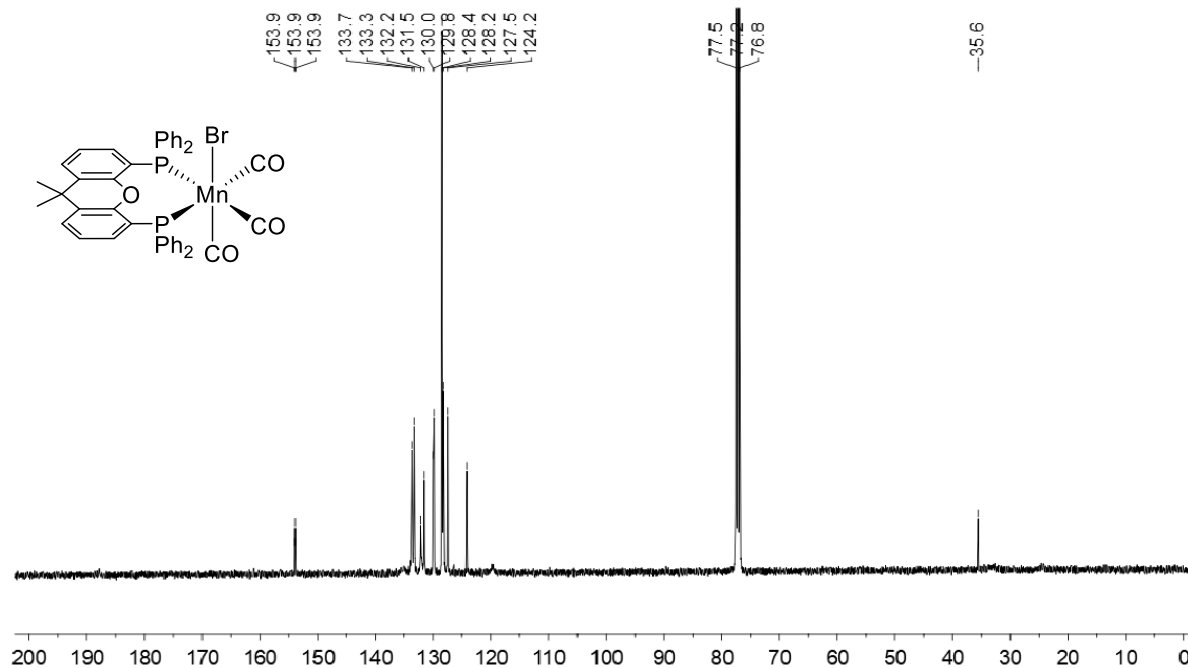


**Figure 2.3**  $^{13}\text{C}\{^1\text{H}\}$  NMR (101 MHz) spectrum of complex **1** in  $\text{CDCl}_3$  at r.t.

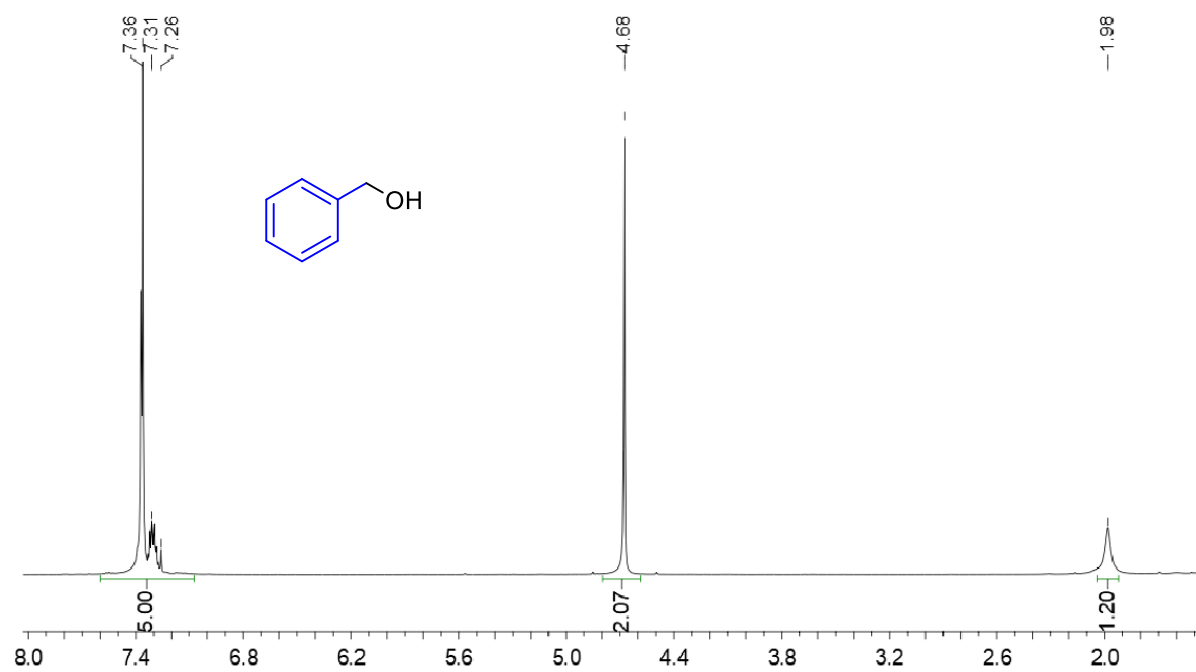


**Figure 2.4**  $^1\text{H}$  NMR (400 MHz) spectrum of benzyl alcohol (**1a'**/**4a'**/**7a'**) in  $\text{CDCl}_3$  at r.t.

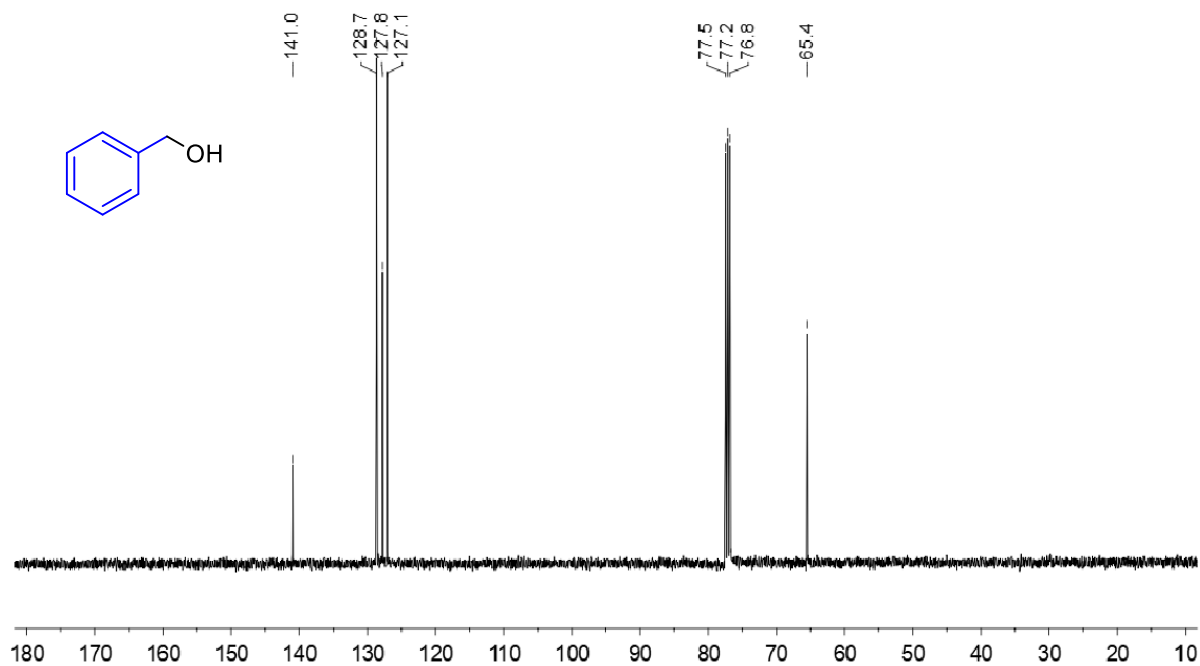


**Figure 2.5**  $^{13}\text{C}$  NMR (101 MHz) spectrum of benzyl alcohol ( $1\text{a}'/4\text{a}'/7\text{a}'$ ) in  $\text{CDCl}_3$  at r.t.

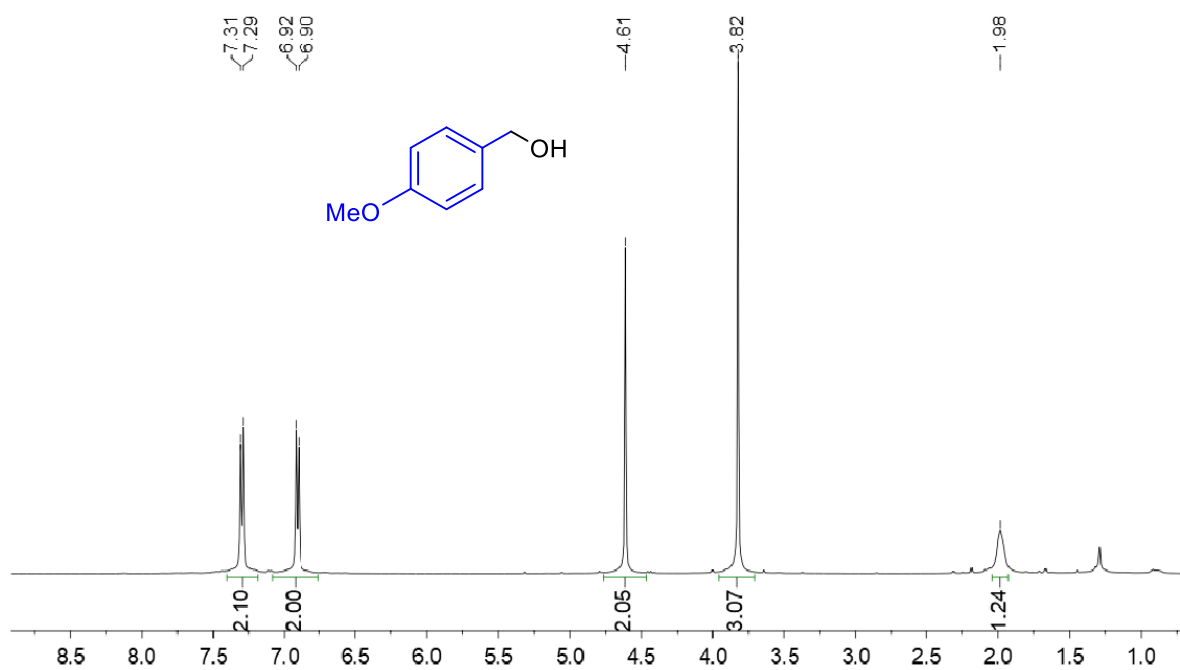


**Figure 2.6**  $^1\text{H}$  NMR (400 MHz) spectrum of 4-methoxybenzyl alcohol ( $1\text{b}'/7\text{b}'$ ) in  $\text{CDCl}_3$  at r.t.

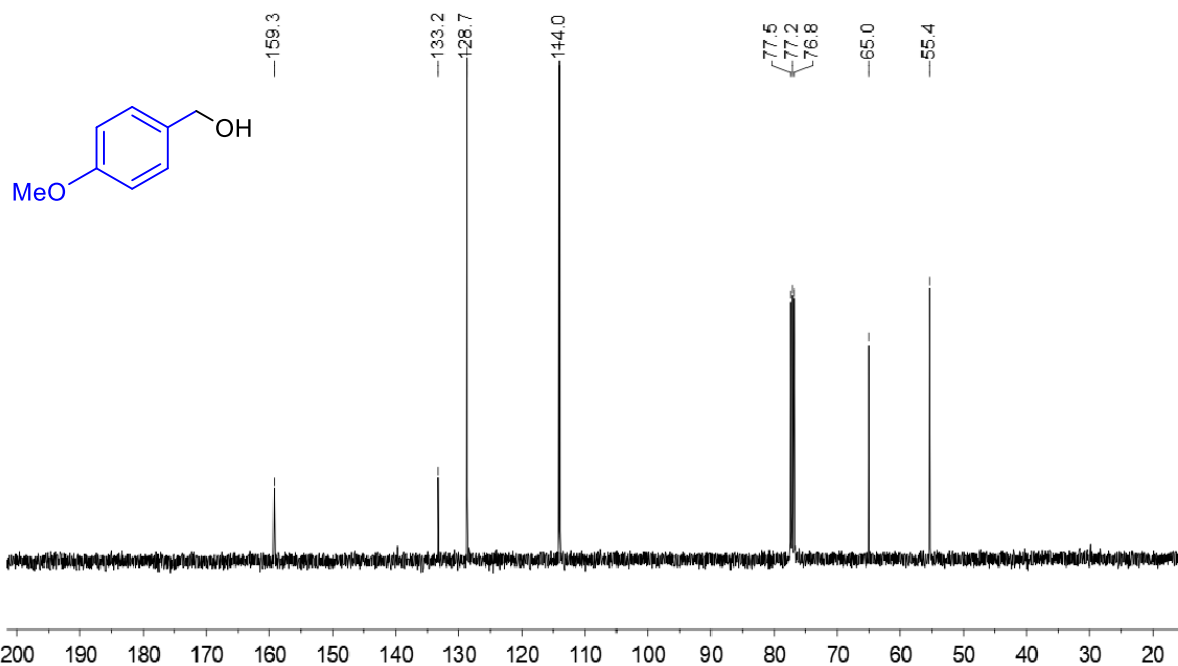


**Figure 2.7**  $^{13}C$  NMR (101 MHz) spectrum of 4-methoxybenzyl alcohol ( $1b'/7b'$ ) in  $CDCl_3$  at r.t.

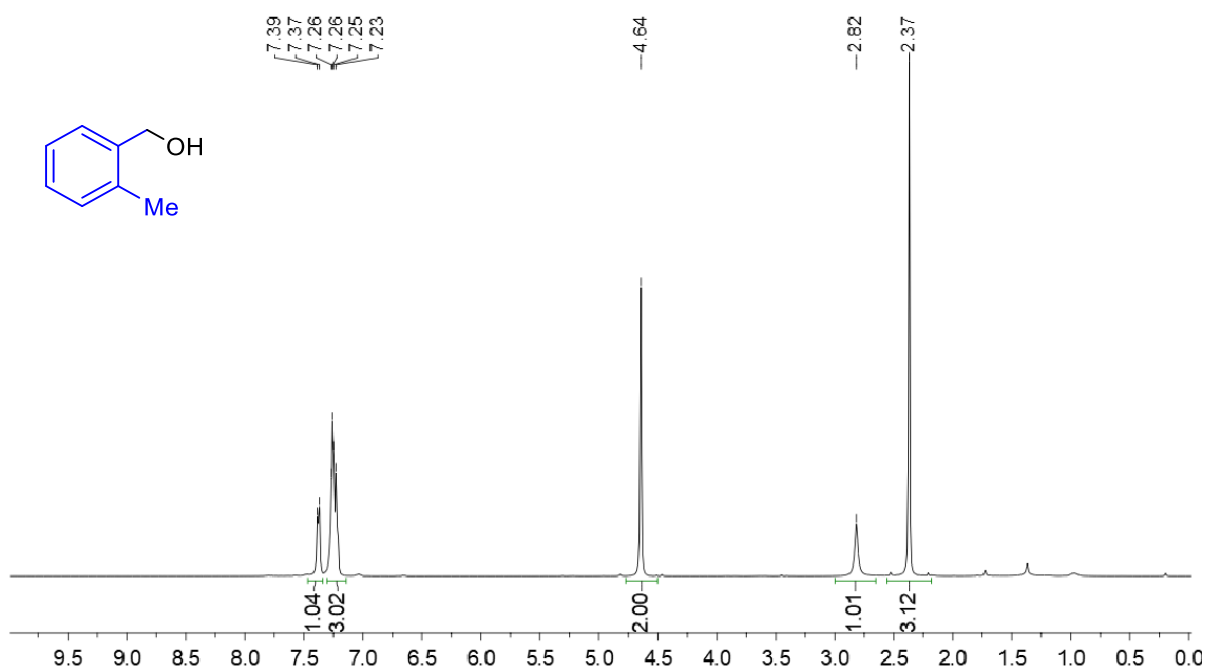


**Figure 2.8**  $^1H$  NMR (400 MHz) spectrum of 2-methylbenzyl alcohol ( $2a'$ ) in  $CDCl_3$  at r.t.

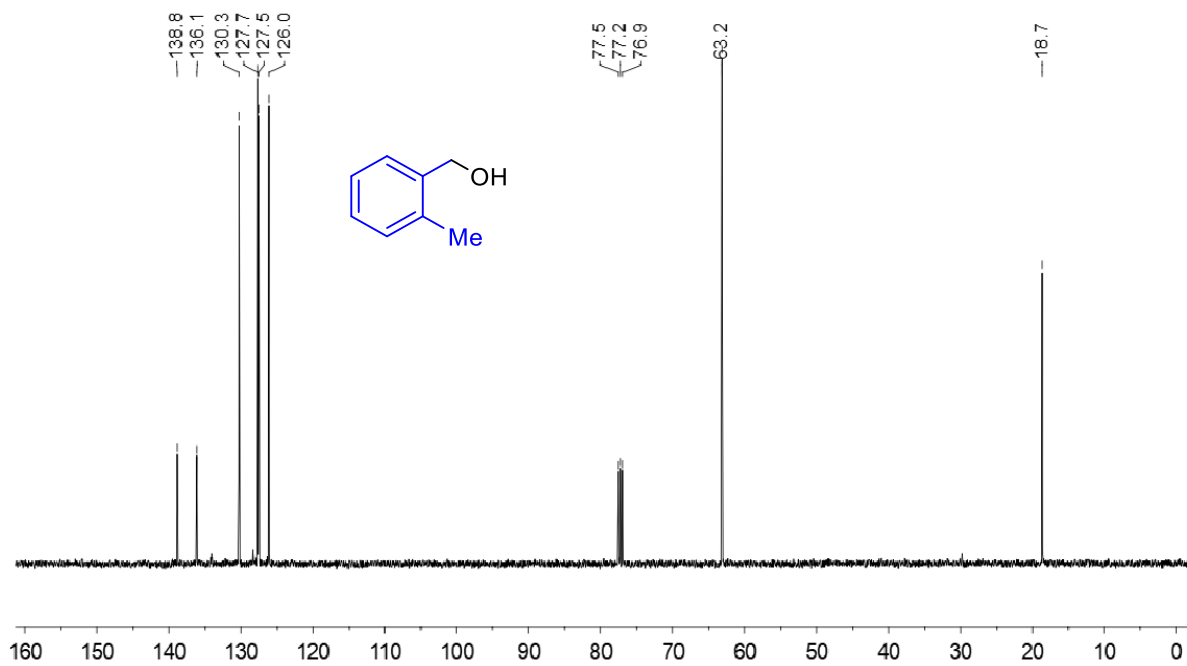


**Figure 2.9**  $^{13}\text{C}$  NMR (101 MHz) spectrum of 2-methylbenzyl alcohol (**2a'**) in  $\text{CDCl}_3$  at r.t.

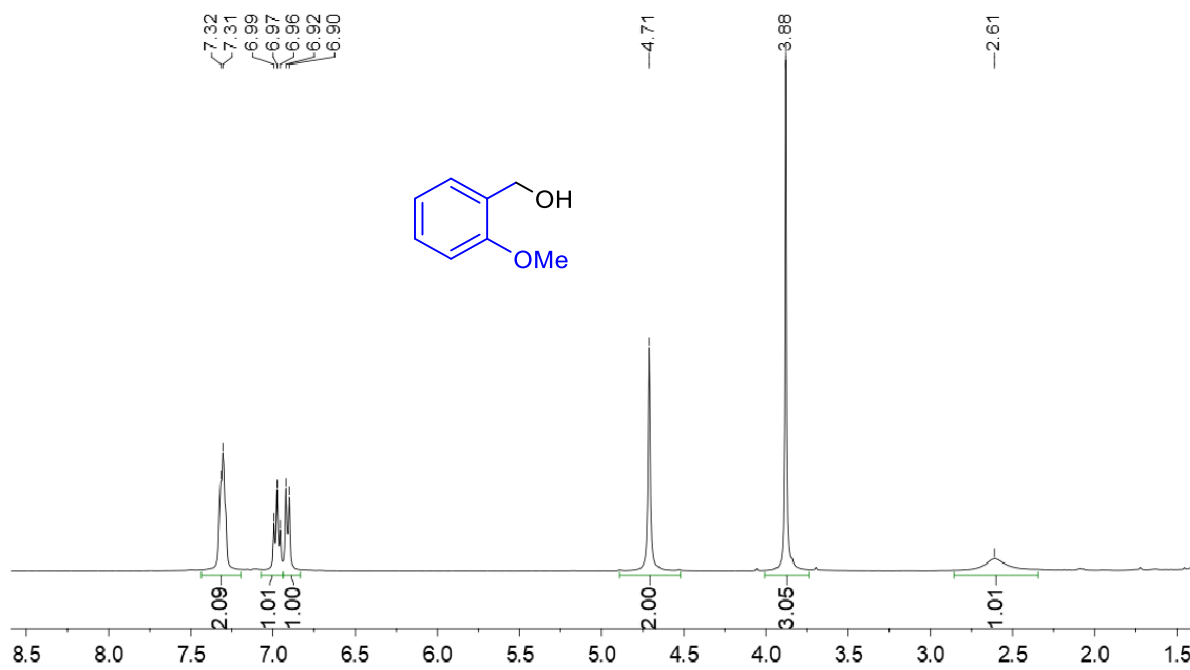


**Figure 2.10**  $^1\text{H}$  NMR (400 MHz) spectrum of 2-methoxybenzyl alcohol (**2b'**) in  $\text{CDCl}_3$  at r.t.

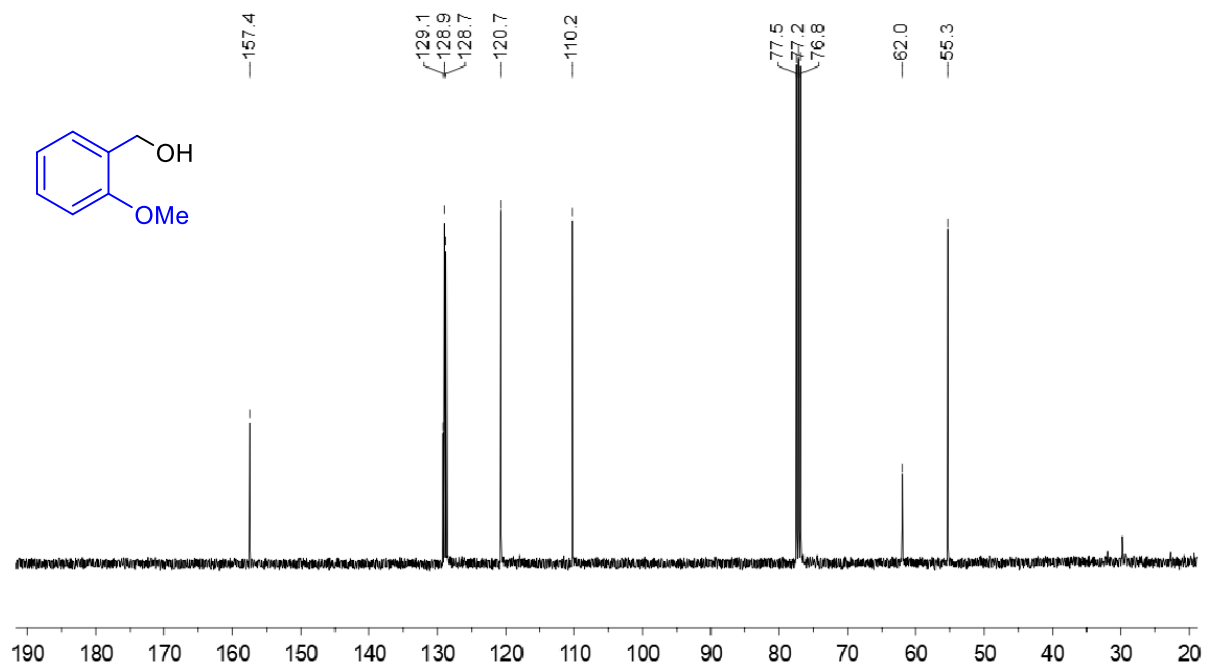


**Figure 2.11**  $^{13}\text{C}$  NMR (101 MHz) spectrum of 2-methoxybenzyl alcohol ( $2b'$ ) in  $\text{CDCl}_3$  at r.t.

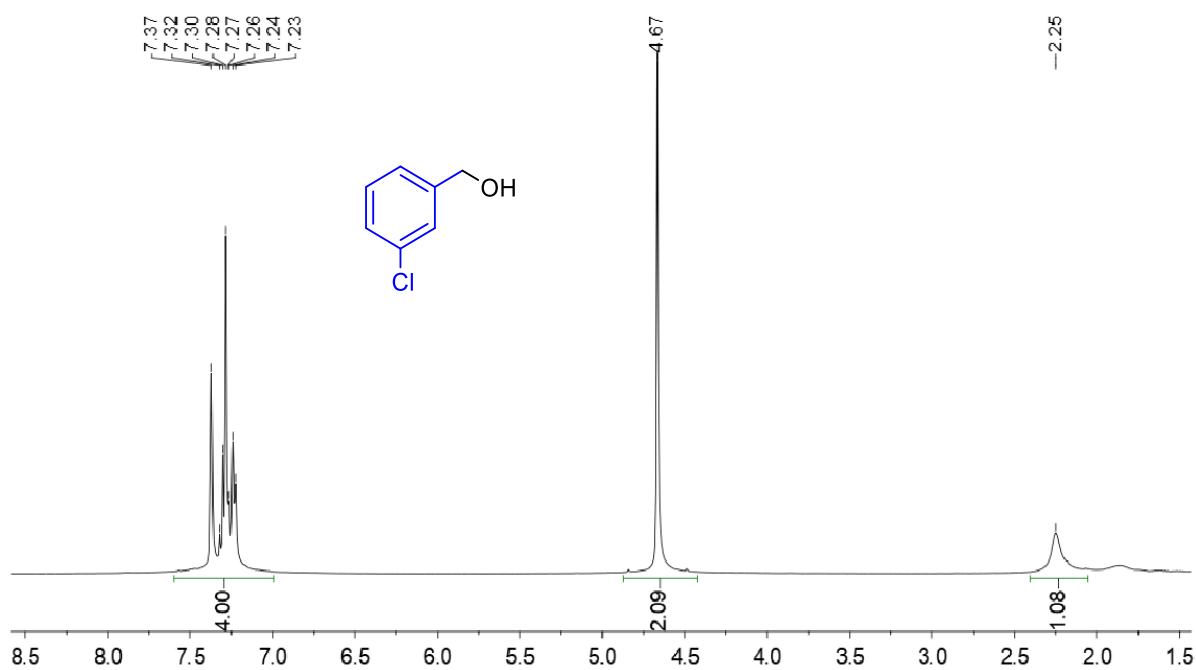


**Figure 2.12**  $^1\text{H}$  NMR (400 MHz) spectrum of 3-chlorobenzyl alcohol ( $3'$ ) in  $\text{CDCl}_3$  at r.t.

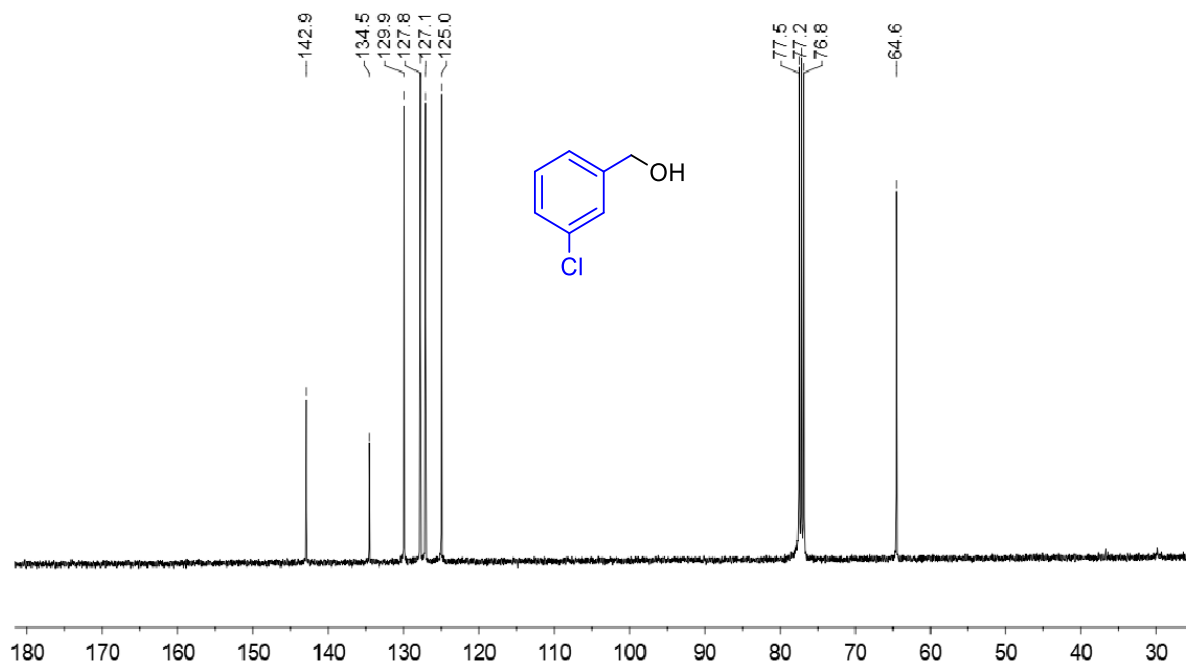


**Figure 2.13**  $^{13}\text{C}$  NMR (101 MHz) spectrum of 3-chlorobenzyl alcohol ( $3'$ ) in  $\text{CDCl}_3$  at r.t.

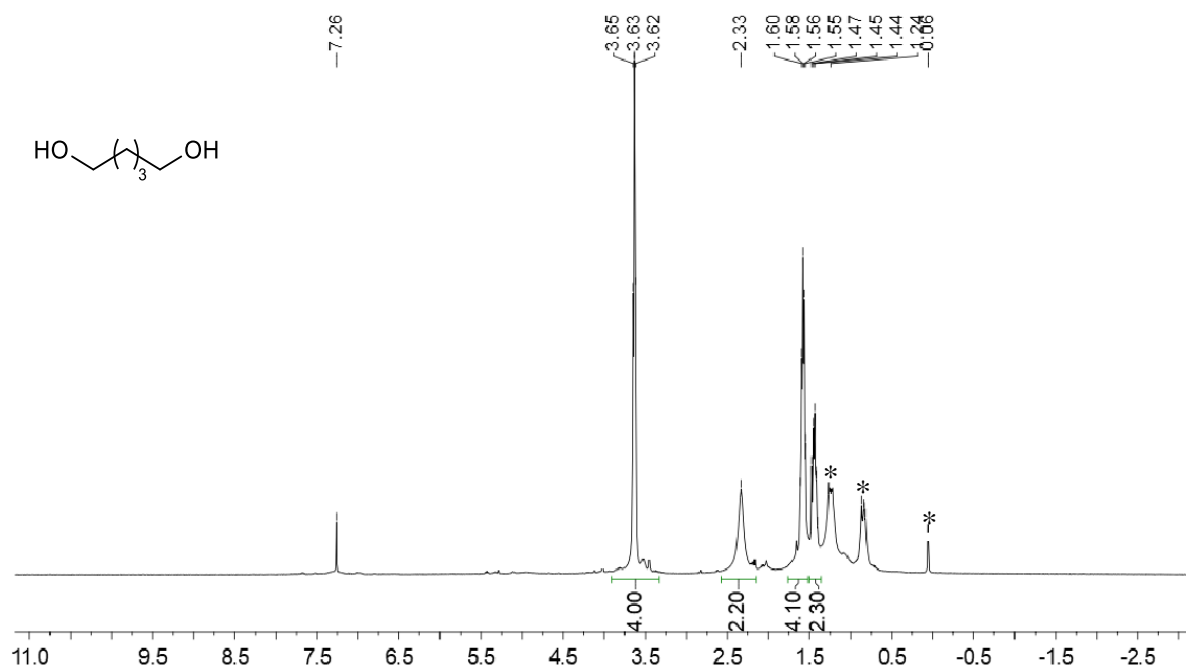


**Figure 2.14**  $^1\text{H}$  NMR (400 MHz) spectrum of 1,5-pentandiol ( $19'$ ) in  $\text{CDCl}_3$  at r.t. (\* indicates silicone grease).

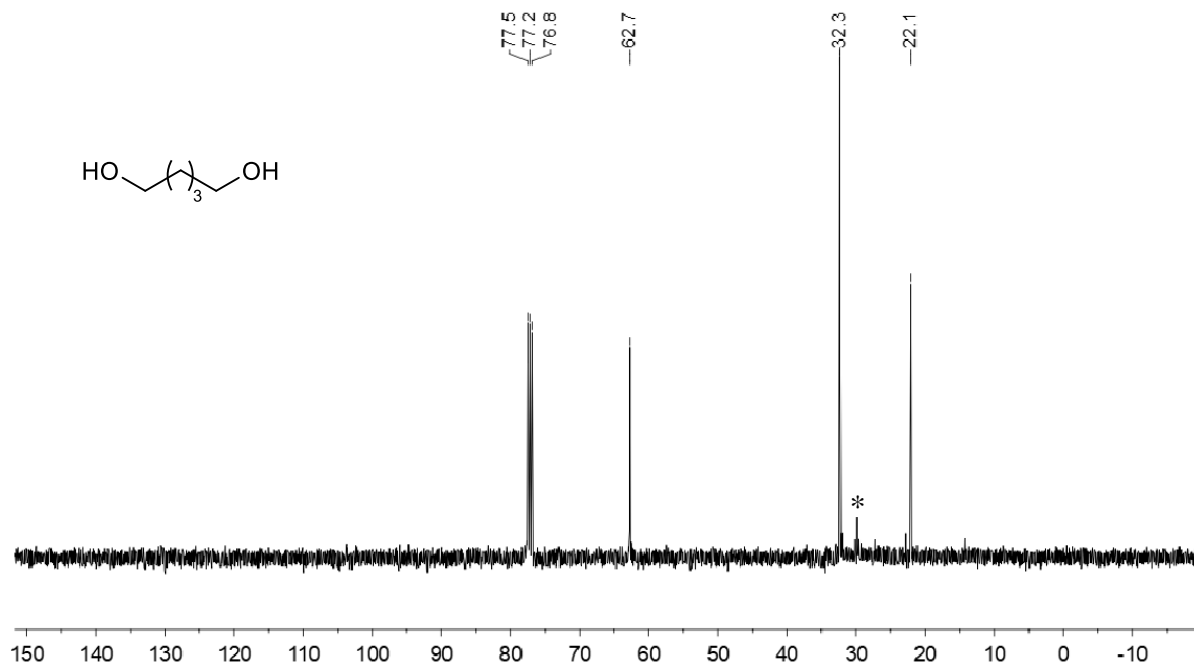


**Figure 2.15**  $^{13}\text{C}$  NMR (101 MHz) spectrum of 1,5-pentanediol ( $19'$ ) in  $\text{CDCl}_3$  at r.t. (\* indicates silicone grease).

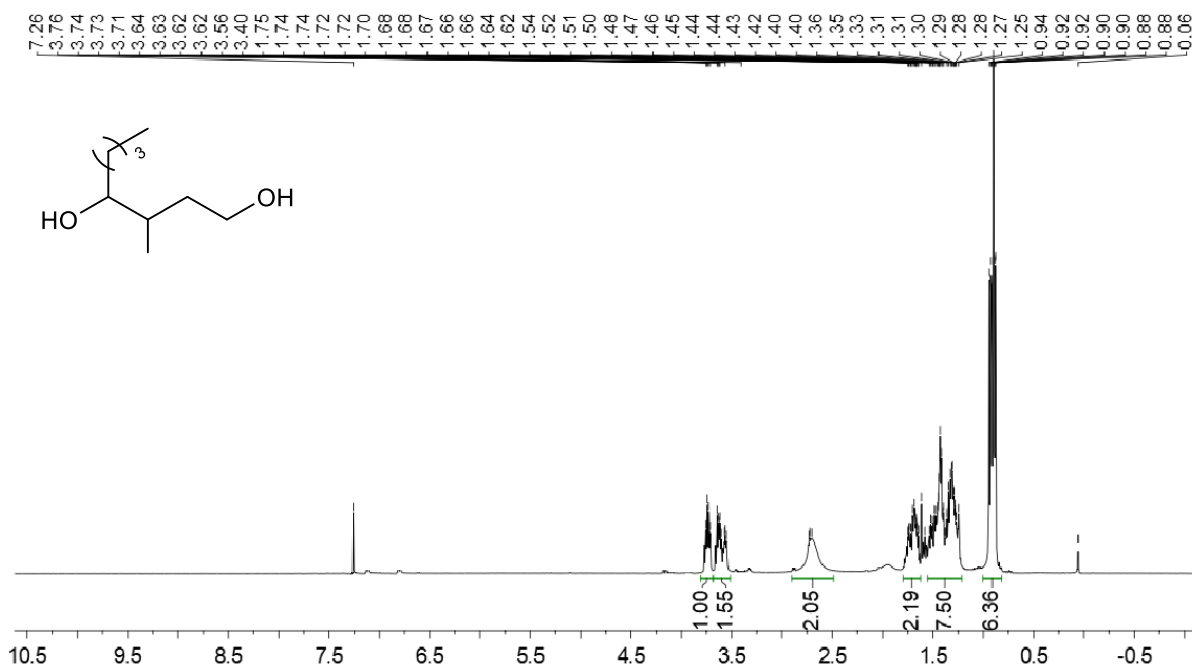


**Figure 2.16**  $^1\text{H}$  NMR (400 MHz) spectrum of 3-methyl-1,4-octanediol ( $21'$ ) in  $\text{CDCl}_3$  at r.t.

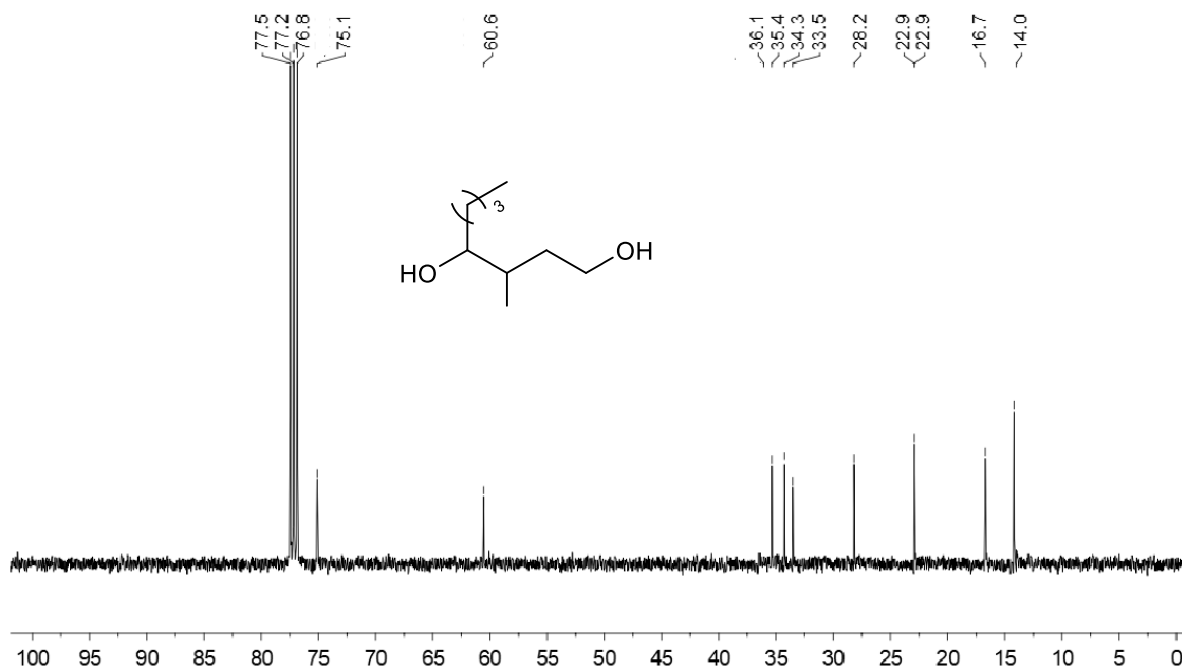


**Figure 2.17**  $^{13}\text{C}$  NMR (101 MHz) spectrum of 3-methyl-1,4-octanediol (**21'**) in  $\text{CDCl}_3$  at r.t.

### References

1. Ege, S. N. *Organic Chemistry*; D. C. Heath Company: Lexington, MA, 1989; p 596.
2. (a) van Putten, R.; Uslamin, E. A.; Garbe, M.; Liu, C.; Gonzalez-de-Castro, A.; Lutz, M.; Junge, K.; Hensen, E. J. M.; Beller, M.; Lefort, L.; Pidko, E. A. Non-Pincer-Type Manganese Complexes as Efficient Catalysts for the Hydrogenation of M.-C. Daniel, D. Astruc, *Chem. Rev.* **2004**, *104*, 293–346. (b) EspinosaJalapa, N. A.; Nerush, A.; Shimon, L. J. W.; Leitun, G.; Avram, L.; BenDavid, Y.; Milstein, D. Manganese-Catalyzed Hydrogenation of Esters to Alcohols. *Chem. - Eur. J.* **2017**, *23*, 5934–5938. (c) Widegren, M. B.; Harkness, G. J.; Slawin, A. M. Z.; Cordes, D. B.; Clarke, M. L. A Highly Active Manganese Catalyst for Enantioselective ketone and Ester Hydrogenation. *Angew. Chem., Int. Ed.* **2017**, *56*, 5825–5828. (d) Chen, J.; Zhu, H.; Chen, J.; Le, Z.-G.; Tu, T. Synthesis, Characterization and Catalytic Application of Pyridine Bridged NHeterocyclic Carbene–Ruthenium Complexes in the Hydrogenation of Carbonates. *Chem. - Asian J.* **2017**, *12*, 2809–2812. (e) Henrion, M.; Roisnel, T.; Couturier, J.-L.; Dubois, J.-L.; Sortais, J.-B.; Darcel, C.; Carpentier, J.-F. Ruthenium complexes bearing amino-bis- (phosphinite) or amino-bis(aminophosphine) ligands:

- Applications in catalytic ester hydrogenation. *Mol. Catal.* **2017**, *432*, 15–22. (f) Kim, D.; Le, L.; Drance, M. J.; Jensen, K. H.; Bogdanovski, K.; Cervarich, T. N.; Barnard, M. G.; Pudalov, N. J.; Knapp, S. M. M.; Chianese, A. R. Ester Hydrogenation Catalyzed by CNN-Pincer Complexes of Ruthenium. *Organometallics* **2016**, *35*, 982–989. (g) Srimani, D.; Mukherjee, A.; Goldberg, A. F. G.; Leitun, G.; DiskinPosner, Y.; Shimon, L. J. W.; Ben David, Y.; Milstein, D. Cobalt-Catalyzed Hydrogenation of Esters to Alcohols: Unexpected Reactivity Trend Indicates Ester Enolate Intermediacy. *Angew. Chem., Int. Ed.* **2015**, *54*, 12357–12360. (h) Chakraborty, S.; Dai, H.; Bhattacharya, P.; Fairweather, N. T.; Gibson, M. S.; Krause, J. A.; Guan, H. Iron-Based Catalysts for the Hydrogenation of Esters to Alcohols. *J. Am. Chem. Soc.* **2014**, *136*, 7869–7872. (i) Carpenter, I.; Eckelmann, S. C.; Kuntz, M. T.; Fuentes, J. A.; France, M. B.; Clarke, M. L. Convenient and improved protocols for the hydrogenation of esters using Ru catalysts derived from (P,P), (P,N,N) and (P,N,O) ligands. *Dalton Trans* **2012**, *41*, 10136–10140. (j) Fogler, E.; Balaraman, E.; Ben-David, Y.; Leitun, G.; Shimon, L. J. W.; Milstein, D. New CNN-Type Ruthenium Pincer NHC Complexes. Mild, Efficient Catalytic Hydrogenation of Esters. *Organometallics* **2011**, *30*, 3826–3833. (k) Sun, Y.; Koehler, C.; Tan, R.; Annibale, V. T.; Song, D. Ester hydrogenation catalyzed by Ru-CNN pincer complexes. *Chem. Commun.* **2011**, *47*, 8349–8351. (l) Ito, M.; Ootsuka, T.; Watari, R.; Shiibashi, A.; Himizu, A.; Ikariya, T. Catalytic Hydrogenation of Carboxamides and Esters by Well-Defined Cp\**Ru* Complexes Bearing a Protic Amine Ligand. *J. Am. Chem. Soc.* **2011**, *133*, 4240–4242.
3. (a) Ai, W.; Zhong, R.; Liu, X.; Liu, Q. Hydride Transfer Reactions Catalyzed by Cobalt Complexes. *Chem. Rev.* **2019**, *119*, 2876–2953. (b) Zhang, Z.; Butt, N. A.; Zhou, M.; Liu, D.; Zhang, W. Asymmetric Transfer and Pressure Hydrogenation with Earth-Abundant Transition Metal Catalysts. *Chin. J. Chem.* **2018**, *36*, 443–454. (c) Morris, R. H. Mechanisms of the H<sub>2</sub>- and transfer hydrogenation of polar bonds catalyzed by iron

- group hydrides. *Dalton Trans* **2018**, *47*, 10809–10826. (d) Matsunami, A.; Kayaki, Y. Upgrading and expanding the scope of homogeneous transferhydrogenation. *Tetrahedron Lett.* **2018**, *59*, 504–513. (e) Stefane, B.; Pozgan, F. Metal-Catalysed Transfer Hydrogenation of Ketones. *Top. Curr. Chem.* **2016**, *374*, 1–67. (f) Echeverria, P.-G.; Ayad, T.; Phansavath, P.; Ratovelomanana-Vidal, V. Recent Developments in Asymmetric Hydrogenation and Transfer Hydrogenation of Ketones and Imines through Dynamic Kinetic Resolution. *Synthesis* **2016**, *48*, 2523–2539. (g) Foubelo, F.; Najera, C.; Yus, M. Catalytic asymmetric transfer hydrogenation of ketones: Recent advances. *Tetrahedron: Asymmetry* **2015**, *26*, 769–790. (h) Morris, R. H. Exploiting Metal–Ligand Bifunctional Reactions in the Design of Iron Asymmetric Hydrogenation Catalysts. *Acc. Chem. Res.* **2015**, *48*, 1494–1502. (i) Wang, D.; Astruc, D. The Golden Age of Transfer Hydrogenation. *Chem. Rev.* **2015**, *115*, 6621–6686. (j) Li, Y. Y.; Yu, S. L.; Shen, W. Y.; Gao, J. X. Iron-, Cobalt-, and Nickel-Catalyzed Asymmetric Transfer Hydrogenation and Asymmetric Hydrogenation of Ketones. *Acc. Chem. Res.* **2015**, *48*, 2587–2598. (k) Vaclavik, J.; Kacer, P.; Kuzma, M.; Cervený, L. Opportunities Offered by Chiral  $\eta^6$ -Arene/N-Arylsulfonyldiamine-RuII Catalysts in the Asymmetric Transfer Hydrogenation of Ketones and Imines. *Molecules* **2011**, *16*, 5460–5495. (l) Robertson, A.; Matsumoto, T.; Ogo, S. The development of aqueous transfer hydrogenation catalysts. *Dalton Trans* **2011**, *40*, 10304–10310. (m) Malacea, R.; Poli, R.; Manoury, E. Asymmetric hydrosilylation, transferhydrogenation and hydrogenation of ketones catalyzed by iridium complexes. *Coord. Chem. Rev.* **2010**, *254*, 729–752.
4. (a) Lee, S.-H.; Nikonov, G. I. Transfer Hydrogenation of Ketones, Nitriles, and Esters Catalyzed by a Half-Sandwich Complex of Ruthenium. *ChemCatChem* **2015**, *7*, 107–113. (b) Dubey, A.; Khaskin, E. Catalytic Ester Metathesis Reaction and Its Application to Transfer Hydrogenation of Esters. *ACS Catal.* **2016**, *6*, 3998–4002. (c)

- Farrar-Tobar, R. A.; Wozniak, B.; Savini, A.; Hinze, S.; Tin, S.; de Vries, J. G. Base-Free Iron Catalyzed Transfer Hydrogenation of Esters Using EtOH as Hydrogen Source. *Angew. Chem., Int. Ed.* **2019**, *58*, 1129–1133.
5. (a) Berk, S. C.; Kreutzer, K. A.; Buchwald, S. L. A Catalytic Method for the Reduction of Esters to Alcohols. *J. Am. Chem. Soc.* **1991**, *113*, 5093–5095. (b) Berk, S. C.; Buchwald, S. L. An Air-Stable Catalyst System for the Conversion of Esters to Alcohols. *J. Org. Chem.* **1992**, *57*, 3751–3753. (c) Barr, K. J.; Berk, S. C.; Buchwald, S. L. Titanocene-Catalyzed Reduction of Esters Using Polymethylhydrosiloxane as the Stoichiometric Reductant. *J. Org. Chem.* **1994**, *59*, 4323–4326. (d) Reding, M. T.; Buchwald, S. L. An Inexpensive Air-Stable Titanium-Based System for the Conversion of Esters to Primary Alcohols. *J. Org. Chem.* **1995**, *60*, 7884–7890. (e) Verdaguer, X.; Hansen, M. C.; Berk, S. C.; Buchwald, S. L. Titanocene-Catalyzed Reduction of Lactones to Lactols. *J. Org. Chem.* **1997**, *62*, 8522–8528.
6. Fernandes, A. C.; Romao, C. C. Silane/MoO<sub>3</sub>·2Cl<sub>2</sub> as an efficient system for the reduction of esters. *J. Mol. Catal. A: Chem.* **2006**, *253*, 96–98.
7. Ohta, T.; Kamiya, M.; Nobutomo, M.; Kusui, K.; Furukawa, I. Reduction of Carboxylic Acid Derivatives Using Diphenylsilane in the Presence of a Rh–PPh<sub>3</sub> Complex. *Bull. Chem. Soc. Jpn.* **2005**, *78*, 1856–1861.
8. Nakanishi, J.; Tatamidani, H.; Fukumoto, Y.; Chatani, N. A New Synthesis of Aldehydes by the Palladium-Catalyzed Reaction of 2-Pyridinyl Esters with Hydrosilanes. *Synlett* **2006**, *2006*, 869–872.
9. Igarashi, M.; Mizuno, R.; Fuchikami, T. Ruthenium complex catalyzed hydrosilylation of esters: a facile transformation of esters to alkyl silyl acetals and aldehydes. *Tetrahedron Lett.* **2001**, *42*, 2149–2151.
10. Matsubara, K.; Iura, T.; Maki, T.; Nagashima, H. A Triruthenium Carbonyl Cluster Bearing a Bridging Acenaphthylene Ligand: An Efficient Catalyst for Reduction of

- Esters, Carboxylic Acids, and Amides by Trialkylsilanes. *J. Org. Chem.* **2002**, *67*, 4985–4988.
11. Elsby, M. R.; Baker, R. T. Strategies and mechanisms of metal-ligand cooperativity in first-row transition metal complex catalysts. *Chem. Soc. Rev.* 2020, *49*, 8933–8987.
12. (a) Bezier, D.; Venkanna, G. T.; Castro, L. C. M.; Zheng, J.; Roisnel, T.; Sortais, J.-B.; Darcel, C. Iron-Catalyzed Hydrosilylation of Esters. *Adv. Synth. Catal.* **2012**, *354*, 1879–1884. (b) Das, S.; Li, Y.; Junge, K.; Beller, M. Synthesis of ethers from esters via Fe-catalyzed hydrosilylation. *Chem. Commun.* **2012**, *48*, 10742–10744. (c) Junge, K.; Wendt, B.; Zhou, S.; Beller, M. Iron-Catalyzed Reduction of Carboxylic Esters to Alcohols. *Eur. J. Org. Chem.* **2013**, *2013*, 2061–2065. (d) Li, H.; Misal Castro, L. C.; Zheng, J.; Roisnel, T.; Dorcet, V.; Sortais, J.-B.; Darcel, C. Selective Reduction of Esters to Aldehydes under the Catalysis of Well-Defined NHC–Iron Complexes. *Angew. Chem., Int. Ed.* **2013**, *52*, 8045–8049.
13. Hanna, P. K.; Gregg, B. T.; Cutler, A. R. Manganese Carbonyl Compounds as Hydrosilation Catalysts for Organoiron Acyl Complexes. *Organometallics* **1991**, *10*, 31–33. (b) DiBiase Cavanaugh, M.; Gregg, B. T.; Cutler, A. R. Manganese Carbonyl Complexes as Catalysts for the Hydrosilation of Ketones: Comparison with  $\text{RhCl}(\text{PPh}_3)_3$ . *Organometallics* **1996**, *15*, 2764–2769. (c) DiBiase Cavanaugh, M.; Gregg, B. T.; Chiulli, R. J.; Cutler, A. R. The reactions of hydrosilanes with the methoxycarbonyl complexes  $\text{Cd}(\text{L})(\text{CO})-\text{MCO}_2\text{Me}$  ( $\text{M} = \text{Fe}, \text{Ru}$ ;  $\text{L} = \text{CO}, \text{PPh}_3$ ) and  $(\text{L})(\text{CO})\text{XMCO}, \text{Me}$  ( $\text{M} = \text{Co}, \text{Mn}$ ;  $\text{L} = \text{CO}, \text{PPh}_3$ ;  $x = 3, 4$ , with and without catalysis. *J. Organomet. Chem.* **1997**, *547*, 173–182. (d) Mao, Z.; Gregg, B. T.; Cutler, A. R. Manganese- and Rhodium-Catalyzed Phenylsilane Hydrosilation-Deoxygenation of Iron Acyl Complexes  $\text{Cp}(\text{L})(\text{CO})-\text{FeC}(\text{O})\text{R}$  ( $\text{L} = \text{CO}, \text{PPh}_3, \text{P}(\text{OMe})_3, \text{P}(\text{OPh})_3$ ;  $\text{R} = \text{CH}_3, \text{Ph}, \text{CHMe}_2, \text{CMe}_3$ ). *Organometallics* **1998**, *17*, 1993–2002. (e) Son, S. U.; Paik, S.-J.; Lee, I. S.; Lee, Y.-A.; Chung, Y. K.; Seok, W. K.; Lee, H. N. Chemistry of [(1H-

hydronaphthalene)Mn(CO)<sub>3</sub>]: The Role of Ring-Slippage in Substitution, Catalytic Hydrosilylation, and Molecular Crystal Structure of [(η<sup>3</sup>-C<sub>10</sub>H<sub>9</sub>)Mn(CO)<sub>3</sub>P(OMe)<sub>3</sub>]. *Organometallics* **1999**, *18*, 4114–4118. (f) Son, S. U.; Paik, S.-J.; Chung, Y. K. Hydrosilylation of ketones catalyzed by tricarbonyl naphthalene manganese cation. *J. Mol. Catal. A: Chem.* **2000**, *151*, 87–90. (g) Riener, K.; Högerl, M. P.; Gigler, P.; Kühn, F. E. RhodiumCatalyzed Hydrosilylation of Ketones: Catalyst Development and Mechanistic Insights. *ACS Catal.* **2012**, *2*, 613–621. (h) Chidara, V. K.; Du, G. An Efficient Catalyst Based on Manganese Salen for Hydrosilylation of Carbonyl Compounds. *Organometallics* **2013**, *32*, 5034–5037. (i) Zheng, J.; Elangovan, S.; Valyaev, D. A.; Brousses, R.; Cesar, V.; Sortais, J.-B.; Darcel, C.; Lugan, N.; Lavigne, G. Hydrosilylation of Aldehydes and Ketones Catalyzed by HalfSandwich Manganese(I) N-Heterocyclic Carbene Complexes. *Adv. Synth. Catal.* **2014**, *356*, 1093–1097. (j) Trovitch, R. Synlett **2014**, *25*, 1638–1642. (k) Ghosh, C.; Mukhopadhyay, T. K.; Flores, M.; Groy, T. L.; Trovitch, R. Comparing Well-Defined Manganese, Iron, Cobalt, and Nickel Ketone Hydrosilylation Catalysts. *Inorg. Chem.* **2015**, *54*, 10398–10406. (l) Ghosh, C.; Mukhopadhyay, T. K.; Flores, M.; Groy, T. L.; Trovitch, R. J. A Pentacoordinate Mn(II) Precatalyst That Exhibits Notable Aldehyde and Ketone Hydrosilylation Turnover Frequencies. *Inorg. Chem.* **2015**, *54*, 10398–10406. (m) Valyaev, D. A.; Wei, D.; Elangovan, S.; Cavailles, M.; Dorcet, V.; Sortais, J.-B.; Darcel, C.; Lugan, N. Half-Sandwich Manganese Complexes Bearing Cp Tethered N-Heterocyclic Carbene Ligands: Synthesis and Mechanistic Insights into the Catalytic Ketone Hydrosilylation. *Organometallics* **2016**, *35*, 4090–4098. (n) Trovitch, R. J. The Emergence of Manganese-Based Carbonyl Hydrosilylation Catalysts. *Acc. Chem. Res.* **2017**, *50*, 2842–2852. (o) Ma, X.; Zuo, Z.; Liu, G.; Huang, Z. Manganese-Catalyzed Asymmetric Hydrosilylation of Aryl Ketones. *ACS Omega* **2017**, *2*, 4688–4692. (p) Wenz, J.; Vasilenko, V.; Kochan, A.; Wadepohl, H.; Gade, L. H.

- Coordination Chemistry of the PdmBOX Pincer Ligand: Reactivity at the Metal and the Ligand. *Eur. J. Inorg. Chem.* **2017**, 2017, 5545–5556.
14. Zheng, J.; Chevance, S.; Darcel, C.; Sortais, J.-B. Selective reduction of carboxylic acids to aldehydes through manganese catalysed hydrosilylation. *Chem. Commun.* **2013**, 49, 10010–10012.
15. (a) Mukhopadhyay, T. K.; Flores, M.; Groy, T. L.; Trovitch, R. J. A Highly Active Manganese Precatalyst for the Hydrosilylation of Ketones and Esters. *J. Am. Chem. Soc.* **2014**, 136, 882–885. (b) Mukhopadhyay, T. K.; Rock, C. L.; Hong, M.; Ashley, D. C.; Groy, T. L.; Baik, M.-H.; Trovitch, R. J. Mechanistic Investigation of Bis(imino)pyridine Manganese Catalyzed Carbonyl and Carboxylate Hydrosilylation. *J. Am. Chem. Soc.* **2017**, 139, 4901–4915. (c) Mukhopadhyay, T. K.; Ghosh, C.; Flores, M.; Groy, T. L.; Trovitch, R. J. Hydrosilylation of Aldehydes and Formates Using a Dimeric Manganese Precatalyst. *Organometallics* **2017**, 36, 3477–3483.
16. Kelly, C. M.; McDonald, R.; Sydora, O. L.; Stradiotto, M.; Turculet, L. A Manganese Pre-Catalyst: Mild Reduction of Amides, Ketones, Aldehydes, and Esters. *Angew. Chem., Int. Ed.* **2017**, 56, 15901–15904.
17. Mao, Z.; Gregg, B. T.; Cutler, A. R. Catalytic Hydrosilylation of Organic Esters Using Manganese Carbonyl Acetyl Complexes,  $(L)(CO)_4MnC(O)CH_3$  ( $L = CO, PPh_3$ ). *J. Am. Chem. Soc.* **1995**, 117, 10139–10140.
18. Martínez-Ferrate, O.; Chatterjee, B.; Werlé, C.; Leitner, W. Hydrosilylation of carbonyl and carboxyl groups catalysed by Mn(I) complexes bearing triazole ligands. *Catal. Sci. Technol.* **2019**, 9, 6370–6378.
19. For selected reviews, see: (a) Bhunia, M.; Sreejyothi, P.; Mandal, S. K. Earth-abundant metal catalyzed hydrosilylative reduction of various functional groups. *Coord. Chem. Rev.* **2020**, 405, 213110. (b) Maji, B.; Barman, M. K. Recent Developments of Manganese Complexes for Catalytic Hydrogenation and Dehydrogenation Reactions.

- Synthesis* **2017**, *49*, 3377–3393. (c) Valyaev, D. A.; Lavigne, G.; Lugan, N. Manganese organometallic compounds in homogeneous catalysis: Past, present, and prospects. *Coord. Chem. Rev.* **2016**, *308*, 191–235. (d) Carney, J. R.; Dillon, B. R.; Thomas, S. P. Recent Advances of Manganese Catalysis for Organic Synthesis. *Eur. J. Org. Chem.* **2016**, *2016*, 3912–3929. (e) Garbe, M.; Junge, K.; Beller, M. Homogeneous Catalysis by Manganese-Based Pincer Complexes. *Eur. J. Org. Chem.* **2017**, *2017*, 4344–4362. (f) Yang, X.; Wang, C. Manganese-Catalyzed Hydrosilylation Reactions. *Chem. - Asian J.* **2018**, *13*, 2307–2315. (g) Filonenko, G. A.; van Putten, R.; Hensen, E. J. M.; Pidko, E. A. Catalytic (de)hydrogenation promoted by non-precious metals – Co, Fe and Mn: recent advances in an emerging field. *Chem. Soc. Rev.* **2018**, *47*, 1459–1483. (h) Gorgas, N.; Kirchner, K. Isoelectronic Manganese and Iron Hydrogenation/Dehydrogenation Catalysts: Similarities and Divergences. *Acc. Chem. Res.* **2018**, *51*, 1558–1569. (i) Hu, Y.; Wang, C. Manganese-Catalyzed C-H Olefination Reactions. *ChemCatChem* **2019**, *11*, 1167–1174.
20. (a) Yadav, V.; Landge, V. G.; Subaramanian, M.; Balaraman, E. Manganese-Catalyzed  $\alpha$ -Olefination of Nitriles with Secondary Alcohols. *ACS Catal.* **2020**, *10*, 947–954. (b) Sousa, S. C. A.; Carrasco, C. J.; Pinto, M. F.; Royo, B. A Manganese N-Heterocyclic Carbene Catalyst for Reduction of Sulfoxides with Silanes. *ChemCatChem* **2019**, *11*, 3839–3843. (c) Tan, Y.-X.; Liu, X.-Y.; Zhao, Y.-S.; Tian, P.; Lin, G.-Q. Arylation/Intramolecular Conjugate Addition of 1,6-Enynes Enabled by Manganese(I)-Catalyzed C–H Bond Activation. *Org. Lett.* **2019**, *21*, 5–9. (d) El-Sepelgy, O.; Matador, E.; Brzozowska, A.; Rueping, M. C-Alkylation of Secondary Alcohols by Primary Alcohols through Manganese-Catalyzed Double Hydrogen Autotransfer. *ChemSusChem* **2019**, *12*, 3099–3102. (e) Hammarback, L. A.; Robinson, A.; Lynam, J. M.; Fairlamb, I. J. S. Delineating the critical role of acid additives in Mn-catalysed C–H bond functionalisation processes. *Chem. Commun.* **2019**, *55*, 3211–3214. (f)

Kaithal, A.; Gracia, L.-L.; Camp, C.; Quadrelli, E. A.; Leitner, W. Direct Synthesis of Cycloalkanes from Diols and Secondary Alcohols or Ketones Using a Homogeneous Manganese Catalyst. *J. Am. Chem. Soc.* **2019**, *141*, 17487–17492. (g) Dutta, P. K.; Chauhan, J.; Ravva, M. K.; Sen, S. Directing-Group-Assisted Manganese-Catalyzed Cyclopropanation of Indoles. *Org. Lett.* **2019**, *21*, 2025–2028. (h) Ling, F.; Hou, H.; Chen, J.; Nian, S.; Yi, X.; Wang, Z.; Song, D.; Zhong, W. Highly Enantioselective Synthesis of Chiral Benzhydrols via Manganese Catalyzed Asymmetric Hydrogenation of Unsymmetrical Benzophenones Using an Imidazole-Based Chiral PNN Tridentate Ligand. *Org. Lett.* **2019**, *21*, 3937–3941. (i) Kaplaneris, N.; Rogge, T.; Yin, R.; Wang, H.; Sirvinskaite, G.; Ackermann, L. Late-Stage Diversification through Manganese-Catalyzed C-H Activation: Access to Acyclic, Hybrid, and Stapled Peptides. *Angew. Chem., Int. Ed.* **2019**, *58*, 3476–3480. (j) Zhang, L.; Tang, Y.; Han, Z.; Ding, K. Lutidine-Based Chiral Pincer Manganese Catalysts for Enantioselective Hydrogenation of Ketones. *Angew. Chem., Int. Ed.* **2019**, *58*, 4973–4977. (k) BruneauVoisine, A.; Pallova, L.; Bastin, S.; Cesar, V.; Sortais, J.-B. Manganese<sup>I</sup> catalyzed  $\alpha$ -methylation of ketones with methanol as a C1 source. *Chem. Commun.* **2019**, *55*, 314–317. (l) Das, U. K.; Kumar, A.; BenDavid, Y.; Iron, M. A.; Milstein, D. Manganese Catalyzed Hydrogenation of Carbamates and Urea Derivatives. *J. Am. Chem. Soc.* **2019**, *141*, 12962–12966. (m) Gawali, S. S.; Pandia, B. K.; Gunanathan, C. Manganese(I)-Catalyzed  $\alpha$ -Alkenylation of Ketones Using Primary Alcohols. *Org. Lett.* **2019**, *21*, 3842–3847. (n) Waiba, S.; Barman, M. K.; Maji, B. Manganese-Catalyzed Acceptorless Dehydrogenative Coupling of Alcohols with Sulfones: A Tool to Access Highly Substituted Vinyl Sulfones. *J. Org. Chem.* **2019**, *84*, 973–982. (o) Ali, S.; Huo, J.; Wang, C. Manganese-Catalyzed Aromatic C–H Allylation of Ketones. *Org. Lett.* **2019**, *21*, 6961–6965. (p) Rana, J.; Gupta, V.; Balaraman, E. Manganese-catalyzed direct C–C coupling of  $\alpha$ -C–H bonds of amides and esters with alcohols via hydrogen

- autotransfer. *Dalton Trans* **2019**, *48*, 7094–7099. (q) Thorve, P. R.; Guru, M. M.; Maji, B. Manganese-Catalyzed Divergent Markovnikov Addition and [2+ 2+2] Cycloaddition of 2-Carbonyl Indanone with Terminal Alkyne. *J. Org. Chem.* **2019**, *84*, 8185–8193. (r) Borghs, J. C.; Azofra, L. M.; Biberger, T.; Linnenberg, O.; Cavallo, L.; Rueping, M.; ElSepelgy, O. Manganese-Catalyzed Multicomponent Synthesis of Pyrroles through Acceptorless Dehydrogenation Hydrogen Autotransfer Catalysis: Experiment and Computation. *ChemSusChem* **2019**, *12*, 3083–3088. (s) Wei, D.; Bruneau-Voisine, A.; Dubois, M.; Bastin, S.; Sortais, J.-B. Manganese-Catalyzed Transfer Hydrogenation of Aldimines. *ChemCatChem* **2019**, *11*, 5256–5259. (t) Ryabchuk, P.; Stier, K.; Junge, K.; Checinski, M. P.; Beller, M. Molecularly Defined Manganese Catalyst for Low-Temperature Hydrogenation of Carbon Monoxide to Methanol. *J. Am. Chem. Soc.* **2019**, *141*, 16923–16929. (u) Weber, S.; Veiros, L. F.; Kirchner, K. Old Concepts, New Application – Additive-Free Hydrogenation of Nitriles Catalyzed by an Air Stable Alkyl Mn(I) Complex. *Adv. Synth. Catal.* **2019**, *361*, 5412–5420. (v) Weber, S.; Stoeger, B.; Veiros, L. F.; Kirchner, K. Rethinking Basic Concepts-Hydrogenation of Alkenes Catalyzed by Bench-Stable Alkyl Mn(I) Complexes. *ACS Catal.* **2019**, *9*, 9715–9720.
21. van Leeuwen, P. W. N. M.; Kamer, P. C. J. Featuring Xantphos. *Catal. Sci. Technol.* **2018**, *8*, 26–113.
22. (a) Weber, S.; Stöger, B.; Kirchner, K. Hydrogenation of Nitriles and Ketones Catalyzed by an Air-Stable Bisphosphine Mn(I) Complex. *Org. Lett.* **2018**, *20*, 7212–7215. (b) Garduño, J. A.; Flores-Alamo, M.; García, J. J. Manganese-Catalyzed Transfer Hydrogenation of Nitriles with 2-Butanol as the Hydrogen Source. *ChemCatChem* **2019**, *11*, 5330–5338.

23. Rieke, R. D.; Thakur, D. S.; Roberts, B. D.; White, G. T. Fatty Methyl Ester Hydrogenation to Fatty Alcohol Part II: Process Issues. *J. Am. Oil Chem. Soc.* **1997**, *74*, 333–339.
24. (a) Werpy, T.; Petersen, G. Top Value-Added Chemicals from Biomass: Vol. I-Results of Screening for Potential Candidates from Sugars and Synthesis Gas; DOE/GO-102004-1992; National Renewable Energy Laboratory, U.S. Department of Energy (DOE): Golden, CO, 2004. (b) Holladay, J. E.; White, J. F.; Bozell, J. J.; Johnson, D. Top Value-Added Chemicals from Biomass: Vol. II-Results of Screening for Potential Candidates from Biorefinery Lignin; PNNL-16983; Pacific Northwest National Laboratory, U.S. Department of Energy (DOE): Richland, WA, 2007. (c) Corma, A.; Iborra, S.; Velty, A. Chemical Routes for the Transformation of Biomass into Chemicals. *Chem. Rev.* **2007**, *107*, 2411–2502. (d) Belgacem, M. N.; Gandini, A. Monomers, Polymers and Composites from Renewable Resources; Elsevier: Amsterdam, 2008. (e) Goldbach, V.; Roesle, P.; Mecking, S. Catalytic Isomerizing  $\omega$ -Functionalization of Fatty Acids. *ACS Catal.* **2015**, *5*, 5951–5972. (f) Li, X.; Jia, P.; Wang, T. Furfural: A Promising Platform Compound for Sustainable Production of C4 and C5 Chemicals. *ACS Catal.* **2016**, *6*, 7621–7640.
25. (a) Westhues, S.; Idel, J.; Klankermayer, J. Molecular catalyst systems as key enablers for tailored polyesters and polycarbonate recycling concepts. *Sci. Adv.* **2018**, *4*, 9669–9676. (b) Fuentes, J. A.; Smith, S. M.; Scharbert, M. T.; Carpenter, I.; Cordes, D. B.; Slawin, A. M. Z.; Clarke, M. L. On the Functional Group Tolerance of Ester Hydrogenation and Polyester Depolymerisation Catalysed by Ruthenium Complexes of Tridentate Aminophosphine Ligands. *Chem. - Eur. J.* **2015**, *21*, 10851–10860. (c) Krall, E. M.; Klein, T. W.; Andersen, R. J.; Nett, A. J.; Glasgow, R. W.; Reader, D. S.; Dauphinais, B. C.; McIlrath, S. P.; Fischer, A. A.; Carney, M. J.; Hudson, D. J.; Robertson, N. J. Controlled hydrogenative depolymerization of polyesters and

polycarbonates catalyzed by ruthenium(II) PNN pincer complexes. *Chem. Commun.* **2014**, *50*, 4884–4887.

---

# **Manganese Catalyzed Chemoselective Hydrosilylation of Nitroarenes: Sustainable Route to Aromatic Amines**

---

**2.1 Abstract**

**2.2 Introduction**

**2.3 Result and Discussion**

**2.4 Conclusion**

**2.5 Experimental Section**

### 3.1 Abstract:

Herein we report efficient catalytic hydrosilylations of nitroarenes to the corresponding anilines using a well-defined air-stable manganese(II)-NNO pincer complex in presence of sodium amalgam. The reduction of nitroarene was performed with low catalyst loading under solvent-free conditions. This base metal catalyzed hydrosilylation presents an easy and sustainable alternative for stoichiometric hydride reduction or classical hydrogenation. A large variety of nitroarenes bearing various functionalities were selectively transformed into corresponding anilines in good to excellent isolated yields. The potential utility of this hydrosilylation of nitroarene was demonstrated by preparing commercial drug molecules. Based on experimental evidences and supported by previous reports a plausible catalytic path is proposed which involves the reduction of manganese(II) precatalyst to manganese(0) active species followed by oxidative addition of silicon-hydrogen bond.

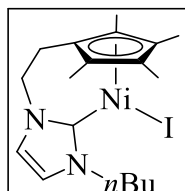
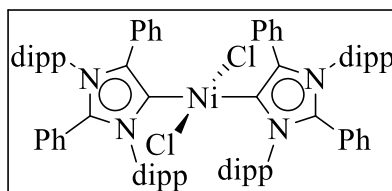
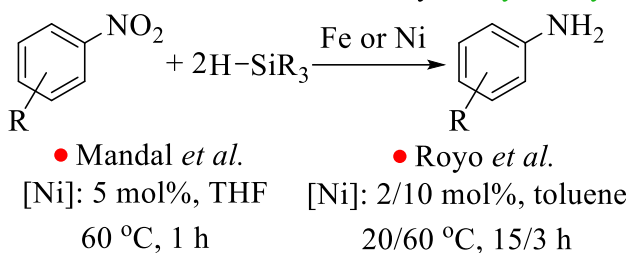
### 3.2 Introduction:

The reduction of nitroarenes to the corresponding anilines is one of the most significant transformations in organic synthesis as anilines are crucial structural motifs in a variety of agrochemicals, pharmaceutical, dyes, natural products and biologically active compounds.<sup>1</sup> Nitroarenes can be transformed into anilines by a number of well-known non-catalytic methods such as Béchamp reduction or by using sulfide reagents (sodium sulfide or hydrogen sulfide and base).<sup>2</sup> The major drawbacks of Béchamp reduction involve the requirement of corrosive hydrochloric acid and excess amounts of iron or ferrous salts. In addition, these traditional processes produce a large amount of waste. Various other reducing agents such as CO/H<sub>2</sub>O,<sup>3</sup> hydroiodic acid,<sup>4</sup> sodium hydrosulfite,<sup>5</sup> tin(II) chloride,<sup>6</sup> hydrazine<sup>7</sup> and ammonia borane<sup>8</sup> have been utilized for the same purpose. Metal hydride reagents are generally not used for the reduction of nitroarenes to anilines as they tend to form azo compounds.<sup>9</sup> However, nitroarenes can be reduced to anilines by sodium borohydride in presence of Ni(OAc)<sub>2</sub>·4H<sub>2</sub>O.<sup>10</sup> Reduction

of nitroarenes by catalytic hydrogenation is considered as the most efficient method<sup>11</sup> and one of two main industrial processes for the synthesis of aniline involve the catalytic hydrogenation of nitrobenzene. In contrast to the use of stoichiometric reducing agents, classical hydrogenation of nitroarenes is much greener as it produces water as the only byproduct. This field of reduction of nitroarenes to anilines by classical hydrogenation is dominated by heterogeneous catalysts. In addition to the commercially available catalysts such as pyrophoric Raney nickel or expensive Pd/C catalysts, various other heterogeneous catalysts have been developed and utilized for the nitroarene hydrogenation.<sup>12</sup> However, heterogeneous catalysts often encounter poor chemoselectivity particularly for the nitroarenes with other reducible or labile groups such as halides, alkene or nitriles. Another disadvantage for the heterogeneous catalysts is the formation of (toxic) impurities or by-products.<sup>13</sup> In this context, homogeneous catalysts are gaining momentum for the hydrogenation of nitroarenes. High chemoselectivity can be achieved by modifying the homogeneous catalyst by changing or adjusting the ligand framework. Various noble metal catalysts (ruthenium,<sup>14</sup> rhodium,<sup>15</sup> iridium,<sup>16</sup> palladium,<sup>17</sup> platinum<sup>18</sup> and gold<sup>19</sup>) have been developed for homogeneous hydrogenation of nitroarenes. However, it is crucial to utilize cheap, earth-abundant and non-toxic base metal catalyst for the development of sustainable catalytic protocol. Several homogeneous iron catalysts were reported for the hydrogenation of nitroarenes.<sup>[20]</sup> Very recently Rueping and coworkers reported an efficient manganese catalyst for selective hydrogenation of nitroarenes in presence of catalytic amount of base (Scheme 1).<sup>21</sup> The reductions were performed at 130 °C under 80 bar of H<sub>2</sub> pressure for 24 h. In order to avoid the use of hydrogen gas and expensive and elaborate experimental set up (high pressure reactor), hydrosilylation can be considered as an easy alternative for the reduction of nitroarenes. Although hydrosilylation has been extensively utilized as an easy alternative for the hydrogenation of a wide variety of unsaturated moieties such as aldehydes, ketones,<sup>22</sup> carboxylic acids,<sup>23</sup> esters,<sup>24</sup> imine<sup>25</sup> and alkenes,<sup>26</sup> reports on the

hydrosilylation of nitroarenes are extremely limited. Few noble metals (rhenium,<sup>27</sup> rhodium,<sup>28</sup> palladium,<sup>29</sup> platinum<sup>30</sup> and gold<sup>31</sup>) were utilized for the nitroarene reduction by catalytic hydrosilylation. Although the utilization of earth-abundant, nonprecious transition metal catalysts is desirable, the reports on the base metal catalyzed hydrosilylation of nitroarenes are extremely limited (Scheme 1). Beller and coworkers used FeBr<sub>2</sub> (10 mol%) in presence of PPh<sub>3</sub> (12 mol%) for the hydrosilylation of nitroarenes.<sup>[32]</sup> Very recently, Darcel and coworkers reported an iron(0)-NHC complex (Fe(CO)<sub>4</sub>(IMes): 5 mol%) as an effective catalyst for the nitroarene reduction under hydrosilylation conditions<sup>[33]</sup> Apart from this, a few reports with nickel catalysts are also known. Quan, Wang and coworkers used Ni(acac)<sub>2</sub> (10 mol%) and polymethylhydrosiloxane for the same purpose.<sup>[34]</sup> Recently, Mandal and coworkers reported a Ni(II)-chloride complex supported by NHC (5 mol%) as an efficient catalyst for the hydrosilylation of nitroarenes.<sup>35</sup> Very recently, Royo and coworkers also utilized Ni-NHC complex for the same purpose.<sup>36</sup>

Previous work: base-metal catalyzed **hydrosilylation** of nitroarenes to anilines

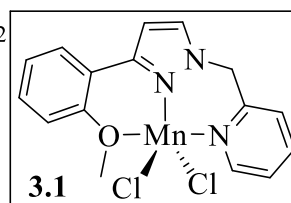
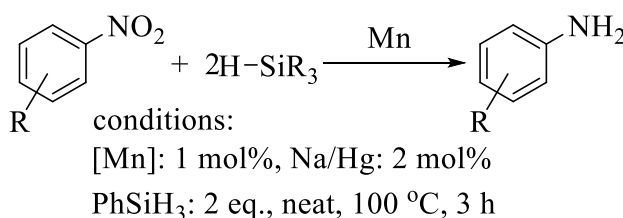


• Beller *et al.*  
 FeBr<sub>2</sub>: 10 mol%  
 PPh<sub>3</sub>: 12 mol%  
 toluene, 110 °C, 16 h

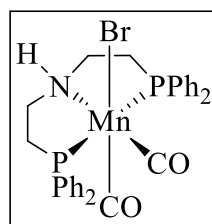
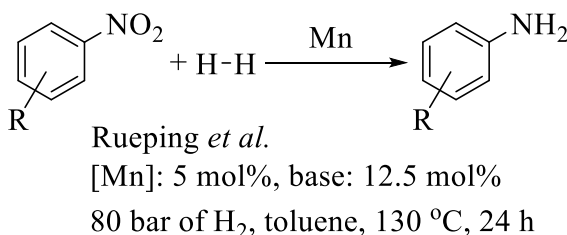
• Darcel *et al.*  
 Fe(CO)<sub>4</sub>(IMes): 5 mol%  
 toluene, 90 °C, *hn*, 20 h

• Quan and wang *et al.*  
 Ni(acac)<sub>2</sub>: 10 mol%  
 1,4-dioxane, 80 °C, 3-5 h

**Present work:** manganese catalyzed **hydrosilylation** of nitroarenes to anilines



Previous work: manganese catalyzed **hydrogenation** of nitroarenes to anilines



### Scheme 3.1 Reduction (hydrosilylation and hydrogenation) of esters by base metal catalysts.

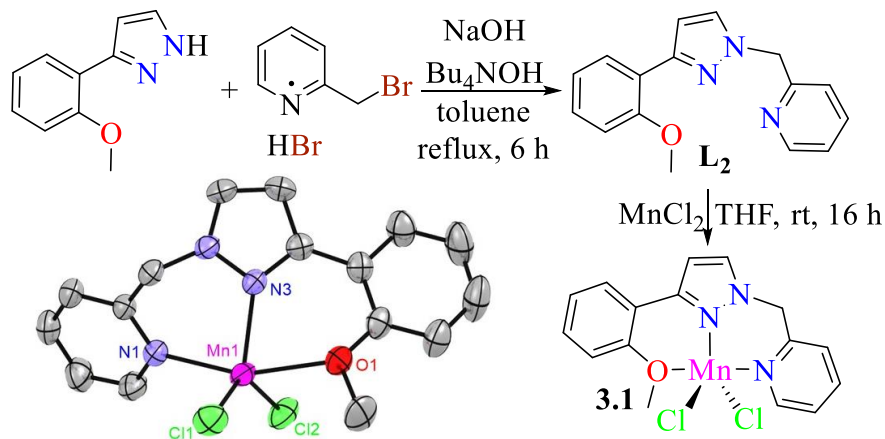
In the field of the development of homogeneous catalysts based on base metals, manganese complexes are getting serious attentions in recent years. As the third most abundant metal on the earth crust, manganese catalysts represent cheap, sustainable and less-toxic alternatives to heavily utilized noble metals such as ruthenium, rhodium, iridium and palladium in various catalytic processes. Manganese complexes have been heavily utilized as efficient catalysts for the hydrosilylation of a wide variety of unsaturated substrates such as aldehydes and ketones,<sup>37</sup> carboxylic acids,<sup>38</sup> ester,<sup>39</sup> alkenes,<sup>40</sup> alkynes<sup>41</sup> and nitriles.<sup>42</sup> Surprisingly, manganese

mediated hydrosilylation of nitroarenes to the corresponding anilines had not been reported (to the best of our knowledge). Herein, we report a readily available and air-stable manganese(II) chloride complex as an effective catalyst (in presence of sodium amalgam) for selective hydrosilylation of aromatic nitro compounds to the corresponding aniline derivatives under solvent-free conditions. Furthermore, the practical utility of this catalytic protocol was extended for the synthesis of various important compounds.

### 3.3 Result and Discussion

The field of homogeneous catalysis utilize a wide range of ligands, which might have various distinctive effects on the reactivity of the corresponding metal catalysts and thus, the outcome of a homogeneous catalytic process is highly dependent on the ligand environments. Pincer ligands are one of the important class of ligands which have been successfully utilized in varieties of chemical transformations in last fifteen to twenty years. A large number of pincer ligands consists of one or more phosphine donor arms (such as PNP, PNN and PCP) which are air-sensitive and difficult to handle. Therefore, phosphine-free ligand synthesis has gained a considerable attention in the field of homogeneous catalysis.<sup>43</sup> We have utilized an air-stable NNO pincer ligand **L1** by reacting 3-(2-methoxyphenyl)-1H-pyrazole with 2-(chloromethyl)-pyridine in presence of base (Scheme 2). Facile coordination of **L1** with  $\text{MnCl}_2$  at r.t. in air resulted in the formation of complex **3.1** as yellow solid (Scheme 2). Air-stable complex **3.1** is paramagnetic and was characterized by mass and elemental analysis. ESI-mass analysis of complex **3.1** displayed a peak at 355.0296 corresponds to  $[\text{M} - \text{Cl}]^+$ . Single crystal X-ray analysis further confirmed the identity of complex **3.1** (Scheme 3.1). Complex **3.1** crystallized in the monoclinic system with  $P2_1/c$  space group. A neutral  $[\text{Mn}(\text{NNO})\text{Cl}_2]$  unit is present in the asymmetric unit. The coordination geometry around the manganese center is strictly described as very distorted square pyramidal (Addison parameter  $\tau = 0.48$ ); however, the geometry lies pretty much in the middle of square pyramidal ( $\tau = 1$ ) and trigonal bipyramidal

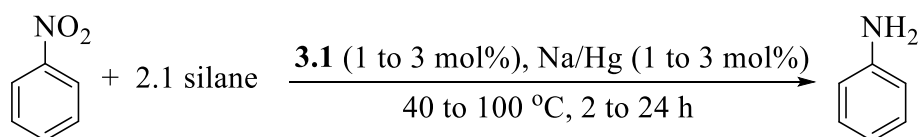
( $\tau = 0$ ). The bond distances and bond angles around the metal center are very consistent with similar manganese(II) complexes.<sup>37i</sup>



**Scheme 3.2** Synthesis of complex **3.1** with the molecular structure of **1** showing 50% ellipsoids<sup>a</sup>

<sup>a</sup>Hydrogen atoms are omitted for clarity. Selected bond distances (Å) and angles (deg): Mn1-Cl1 2.3351(Å), Mn1-Cl2 2.3323(Å), Mn1-N1 2.232(Å), Mn1-N3 2.151(Å), Mn1-O1 2.395(Å) and N1-Mn1-Cl1 97.118(8), Cl1-Mn1-Cl2 130.628(4), N1-Mn1-O1 159.696(9), O1-Mn1-Cl2 89.094(7), N3-Mn1-N1 86.703(9), N3-Mn1-O1 73.157(9).

**Table 3.1.** Catalytic performance of complex **1** for the hydrosilylation of nitrobenzene<sup>a</sup>

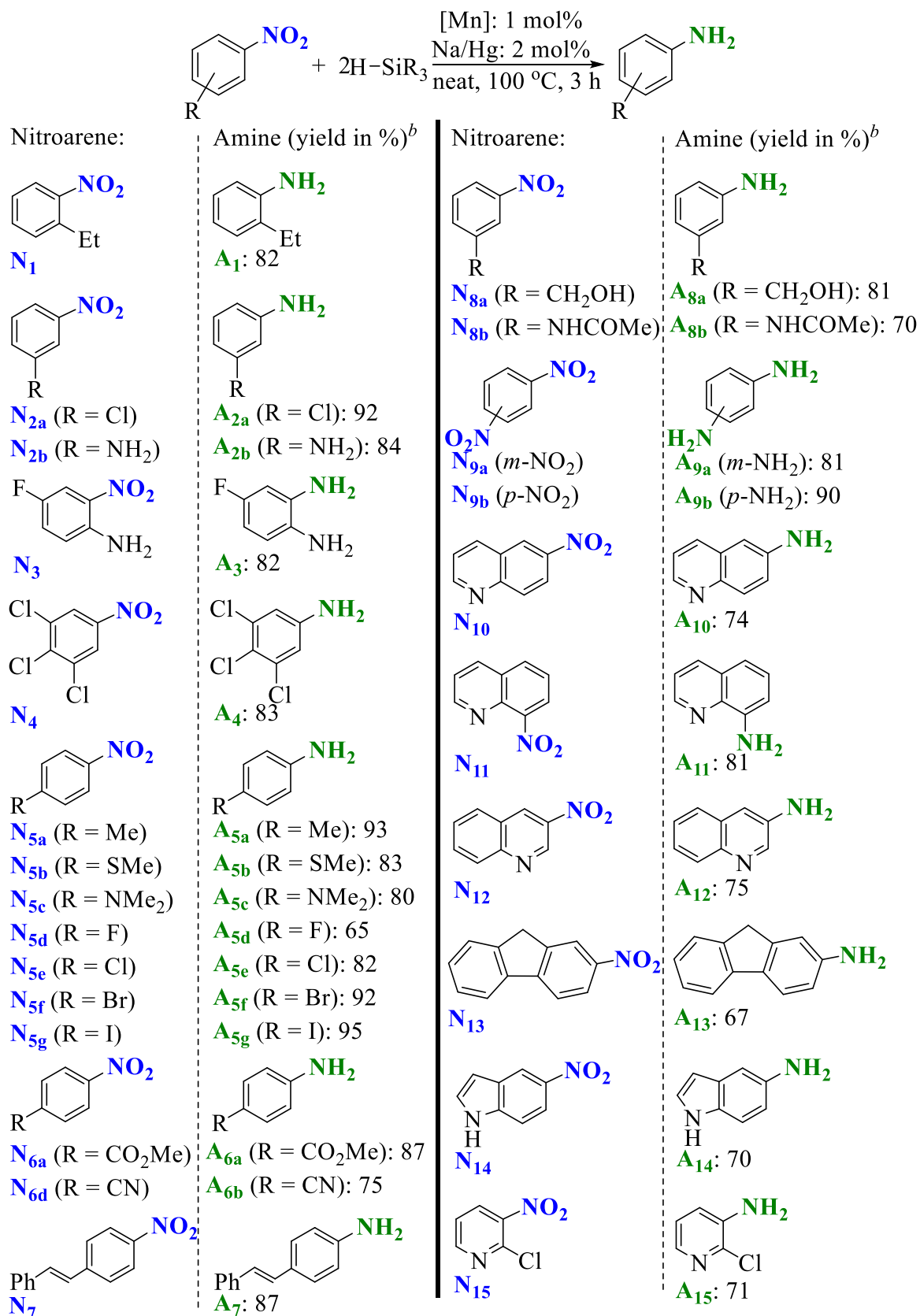


Ent	<b>1</b> , Na/Hg (mol%)	Silane (2.1 eq.)	Temp (° C)	Time (h)	Yield <sup>b</sup> (%)
<b>1</b>	3, 3	PhSiH <sub>3</sub>	100	24/12/6	>99 (98) <sup>c</sup>

<b>2</b>	3, 3	PhSiH <sub>3</sub>	100	5	98
<b>3</b>	no, no	PhSiH <sub>3</sub>	100	6	0
<b>4</b>	3, 3	Ph <sub>2</sub> SiH <sub>2</sub>	100	6	25
<b>5</b>	3, 3	Ph <sub>3</sub> SiH	100	6	<5
<b>6</b>	3, 3	Et <sub>3</sub> SiH	100	6	<10
<b>7</b>	3, 3	<i>i</i> Pr <sub>3</sub> SiH	100	6	<5
<b>8</b>	3, 3	Me <sub>2</sub> PhSiH	100	6	<10
<b>9</b>	2, 2	PhSiH <sub>3</sub>	100	6	82/68
<b>10</b>	2, 2	PhSiH <sub>3</sub>	100	8	>99 (98) <sup>c</sup>
<b>11</b>	2, 2	PhSiH <sub>3</sub>	80/60/40	6	72/50/36
<b>12</b>	1, 1	PhSiH <sub>3</sub>	100	8	88
<b>13</b>	1, 1	PhSiH <sub>3</sub>	100	10	>99 (99) <sup>c</sup>
<b>14</b>	1, 2	PhSiH <sub>3</sub>	100	12/6/3	>99 (99) <sup>c</sup>
<b>15</b>	1, 2	PhSiH <sub>3</sub>	100	2	94
<b>16</b>	1, no	PhSiH <sub>3</sub>	100	3	0

<sup>a</sup>Reactions conducted in pressure tube (15 ml) with 0.50 mmol of nitrobenzene, 1.05 mmol of silane, 3/2/1 mol% of **3.1** and 3/2/1 mol% of Na/Hg. <sup>b</sup>Yields of aniline were determined by GC using p-xylene (0.50 mmol) as standard. <sup>c</sup>Isolated yields.

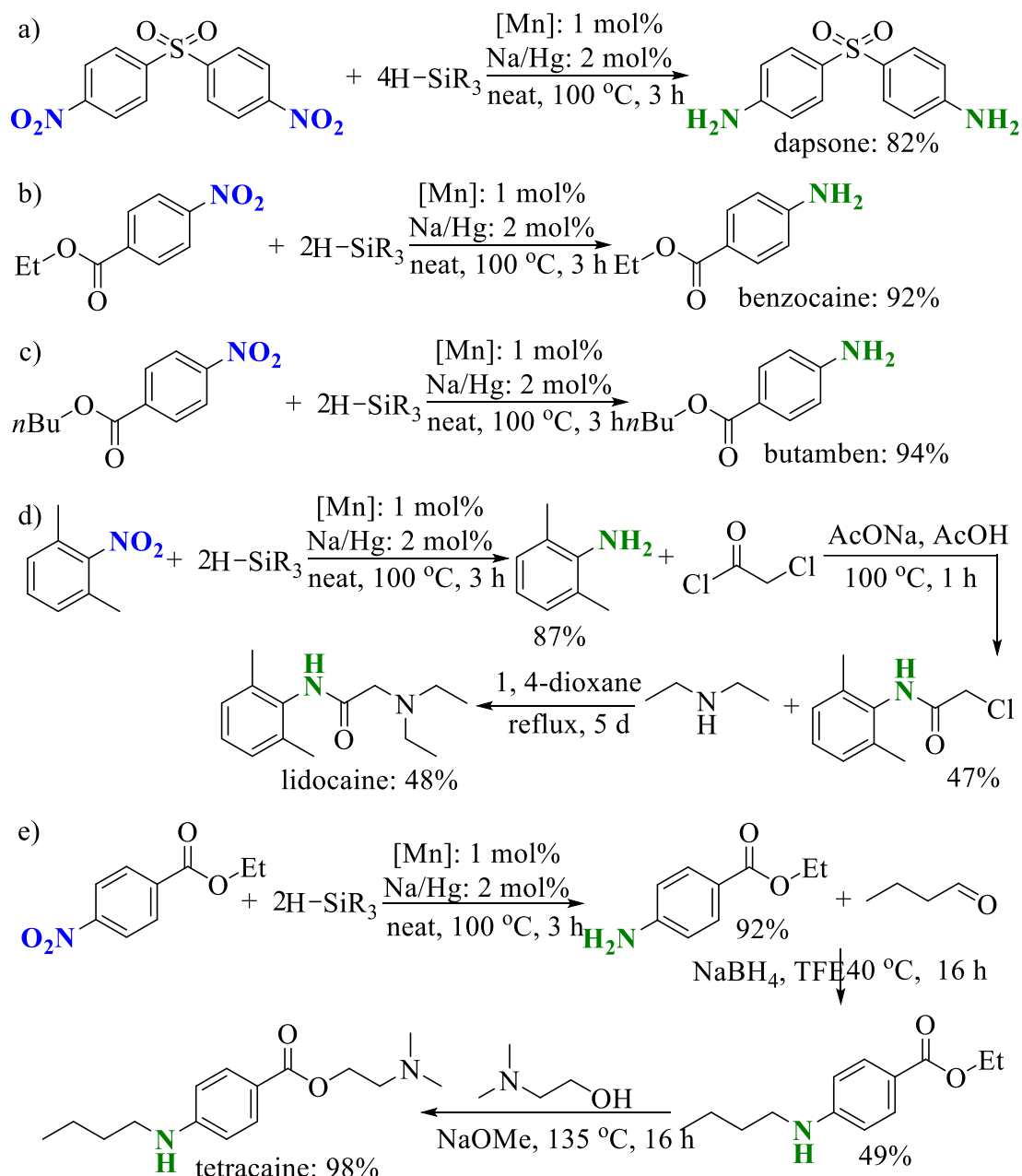
With the air-stable manganese complex **3.1** in hand, we set out to evaluate the catalytic activity of **3.1** for the hydrosilylation of nitroarene using nitrobenzene as standard substrate under various reaction conditions (Table 1). Nitrobenzene was completely reduced to aniline when it was heated with 2.1 eq. of phenylsilane at 100 °C for 24/12/6 h in presence of 3 mol% complex **3.1** and Na/Hg (entry 1). A small amount of unreacted nitrobenzene was observed if the reaction time was reduced to 5 h (entry 2). A blank test was performed and only starting nitrobenzene was recovered (entry 3). Various secondary and tertiary silanes such as diphenylsilane (entry 4), triphenylsilane (entry 5), triethylsilane (entry 6), triisopropylsilane (entry 7) and dimethylphenylsilane (entry 8) were utilized. Approximately 25% conversion of nitrobenzene to aniline was obtained by using diphenylsilane in 6 h and all tertiary silanes gave very poor yield (less than 10%) in 6 h. Reducing the catalyst loading to 2 mol% (both **3.1** and Na/Hg), approximately 80% reduction was achieved in 6 h at 100 °C (entry 9); however, complete reduction was obtained in 8 h (entry 10). The hydrosilylations of nitrobenzene were also carried out at lower temperatures (80, 60 and 40 °C) and much reduced conversions were obtained (entry 11). Catalyst loading (both **3.1** and Na/Hg) was further reduced to 1 mol% and complete reduction was obtained in 10 h at 100 °C (entry 13). So far, 1:1 stoichiometric ratio of complex **3.1** and Na/Hg was used and this is suitable for the reduction of Mn(II) to Mn(I). However, 1:2 stoichiometric ratio of **3.1** and Na/Hg is essential for the reduction of Mn(II) to Mn(0) which is also a likely scenario. Therefore, we utilized 1 mol% of **3.1** and 2 mol% of Na/Hg for the following hydrosilylations (entry 14 and 15). Nitrobenzene was completely reduced to aniline in just 3 h in presence of 1 mol% of complex **3.1** and 2 mol% of Na/Hg (entry 14). The reduction of Mn(II) complex (**3.1**) is essential for the hydrosilylation of nitrobenzene as only starting material was recovered from the hydrosilylation in absence of Na/Hg (entry 16). Therefore, following condition was regarded as the optimized reaction condition: 1 mol% **3.1**, 2 mol% Na/Hg, 2.1 eq. of PhSiH<sub>3</sub>, 3 h, 100 °C (entry 14).



**Scheme 3.3** Selective hydrosilylation of nitroarenes with various functionalities catalyzed by complex 3.1<sup>a</sup>

<sup>a</sup>Reactions conducted in pressure tube (15 ml) with 0.50 mmol of nitroarene, 1.05 mmol of PhSiH<sub>3</sub>, 1 mol% of **3.1** and 2 mol% of Na/Hg. <sup>b</sup>Isolated yields.

Thereafter, the optimized reaction conditions were evaluated for the hydrosilylations of various nitroarenes with a wide range of functionalities to expand the substrate scope (Scheme 3). A large number of substituted nitrobenzenes with various electron donating groups such alkyls, thiomethyl, halides and amino groups (**N**<sub>1</sub>, **N**<sub>2a</sub>, **N**<sub>2b</sub>, **N**<sub>3</sub>, **N**<sub>4</sub>, **N**<sub>5a</sub>, **N**<sub>5b</sub>, **N**<sub>5c</sub>, **N**<sub>5d</sub>, **N**<sub>5e</sub>, **N**<sub>5f</sub>, and **N**<sub>5g</sub>) at *ortho*, *meta* and *para*-positions were effectively reduced to the corresponding anilines in good to excellent isolated yields (**A**<sub>1</sub>: 82%, **A**<sub>2a</sub>: 92%, **A**<sub>2b</sub>: 84%, **A**<sub>3</sub>: 82%, **A**<sub>4</sub>: 83%, **A**<sub>5a</sub>: 93%, **A**<sub>5b</sub>: 83%, **A**<sub>5c</sub>: 80%, **A**<sub>5d</sub>: 65%, **A**<sub>5e</sub>: 82%, **A**<sub>5f</sub>: 92%, and **A**<sub>5g</sub>: 95%). It should be underlined that the halogenated substrates were tolerated well. Reductions were also well conducted with nitroarenes with electron withdrawing substituents such as esters, cyano, hydroxymethyl and amide (**N**<sub>6a</sub>, **N**<sub>6b</sub>, **N**<sub>8a</sub> and **N**<sub>8b</sub>). 4-Nitrostilbene (**N**<sub>7</sub>) was easily reduced to 4-styrylaniline (**A**<sub>7</sub>: 87%). Interestingly reduction was selective to nitro group and reducible functionalities such as ester, cyano, amide and alkene were unaltered. Both nitro groups of 1,3-dinitrobenzene (**N**<sub>9a</sub>) and 1,4-dinitrobenzene (**N**<sub>9b</sub>) were efficiently reduced to the corresponding phenylenediamine (**A**<sub>9a</sub>: 81%, and **A**<sub>9b</sub>: 90%). Hydrosilylations of various nitroquinolines (**N**<sub>10</sub>, **N**<sub>11</sub> and **N**<sub>12</sub>) gave corresponding aminoquinolines in good yields (**A**<sub>10</sub>: 74%, **A**<sub>11</sub>: 81%, and **A**<sub>12</sub>: 75%). Polycyclic aromatic nitrocompound 2-nitrofluorene (**A**<sub>13</sub>: 67%) was also successfully tested. Finally, heteroaromatic nitro species 5-nitroindole (**N**<sub>14</sub>) and 2-chloro-3-nitropyridine (**N**<sub>15</sub>) were successfully reduced to 5-aminoindole (**A**<sub>14</sub>: 70%) and 3-amino-2-chloropyridine (**A**<sub>15</sub>: 71%), respectively.



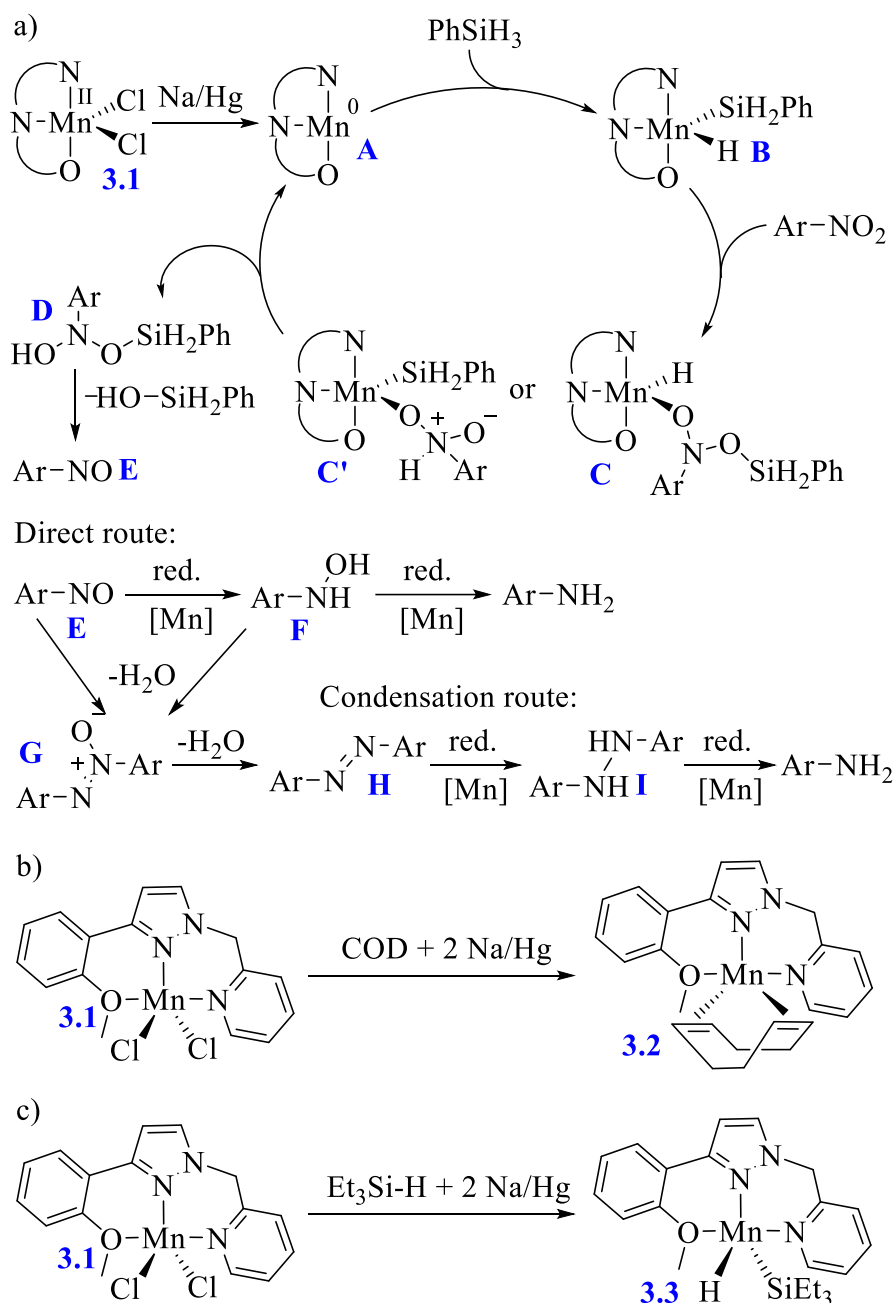
**Scheme 3.4** Syntheses of drug molecules a) dapsone, b) benzocaine, c) butamben, d) lidocaine and e) tetracaine by utilizing present hydrosilylation protocol.

Inspired by the successful reductions of various nitroarenes, we explored the possibility to diversify the application of this catalytic hydrosilylation of nitroarenes. The syntheses of several important drug molecules were explored (Scheme 4). At first, we targeted the synthesis of dapsone (diaminodiphenyl sulfone) which is an antibiotic commonly used for the treatment of leprosy and various other skin diseases. Commonly the synthesis of dapsone involves the

reduction of dinitrodiphenyl sulfone with toxic  $\text{SnCl}_2/\text{HCl}$  (stoichiometric). Using the present optimized hydrosilylation conditions, we synthesized dapsone in excellent isolated yield (Scheme 4a). Syntheses of benzocaine (ethyl 4-aminobenzoate) and butamben (butyl 4-aminobenzoate), important anesthetics commonly used as topical pain reliever, are another important example to demonstrate the scope of the present catalytic protocol (Scheme 4b and 4c). Present syntheses of benzocaine and butamben is superior as the common synthetic procedures involve the reduction of p-nitrobenzoates with highly toxic  $\text{Sn}/\text{HCl}$  (stoichiometric). Dapsone, benzocaine and butamben were also synthesized in gram-scale. As an extension of present hydrosilylation protocol, we also synthesized lidocaine and tetracaine which are also important local anesthetics (Scheme 4d and 4e).

A plausible catalytic path for the hydrosilylation of nitroarene is proposed (Scheme 5a), which is also supported by the previous studies.<sup>33</sup> During reaction optimization, we noted that manganese(II) catalyst (**3.1**) in presence of 2 equivalent of  $\text{Na}/\text{Hg}$  displayed much enhanced activity as compared to the 1:1 stoichiometric ratio of complex **3.1** and  $\text{Na}/\text{Hg}$ . This suggests the reduction of manganese(II) pre-catalyst **3.1** to manganese(0) species (**A**) as active catalyst. Oxidative addition of silicon-hydrogen bond to **A** resulted in the formation of silyl manganese(II) hydride species **B**. Thereafter, binding of nitroarene gave either species **C** or **C'**. Finally, reductive elimination of  $\text{Ar-N}(\text{OSiH}_2\text{Ph})\text{OH}$  (**D**) regenerates active catalyst **A**. Thereafter,  $\text{Ar-N}(\text{OSiH}_2\text{Ph})\text{OH}$  (**D**) forms nitrosoarene (**E**) which is further reduced to aniline either by direct route or via condensation route. Direct route involves the reduction of aryl nitroso  $\text{Ar-NO}$  (**E**) to N-hydroxylaniline  $\text{Ar-NHOH}$  (**F**) to aniline  $\text{Ar-NH}_2$ . Condensation route involves the condensation of aryl nitroso  $\text{Ar-NO}$  (**E**) and N-hydroxylaniline  $\text{Ar-NHOH}$  (**F**) to azoxyarene (**G**) followed by the formation of dehydration product azoarene (**H**). Azoarene (**H**) is finally reduced to aniline via hydrazine intermediate (**I**). Based on

experimental evidences, Rueping et al. previously suggested manganese catalyzed hydrogenation of nitroarene proceeds via direct reduction route with the formation of N-hydroxyaniline Ar-NHOH (**F**). We performed mass analysis from the reaction mixture to detect any intermediate. We could not identify any mass peak for N-hydroxyaniline Ar-NHOH (**F**); however, the formation of azoarene (**H**) was clearly detected by mass analysis ( $M^+$ : 242.1103). Therefore, the possibility of condensation route could not be ruled out in present manganese catalyzed hydrosilylation of nitroarene. To shed further light on the reaction mechanism, we performed several control experiments (Scheme 5b and 5c). Reaction of **3.1** with 1 and 2 eq. of Na/Hg resulted in NMR inactive species which could not be isolated in pure form. As Mn(I) compounds are generally NMR active, it is expected that reduction of Mn(II) complex **3.1** gave Mn(0) species. To trap the proposed Mn(0) species, further reduction of **3.1** with Na/Hg (2 eq.) was performed in presence of COD (Scheme 5d). We isolated COD stabilized Mn(0) species **3.2** which was characterized by HRMS and elemental analysis. Thereafter, we carried out the reduction of **3.1** with Na/Hg (2 eq.) performed in presence of Et<sub>3</sub>SiH and complex **3.3** was isolated as product (Scheme 5e). Complex **3.1** was reduced to Mn(0) species and oxidative addition of silicon-hydrogen bond yielded complex **3**, which is in agreement with initial steps of the proposed catalytic cycle. Despite several attempts, we could not get solid state structural information due to the poor quality of those crystals. Catalytic hydrosilylation of 4-nitroanisole in presence of TEMPO radical took place without the loss of any catalytic activity which suggests to exclude radical process. Hydrosilylation of 4-nitroanisole was also unaltered in presence of excess mercury, which suggests to exclude the formation nano-particles.



**Scheme 3.5** Plausible catalytic path for the hydrosilylation of nitroarene and control experiments.

### 3.5 Conclusion

In conclusion, we have developed an air-stable manganese complex for the efficient hydrosilylation of nitroarenes. Number of reports on hydrosilylation of nitroarenes by base metal homogeneous catalysts is extremely limited; only iron and nickel catalysts are known.

However, utilization of base metal catalysts is essential for the sustainable reduction of nitroarenes. To the best of our knowledge, this is the first report on manganese-catalyzed hydrosilylation of nitroarenes. Various nitroarenes with different electron donating and electron withdrawing functionalities were effectively reduced to the corresponding aromatic amines. Several reducible functionalities such as ester, cyano, amide and alkene were tolerated and this chemoselective reduction of nitro group is an attractive development. Application of this catalytic hydrosilylation protocol was diversified in the syntheses of several important drug molecules such as dapson, benzocaine, butamben, lidocaine and tetracaine. Instead of using toxic reduction route (e.g. Sn/HCl), present catalytic protocol is much appealing. Based on previous reports and supported by experimental evidences, we propose a catalytic path which involve the reduction of manganese(II) to manganese(0) followed by the oxidative addition of silane. Further investigation will involve the use of the present catalytic protocol for the reduction of unsaturated substrates in different hydrofunctionalization reactions.

## 3.6 EXPERIMENTAL SECTION

### 3.6.1 Materials:

All air and moisture sensitive experiments such as catalytic hydrosilylations of nitroarenes were performed under dry nitrogen atmosphere using standard Schlenk or glovebox (MBraun) techniques. Hydrosilylations of nitroarenes were performed in Ace pressure tubes purchased from Sigma-Aldrich. For the air sensitive experiments, solvents (acetonitrile, hexanes, diethyl ether, pentane and THF) were distilled, degassed and stored over 3 Å molecular sieves. Solvents (acetonitrile, hexanes, pentane, ethyl acetate, DCM, MeOH and THF) were purchased from Merck, Finar and Rankem. For recording NMR spectra of air and moisture sensitive samples, CDCl<sub>3</sub> was degasses and stored over 3 Å molecular sieves. CDCl<sub>3</sub> was purchased from Sigma Aldrich. MnCl<sub>2</sub>, PhSiH<sub>3</sub>, Ph<sub>2</sub>SiH<sub>2</sub>,

Ph<sub>3</sub>SiH, *i*Pr<sub>3</sub>SiH, , Me<sub>2</sub>PhSiH, Et<sub>3</sub>SiH, Na/Hg (20% Sodium) and all nitroarenes as substrates for hydrosilylations were purchased from Sigma Aldrich, Alfa Aesar and TCI Chemicals and used without further purification.

### 3.6.2 Physical Measurements:

<sup>1</sup>H and <sup>13</sup>C NMR spectra were recorded at Bruker AV-400 and JEOL-400 (<sup>1</sup>H at 400 MHz and <sup>13</sup>C at 101 MHz). <sup>1</sup>H NMR chemical shifts are referenced in parts per million (ppm) with respect to tetramethylsilane ( $\delta$  0.00 ppm) and <sup>13</sup>C{<sup>1</sup>H} NMR chemical shifts are referenced in ppm with respect to CDCl<sub>3</sub> ( $\delta$  77.16 ppm). The coupling constants (*J*) are reported in hertz (Hz). The following abbreviations are used to describe multiplicity: s = singlet, brs = broad signal, d = doublet, t = triplet, q = quadrate, m = multiplate. High resolution mass spectra were recorded on a Bruker micrOTOF-Q II Spectrometer. Elemental analysis was carried out on a EuroEA Elemental Analyser. GC analyses were performed on a Shimadzu GC-2014 spectrometer. GC-MS analyses were performed on a Shimadzu GCMS-QP2010 Plus spectrometer. Crystal data were collected with Rigaku Oxford diffractometer and with INCOATEC micro source (Mo-K $\alpha$  radiation,  $\lambda = 0.71073$  Å, multilayer optics) at 293 K.

### 3.6.3 Crystal Structure Determination:

A crystal of complex **1** (CCDC 2176244) was mounted in air at ambient conditions. All measurements were made on an *Oxford Diffraction SuperNova* area-detector diffractometer<sup>[S16]</sup> using mirror optics monochromated Mo K $\alpha$  radiation ( $\lambda = 0.71073$  Å) and Al filtered.<sup>[S17]</sup> The unit cell constants and an orientation matrix for data collection were obtained from a leastsquares refinement of the setting angles of reflections in the range  $2.1 < \theta < 26.4^\circ$ . A total of 1090 frames were collected using  $\omega$  scans, with 30+30 seconds exposure time, a rotation angle of  $1.0^\circ$  per frame, a crystal-detector distance of 65.0 mm, at T = 123(2) K. Data reduction

was performed using the *CrysAlisPro* <sup>[S16]</sup> program. The intensities were corrected for Lorentz and polarization effects, and an absorption correction based on the multiscan method using SCALE3 ABSPACK in *CrysAlisPro* <sup>[S16]</sup> was applied. Data collection and refinement parameters are given in Table 1. The structure was solved by direct methods using *SHELXT* <sup>[S18]</sup>, which revealed the positions of all non-hydrogen atoms of the title compound. The non-hydrogen atoms were refined anisotropically. All H-atoms were placed in geometrically calculated positions and refined using a riding model where each H-atom was assigned a fixed isotropic displacement parameter with a value equal to 1.2Ueq of its parent atom. Refinement of the structure was carried out on  $F^2$  <sup>[S17]</sup> using full-matrix least-squares procedures, which minimized the function  $\sum w(F_o^2 - F_c^2)^2$  <sup>[S17]</sup>. The weighting scheme was based on counting statistics and included a factor to downweight the intense reflections. All calculations were performed using the *SHELXL-2014/7* <sup>[S19]</sup> program.

### 3.6.4 Syntheses:

#### Syntheses of ligand and corresponding manganese complex

**Synthesis of L<sub>1</sub>.** In a pressure tube, 3-(2-methoxyphenyl)-1H-pyrazole (1.74 g, 10.0 mmol), 2-(chloromethyl) pyridine hydrochloride (1.64 g, 10.0 mmol), NaOH solution (40%, 5 mL) and toluene (15 mL) were added and the reaction mixture was stirred at r.t. for 15 mins. Then tert-butylammonium hydroxide (4 mL) was added and the reaction mixture was stirred at 130 °C temperature for 24 h. The resulting red mixture was cooled down to r.t. and extracted with ethyl acetate (3 x 50 mL). All volatiles were removed under high vacuum to give **L<sub>1</sub>** as pure procedure (2.27 g, 73%). <sup>1</sup>H NMR (400 MHz, CDCl<sub>3</sub>) δ 8.57 (d,  $J = 4.6$  Hz, 1H), 7.96 (d,  $J = 7.6$  Hz, 1H), 7.61 (t,  $J = 7.7$  Hz, 1H), 7.54 (s, 1H), 7.31 – 7.26 (m, 1H), 7.22 – 7.14 (m, 1H), 7.06 – 6.94 (m, 3H), 6.85 (s, 1H), 5.51 (s, 2H), 3.90 (s, 3H). <sup>13</sup>C NMR (101 MHz, CDCl<sub>3</sub>) δ 156.7, 156.5, 149.00, 148.6, 136.8, 130.3, 128.6, 128.47, 122.43, 122.1, 121.4, 120.6, 111.1, 107.5, 57.4, 55.2. HRMS (ESI-TOF)  $m/z$ : [M]<sup>+</sup> calcd for C<sub>16</sub>H<sub>15</sub>N<sub>3</sub>O 265.1215; found

265.1289. Anal. Calcd for  $C_{16}H_{15}N_3O$  (265.1215): C, 72.43; H, 5.70; N, 15.89. Found: C, 72.41; H, 5.65; N, 15.71.

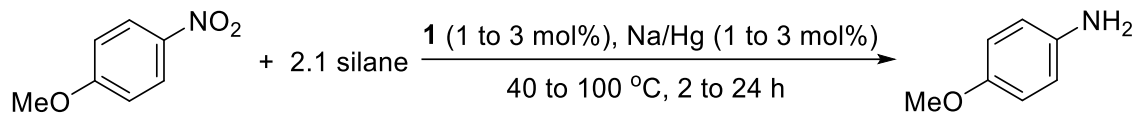
**Synthesis of 1.** A dried 50ml schlenk tube was charged with a mixture of  $MnCl_2$  (0.063 g, 0.50 mmol) and NNO pincer ligand (0.146 g, 0.55 mmol) in THF (10mL). The reaction vessel was sealed and stirred at ambient condition for overnight. After the completion of reaction, the resulting in a white precipitate was syringed off and the solid was washed with hexanes (3 x 10 mL) and was dried under high vacuum to give complex 1 (0.185 g, 95%) as pure compound. Note: Single crystals suitable for X-ray structural analysis were obtained by slow diffusion of DEE into a solution of complex 1 in Methanol or by slow diffusion of pentane into a solution of complex 1 in acetone. Complex 1 is a new compound and was characterized by high resolution mass spectrometry, elemental analysis and single crystal X-ray analysis. HRMS (ESI-TOF)  $m/z$ :  $[M - Cl]^+$  calcd for  $C_{16}H_{15}ClMnN_3O$ : 355.70, found 355.0296  $[M - Cl]^+$ . Anal. Calcd for  $C_{16}H_{15}Cl_2MnN_3O$  (391.15): C, 49.13; H, 3.87; N, 10.74. Found: C, 49.06; H, 3.91; N, 10.71.

### Crystal data of complexes

(NNO) $MnCl_2$ (3.1):  $C_{16}H_{15}Cl_2MnN_3O$ , white niddle shaped, crystal size: 0.3 x 0.2 x 0.2 mm<sup>3</sup>,  $M = 372.11$ , Monoclinic with space group  $P2_1/c$ ,  $a = 13.1725(4)\text{\AA}$ ,  $b = 16.8592(5)\text{\AA}$ ,  $c = 8.3349(2)\text{\AA}$ ,  $\alpha = 90^\circ$ ,  $\beta = 102.266(3)^\circ$ ,  $\gamma = 90^\circ$ ,  $V = 1808.74(9)\text{\AA}^3$ ,  $Z = 21$ ,  $F(000) = 796.0$ ,  $\mu$ -( $MoK\alpha$ ) = 1.031 mm<sup>-1</sup>,  $\theta$  Range = 6.776-60.94°,  $D_{calc} = 1.436\text{ g/cm}^{-3}$ ,  $T = 293(2)K$ , Data/Restraints/parameters = 4703/0/209, Reflections collected, 39369 unique ( $R_1 = 0.0596$ ,  $wR_2 = 0.1136$ ) (all data). The structure has been deposited at the CCDC data center and can be retrieved using the deposit number 2176244.

## General procedure for the hydrosilylation of nitroarenes

General conditions for reaction optimization:



In a dried pressure tube fitted with a magnetic stir bar, complex **1** (1/2/3 mol%), Na/Hg (1.1/2.2/3.3 mol%), *p*-nitroanisole (77 mg, 0.5 mmol), phenylsilane (109 mg, 1.05 mmol) were added successively under nitrogen atmosphere. The reaction mixture was heated at appropriate temperature (40/60/80/100 °C) in a preheated oil bath for 2 to 24 h. After cooling to r.t., MeOH (2 mL) and *p*-xylene (53 mg, 0.5 mmol) was added to the resultant mixture. The mixture was then analyzed by GC to determine the conversion of the nitroarene to the amine. Thereafter, water (6 mL) was added to the previous mixture and the mixture was extracted with DCM or ethylacetate (3 x 12 mL). The organic layer was collected and dried over anhydrous Na<sub>2</sub>SO<sub>4</sub>. All volatiles were removed under high vacuum to give crude product. Occasionally, the crude product was purified by column chromatography using silica as stationary phase and a mixture of hexanes and ethyl acetate as eluent.

Reaction optimization with other reducing agents: We used Zn, Mg, NaBH<sub>4</sub>, LiBHET<sub>3</sub> and KC<sub>8</sub> instead of Na/Hg. The results are summarized in Table S2:

**Table 3.2 Catalytic performance of complex 1<sup>a</sup> using Zn, Mg, NaBH<sub>4</sub>, LiBHET<sub>3</sub> and KC<sub>8</sub> instead of Na/Hg.**

entry	1	reductant	silane	temp	time	yield <sup>b</sup>
	(mol%)	(mol%)	(2.1 eq.)	(°C)	(h)	(%)
1	1	Zn (2)	PhSiH <sub>3</sub>	100	3	<10

2	1	Mg (2)	PhSiH <sub>3</sub>	100	3	<5
3	1	NaBHET <sub>3</sub> (2)	PhSiH <sub>3</sub>	100	3	0
4	1	LiBHET <sub>3</sub> (2)	PhSiH <sub>3</sub>	100	3	0
5	1	KC <sub>8</sub> (2)	PhSiH <sub>3</sub>	100	3	>99 (98) <sup>c</sup>
6	1	KC <sub>8</sub> (2)	PhSiH <sub>3</sub>	100	2	91

<sup>a</sup>Reactions conducted in pressure tube (15 ml) with 0.50 mmol of 4-nitroanisole, 1.05 mmol of silane, 3/2/1 mol% of **1** and 3/2/1 mol% of Na/Hg. <sup>b</sup>Yields of 4-methoxyaniline were determined by GC using *p*-xylene (0.50 mmol) as standard. <sup>c</sup>Isolated yields.

Following are the representative GCMS data of crude product and <sup>1</sup>H NMR spectra of pure product.

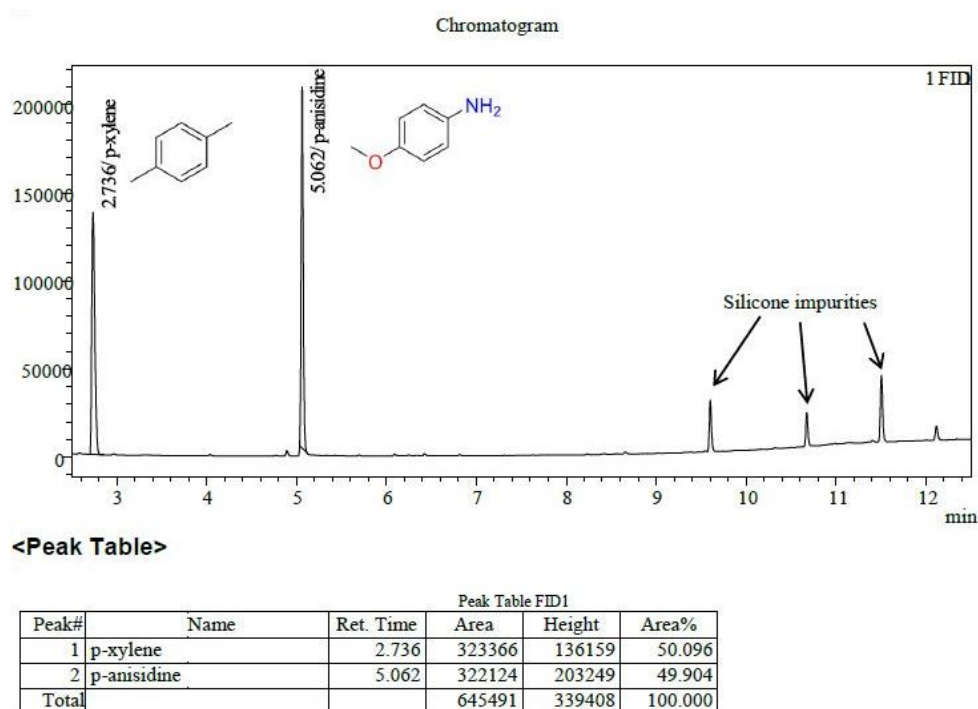


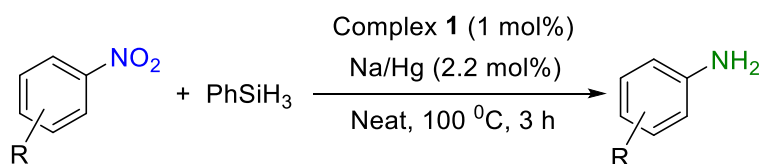
**Figure 3.1** Representative GCMS spectrum of the crude reaction mixture from catalytic hydrosilylation of *p*-nitroanisole performed in presence of 2.1 eq. of PhSiH<sub>3</sub>, 1 mol% of complex **1**, and 2.2 mol% of Na/Hg at 100 °C for 3 h (*p*-xylene as standard).

**Attempted isolation of silylated amine derivative:**

**Attempt 1:** In a dried pressure tube fitted with a magnetic stir bar, complex **1** (1 mol%), Na/Hg (2.2 mol%), *p*-nitroanisole (77 mg, 0.5 mmol), phenylsilane (109 mg, 1.05 mmol) were added successively under nitrogen atmosphere. The reaction mixture was heated at 100 °C in a preheated oil bath for 3 h. After cooling to r.t., dry MeOH (2 mL) was added (no water). The mixture was then analyzed by GC and we observed that *p*-nitroanisole converted to 4-methoxyaniline.

**Attempt 2:** In a dried pressure tube fitted with a magnetic stir bar, complex **1** (1 mol%), Na/Hg (2.2 mol%), *p*-nitroanisole (77 mg, 0.5 mmol), phenylsilane (109 mg, 1.05 mmol) were added successively under nitrogen atmosphere. The reaction mixture was heated at 100 °C in a preheated oil bath for 3 h. After cooling to r.t., dry THF (2 mL) was added (no water). The mixture was then analyzed by GC and we observed that *p*-nitroanisole converted to 4-methoxyaniline.

**Note:** We could not detect the formation of silylated amine derivative even in absence of added water at the end of hydrosilylation. Siloxanes are the final byproducts in this type of hydrosilylation. Silynol ( $R_3Si-OH$ ) is an initial byproduct which condenses to give siloxanes and water. This water may hydrolyzed silylated amine derivative. In addition, we would like to point out that proposed mechanism involves the reductive elimination of  $Ar-N(OSiH_2Ph)OH$  which gradually reduced to arylnitroso ( $Ar-NO$ ) to *N*-hydroxylaniline ( $Ar-NHOH$ ) to aniline ( $Ar-NH_2$ ).

**General conditions for substrate screening:**

In a dried pressure tube fitted with a magnetic stir bar, complex **1** (1 mol%), Na/Hg or  $KC_8$

(2.2 mol%), *p*-nitroanisole (77 mg, 0.5 mmol), phenylsilane (109 mg, 1.05 mmol) were added successively under nitrogen atmosphere. The reaction mixture was heated at an appropriate temperature (100 °C) in a preheated oil bath for 3 h. After cooling to r.t., MeOH (2 mL) and water (6 mL) (occasionally 10 wt% of NaOH solution (6 mL)) were added to the resultant mixture. The mixture was then extracted with DCM (3 x 12 mL). The organic layer was collected and dried over anhydrous Na<sub>2</sub>SO<sub>4</sub>. All volatiles were removed under high vacuum to give crude product. The crude product was purified by column chromatography using silica as stationary phase and a mixture of hexanes and ethyl acetate as eluent.

**Note:** 3-nitrothiophene, 2-bromo-5-nitrofurane, 1-ethynyl-4-nitrobenzene, 4-nitrobenzamide, 4-nitrocinnamic acid and 2-hydroxy-4-nitrobenzoic acid did not undergo hydrosilylation and (2-nitroethyl)benzene gave mixture of products under present reaction conditions.

Following are possible reasons:

Nitro group on pyridyl (or phenyl) moiety was reduced successfully. However, respective furyl and thienyl compound did not give any conversion. Five membered heterocycles with an electronegative heteroatom (such as furan and thiophene) are generally electron rich compared to benzene or pyridine (six electrons for five-atoms vs. six-atoms). Therefore, furan and thiophene are considered as  $\pi$ -excessive and pyridine is considered as  $\pi$ -deficient. The  $\pi$ -excessive nature of furyl and thienyl group in 2-bromo-5-nitrofurane and 3-nitrothiophene makes the nitro groups very electron rich. Thus, nucleophilic hydride-shift (from silane) is less likely.

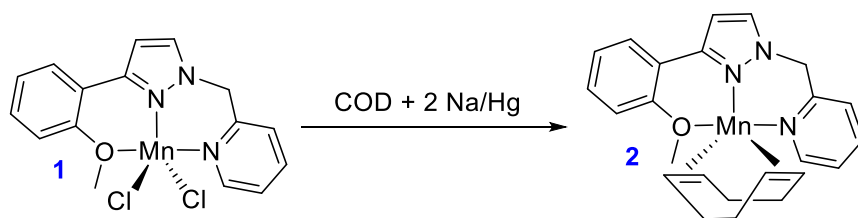
Solubility issue might be the possible reason for unsuccessful hydrosilylation of 1-ethynyl-4-nitrobenzene, 4-nitrobenzamide, 4-nitrocinnamic acid and 2-hydroxy-4-nitrobenzoic acid. If the above substrates were subjected to hydrosilylation under optimized conditions, those substrates remained solid and did not dissolve in the reaction medium.

**Proposed reaction pathway:** Condensation route involves the condensation of aryl nitroso Ar-NO (E) and N-hydroxylaniline Ar-NHOH (F) to azoxyarene (G) followed by the formation of dehydration product azoarene (H). Azoarene (H) is finally reduced to aniline via hydrazine intermediate (I). Based on experimental evidences, Rueping et al. previously suggested manganese catalyzed hydrogenation of nitroarene proceeds via direct reduction route with the formation of N-hydroxylaniline Ar-NHOH (F).<sup>S15</sup> We performed mass analysis from the reaction mixture to detect any intermediate. We could not identify any mass peak for N-hydroxylaniline Ar-NHOH (F); however, the formation of azoarene (H) was clearly detected by mass analysis ( $M^+$ : 242.1103). Therefore, the possibility of condensation route could not be ruled out in present manganese catalyzed hydrosilylation of nitroarene. To shed further light on the reaction mechanism, the possible intermediates N-phenylhydroxylamine, azobenzene and 1,2-diphenylhydrazine were purchased and subjected to catalytic hydrosilylation (above Scheme, equation a, b and c) using following conditions (PhSiH<sub>3</sub>: 2 eq., 1: 1 mol%, Na/Hg: 2 mol%, neat, 100 °C, 1 h). The reduction of N-phenylhydroxylamine led to the formation of 38% of aniline, whereas azobenzene and 1,2-diphenylhydrazine gave only 5 and 8% of aniline, respectively. These results suggested that the reduction of nitroarene via direct route is more favorable in the presence of the present catalytic system.

We performed several other control experiments (Above Scheme, equation d and e). Reaction of 1 with 1 and 2 eq. of Na/Hg resulted in NMR inactive species which could not be isolated in pure form. As Mn(I) compounds are generally NMR active, it is expected that reduction of Mn(II) complex 1 gave Mn(0) species. To trap the proposed Mn(0) species, further reduction of 1 with Na/Hg (2 eq.) was performed in presence of COD (equation d). We isolated COD stabilized Mn(0) species 2 which was characterized by HRMS and elemental analysis. Species 2 was utilized as a catalyst (in absence of Na/Hg) and catalytic activity very similar to complex 1 (in presence of Na/Hg) was observed. Thereafter, we carried out the reduction of 1 with Na/Hg (2 eq.) performed in presence of Et<sub>3</sub>SiH and complex 3 was isolated as product (equation e). Complex 1 was reduced to Mn(0) species and oxidative addition of silicon-hydrogen bond yielded complex 3, which is in agreement with initial steps of the proposed catalytic cycle. Despite several attempts, we could not get solid state structural information due to the poor quality of those crystals.

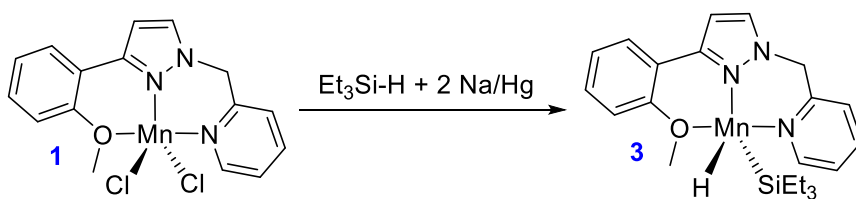
Catalytic hydrosilylations of 4-nitroanisole and nitrobenzene in presence of TEMPO radical took place without the loss of any catalytic activity which suggests to exclude radical process. Hydrosilylations of 4-nitroanisole and nitrobenzene were also unaltered in presence of excess mercury, which suggests to exclude the formation nano-particles.

### Synthesis of complex 2



The following synthesis and characterization of complex 2 was done in dry N<sub>2</sub> atmosphere. 1,5-COD (0.05 mmol, 0.054g) was added to a suspension of complex 1 (0.020 g, 0.05 mmol) in CH<sub>3</sub>CN (2 mL). The mixture was stirred at r.t. for 20 minutes. Then 20 % Na/Hg (0.1 mmol, 0.012g) was added to the reaction mixture and the resultant mixture was stirred at refluxed for 16 h. A grey precipitate was formed and the liquid was decanted off. The solid was dried under high vacuum. Then solid was washed with Et<sub>2</sub>O (3 x 2 mL) and subsequently dried under high vacuum to give complex 2 (0.018 g, 78%). HRMS (ESI-TOF) *m/z*: [M + Na]<sup>+</sup> calcd for C<sub>24</sub>H<sub>27</sub>MnN<sub>3</sub>NaO: 451.4300, found 451.3268. Anal. Calcd for C<sub>24</sub>H<sub>27</sub>MnN<sub>3</sub>O (428.44): C, 67.28; H, 6.35; N, 9.81. Found: C, 67.43; H, 6.47; N, 10.04.

### Synthesis of complex 3



The following synthesis and characterization of complex 2 was done in dry N<sub>2</sub> atmosphere. A mixture of complex 1 (0.05 mmol, 0.020 g), 20 % Na/Hg (2eq, 0.1 mmol, 0.012g) and Et<sub>3</sub>SiH (5eq, 0.25 mmol, 0.029g) was stirred at 100<sup>0</sup>C for 16 h. The resultant grey solution was then cooled down to r.t. Then it was dried under high vacuum and washed with hexane (3 x 2 mL) to remove excess Et<sub>3</sub>SiH. The resultant solid was then extracted with THF (5 mL). The solution was dried under high vacuum to give complex 3 (0.015 g, 69%). HRMS (ESI-TOF) *m/z*: [M + H]<sup>+</sup> calcd for C<sub>22</sub>H<sub>32</sub>MnN<sub>3</sub>OSi: 437.5400, found 437.1690. Anal. Calcd for C<sub>22</sub>H<sub>31</sub>MnN<sub>3</sub>OSi (436.53): C, 60.53; H, 7.16; N, N, 9.63. Found: C, 60.83; H, 7.37; N, 9.84.

Note: Several attempts to crystalize complex 2 and 3 gave poor quality crystals and solid state structural information by single crystal XRD could not be achieved.

### NMR data of aromatic amines

Following anilines (obtained by hydrosilylations of nitroarenes followed by column chromatography) are known compounds and they are characterized by  $^1\text{H}$  and  $^{13}\text{C}$  NMR spectroscopies. For several compounds two yields are mentioned (yield<sup>a</sup>: obtained with Na/Hg; yield<sup>b</sup>: obtained with  $\text{KC}_8$ ).

*p*-anisidine: A mixture of hexanes and ethyl acetate (3:2) was used as eluent for column chromatography. Isolated as a brown oil [(0.060 g, 98%)<sup>a</sup>; [(0.060 g, 98%)<sup>b</sup>].  $^1\text{H}$  NMR (400 MHz,  $\text{CDCl}_3$ )  $\delta$  6.78 (d,  $J = 6.9$  Hz, 2H), 6.66 (d,  $J = 7.9$  Hz, 2H), 3.77 (s, 3H), 3.45 (brs, 2H).  $^{13}\text{C}$  NMR (101 MHz,  $\text{CDCl}_3$ )  $\delta$  152.7, 140.0, 116.4, 114.8, 55.7.

2-ethylaniline (**A1**): A mixture of petroleum ether and ethyl acetate (3:2) was used as eluent for column chromatography. Isolated as a colorless oil [**A1**: (0.050 g, 82%)<sup>a</sup>; [(0.051 g, 84%)<sup>b</sup>].  $^1\text{H}$  NMR (400 MHz,  $\text{CDCl}_3$ )  $\delta$  7.15 (dd,  $J = 17.4, 7.8$  Hz, 2H), 6.85 (t,  $J = 7.4$  Hz, 1H), 6.75 (d,  $J = 7.8$  Hz, 1H), 3.66 (brs, 2H), 2.60 (q,  $J = 7.5$  Hz, 2H), 1.35 (t,  $J = 7.5$  Hz, 3H).  $^{13}\text{C}$  NMR (101 MHz,  $\text{CDCl}_3$ )  $\delta$  144.10, 128.4, 128.1, 126.9, 118.9, 115.5, 24.10, 13.10.

3-chloroaniline (**A2a**): A mixture of hexanes and ethyl acetate (3:2) was used as eluent for column chromatography. Isolated as a brown liquid [**A2a**: (0.059 g, 92%)<sup>a</sup>; [(0.057 g, 89%)<sup>b</sup>].  $^1\text{H}$  NMR (400 MHz,  $\text{CDCl}_3$ )  $\delta$  7.08 (t,  $J = 8.0$  Hz, 1H), 6.74 (d,  $J = 8.0$  Hz, 1H), 6.69 (s, 1H), 6.56 (d,  $J = 8.0$  Hz, 1H), 3.71 (brs, 2H).  $^{13}\text{C}$  NMR (101 MHz,  $\text{CDCl}_3$ )  $\delta$  147.6, 134.8, 130.3, 118.5, 115., 113.2.

1,3-diaminobenzene (**A2b/ A10a**): A mixture of hexanes and ethyl acetate (3:2) was used as eluent for column chromatography. Isolated as a brown solid (**A2b**: 0.045 g, 84%, **A10a**: 0.044 g, 81%)  $^1\text{H}$  NMR (400 MHz,  $\text{CDCl}_3$ )  $\delta$  6.97 (t,  $J = 7.9$  Hz, 1H), 6.14 (d,  $J = 7.8$  Hz, 2H), 6.01 (s, 1H), 3.57 (brs, 4H).  $^{13}\text{C}$  NMR (101 MHz,  $\text{CDCl}_3$ )  $\delta$  147.6, 130.2, 106.0, 102.1.

4-fluorobenzene-1,2-diamine (**A3**): A mixture of hexanes and ethyl acetate (2:1) was used

as eluent for column chromatography. Isolated as a grey brown solid (**A3**: 0.054 g, 82%).  $^1\text{H}$  NMR (400 MHz,  $\text{CDCl}_3$ )  $\delta$  6.38-6.47(m,2H), 6.62-6.65(m,1H), 3.10(brs, 4H).  $^{13}\text{C}$  NMR (101 MHz,  $\text{CDCl}_3$ )  $\delta$  157.8 (d,  $^1J_{\text{C-F}} = 236.1$  Hz), 136.9 (d,  $^3J_{\text{C-F}} = 10.2$  Hz), 129.8, 117.7 (d,  $^3J_{\text{C-F}} = 9.4$  Hz), 105.3 (d,  $^2J_{\text{C-F}} = 22.0$  Hz), 103.2 (d,  $^2J_{\text{C-F}} = 25.5$  Hz).

3,4,5-trichloroaniline (**A4**): A mixture of hexanes and ethyl acetate (3:2) was used as eluent for column chromatography. Isolated as a brown solid [**A4**: (0.082 g, 83%)<sup>a</sup>; [(0.082 g, 84%)<sup>b</sup>].  $^1\text{H}$  NMR (400 MHz,  $\text{CDCl}_3$ )  $\delta$  6.60 (s, 2H), 3.76 (brs, 2H).  $^{13}\text{C}$  NMR (101 MHz,  $\text{CDCl}_3$ )  $\delta$  145.7, 134.2, 119.8, 115.1.

*p*-toluidine (**A5a**): A mixture of hexanes and ethyl acetate (3:2) was used as eluent for column chromatography. Isolated as a brown liquid (**A5a**: 0.50 g, 93%).  $^1\text{H}$  NMR (400 MHz,  $\text{CDCl}_3$ )  $\delta$  7.02 (d,  $J = 7.5$  Hz, 2H), 6.65 (d,  $J = 7.7$  Hz, 2H), 3.42 (brs, 2H), 2.29 (s, 3H).  $^{13}\text{C}$  NMR (101 MHz,  $\text{CDCl}_3$ )  $\delta$  143.8, 129.8, 127.9, 115.4, 20.5.

4-(methylthio)aniline (**A5b**): A mixture of hexanes and ethyl acetate (3:2) was used as eluent for column chromatography. Isolated as a brown solid (**A5b**: 0.058 g, 83%)  $^1\text{H}$  NMR (400 MHz,  $\text{CDCl}_3$ )  $\delta$  7.21 (d,  $J = 8.3$  Hz, 2H), 6.66 (d,  $J = 8.3$  Hz, 2H), 3.67 (brs, 2H), 2.44 (s, 3H).  $^{13}\text{C}$  NMR (101 MHz,  $\text{CDCl}_3$ )  $\delta$  145.1, 131.1, 125.8, 115.8, 18.8.

*N,N*-dimethyl-*p*-phenylenediamine (**A5c**): A mixture of hexanes and ethyl acetate (2:1) was used as eluent for column chromatography. Isolated as a reddish brown solid (**A5c**: 0.055 g, 80%)  $^1\text{H}$  NMR (400 MHz,  $\text{CDCl}_3$ )  $\delta$  6.75 (d,  $J = 8.3$  Hz, 2H), 6.69 (d,  $J = 8.0$  Hz, 2H), 3.37 (brs, 2H), 2.87 (s, 6H).  $^{13}\text{C}$  NMR (101 MHz,  $\text{CDCl}_3$ )  $\delta$  144.9, 138.1, 116.7, 115.6, 42.2.

4-fluoroaniline (**A5d**): A mixture of hexanes and ethyl acetate (3:2) was used as eluent for column chromatography. Isolated as a brown solid [**A5d**: (0.036g, 65% <sup>a</sup>; [(0.038 g, 68%)<sup>b</sup>].  $^1\text{H}$  NMR (400 MHz,  $\text{CDCl}_3$ )  $\delta$  6.88 (t,  $J = 8.5$  Hz, 2H), 6.63 (dd,  $J = 8.1, 4.4$  Hz, 2H), 3.51 (brs, 2H).  $^{13}\text{C}$  NMR (101 MHz,  $\text{CDCl}_3$ )  $\delta$  156.5 (d,  $^1J_{\text{C-F}} = 235.7$  Hz), 142.3, 116.1 (d,  $^3J_{\text{C-F}}$

= 7.4 Hz), 115.6 (d,  $^2J_{\text{C-F}} = 22.4$  Hz).

4-chloroaniline (**A5e**): A mixture of hexanes and ethyl acetate (3:2) was used as eluent for column chromatography. Isolated as a pale yellow solid (**A5e**: 0.053 g, 82%)  $^1\text{H}$  NMR (400 MHz,  $\text{CDCl}_3$ )  $\delta$  7.12 (d,  $J = 8.6$  Hz, 2H), 6.62 (d,  $J = 8.5$  Hz, 2H), 3.68 (brs, 2H).  $^{13}\text{C}$  NMR (101 MHz,  $\text{CDCl}_3$ )  $\delta$  145.0, 129.1, 123.2, 116.2.

4-bromoaniline (**A5f**): A mixture of hexanes and ethyl acetate (3:2) was used as eluent for column chromatography. Isolated as a brown solid (**A5f**: 0.079 g, 92%)  $^1\text{H}$  NMR (400 MHz,  $\text{CDCl}_3$ )  $\delta$  7.25 (d,  $J = 8.6$  Hz, 2H), 6.58 (d,  $J = 8.6$  Hz, 2H), 3.68 (brs, 2H).  $^{13}\text{C}$  NMR (101 MHz,  $\text{CDCl}_3$ )  $\delta$  145.4, 132.0, 116.7, 110.2.

4-iodoaniline (**A5g**): A mixture of hexanes and ethyl acetate (3:2) was used as eluent for column chromatography. Isolated as a brown solid [**A5g**: (0.104 g, 95%)<sup>a</sup>; [(0.105 g, 96%)<sup>b</sup>]  $^1\text{H}$  NMR (400 MHz,  $\text{CDCl}_3$ )  $\delta$  7.43 (d,  $J = 8.2$  Hz, 2H), 6.47 (d,  $J = 8.3$  Hz, 2H), 3.67 (brs, 2H).  $^{13}\text{C}$  NMR (101 MHz,  $\text{CDCl}_3$ )  $\delta$  146.1, 137.9, 124.8, 117.4.

methyl 4-aminobenzoate (**A6a**): A mixture of hexanes and ethyl acetate (3:2) was used as eluent for column chromatography. Isolated as a pale yellow solid (**A6a**: 0.066 g, 87%).  $^1\text{H}$  NMR (400 MHz,  $\text{CDCl}_3$ )  $\delta$  7.86 (d,  $J = 8.4$  Hz, 2H), 6.64 (d,  $J = 8.5$  Hz, 2H), 4.13 (s, 3H), 3.86 (brs, 2H).  $^{13}\text{C}$  NMR (101 MHz,  $\text{CDCl}_3$ )  $\delta$  167.2, 151.0, 131.6, 119.6, 113.8, 51.6.

4-aminobenzonitrile (**A6b**): A mixture of hexanes and ethyl acetate (3:2) was used as eluent for column chromatography. Isolated as a yellow solid [**A6b**: (0.045 g, 75%)<sup>a</sup>; [(0.042 g, 72%)<sup>b</sup>]  $^1\text{H}$  NMR (400 MHz,  $\text{CDCl}_3$ )  $\delta$  7.37 (d,  $J = 8.4$  Hz, 2H), 6.64 (d,  $J = 8.4$  Hz, 2H), 4.30 (brs, 2H).  $^{13}\text{C}$  NMR (101 MHz,  $\text{CDCl}_3$ )  $\delta$  150.8, 133.8, 120.5, 114.4, 99.5.

4-[(*E*)-2-phenylethenyl]aniline (**A7**): A mixture of hexanes and ethyl acetate (3:1) was used as eluent for column chromatography. Isolated as a pale-yellow solid (**A7**: 0.085 g, 87%).  $^1\text{H}$  NMR (400 MHz,  $\text{CDCl}_3$ )  $\delta$  7.52 (d,  $J = 7.7$  Hz, 2H), 7.37 (dd,  $J = 7.7, 5.8$  Hz, 4H), 7.24

(dd,  $J = 16.1, 8.8$  Hz, 1H), 7.13 – 6.93 (m, 2H), 6.71 (d,  $J = 8.3$  Hz, 2H), 3.76 (brs, 2H).  $^{13}\text{C}$  NMR (101 MHz,  $\text{CDCl}_3$ )  $\delta$  146.2, 138.0, 128.7, 128.6, 128.0, 127.8, 126.9, 126.1, 125.1, 115.2.

4-vinylaniline (**A<sub>8</sub>**): A mixture of hexanes and ethyl acetate (3:1) was used as eluent for column chromatography. Isolated as a colourless liquid [**A<sub>8</sub>**: (0.040 g, 66%)<sup>a</sup>; [(0.041 g, 68%)<sup>b</sup>].  $^1\text{H}$  NMR (400 MHz,  $\text{CDCl}_3$ )  $\delta$  7.26 (d,  $J = 8.4$  Hz, H), 6.70 – 6.59 (m, 3H), 5.57 (dd,  $J = 17.6, 0.8$  Hz, 1H), 5.07 (dd,  $J = 10.9, 0.8$  Hz, 1H), 3.17 (brs, 2H).  $^{13}\text{C}$  NMR (101 MHz,  $\text{CDCl}_3$ )  $\delta$  146.2, 136.7, 128.6, 127.5, 115.2, 110.2.

3-aminobenzyl alcohol (**A<sub>9a</sub>**): A mixture of hexanes and ethyl acetate (3:2) was used as eluent for column chromatography. Isolated as a yellow oil (**A<sub>9a</sub>**: 0.050g, 81%).  $^1\text{H}$  NMR (400 MHz,  $\text{CDCl}_3$ )  $\delta$  7.16 (t,  $J = 7.7$  Hz, 1H), 6.76 (d,  $J = 7.5$  Hz, 1H), 6.72 (s, 1H), 6.64 (d,  $J = 7.9$  Hz, 1H), 4.62 (s, 1H), 3.73 (brs, 2H).  $^{13}\text{C}$  NMR (101 MHz,  $\text{CDCl}_3$ )  $\delta$  147.2, 142.2, 129.5, 117.1, 114.4, 113.5, 65.3.

4-aminoacetanilide (**A<sub>9b</sub>**): A mixture of hexanes and ethyl acetate (3:2) was used as eluent for column chromatography. Isolated as a pale yellow solid (**A<sub>9b</sub>**: 0.053 g, 70%).  $^1\text{H}$  NMR (400 MHz,  $\text{CDCl}_3$ )  $\delta$  7.27 (d,  $J = 8.4$  Hz, 2H), 7.25 (brs, 1H), 6.6 (d,  $J = 8.4$  Hz, 2H), 3.62 (brs, 2H), 2.14 (s, 3H).  $^{13}\text{C}$  NMR (101 MHz,  $\text{CDCl}_3$ )  $\delta$  168.2, 143.4, 129.2, 122.2, 115.4, 24.3.

1,4-diaminobenzene (**A<sub>10b</sub>**): A mixture of hexanes and ethyl acetate (3:2) was used as eluent for column chromatography. Isolated as a brown solid (**A<sub>10b</sub>**: 0.046 g, 90%).  $^1\text{H}$  NMR (400 MHz,  $\text{CDCl}_3$ )  $\delta$  6.59 (s, 4H), 3.22 (brs, 4H).  $^{13}\text{C}$  NMR (101 MHz,  $\text{CDCl}_3$ )  $\delta$  138.6, 116.7.

(4-aminophenyl)methanol (**A<sub>11</sub>**): A mixture of hexane and ethyl acetate (4:1) was used as eluent for column chromatography. Isolated as a yellow solid [**A<sub>11</sub>**: (0.056 g, 91%)<sup>a</sup>; [(0.054 g, 88%)<sup>b</sup>].  $^1\text{H}$  NMR (400 MHz,  $\text{CDCl}_3$ )  $\delta$  7.16 (d,  $J = 8.3$  Hz, 2H), 6.68 (d,  $J = 8.3$  Hz, 2H),

4.55 (s, 2H), 2.96 (s, 3H).  $^{13}\text{C}$  NMR (101 MHz,  $\text{CDCl}_3$ )  $\delta$  146.1, 131.2, 128.9, 115.3, 65.3.

1-(2-aminophenyl)ethanol (**A12**): A mixture of hexane and ethyl acetate (4:1) was used as eluent for column chromatography. Isolated as a yellow solid [**A12**: (58 mg, 85%<sup>a</sup>; [(0.060 g, 88%)<sup>b</sup>].  $^1\text{H}$  NMR (400 MHz,  $\text{CDCl}_3$ )  $\delta$  7.12 (ddd,  $J = 7.1, 4.0, 1.7$  Hz, 2H), 6.75 (td,  $J = 7.5, 1.1$  Hz, 1H), 6.69 (dd,  $J = 8.3, 1.1$  Hz, 1H), 4.95 (q,  $J = 6.6$  Hz, 1H), 3.15 (s, 3H), 1.61 (d,  $J = 6.6$  Hz, 3H).  $^{13}\text{C}$  NMR (101 MHz,  $\text{CDCl}_3$ )  $\delta$  145.2, 128.7, 128.5, 126.7, 118.3, 116.8, 69.7, 21.6.

N-(4-aminobenzyl)aniline (**A13**): A mixture of hexanes and ethyl acetate (7:3) was used as eluent for column chromatography. Isolated as a yellow liquid (**A13**: 69 mg, 69%).  $^1\text{H}$  NMR (400 MHz,  $\text{CDCl}_3$ )  $\delta$  8.79 (s, 1H), 8.08 (t,  $J = 12.9$  Hz, 1H), 7.36 (s, 2H), 7.17 (s, 1H), 6.94 (s, 1H), 5.04 (s, 1H).  $^{13}\text{C}$  NMR (101 MHz,  $\text{CDCl}_3$ )  $\delta$  147.5, 138.5, 136.0, 128.9, 127.4, 121.3, 116.1, 115.1, 110.1.

6-aminoquinoline (**A14**): A mixture of hexanes and ethyl acetate (3:2) was used as eluent for column chromatography. Isolated as a brown grey solid [**A14**: (0.054 g, 74%)<sup>a</sup>; [(0.050 g, 70%)<sup>b</sup>].  $^1\text{H}$  NMR (400 MHz,  $\text{CDCl}_3$ )  $\delta$  8.68 (s, 1H), 7.84 (t,  $J = 12.9$  Hz, 2H), 7.18 (t,  $J = 12.9$  Hz, 1H), 7.08 (t,  $J = 12.9$  Hz, 1H), 6.82 (s, 1H) 3.8 (brs, 2H).  $^{13}\text{C}$  NMR (101 MHz,  $\text{CDCl}_3$ )  $\delta$  146.8, 144.7, 143.4, 133.8, 130.5, 129.8, 121.6, 121.4, 107.4.

8-aminoquinoline (**A15**): A mixture of hexanes and ethyl acetate (3:2) was used as eluent for column chromatography. Isolated as a brown grey solid (**A15**: 0.059 g, 81%).  $^1\text{H}$  NMR (400 MHz,  $\text{CDCl}_3$ )  $\delta$  8.79 (s, 1H), 8.08 (t,  $J = 12.9$  Hz, 1H), 7.36 (m, 2H), 7.17 (d, 1H), 6.94 (d, 1H), 4.83 (brs, 2H).  $^{13}\text{C}$  NMR (101 MHz,  $\text{CDCl}_3$ )  $\delta$  147.5, 138.5, 136.0, 128.9, 127.4, 121.3, 116.1, 115.1, 110.1.

3-aminoquinoline (**A16**): A mixture of hexanes and ethyl acetate (3:2) was used as eluent for column chromatography. Isolated as a brown grey solid [**A16**: (0.055 g, 75%)<sup>a</sup>; [(0.056 g,

77%)<sup>b</sup>]. <sup>1</sup>H NMR (400 MHz, CDCl<sub>3</sub>) δ 8.50 (d, *J* = 2.3 Hz, 1H), 7.98 (d, *J* = 8.7 Hz, 1H), 7.57 (dd, *J* = 6.2, 2.9 Hz, 1H), 7.47 – 7.39 (m, 2H), 7.19 (d, *J* = 2.2 Hz, 1H), 4.03 (brs, 2H). <sup>13</sup>C NMR (101 MHz, CDCl<sub>3</sub>) δ 143.2, 142.7, 139.9, 129.2, 129.0, 127.0, 125.9, 125.6, 114.9.

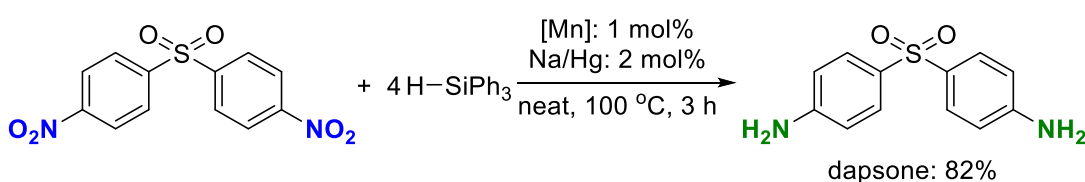
2-aminofluorene (**A17**): A mixture of hexanes and ethyl acetate (3:2) was used as eluent for column chromatography. Isolated as a brown yellow solid (**A17**: 0.061 g, 67%). <sup>1</sup>H NMR (400 MHz, CDCl<sub>3</sub>) δ 7.67 (d, *J* = 2.2 Hz, 1H), 7.60 (d, *J* = 2.2 Hz, 1H), 7.50 (d, *J* = 2.2 Hz, 1H), 7.35 (t, *J* = 12.9 Hz, 1H), 7.22 (d, *J* = 2.2 Hz, 1H), 6.90 (s, 1H), 6.74 (d, *J* = 2.2 Hz, 1H), 3.84 (s, 1H), 3.76 (brs, 1H). <sup>13</sup>C NMR (101 MHz, CDCl<sub>3</sub>) δ 145.8, 145.2, 142.3, 142.2, 133.0, 126.7, 125.1, 124.8, 120.7, 118.6, 114.0, 111.8, 36.8.

6-aminoindole (**A18**): A mixture of hexanes and ethyl acetate (2:1) was used as eluent for column chromatography. Isolated as a yellow solid (**A18**: 0.047 mg, 70%). <sup>1</sup>H NMR (400 MHz, CDCl<sub>3</sub>) δ 7.93 (brs, 1H), 7.10(d, *J* = 2.2 Hz, 1H), 7.03(t, *J* = 12.9 Hz, 1H), 6.87 (d, *J* = 2.2 Hz, 1H), 6.58 (dd, *J* = 7.7, 5.8 Hz, 1H), 6.29 (dd, *J* = 7.7, 5.8 Hz, 1H), 2.91(brs, 2H). <sup>13</sup>C NMR (101 MHz, CDCl<sub>3</sub>) δ 139.5, 130.7, 128.8, 124.7, 112.9, 111.5, 105.6, 101.6.

3-amino-2-chloropyridine (**A19**): A mixture of hexanes and ethyl acetate (2:1) was used as eluent for column chromatography. Isolated as a light brown solid [**A19**: (0.046 g, 71%)<sup>a</sup>; [(0.048 g, 75%)<sup>b</sup>]. <sup>1</sup>H NMR (400 MHz, CDCl<sub>3</sub>) δ 7.71 (s, 1H), 6.97 (s, 2H), 4.11 (brs, 2H). <sup>13</sup>C NMR (101 MHz, CDCl<sub>3</sub>) δ 139.8, 138.5, 136.9, 123.4, 122.5.

### Synthesis of drug molecules:

#### Synthesis of dapsone

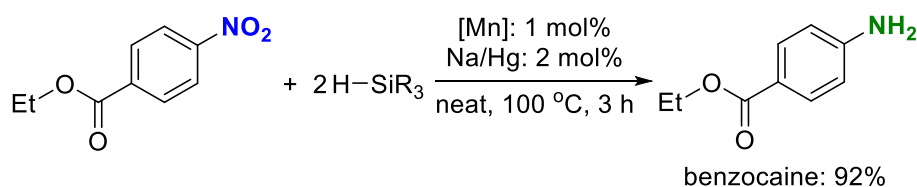


**Synthesis of dapsone:**<sup>S9</sup> In a dried pressure tube fitted with a magnetic stir bar, complex **1**

(1 mol%), Na/Hg (2.2 mol%), 4,4'-sulfonylbis(nitrobenzene) (154 mg, 0.5 mmol), phenylsilane (0.218 g, 2.10 mmol) were added successively under nitrogen atmosphere. The reaction mixture was heated at appropriate temperature (100 °C) in a preheated oil bath for 3 h. After cooling to r.t., MeOH (2 mL) and 10 wt% of NaOH solution (6 mL) were added to the resultant mixture. The mixture was then extracted with DCM (3 x 12 mL). The organic layer was collected and dried over anhydrous Na<sub>2</sub>SO<sub>4</sub>. All volatiles were removed under high vacuum to give crude product. The crude product was purified by column chromatography (using silica as stationary phase and a mixture of hexanes and ethyl acetate (2:1) as eluent) to give a yellow solid as pure product (0.102 g, 82%). <sup>1</sup>H NMR (400 MHz, CDCl<sub>3</sub>) δ 7.68 (d, *J* = 8.4 Hz, 4H), 6.66 (d, *J* = 8.4 Hz, 4H), 4.25 – 3.96 (brs, 4H). <sup>13</sup>C NMR (101 MHz, CDCl<sub>3</sub>) δ 150.4, 131.2, 129.3, 114.1.

Gram-scale synthesis: Under identical reaction conditions, 1.54 g (5 mmol) of 4,4'-sulfonylbis(nitrobenzene) gave 1.06 g (85%) of dapsone.

### Synthesis of benzocaine

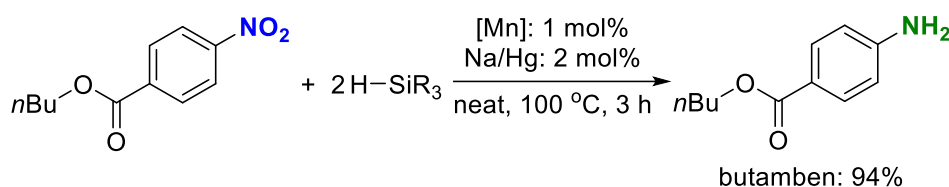


**Synthesis of benzocaine:**<sup>S4</sup> In a dried pressure tube fitted with a magnetic stir bar, complex **1** (1 mol%), Na/Hg (2.2 mol%), ethyl 4-nitrobenzoate (92 mg, 0.5 mmol), phenylsilane (0.109 g, 1.05 mmol) were added successively under nitrogen atmosphere. The reaction mixture was heated at appropriate temperature (100 °C) in a preheated oil bath for 3 h. After cooling to r.t., MeOH (2 mL) and 10 wt% of NaOH solution (6 mL) were added to the resultant mixture. The mixture was then extracted with DCM (3 x 12 mL). The organic layer was collected and dried over anhydrous Na<sub>2</sub>SO<sub>4</sub>. All volatiles were removed under high vacuum to give crude product. The crude product was purified by column chromatography

(using silica as stationary phase and a mixture of hexanes and ethyl acetate (2:1) as eluent) to give a yellow solid as pure product (0.076 g, 82%).  $^1\text{H}$  NMR (400 MHz,  $\text{CDCl}_3$ )  $\delta$  7.87 (d,  $J = 8.4$  Hz, 2H), 6.66 (d,  $J = 8.4$  Hz, 2H), 4.33 (q,  $J = 7.1$  Hz, 2H), 4.06 (brs, 2H), 1.38 (t,  $J = 7.1$  Hz, 3H).  $^{13}\text{C}$  NMR (101 MHz,  $\text{CDCl}_3$ )  $\delta$  166.8, 150.8, 131.7, 120.3, 113.9, 60.4, 14.6.

Gram-scale synthesis: Under identical reaction conditions, 1.95 g (10 mmol) of ethyl 4-nitrobenzoate gave 1.55 g (94%) of benzocaine.

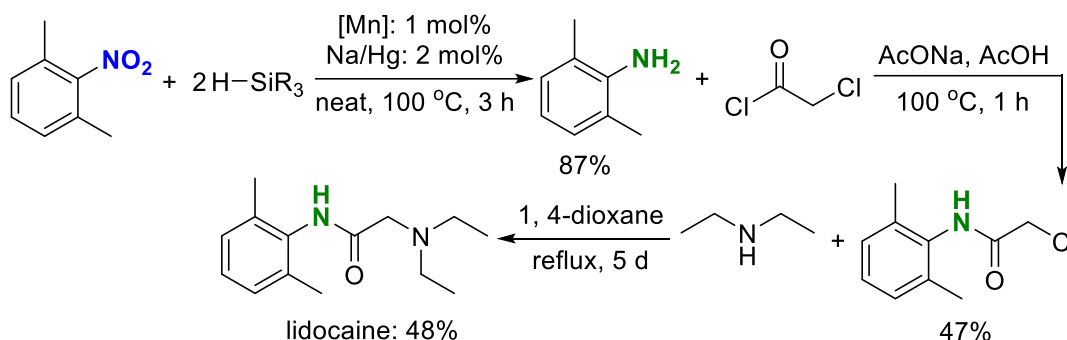
### Synthesis of butamben



**Synthesis of butamben:**<sup>S10</sup> In a dried pressure tube fitted with a magnetic stir bar, complex **1** (1 mol%), Na/Hg (2.2 mol%), butyl 4-nitrobenzoate (111 mg, 0.5 mmol), phenylsilane (0.109 g, 1.05 mmol) were added successively under nitrogen atmosphere. The reaction mixture was heated at appropriate temperature (100 °C) in a preheated oil bath for 3 h. After cooling to r.t., MeOH (2 mL) and 10 wt% of NaOH solution (6 mL) were added to the resultant mixture. The mixture was then extracted with DCM (3 x 12 mL). The organic layer was collected and dried over anhydrous  $\text{Na}_2\text{SO}_4$ . All volatiles were removed under high vacuum to give crude product. The crude product was purified by column chromatography (using silica as stationary phase and a mixture of hexanes and ethyl acetate (2:1) as eluent) to give a yellow solid as pure product (0.091 g, 94%).  $^1\text{H}$  NMR (400 MHz,  $\text{CDCl}_3$ )  $\delta$  7.78 (d,  $J = 8.0$  Hz, 2H), 6.57 (d,  $J = 8.0$  Hz, 2H), 4.19 (t,  $J = 6.6$  Hz, 2H), 3.97 (brs, 2H), 1.70 – 1.60 (m, 2H), 1.40 (dt,  $J = 14.8, 7.4$  Hz, 2H), 0.90 (t,  $J = 7.4$  Hz, 3H).  $^{13}\text{C}$  NMR (101 MHz,  $\text{CDCl}_3$ )  $\delta$  166.8, 150.7, 131.6, 120.2, 113.8, 64.2, 30.9, 19.3, 13.8.

Gram-scale synthesis: Under identical reaction conditions, 1.79 g (8 mmol) of butyl 4-nitrobenzoate gave 1.47 g (95%) of butamben.

### Synthesis of lidocaine<sup>S11, S12</sup>



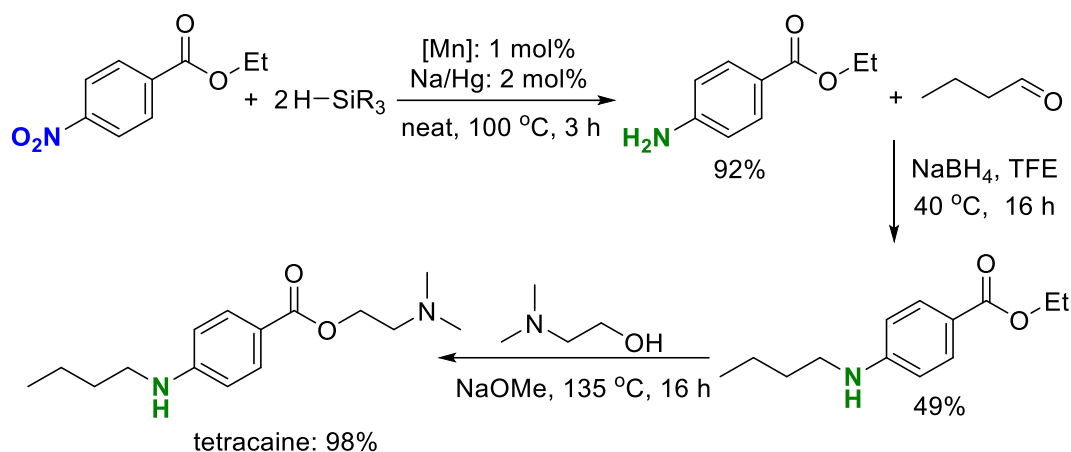
**Synthesis of 2,6-dimethylaniline (step 1):** In a dried pressure tube fitted with a magnetic stir bar, complex **1** (1 mol%), Na/Hg (2.2 mol%), 1,3-dimethyl-2-nitrobenzene (0.075 g, 0.5 mmol), phenylsilane (0.109 g, 1.05 mmol) were added successively under nitrogen atmosphere. The reaction mixture was heated at appropriate temperature (100 °C) in a preheated oil bath for 3 h. After cooling to r.t., MeOH (2 mL) and 10 wt% of NaOH solution (6 mL) were added to the resultant mixture. The mixture was then extracted with DCM (3 x 12 mL). The organic layer was collected and dried over anhydrous Na<sub>2</sub>SO<sub>4</sub>. All volatiles were removed under high vacuum to give crude product. The crude product was purified by column chromatography (using silica as stationary phase and a mixture of hexanes and ethyl acetate (2:1) as eluent) to give a brown liquid as pure product (0.053 g, 87%). <sup>1</sup>H NMR (400 MHz, CDCl<sub>3</sub>) δ 6.99 (d, *J* = 7.3 Hz, 2H), 6.69 (td, *J* = 7.5, 1.9 Hz, 1H), 3.61 (brs, 1H), 2.23 (s, 6H). <sup>13</sup>C NMR (101 MHz, CDCl<sub>3</sub>) δ 142.7, 128.3, 121.7, 118.03, 17.64.

**Synthesis of 2-chloro-N-(2,6-dimethylphenyl)acetamide (step 2):** The Synthetic process was previously reported.<sup>S1</sup> This is a modified procedure. In a dried round-bottom flask fitted with a magnetic stirring bar, chloroacetyl chloride (0.145 g, 1.5 mmol) and 2, 6-

dimethylaniline (0.197 g, 1 mmol) were added and the mixture was stirred until slurry was observed. Sodium acetate (0.164 g, 2 mmol) was added into the mixture and it was allowed to run at reflux condition for 1 h. After completion of the reaction, it was cooled to 0 °C for 20 minutes. The solid material was filtered off and washed with cold water to obtain the crude. The crude was dried under vacuum to get white crystalline solid as pure compound (0.093 g, 47%).  $^1\text{H}$  NMR (700 MHz,  $\text{CDCl}_3$ )  $\delta$  7.87 (brs, 1H), 7.19 – 7.15 (m, 1H), 7.12 (d,  $J=8.0$  Hz, 2H), 4.27 (s, 2H), 2.27 (s, 6H).  $^{13}\text{C}$  NMR (176 MHz,  $\text{CDCl}_3$ )  $\delta$  164.36, 135.36, 132.69, 128.39, 127.91, 42.80, 18.30.

**Synthesis of lidocaine (step 3):** The Synthetic process was previously reported.<sup>S2</sup> This is a modified procedure. In a dried pressure tube fitted with magnetic stirring bar, 2-chloro-N-(2,6-dimethylphenyl)-acetamide (0.197 g, 1 mmol), diethyl amine (0.136 g, 3 mmol) and triethyl amine (0.600 g, 6 mmol) were taken and 1,4 dioxane (4 ml) was added into it. Then the reaction mixture was allowed to run for five days in reflux condition. After completion of the reaction, the resultant mixture was dried under high vacuum to remove all the volatiles. After drying a dark red solid was isolated as crude product. The crude product was purified by column chromatography (silica gel as stationary phase and 1:1 mixture of ethyl acetate and hexanes as eluent) to give red solid as pure product (0.112 g, 48%).  $^1\text{H}$  NMR (400 MHz,  $\text{CDCl}_3$ )  $\delta$  9.05 (s, 1H), 7.10 (m, 3H), 3.31 (s, 2H), 2.76 (t,  $J = 6.0$  Hz, 2H), 1.18 (m, 2H).  $^{13}\text{C}$  NMR (101 MHz,  $\text{CDCl}_3$ )  $\delta$  135.12, 133.85, 128.27, 127.16, 48.96, 18.56, 12.46.

### Synthesis of tetracaine<sup>S13, S14</sup>



**Synthesis of ethyl 4-aminobenzoate (step 1):** In a dried pressure tube fitted with a magnetic stir bar, complex **1** (1 mol%),  $\text{Na/Hg}$  (2.2 mol%), ethyl 4-nitrobenzoate (92 mg, 0.5 mmol), phenylsilane (0.109 g, 1.05 mmol) were added successively under nitrogen atmosphere. The reaction mixture was heated at appropriate temperature ( $100^\circ\text{C}$ ) in a preheated oil bath for 3 h. After cooling to r.t.,  $\text{MeOH}$  (2 mL) and 10 wt% of  $\text{NaOH}$  solution (6 mL) were added to the resultant mixture. The mixture was then extracted with  $\text{DCM}$  (3 x 12 mL). The organic layer was collected and dried over anhydrous  $\text{Na}_2\text{SO}_4$ . All volatiles were removed under high vacuum to give crude product. The crude product was purified by column chromatography (using silica as stationary phase and a mixture of hexanes and ethyl acetate (2:1) as eluent) to give a yellow solid as pure products. (0.076 g, 92%)  $^1\text{H NMR}$  (400 MHz,  $\text{CDCl}_3$ )  $\delta$  7.88 (d,  $J = 8.8$  Hz, 1H), 6.55 (d,  $J = 8.8$  Hz, 1H), 4.33 (q,  $J = 7.1$  Hz, 1H), 4.10 (s, 1H), 3.18 (dd,  $J = 10.7, 6.8$  Hz, 1H), 1.62 (dd,  $J = 14.8, 7.4$  Hz, 1H), 1.45 (dd,  $J = 15.0, 7.4$  Hz, 1H), 1.38 (t,  $J = 7.1$  Hz, 2H), 0.98 (t,  $J = 7.3$  Hz, 2H).

**Synthesis of ethyl 4-(butylamino)benzoate (step 2):** The Synthetic process was previously reported.<sup>S3</sup> This is a modified procedure. In a round bottom flask, a solution of the appropriate carbonyl compound (1 mmol) and TFE (2 mL) was magnetically stirred at 40

°C. After 5 min, the ethyl 4-aminobenzoate (1 mmol) was added, and the mixture vigorously stirred. After stirring for 5 min, NaBH<sub>4</sub> (1.2 mmol) was added and the progress of the reaction conversion was followed by TLC (hexane–EtOAc, 4:1). After completion of the reaction, the mixture was filtered and the residue was washed with TFE (2 mL). The solvent was distilled off (to recover for the next run) and the pure product was obtained. The crude product was further purified by silica gel column chromatography with EtOAc–petroleum ether (8:2) as eluent. (0.108 g, 49%). <sup>1</sup>H NMR (400 MHz, CDCl<sub>3</sub>) δ 7.88 (d, *J* = 8.8 Hz, 2H), 6.55 (d, *J* = 8.8 Hz, 2H), 4.33 (q, *J* = 7.1 Hz, 2H), 4.10 (brs, 1H), 3.18 (dd, *J* = 10.7, 6.8 Hz, 2H), 1.62 (dd, *J* = 14.8, 7.4 Hz, 2H), 1.45 (dd, *J* = 15.0, 7.4 Hz, 2H), 1.38 (t, *J* = 7.1 Hz, 3H), 0.98 (t, *J* = 7.3 Hz, 3H). <sup>13</sup>C NMR (101 MHz, CDCl<sub>3</sub>) δ 166.88, 152.36, 131.78, 117.94, 111.40, 57.97, 45.78, 43.16, 31.5, 20.31, 13.95.

**Synthesis of tetracaine (step 3):** The Synthetic process was previously reported.<sup>S4</sup> This is a modified procedure. In a round bottom flask a solution of ethyl 4-(butylamino)benzoate (154 mg, 0.7 mmol) in 2-(dimethylamino)ethan-1-ol (2.0 mL) was treated with NaOMe (5 mg, 0.1 mmol), heated to 135 °C and stirred at the same temperature for 16 h. The mixture was cooled to room temperature and diluted with H<sub>2</sub>O (10 mL) and CH<sub>2</sub>Cl<sub>2</sub> (10 mL). The layers were separated and the aqueous layer was extracted with CH<sub>2</sub>Cl<sub>2</sub> (2 x 10 mL). The combined organic layers were washed with brine, dried (MgSO<sub>4</sub>) and evaporated. Purification by column chromatography on silica gel eluting with petrol–EtOAc (70:30) gave pure product (0.181 g, 98%). <sup>1</sup>H NMR (400 MHz, CDCl<sub>3</sub>) δ 7.79 (d, *J* = 8.5 Hz, 2H), 6.46 (d, *J* = 8.5 Hz, 2H), 4.31 (s, 2H), 4.05 (s, 1H), 3.09 (dd, *J* = 11.7, 6.9 Hz, 2H), 2.66 (s, 2H), 2.29 (s, 6H), 1.54 (dt, *J* = 14.8, 7.2 Hz, 2H), 1.34 (dt, *J* = 18.6, 5.8 Hz, 2H), 0.89 (t, *J* = 7.3 Hz, 3H). <sup>13</sup>C NMR (101 MHz, CDCl<sub>3</sub>) δ 166.80, 152.24, 131.67, 117.86, 111.30, 62.06, 57.88, 45.70, 43.05, 31.39, 20.21, 13.84.

### <sup>1</sup>H and <sup>13</sup>C NMR spectra of aromatic amines

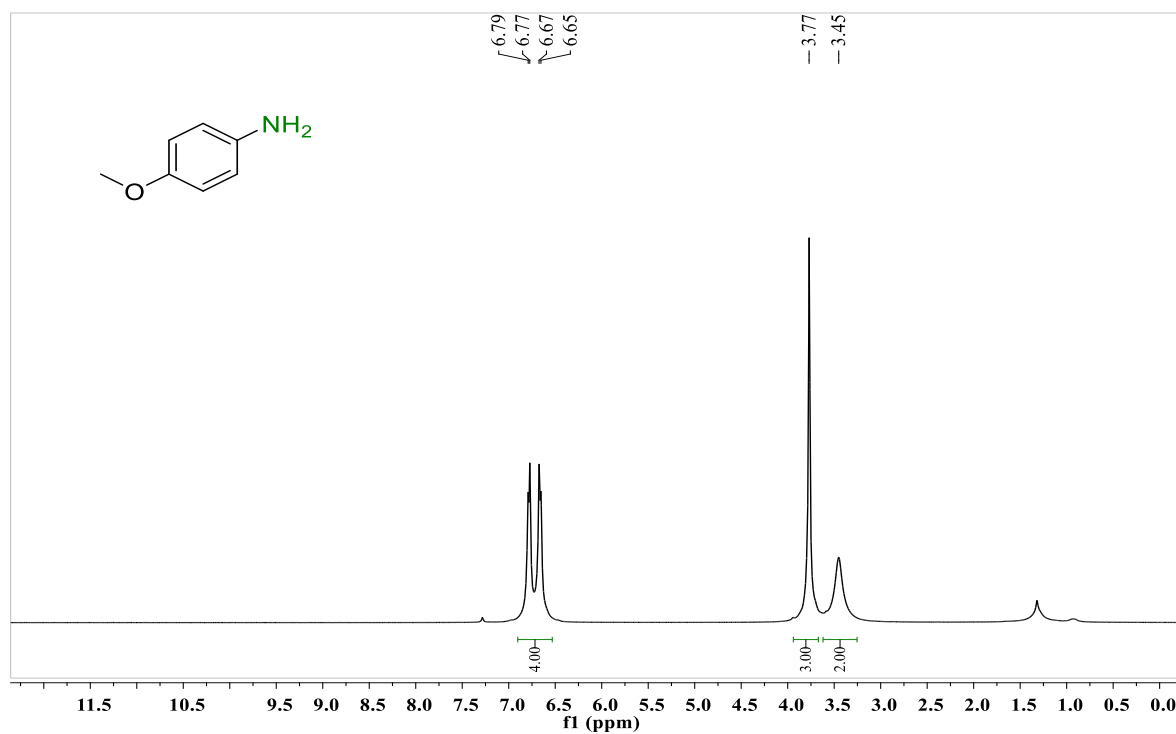


**Figure 3.2.**  $^1\text{H}$  NMR (400 MHz) spectrum of *p*-anisidine in  $\text{CDCl}_3$  at r.t.

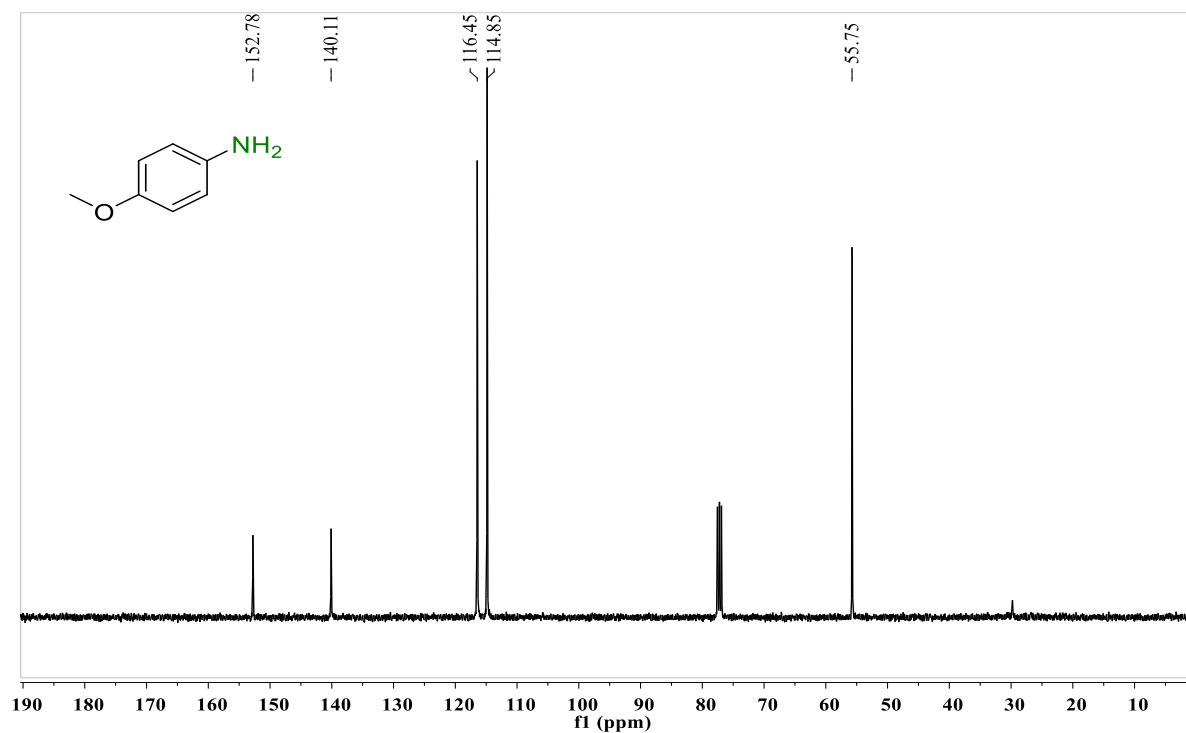


**Figure 3.3.**  $^{13}\text{C}$  NMR (101 MHz) spectrum of *p*-anisidine in  $\text{CDCl}_3$  at r.t.

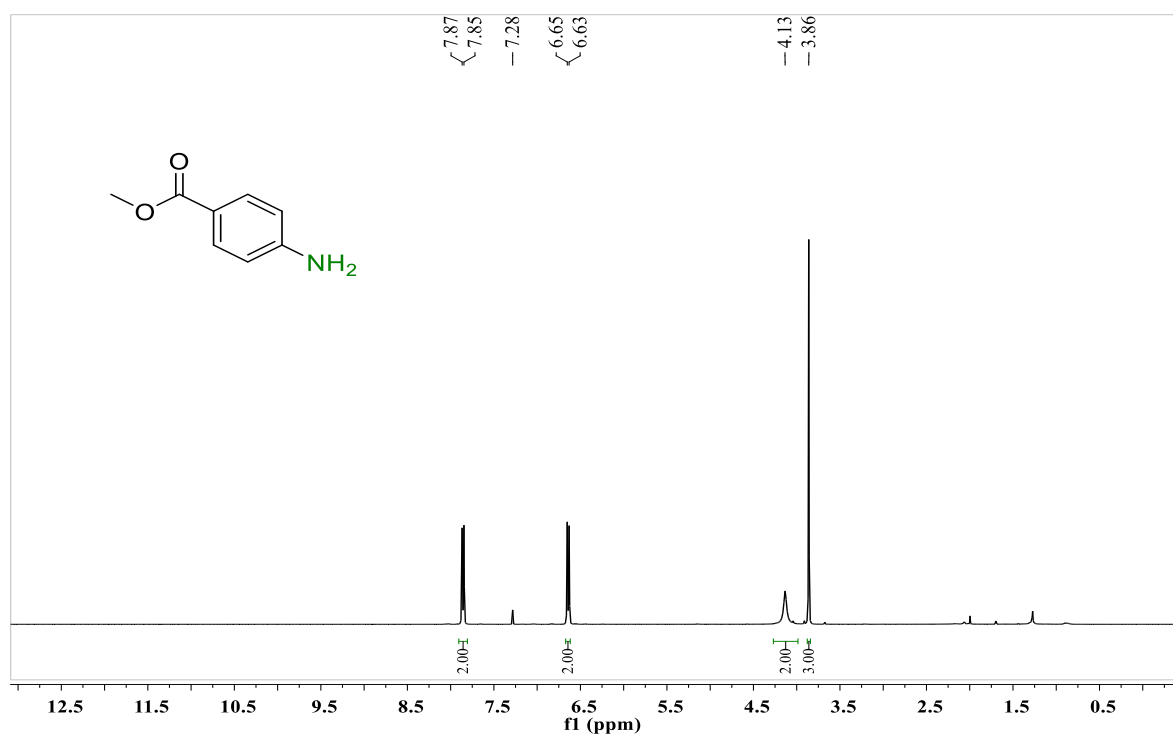


**Figure 3.4.** <sup>1</sup>H NMR (400MHz) spectrum of methyl 4-aminobenzoate (A<sub>6a</sub>) in CDCl<sub>3</sub> at r.t.

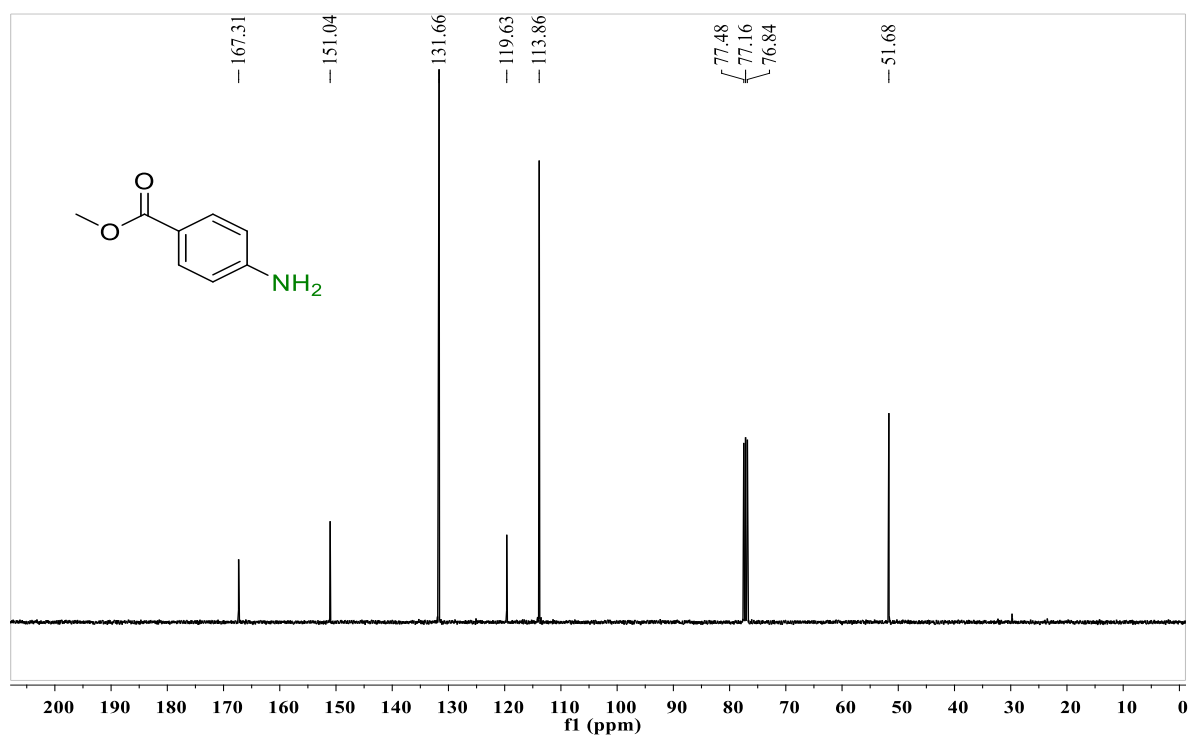


**Figure 3.5.** <sup>13</sup>C NMR (101MHz) spectrum of methyl 4-aminobenzoate (A<sub>6a</sub>) in CDCl<sub>3</sub> at r.t.

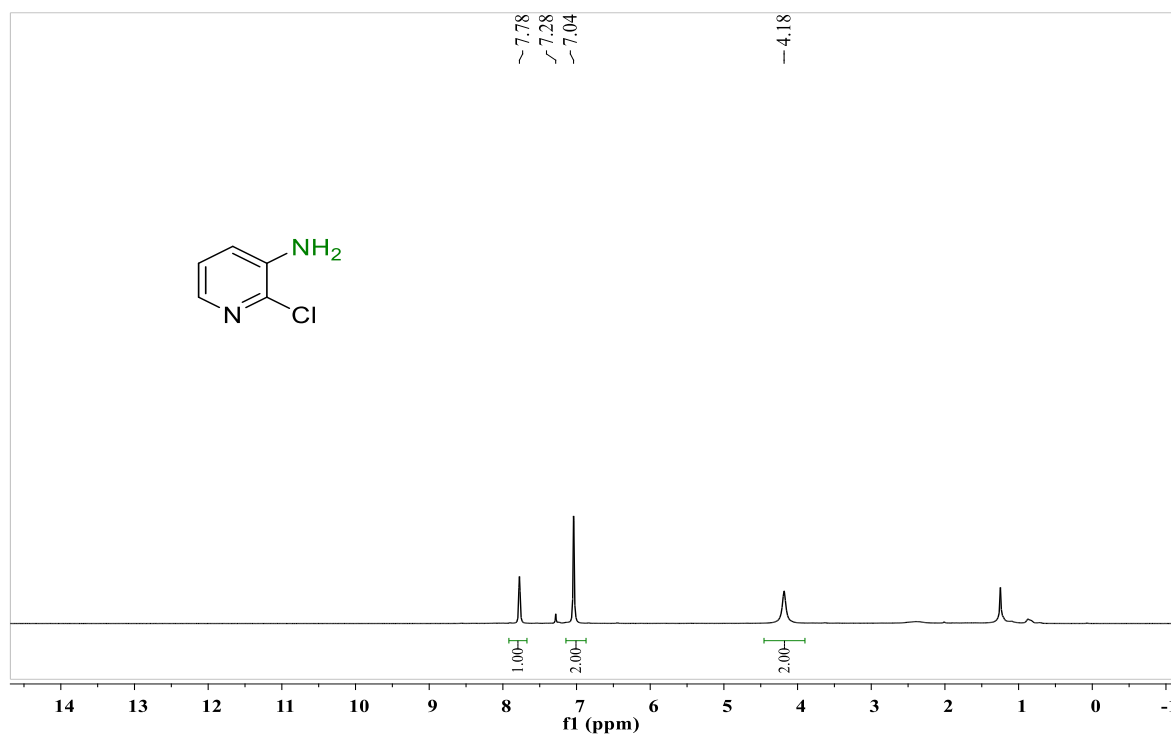


**Figure 3.6.** <sup>1</sup>H NMR (400MHz) spectrum of 3-amino-2-chloropyridine (A19) in CDCl<sub>3</sub> at r.t.

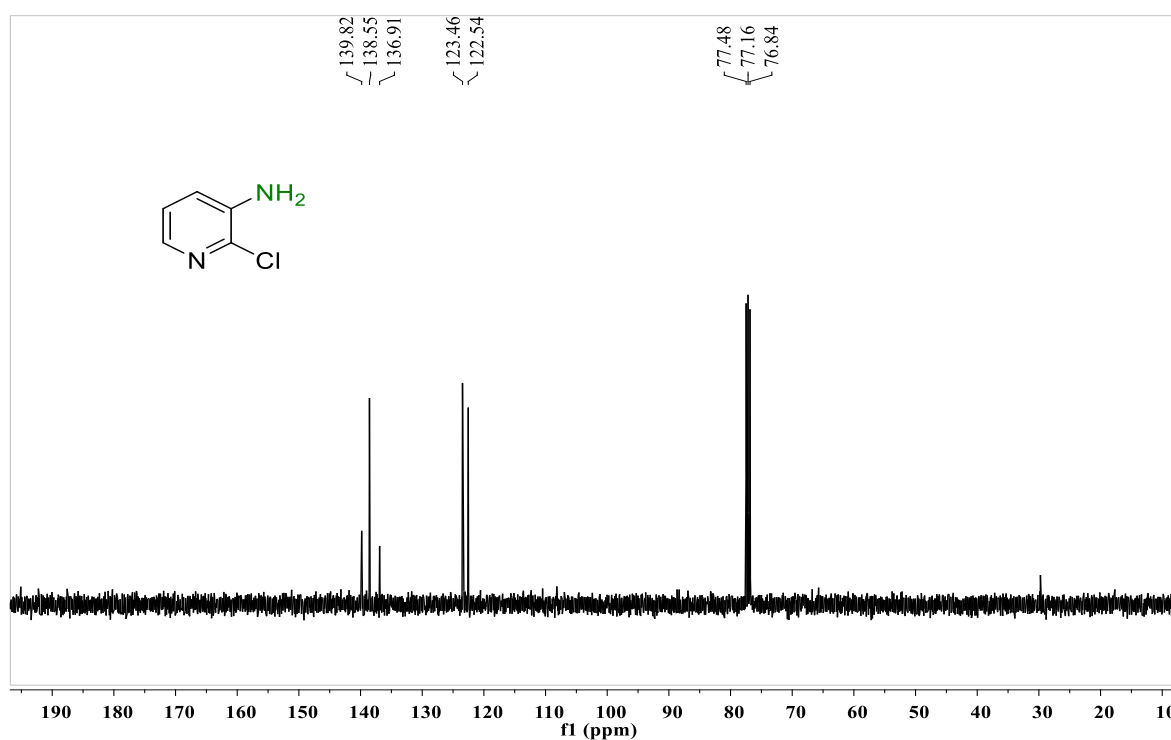


**Figure 3.7.** <sup>13</sup>C NMR (101MHz) spectrum of 3-amino-2-chloropyridine (A19) in CDCl<sub>3</sub> at r.t.

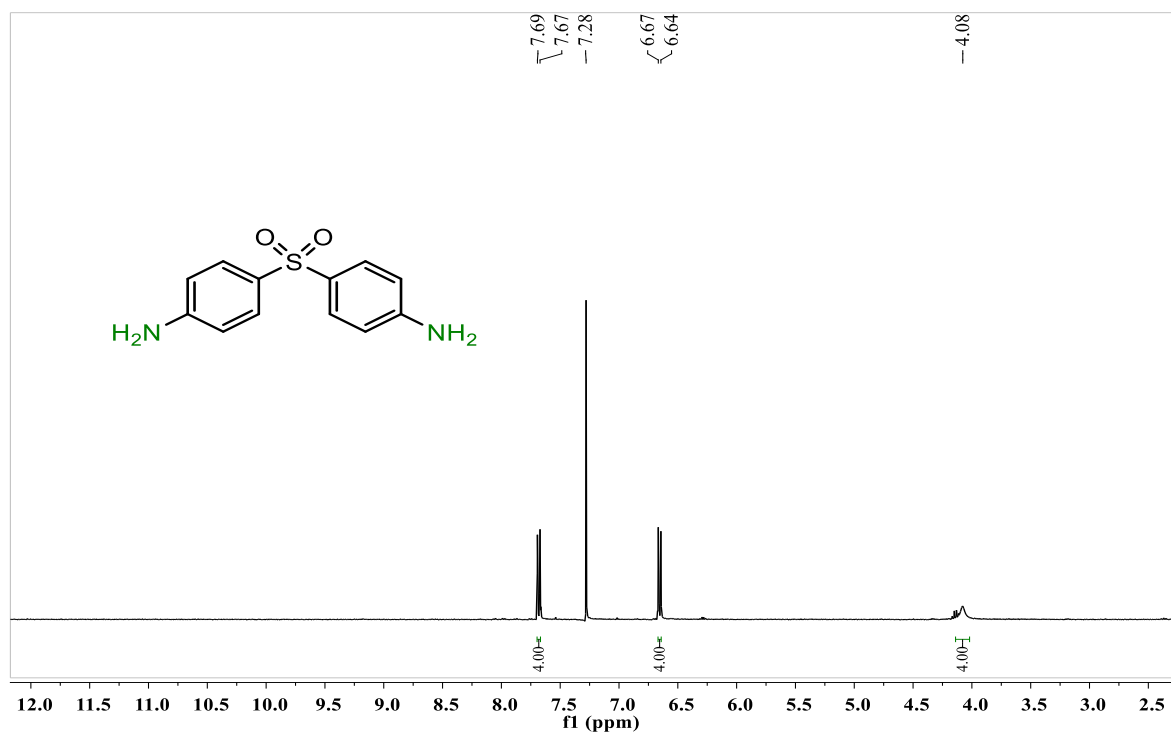


**Figure 3.8.**  $^1\text{H}$  NMR (400MHz) spectrum of 4,4'-sulfonyldianiline in  $\text{CDCl}_3$  at r.t.

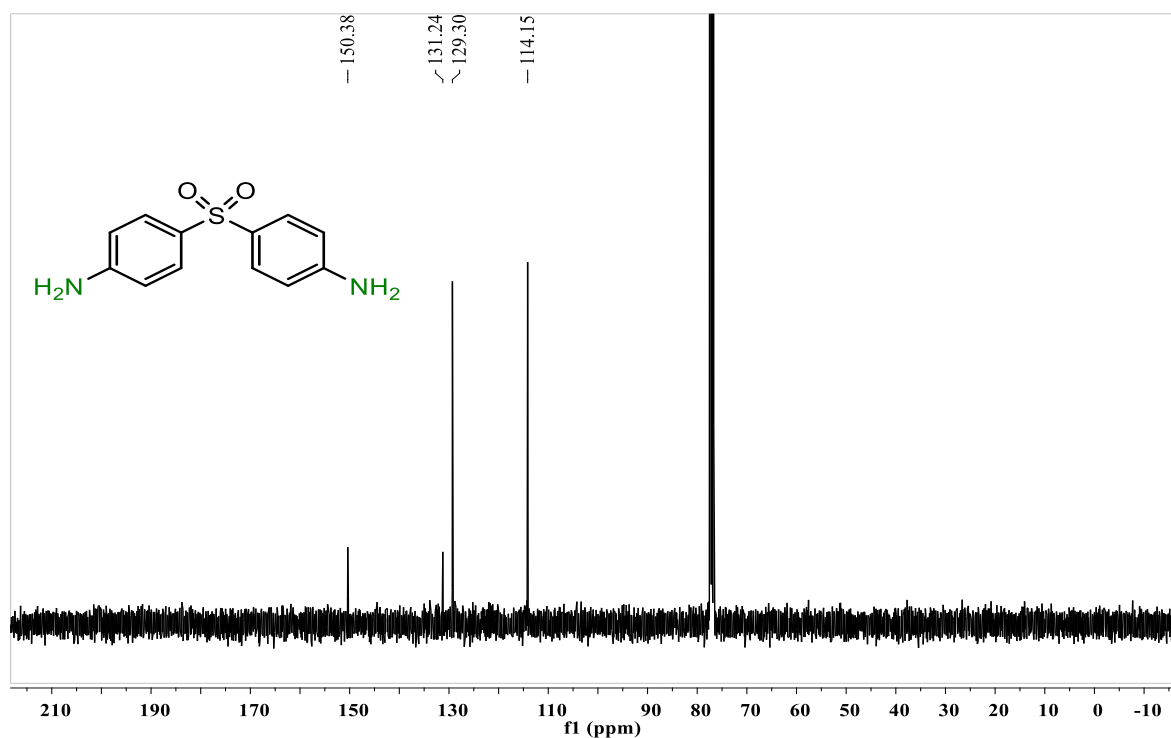


**Figure 3.9.**  $^{13}\text{C}$  NMR (101MHz) spectrum of 4,4'-sulfonyldianiline in  $\text{CDCl}_3$  at r.t.

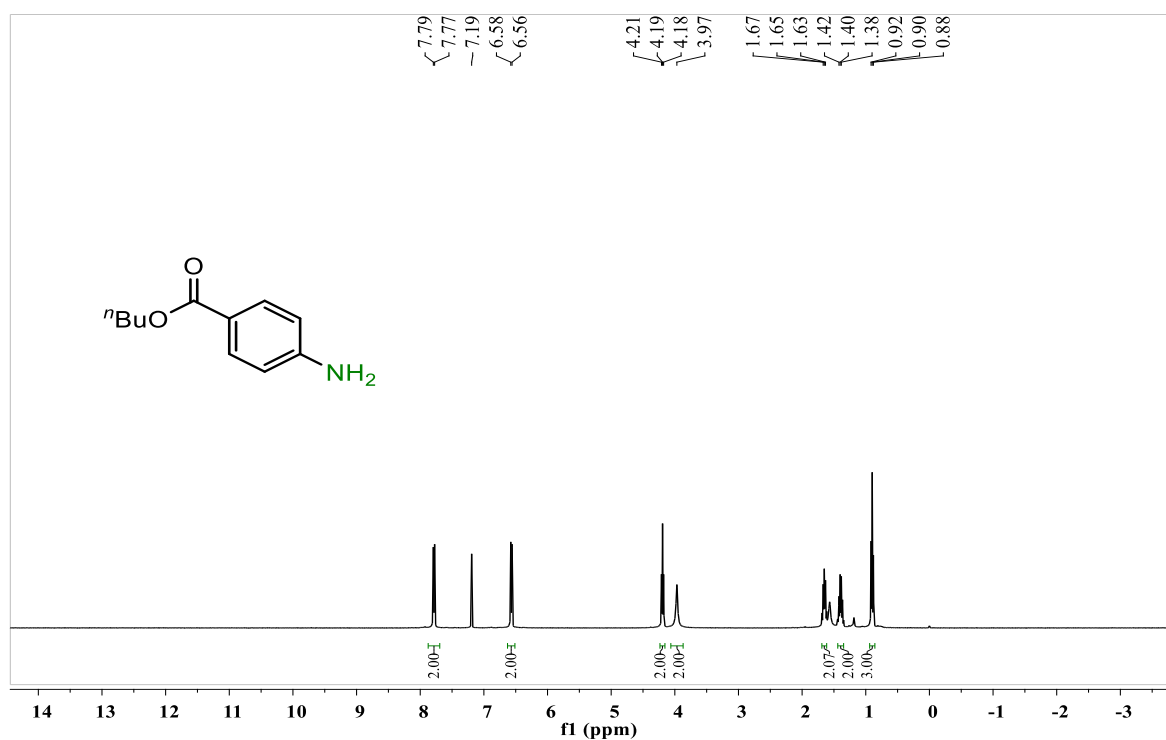


**Figure 3.10.**  $^1\text{H}$  NMR (400 MHz) spectrum of butyl 4-aminobenzoate  $\text{CDCl}_3$  at r.t.

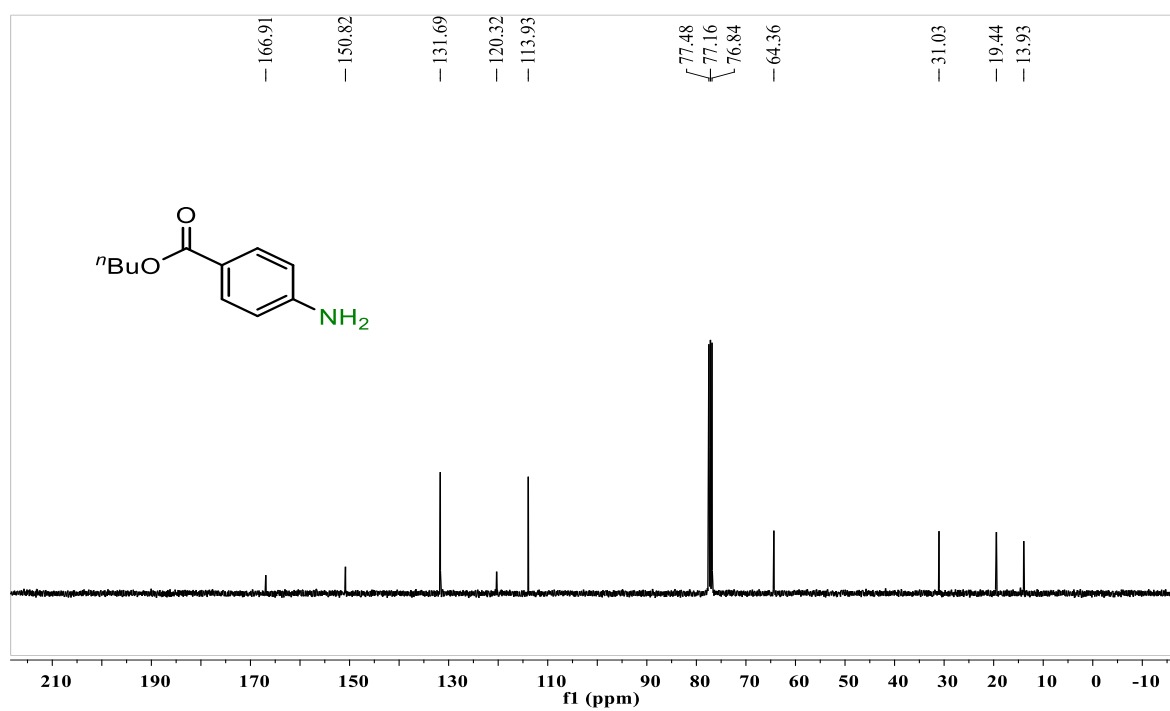


**Figure 3.11.**  $^{13}\text{C}$  NMR (101 MHz) spectrum of butyl 4-aminobenzoate in  $\text{CDCl}_3$  at r.t.

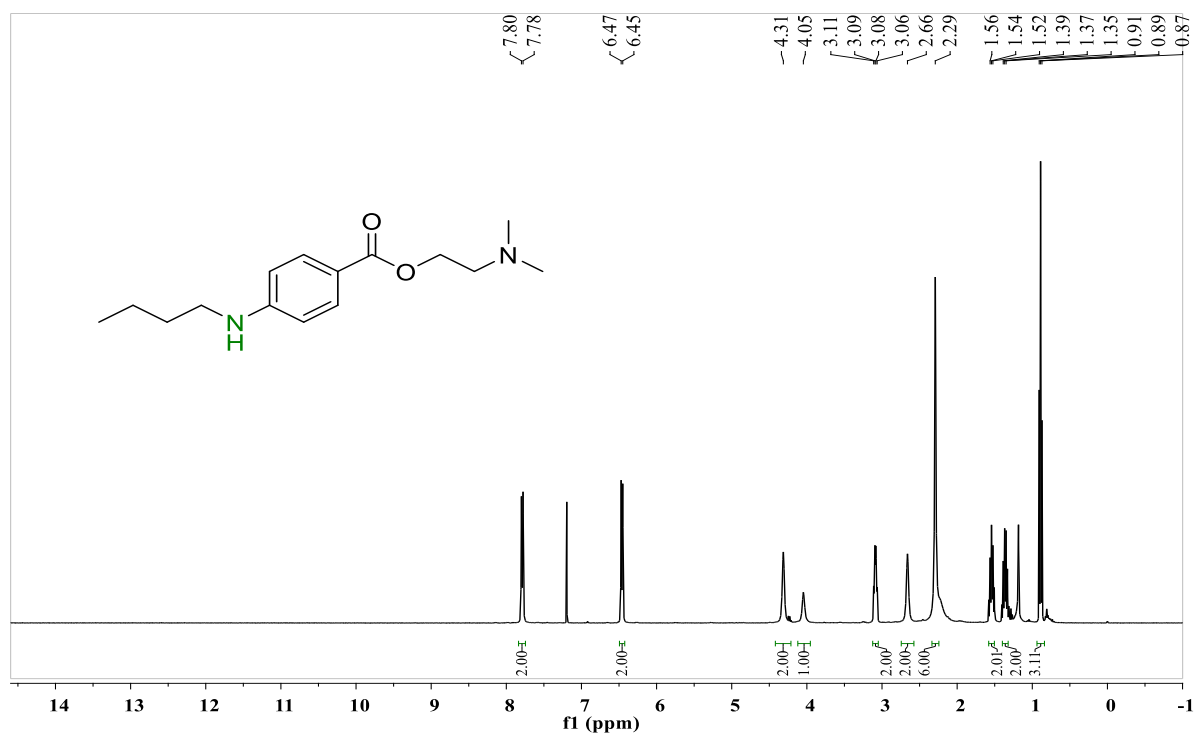


**Figure 3.12.**  $^1\text{H}$  NMR (400MHz) spectrum of 2-(dimethylamino)ethyl 4-(butylamino)benzoate in  $\text{CDCl}_3$  at r.t.

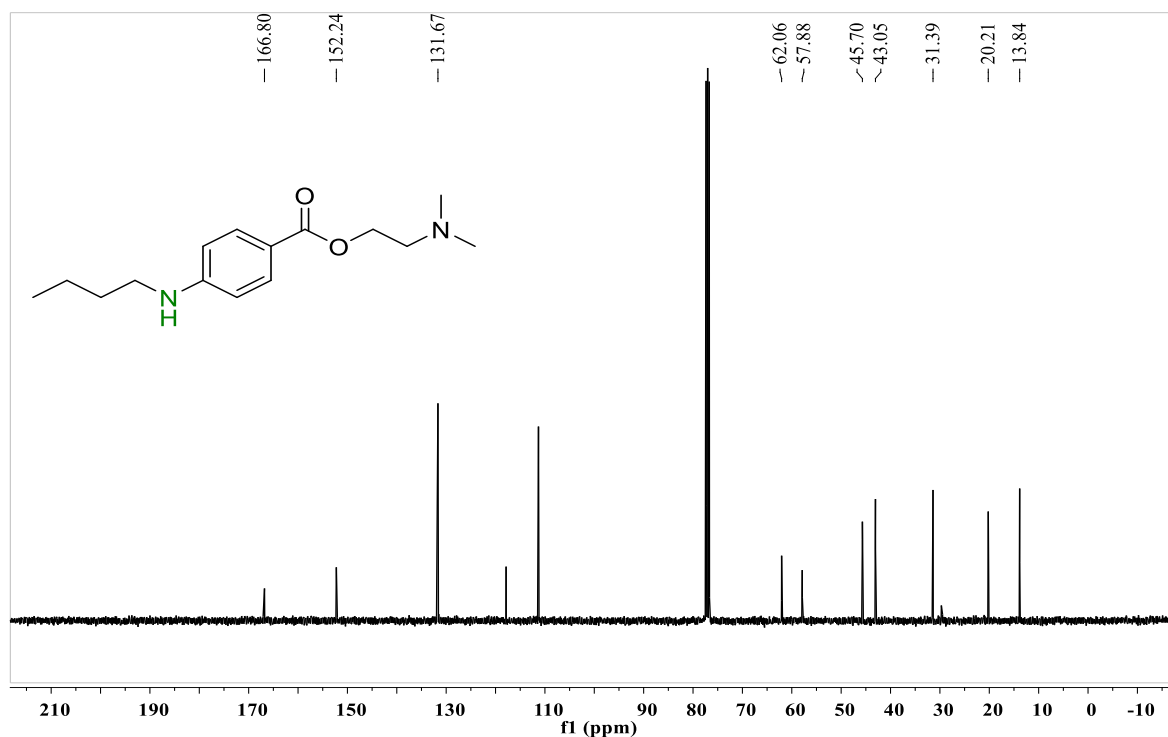
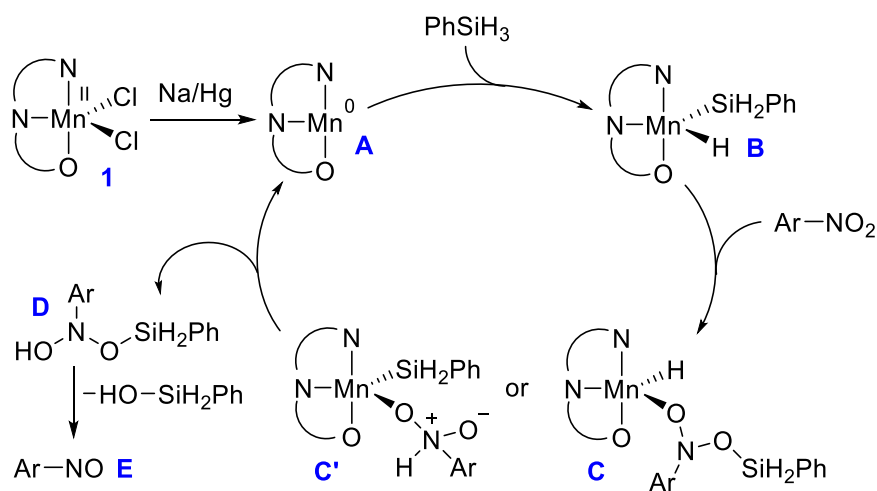


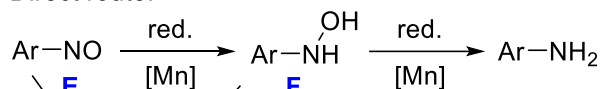
**Figure 3.13.**  $^{13}\text{C}$  NMR (101MHz) spectrum of 2-(dimethylamino)ethyl 4-(butylamino)benzoate in  $\text{CDCl}_3$  at r.t.

## Mechanistic analysis

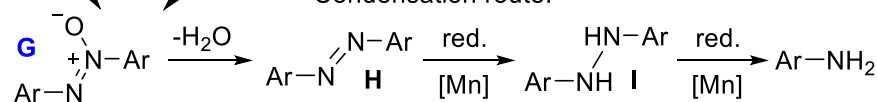
Plausible reaction mechanism:



Direct route:

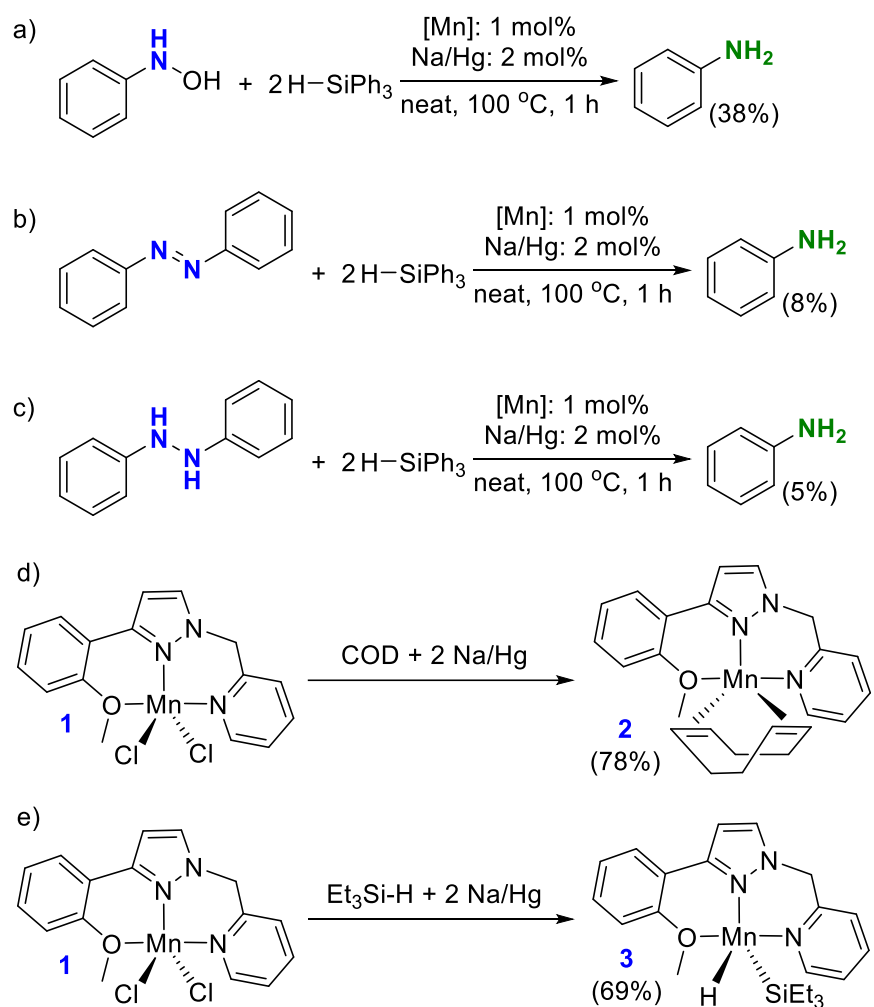


Condensation route:



Proposed reaction pathway: A plausible catalytic path for the hydrosilylation of nitroarene is proposed (above Scheme). During reaction optimization, we noted that manganese(II) catalyst (1) in presence of 2 equivalent of Na displayed much enhanced activity as compared to the 1:1 stoichiometric ratio of complex 1 and Na. This suggests the reduction of manganese(II) pre-catalyst 1 to manganese(0) species (A) as active catalyst. Oxidative addition of silicon-hydrogen bond to A resulted in the formation of silyl manganese(II) hydride species B. Thereafter, binding of nitroarene gave either species C or C'. Finally, reductive elimination of Ar-N(OSiH<sub>2</sub>Ph)OH (D) regenerates active catalyst A. Thereafter, Ar-N(OSiH<sub>2</sub>Ph)OH (D) forms nitrosoarene (E) which is further reduced to aniline either by direct route or via condensation route. Direct route involves the reduction of aryl nitroso Ar-NO (E) to N-hydroxylaniline Ar-NHOH (F) to aniline Ar-NH<sub>2</sub>. Condensation route involves the condensation of aryl nitroso Ar-NO (E) and N-hydroxylaniline Ar-NHOH (F) to azoxyarene (G) followed by the formation of dehydration product azoarene (H). Azoarene (H) is finally reduced to aniline via hydrazine intermediate (I).

## Control Experiments:

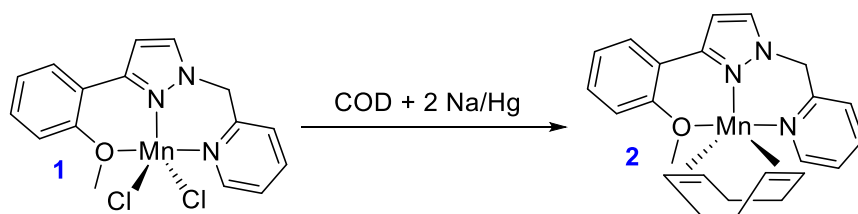


**Proposed reaction pathway:** Condensation route involves the condensation of aryl nitroso Ar-NO (E) and N-hydroxyaniline Ar-NHOH (F) to azoxyarene (G) followed by the formation of dehydration product azoarene (H). Azoarene (H) is finally reduced to aniline via hydrazine intermediate (I). Based on experimental evidences, Rueping et al. previously suggested manganese catalyzed hydrogenation of nitroarene proceeds via direct reduction route with the formation of N-hydroxyaniline Ar-NHOH (F).<sup>S15</sup> We performed mass analysis from the reaction mixture to detect any intermediate. We could not identify any mass peak for N-hydroxyaniline Ar-NHOH (F); however, the formation of azoarene (H) was clearly detected by mass analysis ( $M^+$ : 242.1103). Therefore, the possibility of condensation route could not be ruled out in present manganese catalyzed hydrosilylation of nitroarene. To shed further light on the reaction mechanism, the possible intermediates N-phenylhydroxylamine, azobenzene and 1,2-diphenylhydrazine were purchased and subjected to catalytic hydrosilylation (above Scheme, equation a, b and c) using following conditions (PhSiH<sub>3</sub>: 2 eq., 1: 1 mol%, Na/Hg: 2 mol%, neat, 100 °C, 1 h). The reduction of N-phenylhydroxylamine led to the formation of 38% of aniline, whereas azobenzene and 1,2-diphenylhydrazine gave only 5 and 8% of aniline, respectively. These results suggested that the reduction of nitroarene via direct route is more favorable in the presence of the present catalytic system.

We performed several other control experiments (Above Scheme, equation d and e). Reaction of **1** with 1 and 2 eq. of Na/Hg resulted in NMR inactive species which could not be isolated in pure form. As Mn(I) compounds are generally NMR active, it is expected that reduction of Mn(II) complex **1** gave Mn(0) species. To trap the proposed Mn(0) species, further reduction of **1** with Na/Hg (2 eq.) was performed in presence of COD (equation d). We isolated COD stabilized Mn(0) species **2** which was characterized by HRMS and elemental analysis. Species **2** was utilized as a catalyst (in absence of Na/Hg) and catalytic activity very similar to complex **1** (in presence of Na/Hg) was observed. Thereafter, we carried out the reduction of **1** with Na/Hg (2 eq.) performed in presence of Et<sub>3</sub>SiH and complex **3** was isolated as product (equation e). Complex **1** was reduced to Mn(0) species and oxidative addition of silicon-hydrogen bond yielded complex **3**, which is in agreement with initial steps of the proposed catalytic cycle. Despite several attempts, we could not get solid state structural information due to the poor quality of those crystals.

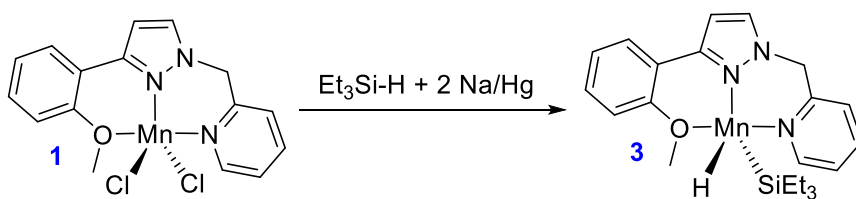
Catalytic hydrosilylations of 4-nitroanisole and nitrobenzene in presence of TEMPO radical took place without the loss of any catalytic activity which suggests to exclude radical process. Hydrosilylations of 4-nitroanisole and nitrobenzene were also unaltered in presence of excess mercury, which suggests to exclude the formation nano-particles.

### Synthesis of complex **2**



The following synthesis and characterization of complex 2 was done in dry N<sub>2</sub> atmosphere. 1,5-COD (0.05 mmol, 0.054g) was added to a suspension of complex 1 (0.020 g, 0.05 mmol) in CH<sub>3</sub>CN (2 mL). The mixture was stirred at r.t. for 20 minutes. Then 20 % Na/Hg (0.1 mmol, 0.012g) was added to the reaction mixture and the resultant mixture was stirred at refluxed for 16 h. A grey precipitate was formed and the liquid was decanted off. The solid was dried under high vacuum. Then solid was washed with Et<sub>2</sub>O (3 x 2 mL) and subsequently dried under high vacuum to give complex 2 (0.018 g, 78%). HRMS (ESI-TOF) *m/z*: [M + Na]<sup>+</sup> calcd for C<sub>24</sub>H<sub>27</sub>MnN<sub>3</sub>NaO: 451.4300, found 451.3268. Anal. Calcd for C<sub>24</sub>H<sub>27</sub>MnN<sub>3</sub>O (428.44): C, 67.28; H, 6.35; N, 9.81. Found: C, 67.43; H, 6.47; N, 10.04.

### Synthesis of complex 3



The following synthesis and characterization of complex 2 was done in dry N<sub>2</sub> atmosphere. A mixture of complex 1 (0.05 mmol, 0.020 g), 20 % Na/Hg (2eq, 0.1 mmol, 0.012g) and Et<sub>3</sub>SiH (5eq, 0.25 mmol, 0.029g) was stirred at 100<sup>0</sup>C for 16 h. The resultant grey solution was then cooled down to r.t. Then it was dried under high vacuum and washed with hexane (3 x 2 mL) to remove excess Et<sub>3</sub>SiH. The resultant solid was then extracted with THF (5 mL). The solution was dried under high vacuum to give complex 3 (0.015 g, 69%). HRMS (ESI-TOF) *m/z*: [M + H]<sup>+</sup> calcd for C<sub>22</sub>H<sub>32</sub>MnN<sub>3</sub>OSi: 437.5400, found 437.1690. Anal. Calcd for C<sub>22</sub>H<sub>31</sub>MnN<sub>3</sub>OSi (436.53): C, 60.53; H, 7.16; N, N, 9.63. Found: C, 60.83; H, 7.37; N, 9.84.

Note: Several attempts to crystallize complex 2 and 3 gave poor quality crystals and solid-state structural information by single crystal XRD could not be achieved.

## REFERENCES

1. (a) Blaser, H.-U.; Baiker, A.; Prins, R., Heterogeneous catalysis and fine chemicals IV. Elsevier: **1997**. (b) Downing, R.; Kunkeler, P.; Van Bekkum, H., Catalytic syntheses of aromatic amines. *Catalysis today* **1997**, *37*, 121-136. (c) Wegener, G.; Brandt, M.; Duda, L.; Hofmann, J.; Kleszczewski, B.; Koch, D.; Kumpf, R.-J.; Orzesek, H.; Pirkl, H.-G.; Six, C., Trends in industrial catalysis in the polyurethane industry. *Appl. Catal., A* **2001**, *221*, 303-335. (d) Lawrence, S. A., Amines: synthesis, properties and applications. Cambridge University Press: **2004**. (e) Rappoport, Z., The Chemistry of Anilines, Part 1. John Wiley & Sons: **2007**. (f) Aniszewski, T., Alkaloids-Secrets of Life: Alkaloid Chemistry, Biological Significance, Applications and Ecological Role. Elsevier: **2007**. (g) Ricci, A., Amino group chemistry: from synthesis to the life sciences. John Wiley & Sons: **2008**.
2. (a) Béchamp, A., De l'action des proto-sels de fer sur la nitronaphtaline et la nitrobenzine; nouvelle méthode de formation des bases organiques artificielles de zinin. **1854**. (b) Sheldon, R. A.; Van Bekkum, H., Fine chemicals through heterogeneous catalysis. John Wiley & Sons: **2008**.
3. (a) Liu, L.; Qiao, B.; Chen, Z.; Zhang, J.; Deng, Y., Novel chemoselective hydrogenation of aromatic nitro compounds over ferric hydroxide supported nanocluster gold in the presence of CO and H<sub>2</sub>O. *Chem. Commun.* **2009**, 653-655. (b) He, L.; Wang, L. C.; Sun, H.; Ni, J.; Cao, Y.; He, H. Y.; Fan, K. N., Efficient and selective room-temperature gold-catalyzed reduction of nitro compounds with CO and H<sub>2</sub>O as the hydrogen source. *Angew. Chem., Int. Ed.* **2009**, *48*, 9538-9541. (c) Huang, J.; Yu, L.; He, L.; Liu, Y.-M.; Cao, Y.; Fan, K.-N., Direct one-pot reductive imination of nitroarenes using aldehydes and carbon monoxide by titania supported gold nanoparticles at room temperature. *Green Chem.* **2011**, *13*, 2672-2677.

4. Kumar, J. D.; Ho, M. M.; Toyokuni, T., Simple and chemoselective reduction of aromatic nitro compounds to aromatic amines: reduction with hydriodic acid revisited. *Tetrahedron Lett.* **2001**, *42*, 5601-5603.
5. Redemann, C. T.; Redemann, C. E., 5-Amino-2, 3-dihydro-1, 4-phthalazinedione: 1, 4-Phthalazinedione, 5-amino-2, 3-dihydro-. *Org. Synth.* **2003**, *29*, 8-8.
6. Panchenko, P. A.; Fedorov, Y. V.; Fedorova, O. A.; Perevalov, V. P.; Jonusauskas, G., Synthesis and spectral properties of 4-amino-and 4-acetylamino-N-arylnaphthalimides containing electron-donating groups in the N-aryl substituent. *Russ. Chem. Bull.* **2009**, *58*, 1233-1240.
7. Gkizis, P. L.; Stratakis, M.; Lykakis, I. N., Catalytic activation of hydrazine hydrate by gold nanoparticles: Chemoselective reduction of nitro compounds into amines. *Catal. Commun.* **2013**, *36*, 48-51.
8. Fountoulaki, S.; Daikopoulou, V.; Gkizis, P. L.; Tamiolakis, I.; Armatas, G. S.; Lykakis, I. N., Mechanistic studies of the reduction of nitroarenes by NaBH<sub>4</sub> or hydrosilanes catalyzed by supported gold nanoparticles. *ACS Catal.* **2014**, *4*, 3504-3511.
9. Amundsen, L. H.; Nelson, L. S., Reduction of nitriles to primary amines with lithium aluminum hydride. *J. Am. Chem. Soc.* **1951**, *73*, 242-244.
10. Setamdideh, D.; Khezri, B.; Mollapour, M., Convenient reduction of nitro compounds to their corresponding Amines with promotion of NaBH<sub>4</sub>/Ni (OAc) 2.4 H<sub>2</sub>O system in wet CH<sub>3</sub>CN. *Orient. J. Chem.* **2011**, *27*, 991.
11. (a) Rylander, P., In *Hydrogenation Methods* Academic Press. New York 1985, 157. (b) Johnstone, R. A.; Wilby, A. H.; Entwistle, I. D., Heterogeneous catalytic transfer hydrogenation and its relation to other methods for reduction of organic compounds. *Chem. Rev.* **1985**, *85*, 129-170. (c) James, B. R., *Homogeneous hydrogenation*. Wiley: 1973. (d) Greenspoon, N.; Keinan, E., Selective deoxygenation of unsaturated

- carbohydrates with Pd (0)/Ph<sub>2</sub>SiH<sub>2</sub>/ZnCl<sub>2</sub>. Total synthesis of (+) -(S, S) -(6-methyltetrahydropyran-2-yl) acetic acid. *J. Org. Chem.* **1988**, *53*, 3723-3731. (e) Rajagopal, S.; Spatola, A., Catalytic transfer hydrogenation. *J. Org. Chem.* **1995**, *56*, 4481-4486.
12. (a) Blaser, H. U.; Steiner, H.; Studer, M., Selective catalytic hydrogenation of functionalized nitroarenes: an update. *ChemCatChem* **2009**, *1*, 210-221. (b) Formenti, D.; Ferretti, F.; Scharnagl, F. K.; Beller, M., Reduction of nitro compounds using 3d-non-noble metal catalysts. *Chem. Rev.* **2018**, *119*, 2611-2680. (c) Orlandi, M.; Brenna, D.; Harms, R.; Jost, S.; Benaglia, M., Recent developments in the reduction of aromatic and aliphatic nitro compounds to amines. *Org. Process Res. Dev.* **2016**, *22*, 430-445.
13. (a) Baumeister, P.; Blaser, H.-U.; Studer, M., Strong reduction of hydroxylamine accumulation in the catalytic hydrogenation of nitroarenes by vanadium promoters. *Catal. Lett.* **1997**, *49*, 219-222. (b) Blaser, H. U.; Malan, C.; Pugin, B.; Spindler, F.; Steiner, H.; Studer, M., Selective hydrogenation for fine chemicals: Recent trends and new developments. *Adv. Synth. Catal.* **2003**, *345*, 103-151.
14. (a) Yu, Z.; Liao, S.; Xu, Y.; Yang, B.; Yu, D., Hydrogenation of nitroaromatics by polymer-anchored bimetallic palladium-ruthenium and palladium-platinum catalysts under mild conditions. *J. Mol. Catal. A: Chem.* **1997**, *120*, 247-255. (b) Knifton, J., Homogeneous catalyzed reduction of nitro compounds. IV. Selective and sequential hydrogenation of nitroaromatics. *J. Org. Chem.* **1976**, *41*, 1200-1206. (c) Toti, A.; Frediani, P.; Salvini, A.; Rosi, L.; Giolli, C., Hydrogenation of single and multiple N–N or N–O bonds by Ru (II) catalysts in homogeneous phase. *J. Organomet. Chem.* **2005**, *690*, 3641-3651. (d) Deshmukh, A. A.; Prashar, A. K.; Kinage, A. K.; Kumar, R.; Meijboom, R., Ru (II) phenanthroline complex as catalyst for chemoselective

- hydrogenation of nitro-aryls in a green process. *Ind. Eng. Chem. Res.* **2010**, *49*, 12180-12184.
15. Chepaikin, E.; Ivanova, V.; Zakhariev, A.; Shopov, D., Homogeneous catalytic hydrogenation of aromatic nitrocompounds by complexes of the platinum group metal with dyes. The reaction of nitrobenzene with a complex of rhodium with the anion-radical of potassium indigodisulfonate. *J. Mol. Catal.* **1980**, *10*, 115-119.
16. Harsy, S. G., Homogeneous hydrogenation of nitroaliphatic compounds catalyzed by group VIII transition metal phosphine complexes. *Tetrahedron* **1990**, *46*, 7403-7412.
17. Xu, S.; Xi, X.; Shi, J.; Cao, S., A homogeneous catalyst made of poly (4-vinylpyridine-co-N-vinylpyrrolidone)-Pd (0) complex for hydrogenation of aromatic nitro compounds. *J. Mol. Catal. A: Chem.* **2000**, *160*, 287-292.
18. Zakhariev, A.; Ivanova, V.; Khidekel, M.; Chepaikin, E.; Shopov, D. Hydrogenation of aromatic nitro-compounds in presence of platinum (ii) complex of 1-phenyl-azo-2-naphthol in dmf. *React. Kinet. Catal. Lett.* **1978**, *8*, 195-201.
19. Corma, A.; Gonzalez-Arellano, C.; Iglesias, M.; Sánchez, F., Gold complexes as catalysts: Chemoselective hydrogenation of nitroarenes. *Appl. Catal., A* **2009**, *356*, 99-102.
20. (a) Deshpande, R. M.; Mahajan, A. N.; Diwakar, M. M.; Ozarde, P. S.; Chaudhari, R., Chemoselective hydrogenation of substituted nitroaromatics using novel water-soluble iron complex catalysts. *J. Org. Chem.* **2004**, *69*, 4835-4838. (b) Wienhöfer, G.; Baseda-Krüger, M.; Ziebart, C.; Westerhaus, F. A.; Baumann, W.; Jackstell, R.; Junge, K.; Beller, M., Hydrogenation of nitroarenes using defined iron-phosphine catalysts. *Chem. Commun.* **2013**, *49*, 9089-9091.
21. Zubar, V.; Dewanji, A.; Rueping, M., Chemoselective Hydrogenation of Nitroarenes Using an Air-Stable Base-Metal Catalyst. *Org. Lett.* **2021**, *23*, 2742-2747.

22. (a) Ohkuma, T.; Ooka, H.; Ikariya, T.; Noyori, R., Preferential hydrogenation of aldehydes and ketones. *J. Am. Chem. Soc.* **1995**, *117*, 10417-10418. (b) Fleischer, S.; Zhou, S.; Junge, K.; Beller, M., General and highly efficient iron-catalyzed hydrogenation of aldehydes, ketones, and  $\alpha$ ,  $\beta$ -unsaturated aldehydes. *Angew. Chem.* **2013**, *125*, 5224-5228. (c) Glatz, M.; Stöger, B.; Himmelbauer, D.; Veiros, L. F.; Kirchner, K., Chemoselective hydrogenation of aldehydes under mild, base-free conditions: manganese outperforms rhenium. *ACS Catal.* **2018**, *8*, 4009-4016. (d) Cantu, D. C.; Padmaperuma, A. B.; Nguyen, M.-T.; Akhade, S. A.; Yoon, Y.; Wang, Y.-G.; Lee, M.-S.; Glezakou, V.-A.; Rousseau, R.; Lilga, M. A., A combined experimental and theoretical study on the activity and selectivity of the electrocatalytic hydrogenation of aldehydes. *ACS Catal.* **2018**, *8*, 7645-7658. (e) Gorgas, N.; Stöger, B.; Veiros, L. F.; Kirchner, K., Highly efficient and selective hydrogenation of aldehydes: a well-defined Fe (II) catalyst exhibits noble-metal activity. *ACS Catal.* **2016**, *6*, 2664-2672.
23. (a) Korstanje, T. J.; Ivar van der Vlugt, J.; Elsevier, C. J.; de Bruin, B., Hydrogenation of carboxylic acids with a homogeneous cobalt catalyst. *Science* **2015**, *350*, 298-302. (b) Cui, X.; Li, Y.; Topf, C.; Junge, K.; Beller, M., Direct Ruthenium-Catalyzed Hydrogenation of Carboxylic Acids to Alcohols. *Angew. Chem.* **2015**, *127*, 10742-10745. (c) Yokoyama, T.; Yamagata, N., Hydrogenation of carboxylic acids to the corresponding aldehydes. *Appl. Catal., A* **2001**, *221*, 227-239. (d) Manyar, H. G.; Paun, C.; Pilus, R.; Rooney, D. W.; Thompson, J. M.; Hardacre, C., Highly selective and efficient hydrogenation of carboxylic acids to alcohols using titania supported Pt catalysts. *Chem. Commun.* **2010**, *46*, 6279-6281.
24. (a) Srimani, D.; Mukherjee, A.; Goldberg, A. F.; Leitus, G.; Diskin-Posner, Y.; Shimon, L. J.; Ben David, Y.; Milstein, D., Cobalt-Catalyzed Hydrogenation of Esters to Alcohols: Unexpected Reactivity Trend Indicates Ester Enolate Intermediacy. *Angew. Chem., Int.*

- Ed.* **2015**, *54*, 12357-12360. (b) Werkmeister, S.; Junge, K.; Wendt, B.; Alberico, E.; Jiao, H.; Baumann, W.; Junge, H.; Gallou, F.; Beller, M., Hydrogenation of esters to alcohols with a well-defined iron complex. *Angew. Chem., Int. Ed.* **2014**, *53*, 8722-8726. (c) Chakraborty, S.; Dai, H.; Bhattacharya, P.; Fairweather, N. T.; Gibson, M. S.; Krause, J. A.; Guan, H., Iron-based catalysts for the hydrogenation of esters to alcohols. *J. Am. Chem. Soc.* **2014**, *136*, 7869-7872. (d) Espinosa-Jalapa, N. A.; Nerush, A.; Shimon, L. J.; Leitun, G.; Avram, L.; Ben-David, Y.; Milstein, D., Manganese-catalyzed hydrogenation of esters to alcohols. *Chem. - Eur. J.* **2017**, *23*, 5934-5938. (e) Adkins, H.; Folkers, K., The catalytic hydrogenation of esters to alcohols. *J. Am. Chem. Soc.* **1931**, *53*, 1095-1097. (f) Zhang, J.; Leitun, G.; Ben-David, Y.; Milstein, D., Efficient homogeneous catalytic hydrogenation of esters to alcohols. *Angew. Chem.* **2006**, *118*, 1131-1133.
25. (a) de Vries, J. G.; Mršić, N., Organocatalytic asymmetric transfer hydrogenation of imines. *Catal. Sci. Technol.* **2011**, *1*, 727-735. (b) Kainz, S.; Brinkmann, A.; Leitner, W.; Pfaltz, A., Iridium-catalyzed enantioselective hydrogenation of imines in supercritical carbon dioxide. *J. Am. Chem. Soc.* **1999**, *121*, 6421-6429. (c) Li, W.; Zhang, X., Asymmetric hydrogenation of imines. In *Stereoselective formation of amines*, Springer: **2013**; pp 103-144. (d) Willoughby, C. A.; Buchwald, S. L., Asymmetric titanocene-catalyzed hydrogenation of imines. *J. Am. Chem. Soc.* **1992**, *114*, 7562-7564. (e) Fleury-Brégeot, N.; de la Fuente, V.; Castillon, S.; Claver, C., Highlights of Transition Metal-Catalyzed Asymmetric Hydrogenation of Imines. *ChemCatChem* **2010**, *2*, 1346-1371.
26. (a) Spielmann, J.; Buch, F.; Harder, S., Early Main-Group Metal Catalysts for the Hydrogenation of Alkenes with H<sub>2</sub>. *Angew. Chem.* **2008**, *120*, 9576-9580. (b) González-Arellano, C.; Corma, A.; Iglesias, M.; Sánchez, F., Enantioselective hydrogenation of alkenes and imines by a gold catalyst. *Chem. Commun.* **2005**, 3451-3453. (c) Xu, R.; Chakraborty, S.; Bellows, S. M.; Yuan, H.; Cundari, T. R.; Jones, W. D., Iron-catalyzed

- homogeneous hydrogenation of alkenes under mild conditions by a stepwise, bifunctional mechanism. *ACS Catal.* **2016**, *6*, 2127-2135.
27. de Noronha, R. G.; Romao, C. C.; Fernandes, A. C., Highly chemo- and regioselective reduction of aromatic nitro compounds using the system silane/oxo-rhenium complexes. *J. Org. Chem.* **2009**, *74*, 6960-6964.
28. Brinkman, H. R.; Miles, W. H.; Hilborn, M. D.; Smith, M. C., The Reduction of Nitrobenzenes by Triethylsilane Using Wilkinson's Catalyst. *Synth. Commun.* **1996**, *26*, 973-980.
29. (a) Rahaim Jr, R. J.; Maleczka Jr, R. E., Palladium-catalyzed silane/siloxane reductions in the one-pot conversion of nitro compounds into their amines, hydroxylamines, amides, sulfonamides, and carbamates. *Synthesis* **2006**, *2006*, 3316-3340. (b) Rahaim, R. J.; Maleczka, R. E., Pd-catalyzed silicon hydride reductions of aromatic and aliphatic nitro groups. *Org. Lett.* **2005**, *7*, 5087-5090. (c) Iovel, I.; Golomba, L.; Fleisher, M.; Popelis, J.; Grinberga, S.; Lukevics, E., Hydrosilylation of (hetero) aromatic aldimines in the presence of a Pd (I) complex. *Chem. Heterocycl. Compd.* **2004**, *40*, 701-714. (d) Lipowitz, J.; Bowman, S. A., Use of polymethylhydrosiloxane as a selective, neutral reducing agent for aldehydes, ketones, olefins, and aromatic nitro compounds. *J. Org. Chem.* **1973**, *38*, 162-165.
30. Andrianov, K.; Sidorov, V.; Filimonova, M., Reaction of triethylsilane with nitrobenzene. *Chem. Informationsdienst* **1977**, *8*, no-no.
31. Fernández, G.; Pleixats, R., Rhodium Nanoparticles Stabilized by PEG-Tagged Imidazolium Salts as Recyclable Catalysts for the Hydrosilylation of Internal Alkynes and the Reduction of Nitroarenes. *Catalysts* **2020**, *10*, 1195.
32. Park, S.; Lee, I. S.; & Park, J., A magnetically separable gold catalyst for chemoselective reduction of nitro compounds. *Organic & Biomolecular Chemistry*, **2013**, *11*, 395-399.

33. Wu, J.; Tongdee, S.; Ammaiyappan, Y.; Darcel, C., A Concise Route to Cyclic Amines from Nitroarenes and Ketoacids under Iron-Catalyzed Hydrosilylation Conditions. *Adv. Synth. Catal.* **2021**, *363*, 3859-3865.
34. Zhang, N.; Quan, Z. J.; Wang, X. C., Nickel-Catalyzed Denitrated Coupling Reaction of Nitroalkenes with Aliphatic and Aromatic Alkenes. *Adv. Synth. Catal.* **2016**, *358*, 3179-3183.
35. Vijaykumar, G.; Mandal, S. K., An abnormal N-heterocyclic carbene based nickel complex for catalytic reduction of nitroarenes. *Dalton Trans.* **2016**, *45*, 7421-7426.
36. Lopes, R.; Pereira, M. M.; & Royo, B., Selective Reduction of Nitroarenes with Silanes Catalyzed by Nickel N-Heterocyclic Carbene Complexes. *ChemCatChem.* **2017**, *15*, 3073-3077.
37. (a) Wenz, J.; Vasilenko, V.; Kochan, A.; Wadehohl, H.; Gade, L. H., Coordination chemistry of the PdmBOX pincer ligand: reactivity at the metal and the ligand. *Eur. J. Inorg. Chem.* **2017**, *2017*, 5545-5556. (b) Ma, X.; Zuo, Z.; Liu, G.; Huang, Z., Manganese-catalyzed asymmetric hydrosilylation of aryl ketones. *ACS omega* **2017**, *2*, 4688-4692. (c) Trovitch, R. J., The emergence of manganese-based carbonyl hydrosilylation catalysts. *Acc. Chem. Res.* **2017**, *50*, 2842-2852. (d) Valyaev, D. A.; Wei, D.; Elangovan, S.; Cavailles, M.; Dorcet, V.; Sortais, J.-B.; Darcel, C.; Lugan, N., Half-sandwich manganese complexes bearing Cp tethered N-heterocyclic carbene ligands: synthesis and mechanistic insights into the catalytic ketone hydrosilylation. *Organometallics* **2016**, *35*, 4090-4098. (e) Trovitch, R. J., Comparing well-defined manganese, iron, cobalt, and nickel ketone hydrosilylation catalysts. *Synlett* **2014**, *25*, 1638-1642. (f) Zheng, J.; Elangovan, S.; Valyaev, D. A.; Brousses, R.; Cesar, V.; Sortais, J. B.; Darcel, C.; Lugan, N.; Lavigne, G., Hydrosilylation of Aldehydes and Ketones Catalyzed by Half-Sandwich Manganese (I) N-Heterocyclic Carbene Complexes. *Adv.*

*Synth. Catal.* **2014**, 356, 1093-1097. (g) Chidara, V. K.; Du, G., An efficient catalyst based on manganese salen for hydrosilylation of carbonyl compounds. *Organometallics* **2013**, 32, 5034-5037. (h) Riener, K.; Högerl, M. P.; Gigler, P.; Kühn, F. E., Rhodium-catalyzed hydrosilylation of ketones: Catalyst development and mechanistic insights. *ACS Catal.* **2012**, 2, 613-621. (i) Ghosh, C.; Mukhopadhyay, T. K.; Flores, M.; Groy, T. L.; Trovitch, R. J., A pentacoordinate Mn (II) precatalyst that exhibits notable aldehyde and ketone hydrosilylation turnover frequencies. *Inorg. Chem.* **2015**, 54, 10398-10406. (j) Son, S. U.; Paik, S.-J.; Chung, Y. K., Hydrosilylation of ketones catalyzed by tricarbonyl (naphthalene) manganese cation. *J. Mol. Catal. A: Chem.* **2000**, 151, 87-90. (k) Son, S. U.; Paik, S.-J.; Lee, I. S.; Lee, Y.-A.; Chung, Y. K.; Seok, W. K.; Lee, H. N., Chemistry of [(1 H-hydronaphthalene)Mn(CO)<sub>3</sub>]: The Role of Ring-Slippage in Substitution, Catalytic Hydrosilylation, and Molecular Crystal Structure of [(η<sup>3</sup>-C<sub>10</sub>H<sub>9</sub>)Mn(CO)<sub>3</sub>P(OMe)<sub>3</sub>]. *Organometallics* **1999**, 18, 4114-4118. (l) Mao, Z.; Gregg, B. T.; Cutler, A. R., Manganese-and Rhodium-Catalyzed Phenylsilane Hydrosilation-Deoxygenation of Iron Acyl Complexes Cp (L)(CO) FeC (O) R (L= CO, PPh<sub>3</sub>, P (OMe)<sub>3</sub>, P (OPh)<sub>3</sub>; R= CH<sub>3</sub>, Ph, CHMe<sub>2</sub>, CMe<sub>3</sub>). *Organometallics* **1998**, 17, 1993-2002. (m) Cavanaugh, M. D.; Gregg, B. T.; Chiulli, R.; Cutler, A. R., The reactions of hydrosilanes with the methoxycarbonyl complexes Cp (L)(CO) MCO<sub>2</sub>Me (M= Fe, Ru; L= CO, PPh<sub>3</sub>) and (L)(CO) xMCO<sub>2</sub>Me (M= Co, Mn; L= CO, PPh<sub>3</sub>; x= 3, 4, with and without catalysis. *J. Organomet. Chem.* **1997**, 547, 173-182. (n) DiBiase Cavanaugh, M.; Gregg, B. T.; Cutler, A. R., Manganese carbonyl complexes as catalysts for the hydrosilation of ketones: Comparison with RhCl(PPh<sub>3</sub>)<sub>3</sub>. *Organometallics* **1996**, 15, 2764-2769. (o) Hanna, P. K.; Gregg, B. T.; Cutler, A. R., Manganese carbonyl compounds as hydrosilation catalysts for organoiron acyl complexes. *Organometallics* **1991**, 10, 31-33.

38. (a) Zheng, J.; Chevance, S.; Darcel, C.; Sortais, J.-B., Selective reduction of carboxylic acids to aldehydes through manganese catalysed hydrosilylation. *Chem. Commun.* **2013**, 49, 10010-10012. (b) Antico, E.; Schlichter, P.; Werlé, C.; Leitner, W., Reduction of Carboxylic Acids to Alcohols via Manganese (I) Catalyzed Hydrosilylation. *JACS Au* **2021**, 1, 742-749.
39. (a) Behera, R. R.; Ghosh, R.; Panda, S.; Khamari, S.; Bagh, B., Hydrosilylation of Esters Catalyzed by Bisphosphine Manganese (I) Complex: Selective Transformation of Esters to Alcohols. *Org. Lett.* **2020**, 22, 3642-3648. (b) Mukhopadhyay, T. K.; Ghosh, C.; Flores, M.; Groy, T. L.; Trovitch, R. J., Hydrosilylation of aldehydes and formates using a dimeric manganese precatalyst. *Organometallics* **2017**, 36, 3477-3483. (c) Mukhopadhyay, T. K.; Rock, C. L.; Hong, M.; Ashley, D. C.; Groy, T. L.; Baik, M.-H.; Trovitch, R. J., Mechanistic investigation of bis (imino) pyridine manganese catalyzed carbonyl and carboxylate hydrosilylation. *J. Am. Chem. Soc.* **2017**, 139, 4901-4915. (d) Mukhopadhyay, T. K.; Flores, M.; Groy, T. L.; Trovitch, R. J., A highly active manganese precatalyst for the hydrosilylation of ketones and esters. *J. Am. Chem. Soc.* **2014**, 136, 882-885.
40. (a) Mukhopadhyay, T. K.; Flores, M.; Groy, T. L.; Trovitch, R. J., A  $\beta$ -diketiminato manganese catalyst for alkene hydrosilylation: substrate scope, silicone preparation, and mechanistic insight. *Chemical science* **2018**, 9, 7673-7680. (b) Carney, J. R.; Dillon, B. R.; Campbell, L.; Thomas, S. P., Manganese-Catalyzed Hydrofunctionalization of Alkenes. *Angew. Chem., Int. Ed.* **2018**, 57, 10620-10624. (c) Yang, X.; Wang, C., Diverse Fates of  $\beta$ -Silyl Radical under Manganese Catalysis: Hydrosilylation and Dehydrogenative Silylation of Alkenes. *Chinese Journal of Chemistry* **2018**, 36, 1047-1051. (d) Dong, J.; Yuan, X.-A.; Yan, Z.; Mu, L.; Ma, J.; Zhu, C.; Xie, J., Manganese-catalysed divergent silylation of alkenes. *Nat. Chem.* **2021**, 13, 182-190.

41. (a) Yang, X.; Wang, C., Dichotomy of manganese catalysis via organometallic or radical mechanism: stereodivergent hydrosilylation of alkynes. *Angew. Chem., Int. Ed.* **2018**, *57*, 923-928. (b) Liang, H.; Ji, Y.-X.; Wang, R.-H.; Zhang, Z.-H.; Zhang, B., Visible-Light-Initiated Manganese-Catalyzed E-Selective Hydrosilylation and Hydrogermylation of Alkynes. *Org. Lett.* **2019**, *21*, 2750-2754.
42. Ganguli, K.; Mandal, A.; Sarkar, B.; Kundu, S., Benzimidazole fragment containing Mn-complex catalyzed hydrosilylation of ketones and nitriles. *Tetrahedron* **2020**, *76*, 131439.

---

# Hydrosilylation of Terminal Alkynes Catalyzed by Air-stable Manganese-NHC Complex

---

**2.1 Abstract**

**2.2 Introduction**

**2.3 Result and Discussion**

**2.4 Conclusion**

**2.5 Experimental Section**

## 2.1 Abstract:

In recent years, catalysis with base metal manganese has received a significant amount of interest. Catalysis with manganese complexes having N-heterocyclic carbenes (NHCs) is relatively underdeveloped in comparison to the extensively investigated manganese catalysts possessing pincer ligands (particularly phosphine-based ligands). Herein, we describe the synthesis of an imidazolium salt decorated with picolyl arms (**L**<sub>2</sub>) as a NHC precursor. Facile coordination of **L**<sub>2</sub> with MnBr(CO)<sub>5</sub> in presence of base resulted in the formation a manganese(I)-NHC complex (**4.1**) as an air-stable solid in good isolated yield. Single crystal X-ray analysis revealed the structure of the cationic complex [Mn(CO)<sub>3</sub>(NHC)][PF<sub>6</sub>] with tridentate N,C,N-binding of the NHC ligand in facile fashion. This manganese complex was utilized as an effective catalyst for the hydrosilylation of terminal alkynes with good selectivity towards the less thermodynamically stable  $\beta$ -(Z)-vinylsilanes. This method provided good regioselectivity (*anti*-Markovnikov addition) and stereoselectivity ( $\beta$ -(Z)-product). Experimental evidences suggested that present hydrosilylation pathway involved a radical mechanism with manganese-hydride species as a possible reactive intermediate.

## 2.2 Introduction:

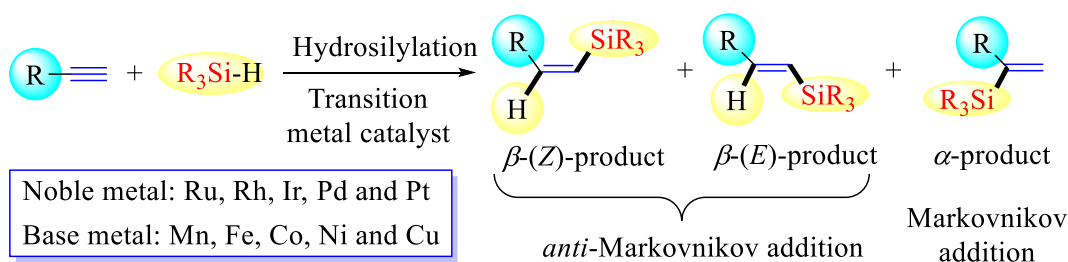
Vinylsilanes are widely used as versatile synthetic key components in organic synthesis and have widespread application in life sciences and material chemistry due to their excellent stability, low toxicity, and simplicity of handling.<sup>1</sup> The most simple and atom-efficient way to produce synthetically useful vinylsilanes is catalytic hydrosilylation of alkynes using transition metal complexes.<sup>2</sup> Controlling the regio- and stereoselectivity is a principal issue in hydrosilylation of alkynes, as this technique may result in a mixture of regio- and stereoisomers such as  $\alpha$ -,  $\beta$ -(Z)-, and  $\beta$ -(E)-vinylsilanes (Scheme 1a).  $\beta$ -(Z)-, and  $\beta$ -(E)-isomers are the results of *anti*-Markovnikov addition of Si-H bond to the alkyne moiety. Since the first report of homogeneous metal-catalyzed hydrosilylation of unsaturated C-C bond published in late

1950s,<sup>3</sup> researchers have investigated this chemical transformation in a variety of ways to develop new metal catalysts that lead to the regio- and stereoselective production of vinylsilanes. Over the last few decades, transition metal catalyzed hydrosilylations of various unsaturated moieties have been advanced immensely.<sup>4</sup> Parallely, various transition metal catalysts particularly with noble metals such as Ru, Rh, Ir, Pd and Pt have been developed for the hydrosilylation of alkynes.<sup>5</sup> However, most noble metal-catalyzed alkyne hydrosilylations yielded  $\beta$ -(*E*)-vinylsilanes.<sup>6</sup> But, the synthesis of the thermodynamically unfavorable  $\beta$ -(*Z*)-isomer is thought to be more difficult than the selective synthesis of  $\beta$ -(*E*)-vinylsilanes and thus,  $\beta$ -(*Z*)-selective hydrosilylation has remained a challenge synthetically.<sup>7</sup> Furthermore, some catalysts have been reported to produce competitive dehydrogenative silylation products, such as alkynylsilane and the corresponding alkene.<sup>8</sup> However, a number of catalysts based on noble metals such as Ru,<sup>9</sup> Rh,<sup>10</sup> and Ir<sup>10g, 11</sup> have been developed for the  $\beta$ -(*Z*)-selective hydrosilylations of terminal alkynes and several silane reagents were suitably applied in those reactions.

The use of earth-abundant and inexpensive base metal catalysts is important for sustainable and economical chemical transformations and in recent years, many efforts have been directed to the use of base metal catalysts which can catalyze hydrosilylation of alkenes and alkynes effectively. In this context, many base metal catalysts have been developed for the hydrosilylation of terminal and internal alkenes,<sup>12</sup> allenes<sup>13</sup> and conjugated dienes.<sup>14</sup> Similarly, several iron,<sup>15</sup> cobalt,<sup>13</sup> nickel<sup>16</sup> and copper<sup>17</sup> complexes have been used as catalysts for the selective hydrosilylations of alkynes. However, cobalt is the major player in this field and many cobalt catalysts have been developed for the selective hydrosilylation of alkynes to give  $\alpha$ -,<sup>18</sup>  $\beta$ -(*Z*)<sup>19</sup> and  $\beta$ -(*E*)-isomers.<sup>20</sup> Cobalt-catalyzed double hydrosilylation<sup>21</sup> and sequential hydrosilylation/hydroboration<sup>22</sup> are also reported. However, reports on manganese catalyzed hydrosilylation of alkynes are very rare. In the last two decades, manganese catalysts have

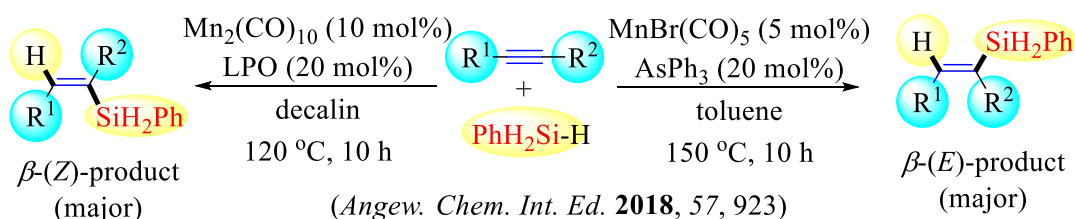
drawn considerable attention due to their fascinating reactivity and the high abundance, low cost and low toxicity of manganese metal is advantageous.<sup>23</sup> A wide variety of manganese complexes have been developed for the hydrosilylation of various unsaturated molecules such as aldehydes and ketones,<sup>24</sup> carboxylic acids,<sup>25</sup> esters,<sup>26</sup> amides,<sup>27</sup> nitriles<sup>28</sup> and alkenes.<sup>29</sup> Very recently, we reported the first example of manganese catalyzed hydrosilylation of nitroarenes.<sup>30</sup> In comparison, only two reports on manganese catalyzed hydrosilylation of alkynes have been published.<sup>31</sup> In 2018, Wang et al. reported the first example of manganese catalyzed hydrosilylation of alkynes and stereodivergent *E/Z* selectivity was highlighted (Scheme 1b).<sup>31a</sup> Various internal alkynes (aryl-aryl and aryl-alkyl alkynes) were subjected to successful hydrosilylation. Interestingly,  $\text{MnBr}(\text{CO})_5$  in presence of  $\text{AsPh}_3$  ligand catalyzed the selective formation of *E*-isomers while  $\text{Mn}_2(\text{CO})_{10}$  in presence of dilauroyl peroxide yielded *Z*-vinylsilane selectively. In the following year, manganese-catalyzed hydrosilylation of both terminal and internal alkynes was reported by Zhang *et al.* (Scheme 1b).<sup>31b</sup>  $\text{Mn}_2(\text{CO})_{10}$  was utilized as an efficient catalyst for visible light induced regio- and stereoselective hydrosilylation of alkynes, which yielded a range of valuable *Z*-vinylsilanes. Very recently, Li and co-workers used DFT calculations to study the mechanistic path for manganese-catalyzed hydrosilylation of alkynes using mononuclear  $\text{Mn}(\text{CO})_5\text{Br}$  and binuclear  $\text{Mn}_2(\text{CO})_{10}$  as catalysts.<sup>32</sup>

**a) Transition metal catalyzed hydrosilylation of alkynes:**

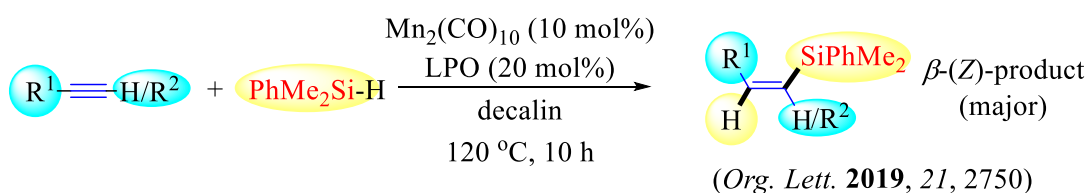


**b) Manganese catalyzed hydrosilylation of alkynes: Two reports**

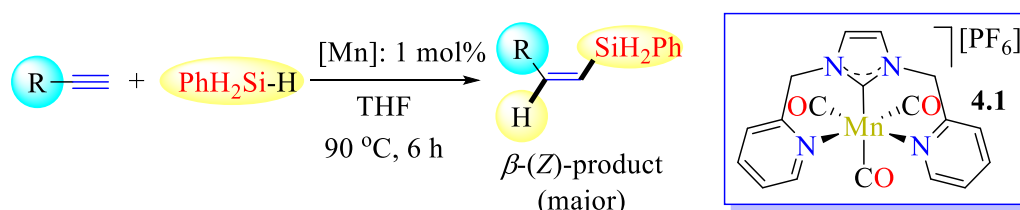
i) Stereodivergent hydrosilylation of internal alkynes by **Wang *et al.***



ii) Visible light initiated hydrosilylation of terminal and internal alkynes by **Zhang and Zhang *et al.***



**c) This work: Hydrosilylation of terminal alkynes catalyzed by manganese-NHC complex**



**Scheme 4.1 Transition metal catalyzed hydrosilylation of alkynes**

The ability of ligands to modify the electronic and steric properties of the metal core is an important consideration for the development of novel metal catalysts. For example, Zhu *et al.* reported iron complexes bearing bidentate 2,9-diaryl-1,10-phenanthroline ligands as excellent catalyst for hydrosilylation of alkynes in which rare ligand-controlled regioselective selectivity was observed by simply altering the substituents on the ligands.<sup>15f</sup> In addition to the steric impact of a ligand, electron-rich ligands can positively influence the hydrosilylation of alkynes by favoring the oxidative addition of Si-H bond. NHCs are widely used electron-rich

ligands in homogeneous catalysis with transition metals due to the accessibility of a wide range of topologies with adjustable electronic and steric properties.<sup>33</sup> In past twenty-year, various noble metal catalysts (Ru,<sup>34</sup> Rh,<sup>35</sup> Ir<sup>36</sup> and Pt<sup>37</sup>) equipped with various NHCs have been utilized for the hydrosilylation of alkynes. Among base metals, a copper-NHC complex<sup>17c</sup> and several cobalt-NHC complexes<sup>18b, 18e, 20a, 20b</sup> showed catalytic activity for alkyne hydrosilylation. Herein, we present an air-stable manganese-NHC complex which was effectively used for the hydrosilylation of both aromatic and aliphatic terminal alkynes (Scheme 1c). Decent selectivity for anti-Markovnikov addition was noted. The catalytic protocol was also stereoselective and a wide range of *Z*-vinylsilanes were produced.

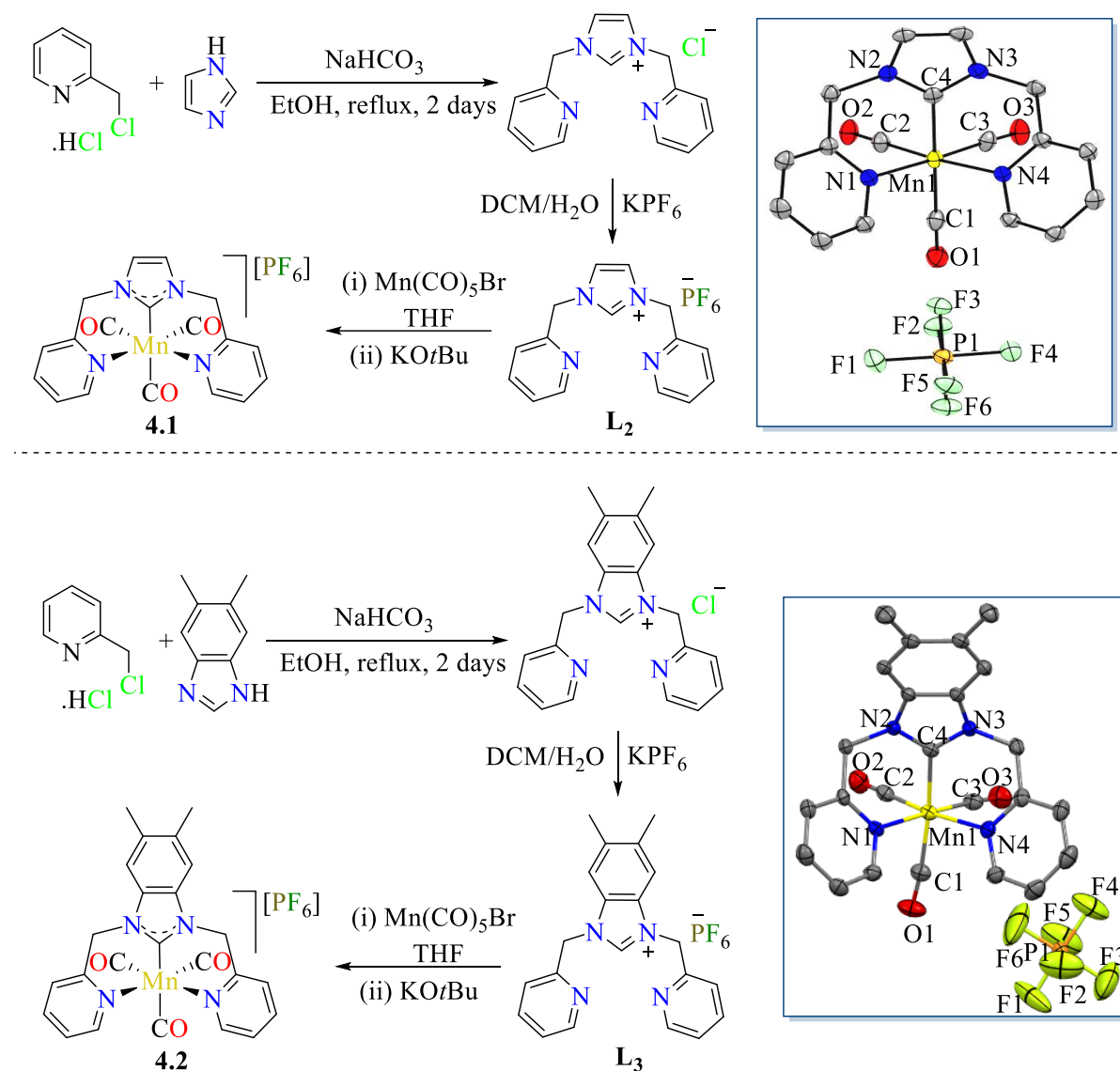
### 2.3 Result and Discussion

There is no example of manganese-NHC complex catalyzed hydrosilylation of alkynes. This motivated us to develop manganese-NHC complex which can be utilized as a catalyst in the hydrosilylation of alkynes. Catalytic use of manganese complexes in hydrosilylations of unsaturated moieties is a topic of continuous research interest in our group.<sup>26a, 30</sup> In addition, steric effect of a bulky ligand can influence the outcome of a stereoselective hydrosilylation of alkynes. For example, Huang et al. and Ge et al. illustrated the effect of bulky tridentate pincer ligands for the selective formation of  $\beta$ -(*Z*)-vinylsilanes in cobalt catalyzed hydrosilylation of alkynes.<sup>19</sup> Therefore, we wanted to develop tridentated NHC ligands which were supposed to give good stability of the resultant metal complexes with tridentate coordination as well provide necessary steric hindrance for selective hydrosilylation of alkynes. We selected two well-known imidazole based NHC precursor (**L**<sub>1</sub> and **L**<sub>2</sub>) decorated with two pendant picolyl donor arms (Scheme 2). These NHCs have already been used for the synthesis of various transition metal complexes, many of which showed good catalytic activity in various organic transformations.<sup>35, 36, 38</sup> Hence, we synthesized 1,3-bis(pyridin-2-ylmethyl)-1H-imidazolium hexafluorophosphates (**L**<sub>1</sub> and **L**<sub>2</sub>) as NHC precursors by using a slightly modified literature

procedure (Scheme 2). Imidazolium chloride salts were prepared by reacting imidazole or substituted imidazole with 2-(chloromethyl)-pyridine hydrochloride in presence of base under reflux. Resonances for the C2 imidazolium protons were observed in the characteristic low field range (10.91 and 11.55 ppm) of the  $^1\text{H}$  NMR spectra. Subsequently imidazolium hexafluorophosphate salts were obtained in good yields by anion exchange using potassium hexafluorophosphate. In the  $^1\text{H}$  NMR spectra of **L1** and **L2**, acidic imidazolium proton was observed at 8.81 and 9.34 ppm, respectively. Thereafter, we proceeded to metalation. By coordinating metal precursors  $\text{Mn}(\text{CO})_5\text{Br}$  with NHC-precursor **L1** having two picolyl wingtips followed by deprotonation of the imidazolium salt using base, we synthesized the manganese complex **4.1** in decent yield (58%). Very similarly, complex **4.2** was also obtained (63%). Both complexes are stable in solid state under atmospheric conditions and they can be kept in the air for weeks without noticeable change. Complex **4.1** and **4.2** were characterized by NMR, IR and UV-visible spectroscopy, mass spectrometry and elemental analysis. The carbene ligand framework was clearly visible in  $^1\text{H}$  and  $^{13}\text{C}\{^1\text{H}\}$  NMR spectra of complex **4.1**. As expected, characteristic C2 imidazolium proton was not observed in the  $^1\text{H}$  NMR spectrum of complex **4.1**. Methylene protons appeared as two characteristic doublets in the range of 5–6 ppm with coupling constants of 16 Hz. This suggests metal coordination of carbene as the methylene protons become diastereotopic after coordination to the manganese atom. The carbene carbon resonance appeared at 191.9 ppm in the  $^{13}\text{C}\{^1\text{H}\}$  NMR spectrum of complex **4.1**. The carbonyl carbons appeared in the expected low field region (210 to 225 ppm). Finally, the presence of hexafluorophosphate anion was shown by distinctive resonances in  $^{31}\text{P}$  (-144.17 ppm, heptate,  $1\text{ JFP } 711.4\text{ Hz}$ ) and  $^{19}\text{F}$  NMR spectra (-70.61 ppm, d,  $\text{JPF} = 706.8\text{ Hz}$ ).<sup>39a</sup> Complex **4.2** was sparingly soluble in all organic solvents and broad resonances for methyl groups, methylene protons and aromatic protons were observed in the expected range of  $^1\text{H}$  NMR spectrum. Low temperature  $^1\text{H}$  NMR measurement of complex **4.2** failed due to precipitation of the dissolved

compound on cooling. However, characteristic peaks in  $^{31}\text{P}$  (- 144.62 ppm, heptate, 1 JFP 711.4 Hz) and  $^{19}\text{F}$  NMR spectra (-72.90 ppm, d, JPF = 708.8 Hz) of complex **4.2** suggested the presence of hexafluorophosphate anion. In the IR spectrum of complex **4.1**, three distinct bands at 2028, 1944, and 1909  $\text{cm}^{-1}$  were observed, which are consistent with the presence of three carbonyl ligands in previously reported fac-isomer.<sup>39</sup> Similar pattern was also noted in the IR spectrum of complex **2** ( $\bar{\nu}$  CO: 2025, 1940 and 1904  $\text{cm}^{-1}$ ). HRMS analysis of complex **4.1** and **4.2** showed the peak at 389.0440 and 467.0506, respectively, corresponds to the molecular ion peak  $[\text{M} - \text{PF}_6]^+$ . The solid-state structure of complex **4.1** and **4.2** was obtained by single crystal X-ray diffraction study which further confirmed the identity of both complexes (Scheme 2). Both **4.1** and **4.2** are cationic in nature with general formula  $[\text{Mn}(\text{CO})_3(\kappa^3\text{N,C,N})][\text{PF}_6]$ . Complex **4.1** and **4.2** have three CO ligands coordinated in facial arrangements. The geometries around manganese metal centers are described as distorted octahedral. The carbene carbon atom (C4) and one CO ligand (C1) occupy the apical positions with C1–Mn1–C4 bond angle of 173.28(14) $^\circ$  and 171.45(16) $^\circ$  for **4.1** and **4.2**, respectively. The remaining two CO ligands (C2 and C3) and the nitrogen atoms of two picolyl moieties (N1 and N4) lie at the equatorial sites. The metal-carbene bond distances are 1.985(3) Å (for 1) and 2.003(3) Å (for 2) which are consistent with previous reports.<sup>40</sup> The metal-carbon distances of coordinated CO ligands are similar; however, very little variation was noted. In complex **4.1**, the metal-carbon distance at apical position (Mn1-C1: 1.845(4) Å) is slightly longer than the metal-carbon distances at the equatorial positions (Mn1-C2: 1.797(4) Å and Mn1-C3: 1.799(4) Å) due to the trans effect of the NHC moiety as well as the larger steric hindrance at the apical positions. Therefore, the carbonyl C-O bond distance at the apical position (C1-O1: 1.146(4) Å) is shorter than the carbonyl C-O bonds at the equatorial positions (C2-O2: 1.150(4) Å and C3-O3: 1.152(4) Å). Similarly in complex **4.2**, the metal-carbon distance at apical position (Mn1-C1: 1.837(4) Å)

is a little longer than the metal-carbon distances at the equatorial positions (Mn1-C2: 1.788(4) Å and Mn1-C3: 1.819(4) Å).



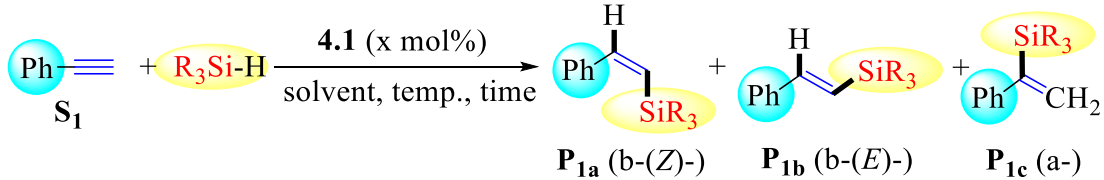
**Scheme 4.2** Synthesis of manganese complexes **4.1** and **4.2** with the molecular structure, using 50% probability ellipsoids (Hydrogen atoms are omitted for clarity)

With a well-characterized Mn(I)-NHC complexes (**4.1** and **4.2**) in hand, we set out to investigate the catalytic activity of complexes under various reaction conditions for the hydrosilylation of terminal alkyne using phenyl acetylene (**S<sub>1</sub>**) as standard substrate (Table 1). We started with complex **4.1** as it did not have any solubility issue in various organic solvents. In addition to those new Mn(I)-NHC complexes, we also screened other known Mn(I)

complexes such as commercially available  $\text{CpMn(CO)}_3$ ,  $\text{Mn(xantphos)(CO)}_2\text{Br}$  and  $\text{Mn(CO)}_3\text{Br}$  in presence of bidentate DPPE ligand (Table 1). A complete hydrosilylation of phenyl acetylene (**S**<sub>1</sub>) was observed when **S**<sub>1</sub> (0.5 mmol) was heated with 2 eq. of phenylsilane (1.0 mmol) at 100 °C in THF for 6 h in presence of 5 mol% of complex **4.1** (entry 1). The catalyst loading was gradually reduced to 1 mol% (entry 4) and again complete hydrosilylation of **S**<sub>1</sub> was observed in 24 h. In all reactions (entry 1 to 4), formation of Markovnikov product **P**<sub>1c</sub> was observed in small quantity (12-14%) and the rest was *anti*-Markovnikov addition products **P**<sub>1a</sub> and **P**<sub>1b</sub>. The major isomer was *Z*-vinylsilane **P**<sub>1a</sub> (81-82%) and a very small amount *E*-vinylsilane **P**<sub>1b</sub> (5-6%) of was noted. A blank test without added manganese catalyst was performed and only starting alkyne was recovered (entry 5). Then we tested secondary and tertiary silanes such as diphenylsilane, triethylsilane and triphenylsilanes, dimethoxymethylsilane, diethoxymethylsilane; methylbis(trimethylsilyloxy)silane, butylsilane and hexylsilane; however, poor catalytic conversion was noted (entry 6 to 13). So, phenylsilane proved to be the best. Thereafter, the reaction time was regularly decreased with constant catalyst loading of 1 mol% (entry 14 to 17). Complete hydrosilylation of **S**<sub>1</sub> was achieved in just 6 h (entry 16). If the reaction was run for 5 h, roughly 20% unreacted starting material **S**<sub>1</sub> was observed (entry 17). Next, we used just 1 eq. of phenylsilane instead of 2 eq. and full conversion of **S**<sub>1</sub> was noted in 6 h at 100 °C in THF in presence of 1 mol% of complex **4.1** (entry 18). A very similar product ratio (**P**<sub>1a</sub>/**P**<sub>1b</sub>/**P**<sub>1c</sub>: 84/3/13) was obtained. In addition to THF, we also used different solvent such as toluene (entry 19) and acetonitrile (entry 20); however, we observed poor conversion to products. The hydrosilylation of **S**<sub>1</sub> was also carried out under neat condition, but only unreacted starting material was isolated (entry 21). Finally, the reaction temperatures were steadily reduced (entry 22 to 25). Complete conversion of **S**<sub>1</sub> was noted at 90 °C in 6 h in THF in presence of 1 mol% of complex **4.1** (entry 22). The *Z/E* ratio was 28:1. If the reaction temperature was reduced to 80 °C, a small amount of unreacted starting material

was noted (entry 23). As expected, the amount of unreacted starting material increased with further lowering of reaction temperature (entry 24 and 25). Therefore, the optimized reaction condition for the hydrosilylation of phenyl acetylene is as follows: 1 mol% catalyst loading, 1 eq. PhSiH<sub>3</sub>, 90 °C, THF, 6 h (entry 22 depicted in blue). Under identical reaction condition (1 mol% catalyst loading, 1 eq. PhSiH<sub>3</sub>, 90 °C, THF, 6 h), we also tested Mn(I)-NHC complex **4.2** and other manganese(I) complexes (entry 26 to 29). Very poor hydrosilylation of phenyl acetylene (roughly 10%) was noted in presence complex **4.2** (entry 26). This poor catalytic activity of complex **4.2** might be due to its insolubility in THF. Other known manganese(I) complexes did not show any conversion under present reaction condition. Therefore, complex **4.1** was proved to be the best. As this catalytic hydrosilylation could be performed at elevated temperature, we wanted to check if present hydrosilylation of alkyne could be performed photochemically. Therefore, we carried out a light experiment to extend the applicability of the present catalyst. UV-vis measurement showed that complex **4.1** had  $\lambda_{\text{max}}$  at 350 nm. Hence, hydrosilylation was carried out using UV light irradiation of 350 nm wavelength. Using 5 mol% catalyst loading, phenylacetylene underwent complete hydrosilylation in 24 h at r.t. with a similar ratio of products ( $\beta$ -(Z)/ $\beta$ -(E)/ $\alpha$ : 80/10/10) that was obtained thermally. This demonstrates that the irradiation can also promote present manganese catalyzed hydrosilylation of alkyne.

**Table 4.1. Catalytic performance of 4.1 for the hydrosilylation of terminal alkynes.<sup>a</sup>**



entry	Mn	Silanes	temp.	Solvent	time	Conversion <sup>b</sup>	Selectivity <sup>b</sup> (%)
	(mol%)	(eq.)	(°C)	(1 mL)	(h)	(%)	$\beta$ -(Z)/ $\beta$ -(E)/ $\alpha$

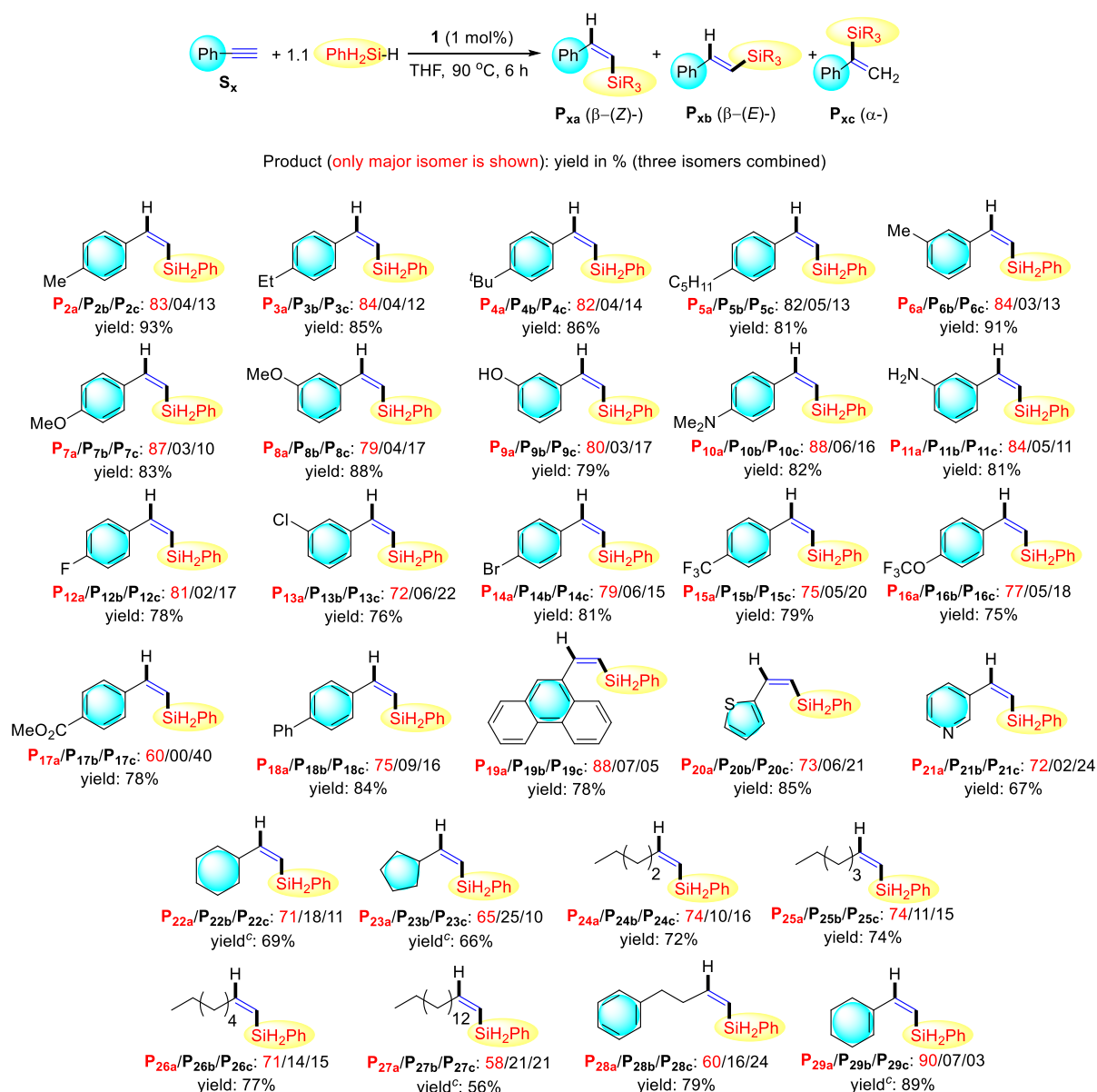
1	4.1 (5)	PhSiH <sub>3</sub> (2)	100	THF	24	>99 (93) <sup>c</sup>	82/06/12
2	4.1 (3)	PhSiH <sub>3</sub> (2)	100	THF	24	>99	81/05/14
3	4.1 (2)	PhSiH <sub>3</sub> (2)	100	THF	24	>99	81/06/13
4	4.1 (1)	PhSiH <sub>3</sub> (2)	100	THF	24	>99 (92) <sup>c</sup>	82/06/12
5	no	PhSiH <sub>3</sub> (2)	100	THF	24	0	
6	4.1 (1)	<b>Et<sub>3</sub>SiH</b> (1)	100	THF	24	25	53/30/17
7	4.1 (1)	<b>Ph<sub>3</sub>SiH</b> (1)	100	THF	24	0	
8	4.1 (1)	<b>Ph<sub>2</sub>SiH<sub>2</sub></b> (1)	100	THF	24	20	95/01/04
9	4.1 (1)	<b>(MeO)<sub>2</sub>MeSiH</b> (1)	100	THF	24	0	
10	4.1 (1)	<b>(EtO)<sub>2</sub>MeSiH</b> (1)	100	THF	24	0	
11	4.1 (1)	<b>(Me<sub>3</sub>SiO)<sub>2</sub>MeSiH</b> (1)	100	THF	24	0	
7	4.1 (1)	<b>nBuSiH<sub>3</sub></b> (1)	100	THF	24	<5	nd
7	4.1 (1)	<b>nHexSiH<sub>3</sub></b> (1)	100	THF	24	0	
14	4.1 (1)	PhSiH <sub>3</sub> (2)	100	THF	<b>18</b>	>99	84/03/13
15	4.1 (1)	PhSiH <sub>3</sub> (2)	100	THF	<b>12</b>	>99	84/04/12
16	4.1 (1)	PhSiH <sub>3</sub> (2)	100	THF	<b>6</b>	>99 (91) <sup>c</sup>	84/03/13
17	4.1 (1)	PhSiH <sub>3</sub> (2)	100	THF	<b>5</b>	79	76/11/13
18	4.1 (1)	PhSiH <sub>3</sub> (1)	100	THF	6	>99 (93) <sup>c</sup>	84/03/13
19	4.1 (1)	PhSiH <sub>3</sub> (1)	100	<b>toluene</b>	6	28	76/11/13
20	4.1 (1)	PhSiH <sub>3</sub> (1)	100	<b>CH<sub>3</sub>CN</b>	6	15	72/11/17
21	4.1 (1)	PhSiH <sub>3</sub> (1)	100	<b>neat</b>	6	0	
22	4.1 (1)	PhSiH <sub>3</sub> (1)	<b>90</b>	THF	6	>99 (92) <sup>c</sup>	84/03/13
23	4.1 (1)	PhSiH <sub>3</sub> (1)	<b>80</b>	THF	6	82 (79) <sup>c</sup>	82/03/15
24	4.1 (1)	PhSiH <sub>3</sub> (1)	<b>70</b>	THF	6	65	77/08/15
25	4.1 (1)	PhSiH <sub>3</sub> (1)	<b>60</b>	THF	6	56	72/09/19
26	4.2 (1)	PhSiH <sub>3</sub> (1)	<b>90</b>	THF	6	~10	64/22/14
27	4.3 (1)	PhSiH <sub>3</sub> (1)	<b>90</b>	THF	6	0	
28	4.4 (1)	PhSiH <sub>3</sub> (1)	<b>90</b>	THF	6	0	

29      4.5 (1)    PhSiH<sub>3</sub> (1)      90      THF      6      0

<sup>a</sup>Reactions conducted with 0.5 mmol of **S**<sub>1</sub>, 1.0/0.5 mmol of silanes, and 5/3/2/1 mol% of **1** in solvent (1.0 mL). <sup>b</sup>Conversion and selectivities were determined by <sup>1</sup>H NMR and GC using *n*-dodecane as standard. <sup>c</sup>Isolated yields.

Since complex **4.1** proved to be an effective catalyst for the hydrosilylation of phenylacetylene, the generality of its performance in the hydrosilylation of various terminal alkynes was tested. Previously optimized hydrosilylation protocol was utilized for catalytic hydrosilylation of various aromatic and aliphatic terminal alkynes to expand the substrate scope (Scheme 3). A wide range of phenylacetylene bearing various electronically and sterically different substituents reacted smoothly under optimized reaction condition yielding the corresponding *Z*-vinylsilanes in good yields and good stereoselectivities. At first, phenylacetylene substituted with various electron donating functionalities such as alkyls (**S**<sub>2</sub>, **S**<sub>3</sub>, **S**<sub>4</sub>, **S**<sub>5</sub>, **S**<sub>6</sub>), alkoxy (**S**<sub>7</sub>, **S**<sub>8</sub>), hydroxyl (**S**<sub>9</sub>) and amines (**S**<sub>10</sub>, **S**<sub>11</sub>) were tested and corresponding hydrosilylation products (**P**<sub>2</sub>: 93%, **P**<sub>3</sub>: 85%, **P**<sub>4</sub>: 86%, **P**<sub>5</sub>: 81%, **P**<sub>6</sub>: 91%, **P**<sub>7</sub>: 83%, **P**<sub>8</sub>: 88%, **P**<sub>9</sub>: 79%, **P**<sub>10</sub>: 82%, **P**<sub>11</sub>: 81%) were obtained in good to excellent yields. Generally good stereoselectivities were noted with *Z*-vinylsilanes as the major products (80 to 90%). Several halogen groups such as fluoro (**S**<sub>12</sub>), chloro (**S**<sub>13</sub>) and bromo (**S**<sub>14</sub>) were well tolerated with similar yields and stereoselectivities. Thereafter, we tested various substituted phenylacetylene with electron withdrawing groups such as trifluoromethyl (**S**<sub>15</sub>), trifluoromethoxy (**S**<sub>16</sub>) and ester (**S**<sub>17</sub>) and lower selectivity to *Z*-vinylsilane (60%) was noted only for methyl 4-ethynylbenzoate (**S**<sub>17</sub>). However, ethynylarenes with nitro (**S**<sub>18</sub>), cyano (**S**<sub>19</sub>), and carboxylic acid (**S**<sub>20</sub>) moieties did not undergo hydrosilylation under the optimized reaction condition. We also used 4-ethynylbiphenyl (**S**<sub>21</sub>) and 9-ethynylphenanthrene (**S**<sub>22</sub>) as substrates and good yields (**P**<sub>18</sub>: 84%, **P**<sub>19</sub>: 78%) and good *Z*-selectivities (*Z*-**P**<sub>18</sub>: 75%, *Z*-**P**<sub>19</sub>: 88%) were obtained. Sulfur and nitrogen containing heteroaromatic alkynes (**P**<sub>20</sub>: 85%, **P**<sub>21</sub>: 67%) were also compatible to this hydrosilylation protocol smoothly giving *Z*-vinylsilanes (*Z*-**P**<sub>20</sub>: 73%,

Z-P21: 72%) in good yields. Thereafter, aliphatic alkynes were also investigated. The catalyst loading was increased to 2 mol% and good yields and stereoselectivities were noted (Z-P22: 71%, Z-P23 : 65%). However, 1-hexyne and 1-heptyne hydrosilylation showed significant selectivity for the  $\beta$ -(Z)-vinylsilane isomers (Z-P24: 74%, Z-P25 : 74%, Z-P26 : 71%, Z-P27 : 58%, Z-P28 : 60%).



Scheme 4.3 Substrate scope for terminal alkyne hydrosilylation.<sup>a,b</sup>

<sup>a</sup>Reaction conditions: alkyne (0.5 mmol), PhSiH<sub>3</sub> (0.5 mmol), Mn(I) catalyst (1 mol%), THF (1.0 mL), 90 °C; yield of isolated product. <sup>b</sup>The  $\beta$ -(Z)/ $\beta$ -(E)/ $\alpha$  ratios were determined by GC. <sup>c</sup>catalyst loading (2 mol%).

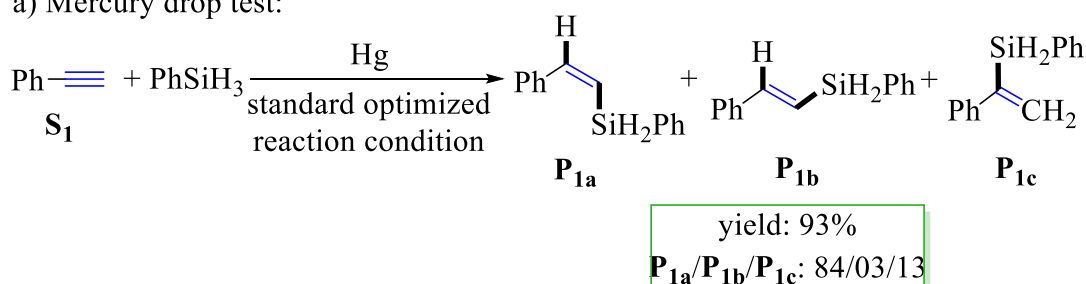
Thereafter, we performed several control experiments in order to get an idea of the reaction mechanism (Scheme 4). At first, mercury drop test was performed to check if the catalytic hydrosilylation was homogeneous in nature (Scheme 4a). In presence of added mercury, hydrosilylation of phenylacetylene was carried out using the optimized reaction condition (1 mol% complex **4.1**, 1 eq. PhSiH<sub>3</sub>, 90 °C, THF, 6 h) and we did not observe any change in product yield and selectivity. One of the two reports on manganese catalyzed hydrosilylation of alkynes described visible light induced radical pathway.<sup>26</sup> The other report described Mn<sub>2</sub>(CO)<sub>10</sub> catalyzed hydrosilylation of alkynes at elevated temperature in presence of dilauroyl peroxide as radical initiator and again radical pathway was proposed.<sup>25</sup> During our study, Royo *et al.* reported a very similar Mn-NHC complex which proved to be an efficient catalyst for the visible light induced hydrosilylation of ketones.<sup>37a</sup> Experimental evidences (radical trap experiments with TEMPO radical) suggested radical pathway. Therefore, we performed hydrosilylation of phenylacetyne using complex **4.1** as catalyst in presence of radical scavenger such as TEMPO radical and bromotrichloromethane (Scheme 4b). Hydrosilylation of phenylacetylene did not proceed at all in presence of those radical scavenger and only starting material was recovered. This clearly suggests that a radical mechanism is in the action in the present hydrosilylation of alkyne. These radical trap experiments with TEMPO radical or CCl<sub>3</sub>Br hint a radical mechanism is in action in the present hydrosilylation of alkyne. However, TEMPO could act as a ligand or oxidizing agent and as a result, it might change the nature of catalyst **4.1** yielding a catalytically inactive manganese complex. To gain further support on possible radical mechanism, we carried out catalytic hydrosilylation of phenyl acetylene in presence of 5,5-dimethyl-1-pyrroline N-oxide (DMPO) and dibutylhydroxytoluene (BHT) as radical scavenger. If a reaction undergoes radical path involving an active radical species, DMPO or BHT present in the reaction medium can trap the radical and form corresponding DMPO radical or BHT radical which can be identified by EPR

experiment (Scheme 4c). Mal *et al.* utilized this technique to establish radical mechanism for several reactions.<sup>44</sup> However, catalytic hydrosilylation of phenyl acetylene in presence of DMPO and BHT did not reveal the presence of EPR active DMPO radical or BHT radical. These negative EPR test does not suggest a radical path for this manganese catalyzed hydrosilylation of alkyne. Therefore, we looked into the possibility of the alternating organometallic path involving the oxidative addition of Si-H bond to the manganese metal center. For the hydrosilylations of unsaturated substrates, metal-hydride species are considered as an active intermediate in the catalytic cycle. Metal-hydrides are formed by the oxidative addition of the Si-H bond. Zhang *et al.* also proposed a manganese-hydride intermediates in the catalytic cycle of terminal alkyne hydrosilylation.<sup>26</sup> We also wanted to check if a manganese-hydride species is part of the catalytic cycle in the present hydrosilylation protocol. Hence, we carried out complex **4.1** catalyzed (1 mol%) hydrosilylation of phenylacetyne in presence of trityl tetrafluoroborate (1 mol%), a well-known hydride abstractor for organometallic compounds (Scheme 4d).<sup>37a, 38</sup> Addition of trityl tetrafluoroborate completely inhibited the hydrosilylation of phenylacetylene; only starting material was recovered. This clearly suggest hints the possible formation of manganese-hydride species in the catalytic cycle. Finally, we wanted to check the possible formation of low-valent manganese-silyl species as a reactive intermediate. Wang *et al.* reported hydrosilylation of alkyne catalyzed by  $\text{Mn}(\text{CO})_5\text{Br}$  in presence of  $\text{AsPh}_3$  ligand and the propose mechanism involves the formation of manganese-silyl species  $(\text{CO})_4(\text{AsPh}_3)\text{Mn-SiH}_2\text{Ph}$  as active catalyst.<sup>25</sup> Very recently, Li *et al.* revisited this reaction mechanism by DFT analysis and computation study also suggested the formation of manganese-silyl species  $(\text{CO})_4(\text{AsPh}_3)\text{Mn-SiH}_2\text{Ph}$  as active catalyst.<sup>27</sup> Therefore, we performed a stoichiometric reaction of complex **4.1** and  $\text{PhSiH}_3$  to identify the corresponding manganese-silyl species (Scheme 4e). Mass analysis from the reaction mixture clearly showed the formation of Mn(I)- $\text{SiH}_2\text{Ph}$  species **A** (HRMS (ESI)  $m/z$ :  $[\text{M}]^+$  calcd for

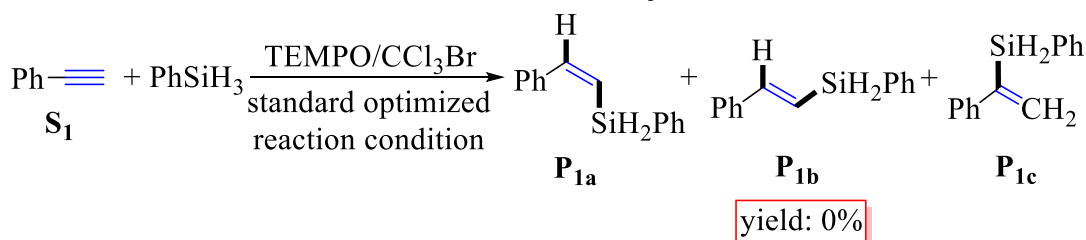
$C_{23}H_{21}MnN_4O_2Si$  468.0814; found 468.0785. However, we could not isolate species **A** in pure form despite of several attempts. The identification of manganese-silyl species **A** suggests that an organometallic mechanism is the likely scenario.

#### Scheme 4.4 Control experiments

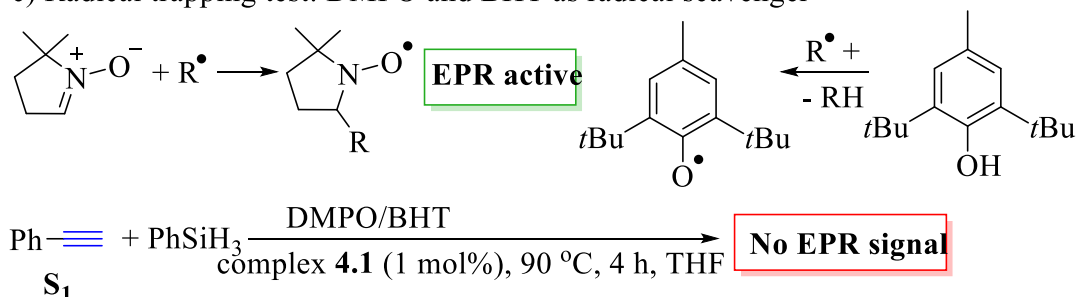
a) Mercury drop test:



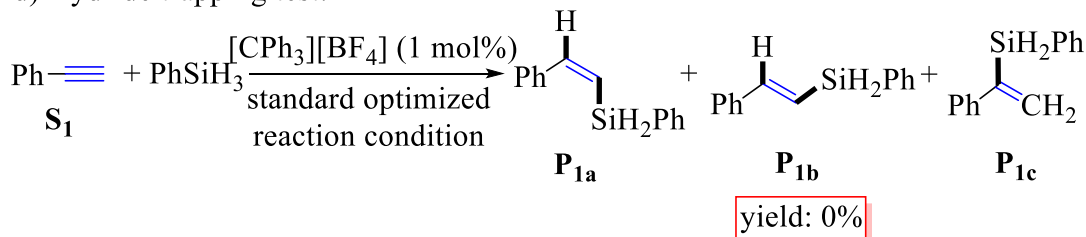
b) Radical trapping test: TEMPO radical and  $\text{CCl}_3\text{Br}$  as radical scavenger



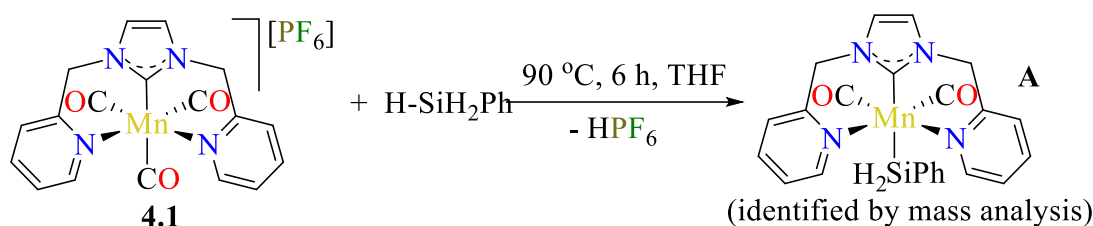
c) Radical trapping test: DMPO and BHT as radical scavenger



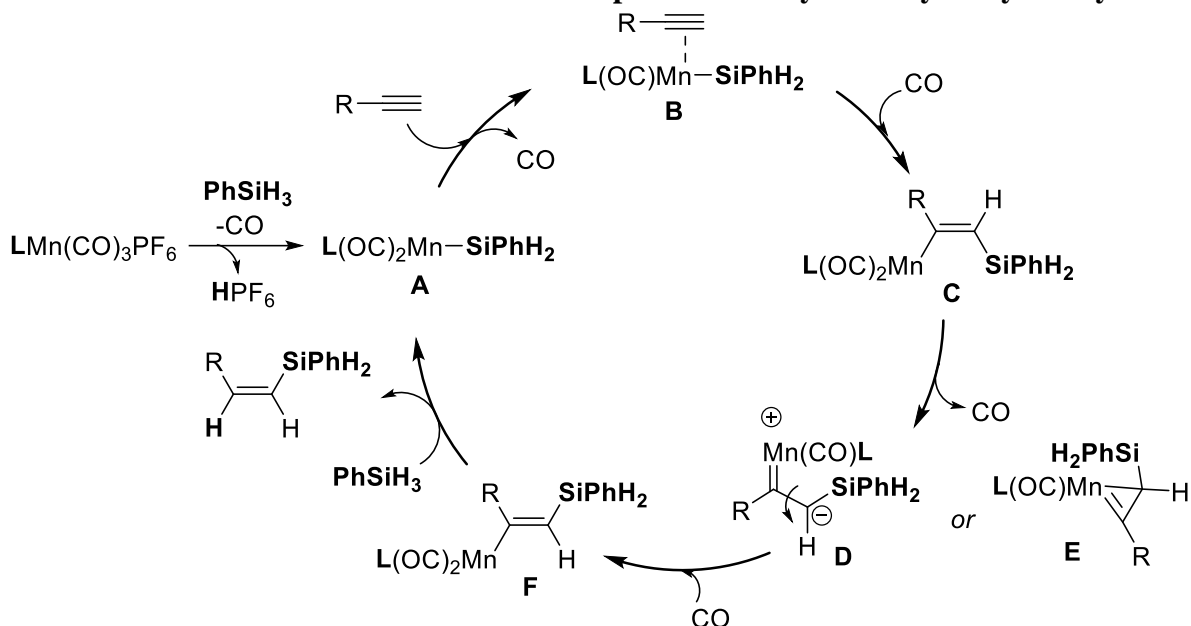
d) Hydride trapping test:



e) Formation of low-valent Mn(I)-silyl intermediate:



**Scheme 4.5 Plausible Reaction Path for Complex 4.1 Catalyzed Alkyne Hydrosilylation.**



Based on the experimental evidences, we propose a plausible catalytic cycle which is very similar to the mechanism proposed by Wang and Li *et al.* for the alkyne hydrosilylation catalyzed by  $\text{Mn(CO)}_5\text{Br}$  in presence of  $\text{AsPh}_3$  as ligand (Scheme 5). A manganese(I)-silyl species was proposed to be the active catalyst. Very similar catalytic paths were proposed for cobalt catalyzed hydrosilylations of alkynes, which also suggested similar low-valent cobalt-silyl species as active catalysts.<sup>19</sup> Our proposed organometallic reaction path starts with the formation of manganese(I)-silyl species **A**, which forms by the addition of  $\text{PhH}_2\text{Si-H}$  followed by the elimination of  $\text{HPF}_6$ . The coordination of the terminal alkyne to manganese followed by the insertion of coordinated alkyne into the Mn-Si bond yields a manganese-vinyl intermediate, (*Z*)-1-silyl-1-alken-2-yl-manganese (**C**). Manganese is coordinated with bulky NCN pincer ligand and thus, intermediate **C** undergoes isomerization possible due to the steric repulsion between the sterically crowded manganese moiety and bulky silyl group. Isomerization of (*Z*)-

l-silyl-1-alken-2-yl-manganese (**C**) via Ojima-Crabtree type rearrangement results in the formation of (*E*)-l-silyl-1-alken-2-yl-manganese intermediate (**F**) as a sterically less challenging species.<sup>10h</sup> Finally, PhSiH<sub>3</sub> reacts with manganese-vinyl intermediate, (*E*)-l-silyl-1-alken-2-yl-manganese (**F**) to give desired (*Z*)-vinylsilane and regenerates active manganese-silyl species **A**.

## 2.5 Conclusion

In conclusion, we have developed an air-stable picolyl-functionalized imidazolyldiene containing manganese(I) complex (**1**) which was utilized as an effective catalyst for the hydrosilylation of terminal alkynes at elevated temperature (90 °C). Only two reports on manganese (commercially available Mn<sub>2</sub>(CO)<sub>10</sub> and MnBr(CO)<sub>5</sub>) catalyzed hydrosilylation of alkynes were previously reported. We used low catalyst loading (1 mol%) in comparison to the previous reports (10 to 20 mol% of manganese loading). A wide range of aromatic and aliphatic terminal alkynes with various functionalities were successfully tested. Both Markovnikov and *anti*-Markovnikov addition products were detected. However, present hydrosilylation protocol was selective to *Z*-vinylsilanes, a thermodynamically less favored isomer. Several control experiments suggested a radical mechanism is in action. Several control experiments suggest an organometallic mechanism is in action and a in situ generated manganese(I)-silyl intermediate acts as active catalyst. The steric hindrance provided by NCN pincer ligand might play a crucial role for Ojima-Crabtree type rearrangement to give (*Z*)-vinylsilane as final product. Involvement of manganese-hydride species as an active intermediate is also established. A bulkier NCN pincer ligand was utilized to form another manganese(I) carbonyl complex (**4.2**). However, we failed to utilize complex **4.2** for the stereoselective hydrosilylation of alkynes due to very poor solubility of complex **4.2** in organic solvents. Further modification of ligand frameworks is presently undergoing to achieve better

selectivity for alkyne hydrosilylation. Further investigations will also involve the utilization of this manganese-NHC complex (**4.1**) for various hydrofunctionalization reactions.

## 2.6 Experimental Section

**General experimental.** Synthesis of the ligand **L**<sub>1</sub> was performed in air. All other experiments such as the synthesis of manganese complex and the catalytic hydrosilylation of terminal alkynes were performed under dry nitrogen atmosphere using standard Schlenk or glovebox (MBraun) techniques. Catalytic hydrosilylation of terminal alkynes were performed in Ace pressure tubes purchased from Sigma-Aldrich. Analysis and purification of the products of hydrosilylation of terminal alkynes were carried out in air. Solvents were purchased from Merck and Spectrochem. For the air-sensitive experiments, solvents (toluene, THF, acetonitrile and Et<sub>2</sub>O) were distilled, degassed and stored over 3 Å molecular sieves. Deuterated solvents (CDCl<sub>3</sub>, CD<sub>3</sub>CN and DMSO-d<sub>6</sub>) were purchased from Sigma-Aldrich. For recording NMR spectra of air and moisture sensitive samples, CD<sub>3</sub>CN and DMSO-d<sub>6</sub> were degassed and stored over 3 Å molecular sieves. Phenylsilane, diphenylsilane, triphenylsilane, triethylsilane and all alkynes were purchased from Sigma Aldrich, Alfa Aesar and TCI Chemicals and used without further purification.

<sup>1</sup>H and <sup>13</sup>C{<sup>1</sup>H} NMR spectra were recorded at Bruker AV-400, AV-700 and JEOL-400 (<sup>1</sup>H at 400 MHz and <sup>13</sup>C{<sup>1</sup>H} at 101 MHz). <sup>1</sup>H and <sup>13</sup>C{<sup>1</sup>H}, (<sup>31</sup>P{<sup>1</sup>H} and <sup>19</sup>F{<sup>1</sup>H}) NMR chemical shifts are referenced in parts per million (ppm) with respect to residual solvent peaks (CDCl<sub>3</sub>: δ 7.26 and 77.16 ppm; DMSO-d<sub>6</sub>: 2.50 and 39.52 ppm). The coupling constants (*J*) are reported in hertz (Hz). The following abbreviations are used to describe multiplicity: s = singlet, br = broad resonance, d = doublet, t = triplet, q = quadrate, m = multiplate, hep = heptate. GC analyses were performed on a Shimadzu GC-2014 spectrometer. High resolution mass spectra were recorded on a Bruker micrOTOF-Q II Spectrometer. Elemental analysis was carried out on a EuroEA Elemental Analyser. Crystal data were collected with Rigaku Oxford

diffractometer and with INCOATEC micro source (Mo-K $\alpha$  radiation,  $\lambda = 0.71073 \text{ \AA}$ , multilayer optics) at 293 K.

### Instrumentation Set Up of photoreactor

Luzchem Photoreactor Model - LZC-4X

Configuration: The LZC-4X photoreactor is equipped with 6 top lamps, and 8 side lamps.

Dimensions: External: 18" wide, 21" deep (with exhaust) and 16.5" high (46 x 53 x 42 cm)

Internal: 12" wide, 12" deep and 8.5" high (30 x 30 x 22 cm)

Power Rating: 110/220 VAC, 50/60 Hz cycle, 3 Amps Ships with North American-style power cable.

Housing Material: External: Stainless Steel

Internal (chamber): Al 5052-H32 (aluminium alloy).

Ambient Temperature: Must be between 10 °C and 35 °C.

Chamber Temperature: Maintained to 3-4 °C above room temperature.

Humidity: Must be between 0% and 95% (non-condensing)

**Synthesis of 1,3-bis(pyridin-2-ylmethyl)-1*H*-imidazolium chloride:** Compound 1,3-bis(pyridin-2-ylmethyl)-1*H*-imidazolium chloride is a known compound and was synthesized by following literature procedure with slight modification.<sup>30</sup> A mixture of imidazole (0.17 g, 2.50 mmol), 2-(chloromethyl)pyridine hydrochloride (0.82 g, 5.00 mmol) and sodium bicarbonate (0.65 g, 7.75 mmol) in anhydrous ethanol (90 mL) was heated in a preheated oil bath under reflux for 48 hours. The resultant reaction mixture was allowed to cool down to r.t. and filtered through a small plug of celite. All volatiles were removed by using rotary evaporation. The brown residue was dissolved in minimal amount of DCM (2-3 mL) and then triturated with THF (25-30 mL) resulting in a brown powder to precipitate. The supernatant was decanted off. The brown solid was washed with THF (3 x 5 mL) and dried in vacuum to give pure product (0.63 g, 88%). <sup>1</sup>H NMR (400 MHz, CDCl<sub>3</sub>)  $\delta$  10.91 (s, 1H, NCHN-

imidazole), 8.67–8.42 (m, 2H, NCHC-imidazole), 7.75 (dd,  $J = 6.3, 1.5$  Hz, 4H, pyridyl-*H*), 7.57 (d,  $J = 1.4$  Hz, 2H, pyridyl-*H*), 7.33–7.24 (m, 2H, pyridyl-*H*), 5.70 (s, 4H, NCH<sub>2</sub>C). <sup>13</sup>C{<sup>1</sup>H} NMR (101 MHz, CDCl<sub>3</sub>)  $\delta$  151.9, 148.9, 136.8, 136.6, 123.1, 122.8, 122.1, 52.9.

**Synthesis of 1,3-bis(pyridin-2-ylmethyl)-1*H*-imidazolium hexafluorophosphate (L<sub>1</sub>):** 1,3-bis(pyridin-2-ylmethyl)-1*H*-imidazolium chloride (0.63g, 2.20 mmol) was dissolved in water and neutralized with Na<sub>2</sub>CO<sub>3</sub> until pH 9. White solid precipitated out. The mixture was extracted with Et<sub>2</sub>O (3 x 20 mL). The aqueous phase was stirred vigorously with KPF<sub>6</sub> (0.81 g, 4.4 mmol) for 1 h to form a turbid emulsion followed by extraction with DCM. Combined organic phases were dried over anhydrous Na<sub>2</sub>SO<sub>4</sub> and evaporated to dryness to produce viscous oil. Removal of residual water from the product was done by co-evaporating water with acetonitrile three times on the rotary evaporation. The resulting brownish amorphous solid was identified as pure product (0.78 g, 90%). <sup>1</sup>H NMR (400 MHz, CD<sub>3</sub>CN)  $\delta$  8.81 (s, 1H, NCHN-imidazole), 8.66–8.51 (m, 2H, NCHC-imidazole), 7.87 (td,  $J = 7.7, 1.8$  Hz, 2H, pyridyl-*H*), 7.50 (d,  $J = 1.6$  Hz, 2H, pyridyl-*H*), 7.46 (d,  $J = 7.8$  Hz, 2H, pyridyl-*H*), 7.42–7.37 (m, 2H, pyridyl-*H*), 5.48 (s, 4H, NCH<sub>2</sub>C). <sup>31</sup>P{<sup>1</sup>H} NMR (162 MHz, CD<sub>3</sub>CN)  $\delta$  -144.59 (hep,  $J = 706.7$  Hz). <sup>19</sup>F{<sup>1</sup>H} NMR (377 MHz, CD<sub>3</sub>CN)  $\delta$  -72.81 (d,  $J = 706.8$  Hz). <sup>13</sup>C{<sup>1</sup>H} NMR (101 MHz, CD<sub>3</sub>CN)  $\delta$  153.4, 150.5, 138.2, 124.5, 123.7, 123.4, 54.5. HRMS (ESI)  $m/z$ : [M – PF<sub>6</sub>]<sup>+</sup> Calcd. for C<sub>15</sub>H<sub>15</sub>N<sub>4</sub> 251.1291; found 251.1273. Anal. Calcd for C<sub>15</sub>H<sub>15</sub>F<sub>6</sub>N<sub>4</sub>P (672.1028): C, 45.46; H, 3.82; N, 14.14. Found: C, 45.39; H, 3.86; N, 14.17.

**Synthesis of 5,6-dimethyl-1,3-bis(pyridin-2-ylmethyl)-1*H*-benzimidazole-3-mum chloride:** Compound 1,3-bis(pyridin-2-ylmethyl)-1*H*-imidazolium chloride is a known compound and was synthesized by following literature procedure with slide modification.<sup>30</sup> A mixture of 5,6-dimethyl benzimidazole (0.365 g, 2.50 mmol), 2-(chloromethyl)pyridine hydrochloride (0.820 g, 5.00 mmol) and sodium bicarbonate (0.65 g, 7.75 mmol) in anhydrous ethanol (90 mL) was heated in a preheated oil bath under reflux for 48 hours. The resultant

reaction mixture was allowed to cool down to r.t. and filtered through a small plug of celite. All volatiles were removed by using rotary evaporation. The brown residue was dissolved in minimal amount of DCM (2-3 mL) and then triturated with THF (25-30 mL) resulting in a grey brownish powder to precipitate. The supernatant was decanted off. The brown solid was washed with THF (3 x 5 mL) and dried in vacuum to give pure product (0.840 g, 92%).  $^1\text{H}$  NMR (400 MHz,  $\text{CDCl}_3$ )  $\delta$  11.55 (s, 1H, NCHN-benzimidazole), 8.67–8.42 (m, 2H, NCHC-benzimidazole), 7.78-7.70 (m, 4H, pyridyl-*H*), 7.52 (s, 2H, phenyl-*CH*), 7.25–7.21 (m, 2H, pyridyl-*H*), 5.92 (s, 4H,  $\text{NCH}_2\text{C}$ ), 2.34 (s, 6H,  $\text{CH}_3$ ).  $^{13}\text{C}\{^1\text{H}\}$  NMR (101 MHz,  $\text{CDCl}_3$ )  $\delta$  152.8, 149.7, 142.9, 137.8, 137.3, 130.2, 123.9, 123.7, 113.8, 77.4, 77.1, 76.8, 52.6, 20.7. HRMS (ESI)  $m/z$ :  $[\text{M} - \text{Cl}]^+$  Calcd. for  $\text{C}_{21}\text{H}_{21}\text{N}_4$  329.1761; found 251.1735. Anal. Calcd for  $\text{C}_{15}\text{H}_{15}\text{F}_6\text{N}_4\text{P}$  (672.1028): C, 76.57; H, 6.43; N, 17.01. Found: C, 76.54; H, 6.41; N, 17.03.

**Synthesis of 5,6-dimethyl-1,3-bis(pyridin-2-ylmethyl)-1*H*-benzimidazole-3-mum hexafluorophosphate (L<sub>2</sub>):** 5,6-dimethyl-1,3-bis(pyridin-2-ylmethyl)-1*H*-benzimidazole-3-mum chloride (0.803g, 2.20 mmol) was dissolved in water and neutralized with  $\text{Na}_2\text{CO}_3$  until pH 9. White solid precipitated out. The mixture was extracted with  $\text{Et}_2\text{O}$  (3 x 20 mL). The aqueous phase was stirred vigorously with  $\text{KPF}_6$  (0.81 g, 4.4 mmol) for 1 h to form a turbid emulsion followed by extraction with DCM. Combined organic phases were dried over anhydrous  $\text{Na}_2\text{SO}_4$  and evaporated to dryness to produce viscous oil. Removal of residual water from the product was done by co-evaporating water with acetonitrile three times on the rotary evaporation. The resulting grey solid was identified as pure product (0.887 g, 85%).  $^1\text{H}$  NMR (400 MHz,  $\text{CDCl}_3$ )  $\delta$  9.32 (s, 1H, NCHN-benzimidazole), 8.50 (m, 2H, NCHC-benzimidazole), 7.79 – 7.65 (m, 2H, pyridyl-*H*), 7.54 (d,  $J = 7.8$  Hz, 2H, pyridyl-*H*), 7.50 (s, 2H, phenyl-*CH*), 7.24 (d,  $J = 5.1$  Hz, 2H, pyridyl-*H*), 5.67 (s, 4H,  $\text{NCH}_2\text{C}$ ), 2.34 (s, 6H,  $\text{CH}_3$ ).  $^{31}\text{P}\{^1\text{H}\}$  NMR (162 MHz,  $\text{CDCl}_3$ )  $\delta$  -141.91 (hep,  $J = 706.7$  Hz).  $^{19}\text{F}\{^1\text{H}\}$  NMR (377 MHz,  $\text{CDCl}_3$ )  $\delta$  -71.76 (d,  $J = 706.8$  Hz).  $^{13}\text{C}\{^1\text{H}\}$  NMR (101 MHz,  $\text{CDCl}_3$ )  $\delta$  152.0, 149.9, 141.0, 137.9, 130.2, 124.1,

123.3, 113.6, 77.4, 77.1, 76.8, 52.4, 20.6. HRMS (ESI)  $m/z$ :  $[M - PF_6]^+$  Calcd. for  $C_{21}H_{21}N_4$  329.1761; found 251.1798. Anal. Calcd for  $C_{15}H_{15}F_6N_4P$  (672.1028): C, 76.57; H, 6.43; N, 17.01. Found: C, 76.59; H, 6.46; N, 16.98.

**Synthesis of complex 4.1:** To the orange suspension of  $[MnBr(CO)_5]$  (0.14 g, 0.50 mmol) in THF (2 mL), a solution of **L1** (0.20 g, 0.50 mmol) in THF (3 mL) was added dropwise and stirred for 3 h at 60 °C in a preheated oil bath. The resulting solution was then cooled down to r.t. and potassium *tert*-butoxide (0.06 g, 0.55 mmol) was added slowly for 20 min followed by stirring for another 16 h. All volatiles were removed under high vacuum. The residual oil was washed with pentane, dissolved in DCM, filtered through a plug of celite and finally evaporated to dryness. The crude product was further purified by crystallization (slow diffusion of  $Et_2O$  into a saturated solution of crude complex **4.1** in THF) to afford complex **4.1** as yellow crystal. The yellow crystals were dried to give pure compound as complex **4.1**·THF (0.176 g, 58%). X-ray quality single crystals were obtained by slow evaporation of a saturated solution of complex **4.1** in  $CH_3CN$ .  $^1H$  NMR (400 MHz,  $DMSO-d_6$ )  $\delta$  9.46 (br, 1H), 8.08 (br, 1H), 7.78 (d,  $J = 6.3$  Hz, 1H), 7.73 (s, 1H), 7.57 (br, 1H), 5.93 (d,  $J = 16.2$  Hz, 1H), 5.52 (d,  $J = 16.2$  Hz, 1H).  $^{31}P\{^1H\}$  NMR (162 MHz,  $DMSO-d_6$ )  $\delta$  -144.17 (hep,  $J = 711.4$  Hz).  $^{19}F\{^1H\}$  NMR (377 MHz,  $DMSO-d_6$ )  $\delta$  -70.61 (d,  $J = 706.8$  Hz).  $^{13}C\{^1H\}$  NMR (101 MHz,  $DMSO-d_6$ )  $\delta$  221.3 (CO), 212.3 (CO), 191.9 (Mn- $C_{carbene}$ ), 157.2 ( $CH_{imid}$ ), 156.4 ( $CH_{imid}$ ), 140.7 ( $CH_{py}$ ), 127.2 ( $CH_{py}$ ), 126.0 ( $CH_{imid}$ ), 123.6 ( $CH_{py}$ ), 53.9 (NCH<sub>2</sub>N). HRMS (ESI)  $m/z$ :  $[M-PF_6-THF]^+$  calcd for  $C_{18}H_{15}MnN_4O_3$  389.0446; found 389.0440. Anal. Calcd for  $C_{18}H_{15}F_6MnN_4O_3P$  (606.34): C, 43.58; H, 3.66; N, 9.24. Found: C, 43.53; H, 3.65; N, 9.26. FTIR-ATR (solid):  $\bar{\nu}$  [ $cm^{-1}$ ] 2027 (s,  $\bar{\nu}$  CO), 1943 (s,  $\bar{\nu}$  CO), 1909 (s,  $\bar{\nu}$  CO).

**Synthesis of complex 4.2:** To the orange suspension of  $[MnBr(CO)_5]$  (0.14 g, 0.50 mmol) in THF (2 mL), a solution of **L2** (0.237 g, 0.50 mmol) in THF (3 mL) was added dropwise and stirred for 3 h at 60 °C. The resulting solution was then cooled down to r.t. and potassium *tert*-

butoxide (0.06 g, 0.55 mmol) was added slowly for 20 min followed by stirring for another 16 h. All volatiles were removed under high vacuum. The residual oil was washed with pentane, dissolved in DCM, filtered through a plug of celite and finally evaporated to dryness. The crude product was further purified by crystallization (slow diffusion of Et<sub>2</sub>O into a saturated solution of crude complex **4.2** in THF) to afford complex **4.2** as yellow crystal. The yellow crystals were dried to give pure compound as complex **4.2** (0.193 g, 63%). <sup>1</sup>H NMR (400 MHz, CD<sub>3</sub>CN) δ 9.26 (br, 1H), 7.96-7.49 (m, 8H), 5.80 (d, *J* = 93.7 Hz, 4H), 2.36 (d, *J* = 55.9 Hz, 6H). <sup>31</sup>P{<sup>1</sup>H} NMR (162 MHz, DMSO-*d*<sub>6</sub>) δ -144.20 (hep, *J* = 711.4 Hz). <sup>13</sup>C{<sup>1</sup>H} NMR (101 MHz, DMSO-*d*<sub>6</sub>) δ 212.3, 203.4, 157.2, 156.2, 140.8, 133.4, 133.0, 127.2, 126.1, 111.7, 50.6, 20.3. HRMS (ESI) *m/z*: [M-PF<sub>6</sub>]<sup>+</sup> calcd for C<sub>24</sub>H<sub>20</sub>MnN<sub>4</sub>O<sub>3</sub> 467.0916; found 467.0506. Anal. Calcd for C<sub>18</sub>H<sub>15</sub>F<sub>6</sub>MnN<sub>4</sub>O<sub>3</sub>P (606.34): C, 61.68; H, 4.31; N, 11.99. Found: C, 61.63; H, 4.35; N, 12.03. FTIR-ATR (solid):  $\bar{\nu}$  [cm<sup>-1</sup>] 2025 (s,  $\bar{\nu}$  CO), 1940 (s,  $\bar{\nu}$  CO), 1904 (s,  $\bar{\nu}$  CO).

**General conditions for hydrosilylation reaction optimization.** A mixture of phenylacetylene (0.051 g, 0.50 mmol, 1.0 equiv), silane (0.5/1.0 mmol, 1.0/2.0 equiv) and manganese catalyst, complex **4.1**·THF (1 to 5 mol%) in THF (1 mL) was added to a pressure tube (15 mL) fitted with a magnetic stir-bar under N<sub>2</sub> atmosphere. The reaction mixture was stirred at an appropriate temperature in a preheated oil bath for appropriate time. To the resultant mixture, *n*-dodecane (0.085 g, 0.50 mmol, 1.0 equiv) was added. Hexane (2 mL) was also added and subsequently the resultant mixture was analyzed by GC to determine the yield. Occasionally the crude product was purified by column chromatography using silica as the stationary phase and a mixture of petroleum ether/hexane and EtOAc (9.8:0.2) as eluent. The ratio of isomers in products were unambiguously characterized on the basis of the <sup>3</sup>*J*<sub>H-H</sub> coupling constants of the vinylic protons in the corresponding <sup>1</sup>H NMR spectra and subsequent comparison to literature data. Values of *J* ranged from 17 to 19 Hz for β-(*E*), 13 to 16 Hz for β-(*Z*), and 1 to 3 Hz for α-vinylsilanes.<sup>33</sup>

**General condition for gram-scale hydrosilylation of 4-ethynyltoluene with PhSiH<sub>3</sub>:** A mixture of 4-ethynyltoluene (1.160 g, 10.0 mmol, 1.0 equiv), PhSiH<sub>3</sub> (1.080 g, 10.0 mmol, 1.0 equiv) and manganese catalyst, complex **1**·THF (0.061 g, 1 mol %) in THF (8 mL) was added to a pressure tube (15 mL) fitted with a magnetic stir-bar under N<sub>2</sub> atmosphere. The reaction mixture was heated at 90 °C in a preheated oil bath for 6 h. Thereafter, the reaction mixture was cooled down to r.t. and the crude product was purified by column chromatography (silica as stationary phase and a mixture of petroleum ether and ethyl acetate (9.8:0.2) as eluent to give colourless oil as a mixture ( $\beta$ -(Z)/ $\beta$ -(E)/ $\alpha$ : 84/3/13) of products (1.970 g, 88%). The ratio of isomers in products were unambiguously characterized on the basis of the <sup>3</sup>J<sub>H-H</sub> coupling constants of the vinylic protons in the corresponding <sup>1</sup>H NMR spectra and subsequent comparison to literature data. Values of *J* ranged from 17 to 19 Hz for  $\beta$ -(E), 13 to 16 Hz for  $\beta$ -(Z), and 1 to 3 Hz for  $\alpha$ -vinylsilanes.<sup>31a</sup>

**General condition for substrate screening.** A mixture of terminal alkynes (0.5 mmol, 1.0 equiv), PhSiH<sub>3</sub> (0.0540 g, 0.5 mmol, 1.0 equiv) and manganese catalyst, complex **1**·THF (0.003 g, 1 mol%) in THF (1 mL) was added to a pressure tube (15 mL) fitted with a magnetic stir-bar under N<sub>2</sub> atmosphere. The reaction mixture was heated at 90 °C in a preheated oil bath for 6 h. Thereafter, the reaction mixture was cooled down to r.t. and dried under vacuum to give the crude product. The crude product was purified by column chromatography (silica as stationary phase and a mixture of hexanes and ethyl acetate or petroleum ether and ethyl acetate as eluent) to give pure product as a mixture of  $\beta$ -(Z)/ $\beta$ -(E)/ $\alpha$ -isomers.

**Mercury drop test.** A mixture of phenylacetylene (0.051 g, 0.50 mmol, 1.0 equiv), PhSiH<sub>3</sub> (0.054 g, 0.5 mmol, 1.0 equiv) and manganese catalyst, complex **4.1**·THF (0.003 g, 1 mol%) in THF (1 mL) was added to a pressure tube (15 mL) fitted with a magnetic stir-bar under N<sub>2</sub> atmosphere. A drop of mercury was added. The reaction mixture was heated at 90 °C in a preheated oil bath for 6 h. Thereafter, the reaction mixture was cooled down to r.t. Thereafter,

the reaction mixture was cooled down to r.t., dried under vacuum. The residue was purified by column chromatography using silica as stationary phase and a mixture of petroleum ether/hexane and EtOAc (9.8:0.2) as eluent. Finally, the mass was analyzed by GC-MS and  $^1\text{H}$  NMR analysis and no loss of catalytic activity were detected.

**Radical trapping test.** A mixture of phenylacetylene (0.051 g, 0.50 mmol, 1.0 equiv),  $\text{PhSiH}_3$  (0.054 g, 0.5 mmol, 1.0 equiv), manganese catalyst, complex **4.1**·THF (0.003 g, 1 mol%) and radical abstractor TEMPO radical (0.156 g, 1.0 mmol, 2.0 equiv) or  $\text{CCl}_3\text{Br}$  (0.198 g, 1.0 mmol, 2.0 equiv) in THF (1 mL) was added to a pressure tube (15 mL) fitted with a magnetic stir-bar under  $\text{N}_2$  atmosphere. The reaction mixture was heated at 90 °C in a preheated oil bath for 6 h. Thereafter, the reaction mixture was cooled down to r.t. and dried under vacuum. The residue was purified by column chromatography using silica as stationary phase and a mixture of petroleum ether/hexane and EtOAc (9.8:0.2) as eluent. Finally, the mass was analyzed by GC-MS and  $^1\text{H}$  NMR analysis and no conversion of substrate was detected.

**Hydrosilylation in presence of UV light.** A mixture of phenylacetylene (0.051 g, 0.50 mmol, 1.0 equiv),  $\text{PhSiH}_3$  (0.054 g, 0.5 mmol, 1.0 equiv) and manganese catalyst, complex **4.1**·THF (0.015 g, 5 mol%) in THF (1 mL) was added to a pressure tube (15 mL) fitted with a magnetic stir-bar under  $\text{N}_2$  atmosphere. The reaction mixture was stirred at r.t. for 24 h under UV-light (8 W, blue LED) of 350 nm wavelength. Thereafter, the reaction mixture was cooled down to r.t. and dried under vacuum. The residue was purified by column chromatography using silica as stationary phase and a mixture of petroleum ether/hexane and EtOAc (9.8:0.2) as eluent. Finally, the mass was analyzed by GC-MS and  $^1\text{H}$  NMR analysis and mass (0.191 g, 91%) was identified as a mixture of  $\beta$ -(Z)/ $\beta$ -(E)/ $\alpha$ -isomers in the ratio of 80/10/10.

**Hydride trapping test.** A mixture of phenylacetylene (0.051 g, 0.50 mmol, 1.0 equiv),  $\text{PhSiH}_3$  (0.054 g, 0.5 mmol, 1.0 equiv), manganese catalyst, complex **4.1**·THF (0.003 g, 1 mol%) and hydride trapping reagent trityl tetrafluoroborate (0.003 g, 1 mol %) in THF (1 mL) was added

to a pressure tube (15 mL) fitted with a magnetic stir-bar under N<sub>2</sub> atmosphere. The reaction mixture was heated at 90 °C in a preheated oil bath for 6 h. Thereafter, the reaction mixture was cooled down to r.t. and dried under vacuum. The residue was purified by column chromatography using silica as stationary phase and a mixture of petroleum ether/hexane and EtOAc (9.8:0.2) as eluent. Finally, the mass was analyzed by GC-MS and <sup>1</sup>H NMR analysis and no conversion of substrate was detected.

Most of the products of hydrosilylations are known compounds and were characterized by <sup>1</sup>H and <sup>13</sup>C{<sup>1</sup>H} NMR spectroscopies. New compounds are characterized by <sup>1</sup>H and <sup>13</sup>C{<sup>1</sup>H} NMR spectroscopies and HRMS.

**(Z)-phenyl(styryl)silane (P<sub>1a</sub>):** Crude product was purified by fast silica gel column chromatography using petroleum ether as the eluent afforded the title compound as a colourless oil (0.096 g, 92%). <sup>1</sup>H NMR (400 MHz, CDCl<sub>3</sub>) δ 7.79 – 7.71 (m, 3H), 7.52 (d, *J* = 8.2 Hz, 4H), 7.48 (dd, *J* = 8.4, 1.4 Hz, 3H), 7.43 – 7.40 (m, 1H), 6.15 (dt, *J* = 14.7, 4.3 Hz, 1H), 4.90 – 4.85 (m, 2H). <sup>13</sup>C{<sup>1</sup>H} NMR (101 MHz, CDCl<sub>3</sub>) δ 150.5, 138.9, 135.4, 132.3, 129.8, 128.5, 128.3, 128.2, 126.6, 122.0.

**(Z)-(4-methylstyryl)(phenyl)silane (P<sub>2a</sub>):** Crude product was purified by fast silica gel column chromatography using petroleum ether as the eluent afforded the title compound as a colourless oil (0.104 g, 93%). <sup>1</sup>H NMR (400 MHz, CDCl<sub>3</sub>) δ 7.55 – 7.50 (m, 2H), 7.49 – 7.43 (m, 1H), 7.32 – 7.25 (m, 3H), 7.20 (d, *J* = 8.0 Hz, 2H), 7.07 (d, *J* = 7.9 Hz, 2H), 5.85 (dt, *J* = 14.7, 4.3 Hz, 1H), 4.64 (d, *J* = 4.3 Hz, 2H), 2.27 (s, 3H). <sup>13</sup>C{<sup>1</sup>H} NMR (101 MHz, CDCl<sub>3</sub>) δ 150.5, 138.2, 136.2, 135.4, 129.8, 129.3, 129.0, 128.5, 128.2, 120.7, 21.4.

**(Z)-(4-ethylstyryl)(phenyl)silane (P<sub>3a</sub>):** Crude product was purified by fast silica gel column chromatography using petroleum ether as the eluent afforded the title compound as a colourless oil (0.101 g, 85%). <sup>1</sup>H NMR (400 MHz, CDCl<sub>3</sub>) δ 7.52 – 7.42 (m, 3H), 7.28 – 7.19 (m, 5H),

7.07 (d,  $J = 8.0$  Hz, 2H), 5.84 (dt,  $J = 14.7, 4.3$  Hz, 1H), 4.64 (d,  $J = 4.3$  Hz, 2H), 2.54 (q,  $J = 7.6$  Hz, 2H), 1.13 (t,  $J = 7.6$  Hz, 3H).  $^{13}\text{C}\{^1\text{H}\}$  NMR (101 MHz,  $\text{CDCl}_3$ )  $\delta$  150.4, 144.5, 136.4, 135.4, 132.4, 129.8, 128.6, 128.2, 127.8, 120.7, 28.8, 15.6. HRMS (ESI)  $m/z$ :  $[\text{M}+\text{H}]^+$  calcd. for  $\text{C}_{16}\text{H}_{19}\text{Si}$  239.1256; found: 239.1256.

**(Z)-(4-(tert-butyl)styryl)(phenyl)silane (P<sub>4a</sub>):** Crude product was purified by fast silica gel column chromatography using petroleum ether as the eluent afforded the title compound as a colourless oil (0.114 g, 86%).  $^1\text{H}$  NMR (400 MHz,  $\text{CDCl}_3$ )  $\delta$  7.76 (dd,  $J = 7.6, 1.7$  Hz, 2H), 7.69 (d,  $J = 14.8$  Hz, 1H), 7.52 – 7.47 (m, 7H), 6.09 (dt,  $J = 14.8, 4.3$  Hz, 1H), 4.92 (d,  $J = 4.3$  Hz, 2H), 1.47 (s, 9H).  $^{13}\text{C}\{^1\text{H}\}$  NMR (101 MHz,  $\text{CDCl}_3$ )  $\delta$  151.3, 150.4, 136.1, 135.4, 129.8, 128.4, 128.2, 126.2, 125.3, 120.7, 34.8, 31.4.

**(Z)-(4-pentylstyryl)(phenyl)silane (P<sub>5a</sub>):** Crude product was purified by fast silica gel column chromatography using petroleum ether as the eluent afforded the title compound as a colourless oil (0.113 g, 81%).  $^1\text{H}$  NMR (400 MHz,  $\text{CDCl}_3$ )  $\delta$  7.75 (dd,  $J = 7.6, 1.8$  Hz, 2H), 7.69 (d,  $J = 14.8$  Hz, 1H), 7.51 – 7.44 (m, 5H), 7.29 (d,  $J = 8.1$  Hz, 2H), 6.08 (dt,  $J = 14.7, 4.3$  Hz, 1H), 4.91 (d,  $J = 4.3$  Hz, 2H), 2.76 – 2.72 (m, 2H), 1.78 – 1.74 (m, 2H), 1.49 – 1.44 (m, 4H), 1.05 (t,  $J = 6.9$  Hz, 3H).  $^{13}\text{C}\{^1\text{H}\}$  NMR (101 MHz,  $\text{CDCl}_3$ )  $\delta$  150.5, 143.2, 136.3, 135.4, 132.4, 129.7, 128.5, 128.4, 128.2, 120.6, 35.8, 31.6, 31.1, 22.7, 14.2. HRMS (ESI)  $m/z$ :  $[\text{M}+\text{H}]^+$  calcd. for  $\text{C}_{19}\text{H}_{25}\text{Si}$  281.1726, found: 281.1716.

**(Z)-(3-methylstyryl)(phenyl)silane (P<sub>6a</sub>):** Crude product was purified by fast silica gel column chromatography using petroleum ether as the eluent afforded the title compound as a colourless oil (0.102 g, 91%).  $^1\text{H}$  NMR (400 MHz,  $\text{CDCl}_3$ )  $\delta$  7.76 (dd,  $J = 7.6, 1.8$  Hz, 2H), 7.70 (d,  $J = 14.7$  Hz, 1H), 7.51 (dd,  $J = 6.0, 4.4$  Hz, 3H), 7.34 (dd,  $J = 8.5, 2.4$  Hz, 3H), 7.24 (d,  $J = 7.0$  Hz, 1H), 6.14 (dt,  $J = 14.7, 4.2$  Hz, 1H), 4.89 (d,  $J = 4.2$  Hz, 2H), 2.48 (s, 3H).  $^{13}\text{C}$

NMR (101 MHz, CDCl<sub>3</sub>)  $\delta$  150.7, 138.9, 137.9, 135.3, 132.4, 131.2, 129.8, 129.3, 129.0, 128.2, 125.5, 121.7, 21.5.

**(Z)-(4-methoxystyryl)(phenyl)silane (P<sub>7a</sub>):** Crude product was purified by fast silica gel column chromatography using petroleum ether as the eluent afforded the title compound as a colourless oil (0.100 g, 83%). <sup>1</sup>H NMR (400 MHz, CDCl<sub>3</sub>)  $\delta$  7.52 (dd,  $J$  = 7.6, 1.7 Hz, 2H), 7.42 (d,  $J$  = 14.7 Hz, 1H), 7.26 (dd,  $J$  = 14.3, 8.0 Hz, 5H), 6.79 – 6.76 (m, 2H), 5.77 (dt,  $J$  = 14.7, 4.3 Hz, 1H), 4.64 (d,  $J$  = 4.3 Hz, 2H), 3.70 (s, 3H). <sup>13</sup>C{<sup>1</sup>H} NMR (101 MHz, CDCl<sub>3</sub>)  $\delta$  159.7, 150.0, 135.4, 132.4, 131.7, 129.9, 129.8, 128.2, 119.1, 113.7, 55.4. HRMS (ESI)  $m/z$ : [M]<sup>+</sup> calcd. for C<sub>15</sub>H<sub>16</sub>OSi 240.0970; found: 240.0969.

**(Z)-(3-methoxystyryl)(phenyl)silane (P<sub>8a</sub>):** Crude product was purified by fast silica gel column chromatography using petroleum ether as the eluent afforded the title compound as a pale yellow oil (0.106 g, 88%). <sup>1</sup>H NMR (700 MHz, CDCl<sub>3</sub>)  $\delta$  7.76 – 7.73 (m, 2H), 7.72 – 7.65 (m, 1H), 7.53 – 7.46 (m, 3H), 7.41 – 7.35 (m, 1H), 7.09 (dd,  $J$  = 15.9, 15.0 Hz, 2H), 6.99 – 6.94 (m, 1H), 6.18 – 6.13 (m, 1H), 4.93 – 4.85 (m, 2H), 3.84 – 3.81 (m, 3H). <sup>13</sup>C{<sup>1</sup>H} NMR (176 MHz, CDCl<sub>3</sub>)  $\delta$  159.6, 150.5, 140.3, 135.3, 132.1, 129.8, 129.3, 128.2, 122.0, 121.1, 114.4, 113.2, 55.1. HRMS (ESI)  $m/z$ : [M]<sup>+</sup> calcd. for C<sub>15</sub>H<sub>16</sub>OSi 240.0970; found: 240.0969.

**(Z)-3-(2-(phenylsilyl)vinyl)phenol (P<sub>9a</sub>):** Crude product was purified by fast silica gel column chromatography using petroleum ether as the eluent afforded the title compound as a pale yellow oil (0.090 g, 79%). <sup>1</sup>H NMR (400 MHz, CDCl<sub>3</sub>)  $\delta$  7.47 (d,  $J$  = 5.3 Hz, 2H), 7.37 (d,  $J$  = 14.7 Hz, 1H), 7.24 (d,  $J$  = 6.7 Hz, 3H), 7.05 (d,  $J$  = 7.7 Hz, 1H), 6.83 (d,  $J$  = 6.2 Hz, 1H), 6.70 (s, 1H), 6.62 (d,  $J$  = 7.1 Hz, 1H), 5.88 (d,  $J$  = 14.5 Hz, 1H), 5.69 (s, 1H), 4.57 (t,  $J$  = 16.7 Hz, 2H). <sup>13</sup>C{<sup>1</sup>H} NMR (101 MHz, CDCl<sub>3</sub>)  $\delta$  155.4, 150.1, 140.6, 135.3, 132.2, 129.8, 129.6, 128.2, 122.4, 121.1, 115.3, 115.2.

**(Z)-N,N-dimethyl-4-(2-(phenylsilyl)vinyl)aniline (P<sub>10a</sub>):** Crude product was purified by fast silica gel column chromatography using petroleum ether as the eluent afforded the title compound as a colourless oil (0.104 g, 82%). <sup>1</sup>H NMR (400 MHz, CDCl<sub>3</sub>) δ 7.77 (dd, *J* = 7.4, 1.9 Hz, 2H), 7.63 – 7.58 (m, 1H), 7.51 – 7.44 (m, 5H), 6.79 (d, *J* = 8.8 Hz, 2H), 5.85 (dt, *J* = 14.7, 4.3 Hz, 1H), 4.94 (d, *J* = 4.3 Hz, 2H), 3.06 (s, 6H). <sup>13</sup>C{<sup>1</sup>H} NMR (101 MHz, CDCl<sub>3</sub>) δ 150.5, 150.4, 135.3, 132.9, 129.9, 129.6, 128.1, 127.3, 115.6, 111.8, 40.3. HRMS (ESI) *m/z*: [M]<sup>+</sup> calcd. for C<sub>16</sub>H<sub>19</sub>NSi 253.1287; found: 253.1281.

**(Z)-3-(2-(phenylsilyl)vinyl)aniline (P<sub>11a</sub>):** Crude product was purified by fast silica gel column chromatography using petroleum ether as the eluent afforded the title compound as a pale yellow oil (0.091 g, 81%). <sup>1</sup>H NMR (400 MHz, CDCl<sub>3</sub>) δ 7.51 (dd, *J* = 7.6, 1.7 Hz, 2H), 7.39 (d, *J* = 14.7 Hz, 1H), 7.32 – 7.24 (m, 3H), 7.03 (t, *J* = 7.7 Hz, 1H), 6.69 (d, *J* = 7.6 Hz, 1H), 6.56 (s, 1H), 6.50 (dd, *J* = 7.9, 1.8 Hz, 1H), 5.86 (dt, *J* = 14.7, 4.2 Hz, 1H), 4.62 (d, *J* = 4.2 Hz, 2H), 3.34 (s, 2H). <sup>13</sup>C{<sup>1</sup>H} NMR (101 MHz, CDCl<sub>3</sub>) δ 150.7, 146.3, 140.0, 135.3, 132.5, 129.7, 129.2, 128.2, 121.6, 119.0, 115.1, 115.0.

**(Z)-(4-fluorostyryl)(phenyl)silane (P<sub>12a</sub>):** Crude product was purified by fast silica gel column chromatography using petroleum ether as the eluent afforded the title compound as a colourless oil (0.089 g, 78%). <sup>1</sup>H NMR (400 MHz, CDCl<sub>3</sub>) δ 7.52 – 7.48 (m, 2H), 7.43 (d, *J* = 14.7 Hz, 1H), 7.32 – 7.28 (m, 2H), 7.27 – 7.22 (m, 3H), 6.92 (t, *J* = 8.6 Hz, 2H), 5.90 (dt, *J* = 14.7, 4.3 Hz, 1H), 4.60 (d, *J* = 4.2 Hz, 2H). <sup>13</sup>C{<sup>1</sup>H} NMR (101 MHz, CDCl<sub>3</sub>) δ 149.3, 135.3, 131.9, 130.2, 130.1, 129.9, 128.3, 121.8, 115.4, 115.2.

**(Z)-(3-chlorostyryl)(phenyl)silane (P<sub>13a</sub>):** Crude product was purified by fast silica gel column chromatography using petroleum ether as the eluent afforded the title compound as a colourless oil (0.093 g, 76%). <sup>1</sup>H NMR (700 MHz, CDCl<sub>3</sub>) δ 7.69 (d, *J* = 7.4 Hz, 2H), 7.61 – 7.56 (m, 1H), 7.49 (d, *J* = 7.0 Hz, 1H), 7.45 (dd, *J* = 12.9, 6.7 Hz, 3H), 7.33 (d, *J* = 4.9 Hz,

3H), 6.18 (dt,  $J = 14.7, 4.1$  Hz, 1H), 4.81 (d,  $J = 4.0$  Hz, 2H).  $^{13}\text{C}\{^1\text{H}\}$  NMR (176 MHz,  $\text{CDCl}_3$ )  $\delta$  148.9, 140.6, 135.3, 134.3, 131.7, 130.0, 129.5, 128.5, 128.3, 128.1, 126.4, 124.1. HRMS (ESI)  $m/z$ :  $[\text{M}]^+$  calcd. for  $\text{C}_{14}\text{H}_{13}\text{ClSi}$  244.0475; found: 244.0477.

**(Z)-(4-bromostyryl)(phenyl)silane (P<sub>14a</sub>):** Crude product was purified by fast silica gel column chromatography using petroleum ether as the eluent afforded the title compound as a colourless oil (0.112 g, 81%).  $^1\text{H}$  NMR (400 MHz,  $\text{CDCl}_3$ )  $\delta$  7.61 (dd,  $J = 7.8, 1.6$  Hz, 2H), 7.49 (d,  $J = 8.5$  Hz, 2H), 7.45 – 7.37 (m, 4H), 7.27 – 7.23 (m, 2H), 6.08 (dt,  $J = 14.7, 4.3$  Hz, 1H), 4.71 (d,  $J = 4.3$  Hz, 1H).  $^{13}\text{C}\{^1\text{H}\}$  NMR (101 MHz,  $\text{CDCl}_3$ )  $\delta$  149.2, 135.7, 135.3, 131.7, 131.5, 130.0, 130.0, 128.3, 128.2, 123.1.

**(Z)-phenyl(4-(trifluoromethyl)styryl)silane (P<sub>15a</sub>):** Crude product was purified by fast silica gel column chromatography using petroleum ether as the eluent afforded the title compound as a colourless oil (0.110 g, 79%).  $^1\text{H}$  NMR (400 MHz,  $\text{CDCl}_3$ )  $\delta$  7.47 (d,  $J = 6.9$  Hz, 4H), 7.33 (d,  $J = 7.1$  Hz, 3H), 7.26 (d,  $J = 6.8$  Hz, 3H), 6.06 (d,  $J = 14.9$  Hz, 1H), 4.59 (d,  $J = 2.7$  Hz, 2H).  $^{13}\text{C}\{^1\text{H}\}$  NMR (101 MHz,  $\text{CDCl}_3$ )  $\delta$  148.9, 142.3, 135.7, 135.3, 133.3, 131.5, 130.0, 128.7, 128.4, 126.9, 125.2. HRMS (ESI)  $m/z$ :  $[\text{M}]^+$  calcd. for  $\text{C}_{15}\text{H}_{13}\text{F}_3\text{Si}$  278.0739; found: 278.0740.

**(Z)-phenyl(4-(trifluoromethoxy)styryl)silane (P<sub>16a</sub>):** Crude product was purified by fast silica gel column chromatography using petroleum ether as the eluent afforded the title compound as a colourless oil (0.110 g, 75%).  $^1\text{H}$  NMR (400 MHz,  $\text{CDCl}_3$ )  $\delta$  7.47 (dd,  $J = 7.7, 1.5$  Hz, 2H), 7.42 (d,  $J = 14.8$  Hz, 1H), 7.25 (d,  $J = 8.2$  Hz, 5H), 7.05 (d,  $J = 8.2$  Hz, 2H), 5.96 (d,  $J = 14.8$  Hz, 1H), 4.60 (d,  $J = 4.2$  Hz, 2H).  $^{13}\text{C}\{^1\text{H}\}$  NMR (101 MHz,  $\text{CDCl}_3$ )  $\delta$  148.9, 137.6, 135.7, 135.4, 132.2, 131.7, 129.9, 128.3, 127.9, 123.4, 120.7.

**(Z)-methyl 4-(2-(phenylsilyl)vinyl)benzoate and phenyl(1-(4-acetoxyphenyl)vinyl)silane (P<sub>17a</sub>/ P<sub>17c</sub>):** Crude product was purified by fast silica gel column chromatography using

petroleum ether as the eluent afforded the title compound as a colourless oil (0.104 g, 78%). For (Z)-methyl 4-(2-(phenylsilyl)vinyl)benzoate<sup>19a</sup>, <sup>1</sup>H NMR (400 MHz, CDCl<sub>3</sub>) δ 8.03 – 7.99 (m, 2H), 7.63 – 7.56 (m, 3H), 7.41 (d, *J* = 2.1 Hz, 2H), 7.40 – 7.36 (m, 3H), 6.22 – 6.09 (m, 1H), 4.70 (t, *J* = 5.5 Hz, 2H), 3.92 (s, 3H). <sup>13</sup>C{<sup>1</sup>H} NMR (101 MHz, CDCl<sub>3</sub>) δ 166.9, 149.3, 143.3, 135.4, 131.7, 130.2, 130.0, 129.7, 128.3, 125.1, 52.3. For phenyl(1-(4-acetoxyphenyl)vinyl)silane, <sup>1</sup>H NMR (400 MHz, CDCl<sub>3</sub>) δ 7.91 – 7.86 (m, 2H), 7.48 (t, *J* = 1.8 Hz, 1H), 7.32 – 7.23 (m, 6H), 6.20 (d, *J* = 2.2 Hz, 1H), 5.84 (t, *J* = 6.0 Hz, 1H), 4.76 (s, 2H), 3.82 (s, 3H). <sup>13</sup>C{<sup>1</sup>H} NMR (101 MHz, CDCl<sub>3</sub>) δ 167.1, 147.2, 144.0, 135.8, 135.7, 133.1, 130.7, 130.2, 129.0, 128.4, 126.6, 52.2. These data are in accordance with the literature.<sup>42</sup>

**(Z)-(2-([1,1'-biphenyl]-4-yl)vinyl)(phenyl)silane (P<sub>18a</sub>):** Crude product was purified by fast silica gel column chromatography using petroleum ether as the eluent afforded the title compound as a colourless oil (0.120 g, 84%). <sup>1</sup>H NMR (400 MHz, CDCl<sub>3</sub>) δ 7.78 – 7.74 (m, 3H), 7.71 (d, *J* = 8.3 Hz, 4H), 7.60 (s, 1H), 7.57 (d, *J* = 9.1 Hz, 2H), 7.53 (d, *J* = 9.1 Hz, 3H), 7.50 – 7.46 (m, 2H), 6.17 (dt, *J* = 14.8, 4.3 Hz, 1H), 4.94 (d, *J* = 4.3 Hz, 2H). <sup>13</sup>C{<sup>1</sup>H} NMR (101 MHz, CDCl<sub>3</sub>) δ 150.0, 140.9, 140.6, 137.8, 135.4, 132.2, 129.8, 129.0, 128.9, 128.3, 127.6, 127.1, 127.0, 122.0. HRMS (ESI) *m/z*: [M]<sup>+</sup> calcd. for C<sub>20</sub>H<sub>18</sub>Si 286.1178; found: 286.1179.

**(Z)-(2-(phenanthren-9-yl)vinyl)(phenyl)silane (P<sub>19a</sub>):** Crude product was purified by fast silica gel column chromatography using petroleum ether as the eluent afforded the title compound as a colourless oil (0.121 g, 78%). <sup>1</sup>H NMR (400 MHz, CDCl<sub>3</sub>) δ 8.59 – 8.51 (m, 2H), 8.08 – 7.98 (m, 1H), 7.96 – 7.88 (m, 1H), 7.67 – 7.63 (m, 1H), 7.54 (dd, *J* = 8.1, 1.4 Hz, 1H), 7.51 (s, 2H), 7.49 (d, *J* = 1.2 Hz, 1H), 7.46 (d, *J* = 8.1 Hz, 1H), 7.43 (dd, *J* = 7.8, 1.5 Hz, 2H), 7.26 – 7.16 (m, 3H), 6.22 (dt, *J* = 14.3, 4.0 Hz, 1H), 4.45 (d, *J* = 4.0 Hz, 2H). <sup>13</sup>C{<sup>1</sup>H} NMR (101 MHz, CDCl<sub>3</sub>) δ 149.2, 135.3, 135.3, 132.6, 131.3, 130.8, 130.5, 130.4, 129.6, 129.0, 128.1, 127.0, 126.9, 126.9, 126.8, 126.7, 125.5, 125.3, 123.1, 122.6.

**(Z)-phenyl(2-(thiophen-2-yl)vinyl)silane (P<sub>20a</sub>):** Crude product was purified by fast silica gel column chromatography using petroleum ether as the eluent afforded the title compound as a pale yellow oil (0.092 g, 85%). <sup>1</sup>H NMR (400 MHz, CDCl<sub>3</sub>) δ 7.58 – 7.55 (m, 2H), 7.50 (d, *J* = 14.9 Hz, 1H), 7.31 (dd, *J* = 7.2, 4.5 Hz, 3H), 7.21 (d, *J* = 5.0 Hz, 1H), 7.04 (d, *J* = 3.5 Hz, 1H), 6.93 (dd, *J* = 5.1, 3.6 Hz, 1H), 5.80 (d, *J* = 14.9 Hz, 1H), 4.77 (d, *J* = 4.1 Hz, 2H). <sup>13</sup>C{<sup>1</sup>H} NMR (101 MHz, CDCl<sub>3</sub>) δ 141.8, 135.4, 131.7, 129.9, 128.9, 128.2, 127.3, 126.9, 124.6, 119.5.

**(Z)-3-(2-(phenylsilyl)vinyl)pyridine (P<sub>21a</sub>):** Crude product was purified by fast silica gel column chromatography using petroleum ether as the eluent afforded the title compound as a pale yellow oil (0.071 g, 67%). <sup>1</sup>H NMR (400 MHz, CDCl<sub>3</sub>) δ 8.65 (s, 1H), 8.55 (d, *J* = 4.0 Hz, 1H), 7.71 (d, *J* = 7.6 Hz, 1H), 7.61 (dd, *J* = 7.8, 1.6 Hz, 2H), 7.57 (d, *J* = 14.9 Hz, 1H), 7.45 – 7.40 (m, 3H), 7.30 (d, *J* = 3.8 Hz, 1H), 6.24 (dt, *J* = 14.9, 4.3 Hz, 1H), 4.73 (d, *J* = 4.3 Hz, 2H). <sup>13</sup>C{<sup>1</sup>H} NMR (101 MHz, CDCl<sub>3</sub>) δ 149.4, 148.7, 146.4, 135.7, 135.3, 133.7, 131.2, 130.0, 128.3, 125.6, 123.2.

**(Z)-(2-cyclohexylvinyl)(phenyl)silane (P<sub>22a</sub>):** Crude product was purified by fast silica gel column chromatography using petroleum ether as the eluent afforded the title compound as a colourless oil (0.074 g, 69%). <sup>1</sup>H NMR (400 MHz, CDCl<sub>3</sub>) δ 7.44 – 7.40 (m, 2H), 7.20 (d, *J* = 6.7 Hz, 3H), 6.33 (dd, *J* = 13.5, 9.7 Hz, 1H), 5.47 – 5.36 (m, 1H), 4.44 (d, *J* = 4.0 Hz, 2H), 2.60 (d, 4.1 Hz, 1H), 1.66 – 1.58 (m, 3H), 1.50 (dd, *J* = 7.2, 3.4 Hz, 4H), 1.44 – 1.37 (m, 3H). <sup>13</sup>C{<sup>1</sup>H} NMR (101 MHz, CDCl<sub>3</sub>) δ 158.7, 135.4, 132.6, 129.6, 128.1, 116.9, 44.3, 33.5, 32.5, 25.7. HRMS (ESI) *m/z*: [M+H]<sup>+</sup> calcd. for C<sub>14</sub>H<sub>21</sub>Si 217.1413; found: 217.1413.

**(Z)-(2-cyclopentylvinyl)(phenyl)silane (P<sub>23a</sub>):** Crude product was purified by fast silica gel column chromatography using petroleum ether as the eluent afforded the title compound as a colourless oil (0.067 g, 66%). <sup>1</sup>H NMR (400 MHz, CDCl<sub>3</sub>) δ 7.52 – 7.49 (m, 2H), 7.29 (d, *J* = 6.5 Hz, 3H), 6.42 (dd, *J* = 13.5, 9.7 Hz, 1H), 5.50 (dt, *J* = 13.6, 4.1 Hz, 1H), 4.52 (d, *J* = 4.1

Hz, 2H), 2.69 (dd,  $J = 16.9, 8.0$  Hz, 1H), 1.59 (dd,  $J = 7.3, 3.6$  Hz, 4H), 1.49 (dd,  $J = 7.8, 4.8$  Hz, 4H).  $^{13}\text{C}\{^1\text{H}\}$  NMR (101 MHz,  $\text{CDCl}_3$ )  $\delta$  158.7, 135.4, 132.6, 129.6, 128.1, 116.8, 44.3, 33.5, 25.7.

**(Z)-hex-1-en-1-yl(phenyl)silane (P<sub>24a</sub>):** Crude product was purified by fast silica gel column chromatography using petroleum ether as the eluent afforded the title compound as a colourless oil (0.068 g, 72%).  $^1\text{H}$  NMR (400 MHz,  $\text{CDCl}_3$ )  $\delta$  7.67 (s, 2H), 7.45 (s, 3H), 6.79 – 6.61 (m, 1H), 5.79 (s, 1H), 4.71 (s, 2H), 2.33 (d,  $J = 5.8$  Hz, 2H), 1.45 (dd,  $J = 15.8, 7.5$  Hz, 4H), 0.98 (s, 3H).  $^{13}\text{C}\{^1\text{H}\}$  NMR (101 MHz,  $\text{CDCl}_3$ )  $\delta$  153.8, 135.4, 132.5, 129.6, 128.1, 119.0, 33.2, 31.6, 22.3, 14.0.

**(Z)-hept-1-en-1-yl(phenyl)silane (P<sub>25a</sub>):** Crude product was purified by fast silica gel column chromatography using petroleum ether as the eluent afforded the title compound as a colourless oil (0.076 g, 74%).  $^1\text{H}$  NMR (400 MHz,  $\text{CDCl}_3$ )  $\delta$  7.48 (s, 2H), 7.27 (s, 3H), 6.58 – 6.47 (m, 1H), 5.58 (d,  $J = 13.7$  Hz, 1H), 4.52 (d,  $J = 4.0$  Hz, 2H), 2.17 – 2.10 (m, 2H), 1.17 (s, 6H), 0.79 (s, 3H).  $^{13}\text{C}\{^1\text{H}\}$  NMR (101 MHz,  $\text{CDCl}_3$ )  $\delta$  153.9, 135.4, 132.5, 129.6, 128.1, 119.0, 33.5, 31.8, 29.0, 22.7, 14.2.

**(Z)-oct-1-en-1-yl(phenyl)silane (P<sub>26a</sub>):** Crude product was purified by fast silica gel column chromatography using petroleum ether as the eluent afforded the title compound as a colourless oil (0.085 g, 78%).  $^1\text{H}$  NMR (400 MHz,  $\text{CDCl}_3$ )  $\delta$  7.67 – 7.58 (m, 2H), 7.39 (dd,  $J = 8.2, 1.7$  Hz, 3H), 6.71 – 6.56 (m, 1H), 5.74 – 5.67 (m, 1H), 4.63 (d,  $J = 4.1$  Hz, 1H), 2.28 – 2.23 (m, 2H), 1.44 – 1.40 (m, 2H), 1.33 – 1.29 (m, 10H), 0.91 (t,  $J = 6.2$  Hz, 3H).  $^{13}\text{C}$  NMR (101 MHz,  $\text{CDCl}_3$ )  $\delta$  153.9, 135.4, 132.5, 129.6, 128.2, 119.0, 33.5, 31.8, 29.4, 29.0, 22.7, 14.2.

**(Z)-hexadec-1-en-1-yl(phenyl)silane (P<sub>27a</sub>):** Crude product was purified by fast silica gel column chromatography using petroleum ether as the eluent afforded the title compound as a colourless oil (0.093 g, 56%).  $^1\text{H}$  NMR (400 MHz,  $\text{CDCl}_3$ )  $\delta$  7.71 – 7.53 (m, 2H), 7.45 – 7.29

(m, 3H), 6.63 (tt,  $J = 20.4, 10.3$  Hz, 1H), 5.76 – 5.67 (m, 1H), 4.65 (d,  $J = 4.1$  Hz, 2H), 2.35 – 2.21 (m, 2H), 1.31 (s, 22H), 0.93 (t,  $J = 6.8$  Hz, 5H).  $^{13}\text{C}$  NMR (101 MHz,  $\text{CDCl}_3$ )  $\delta$  153.9, 135.4, 129.6, 128.1, 120.0, 119.0, 37.6, 37.1, 33.5, 32.1, 29.9, 29.9, 29.8, 29.7, 29.6, 29.6, 29.4, 29.3, 22.9, 14.3. HRMS (ESI)  $m/z$ :  $[\text{M}]^+$  calcd. for  $\text{C}_{22}\text{H}_{38}\text{Si}$  330.2743; found: 330.2738.

**(Z)-phenyl(4-phenylbut-1-en-1-yl)silane (P<sub>28a</sub>):** Crude product was purified by fast silica gel column chromatography using petroleum ether as the eluent afforded the title compound as a colourless oil (0.094 g, 79%).  $^1\text{H}$  NMR (400 MHz,  $\text{CDCl}_3$ )  $\delta$  7.44 (dt,  $J = 9.5, 4.7$  Hz, 2H), 7.29 – 7.27 (m, 3H), 7.21 – 7.16 (m, 2H), 7.10 (dd,  $J = 3.8, 1.8$  Hz, 1H), 7.05 (dd,  $J = 6.4, 4.8$  Hz, 2H), 6.60 – 6.51 (m, 1H), 5.64 (dt,  $J = 13.7, 4.1$  Hz, 1H), 4.48 (d,  $J = 4.1$  Hz, 1H), 2.63 – 2.59 (m, 1H), 2.47 (dd,  $J = 15.1, 7.4$  Hz, 1H).  $^{13}\text{C}$  NMR (101 MHz,  $\text{CDCl}_3$ )  $\delta$  152.3, 141.5, 135.7, 135.4, 129.7, 128.6, 128.5, 128.2, 126.1, 120.1, 35.7, 35.3.

**(Z)-(2-(cyclohex-1-en-1-yl)vinyl)(phenyl)silane (P<sub>29a</sub>):** Crude product was purified by fast silica gel column chromatography using petroleum ether as the eluent afforded the title compound as a colourless oil (0.095 g, 89%).  $^1\text{H}$  NMR (400 MHz,  $\text{CDCl}_3$ )  $\delta$  7.63 (d,  $J = 7.2$  Hz, 2H), 7.41 (dd,  $J = 12.7, 6.9$  Hz, 3H), 7.00 (d,  $J = 14.7$  Hz, 1H), 5.89 (s, 1H), 5.58 – 5.56 (m, 1H), 4.76 (d,  $J = 3.9$  Hz, 2H), 2.26 (d,  $J = 1.5$  Hz, 2H), 2.15 (d,  $J = 1.5$  Hz, 2H), 1.65 (dd,  $J = 11.5, 5.7$  Hz, 2H), 1.59 (dd,  $J = 10.5, 4.9$  Hz, 2H).  $^{13}\text{C}$  NMR (101 MHz,  $\text{CDCl}_3$ )  $\delta$  153.8, 138.7, 135.2, 133.5, 131.9, 129.5, 128.1, 116.2, 27.5, 25.9, 22.6, 22.1.

## NMR Spectra

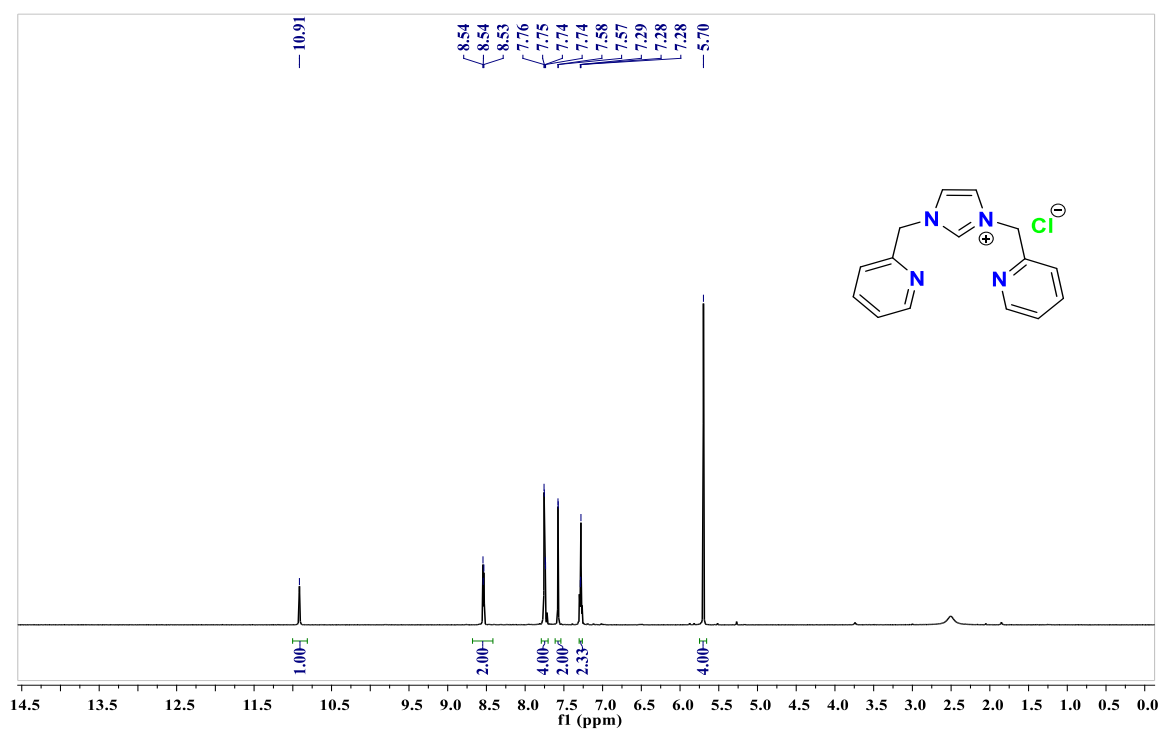


**Figure 4.1.**  $^1\text{H}$  NMR (400 MHz,  $\text{CDCl}_3$ ) of 1,3-bis(pyridin-2-ylmethyl)-1H-imidazolium chloride.

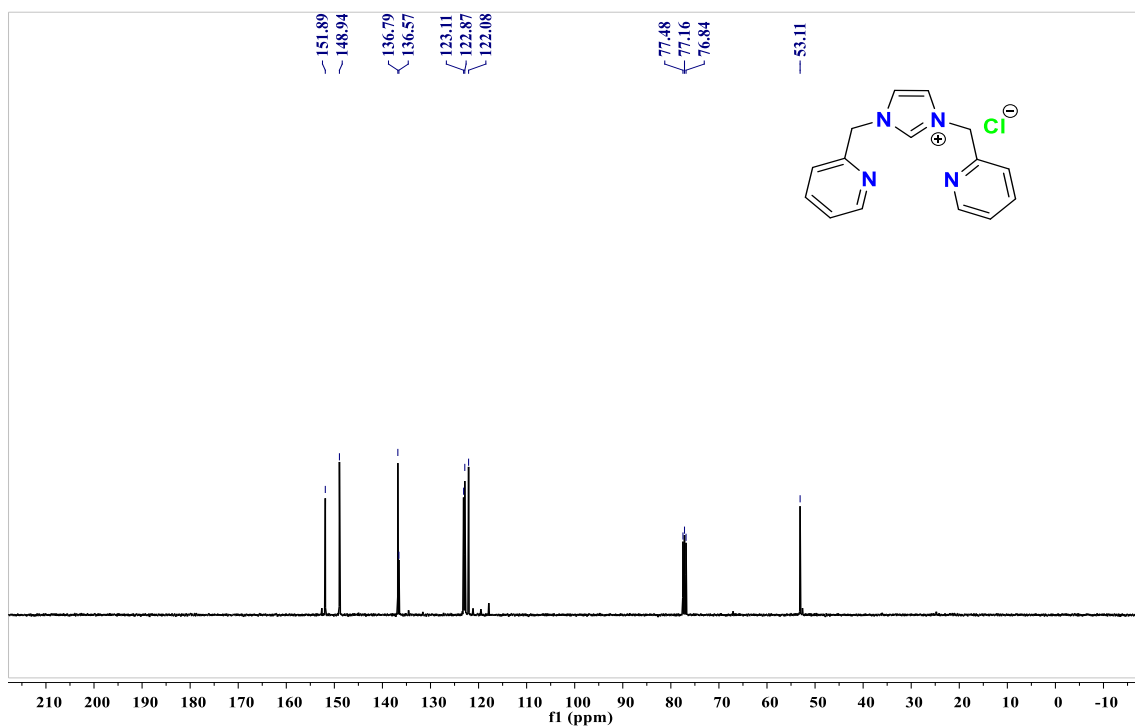


**Figure 4.2.**  $^{13}\text{C}\{^1\text{H}\}$  NMR (101 MHz,  $\text{CDCl}_3$ ) of 1,3-bis(pyridin-2-ylmethyl)-1H-imidazolium chloride.

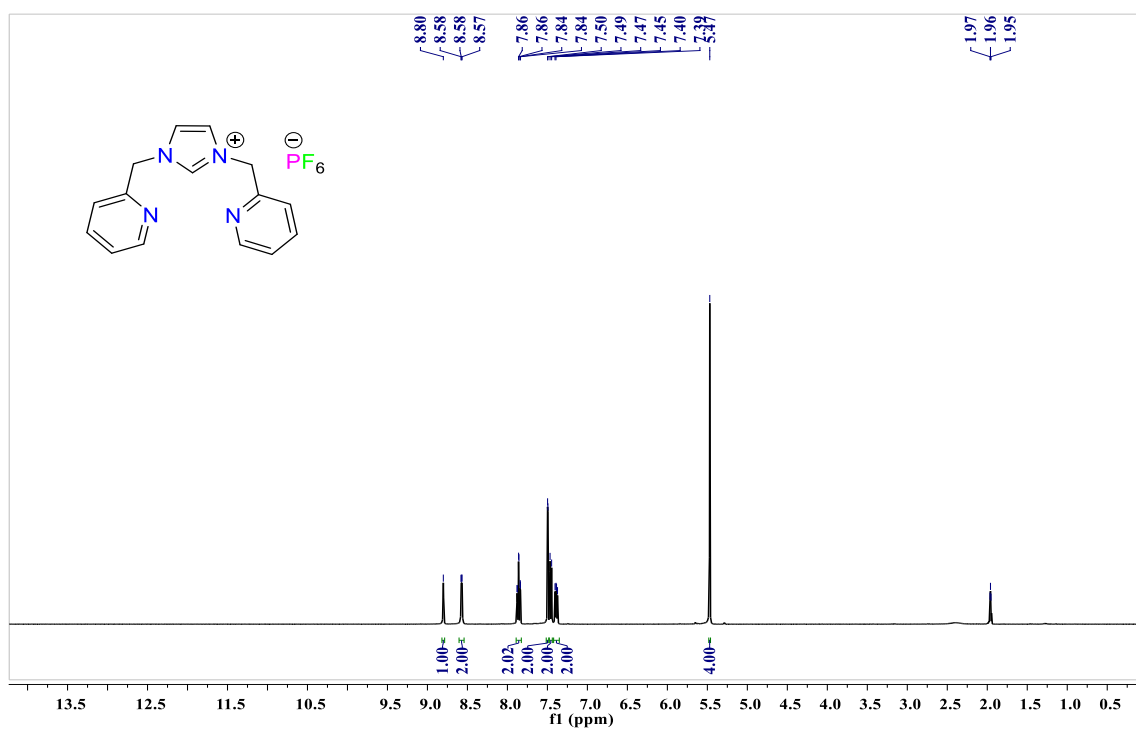


**Figure 4.3.**  $^1\text{H}$  NMR (400 MHz,  $\text{CDCl}_3$ ) of 1,3-bis(pyridin-2-ylmethyl)-1H-imidazolium hexafluorophosphate (**L1**).

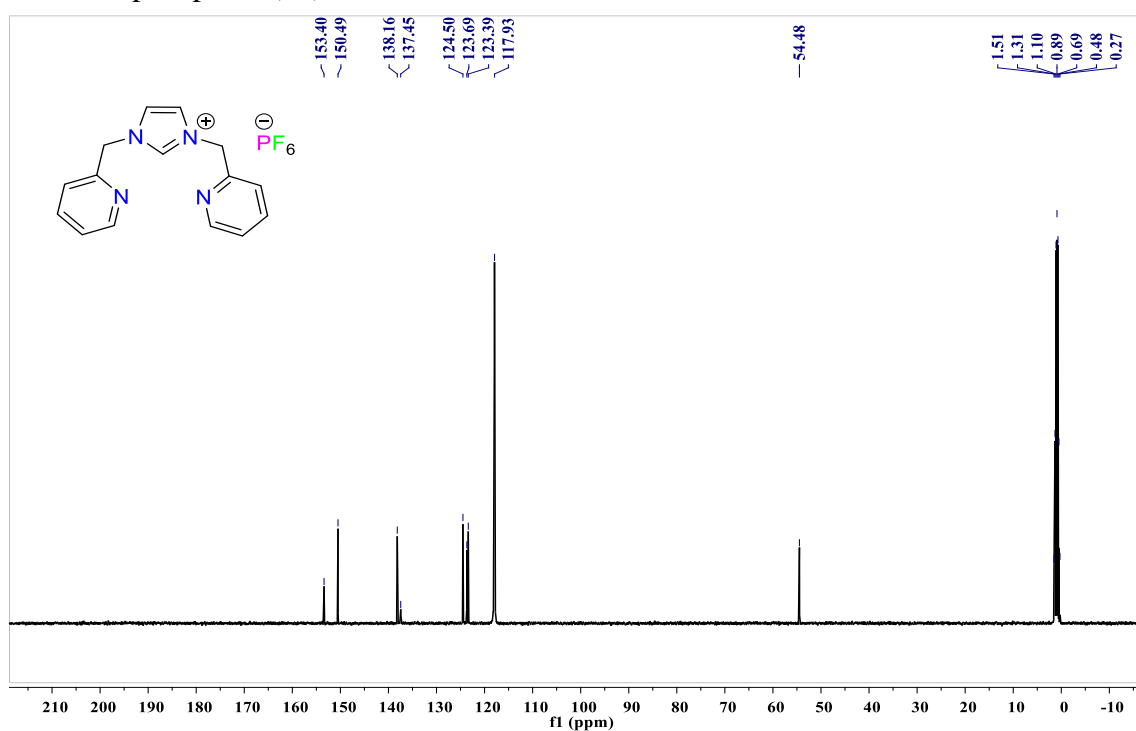


**Figure 4.4.**  $^{13}\text{C}\{^1\text{H}\}$  NMR (101 MHz,  $\text{CD}_3\text{CN}$ ) of 1,3-bis(pyridin-2-ylmethyl)-1H-imidazolium hexafluorophosphate (**L1**).

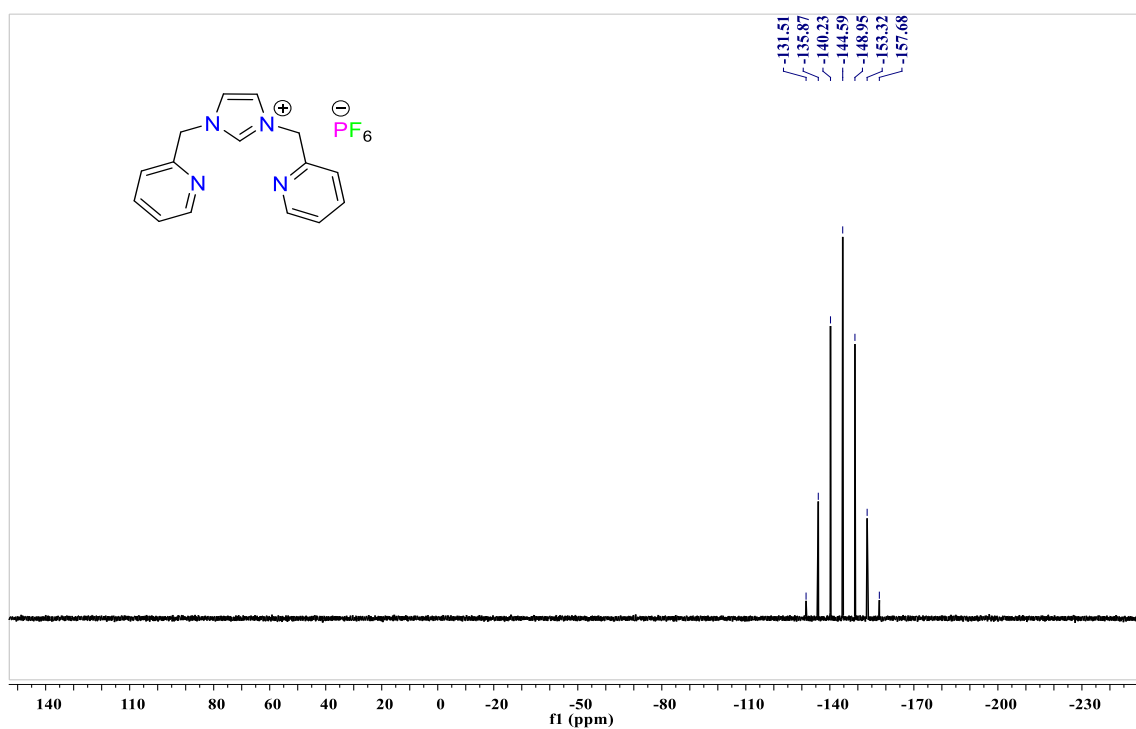


**Figure 4.5.**  $^{31}\text{P}\{^1\text{H}\}$  NMR (162 MHz,  $\text{CD}_3\text{CN}$ ) of 1,3-bis(pyridin-2-ylmethyl)-1H-imidazolium hexafluorophosphate (**L1**).

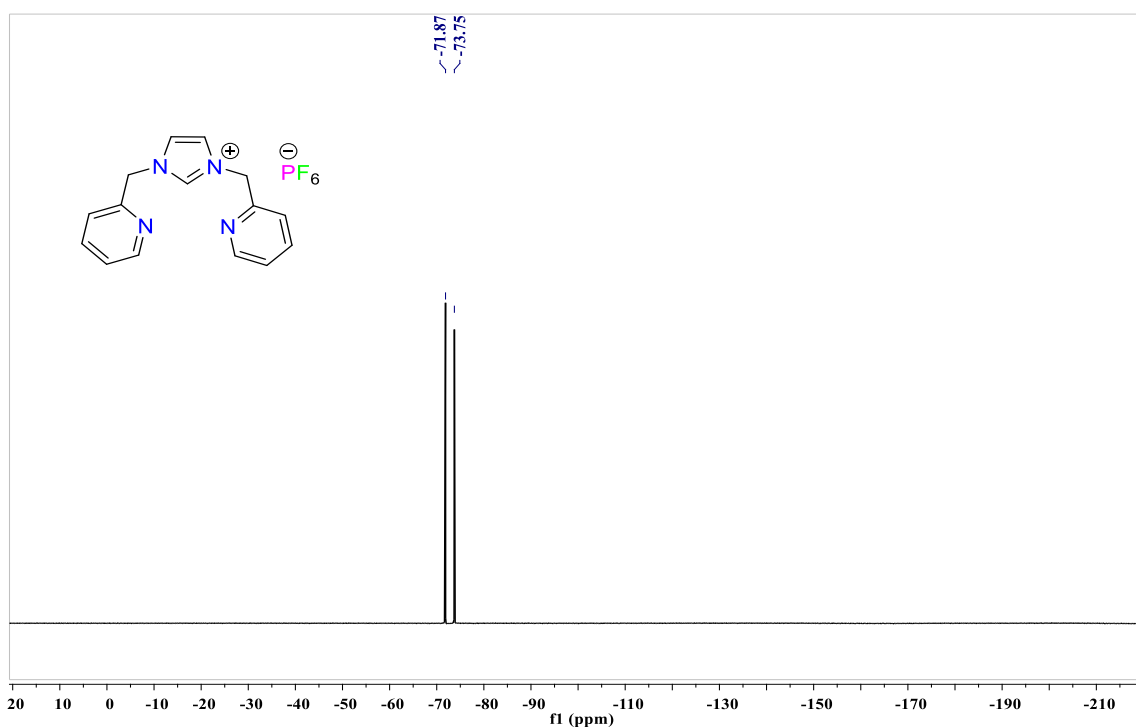


**Figure 4.6.**  $^{19}\text{F}\{^1\text{H}\}$  NMR (377 MHz,  $\text{CD}_3\text{CN}$ ) of 1,3-bis(pyridin-2-ylmethyl)-1H-imidazolium hexafluorophosphate (**L1**).

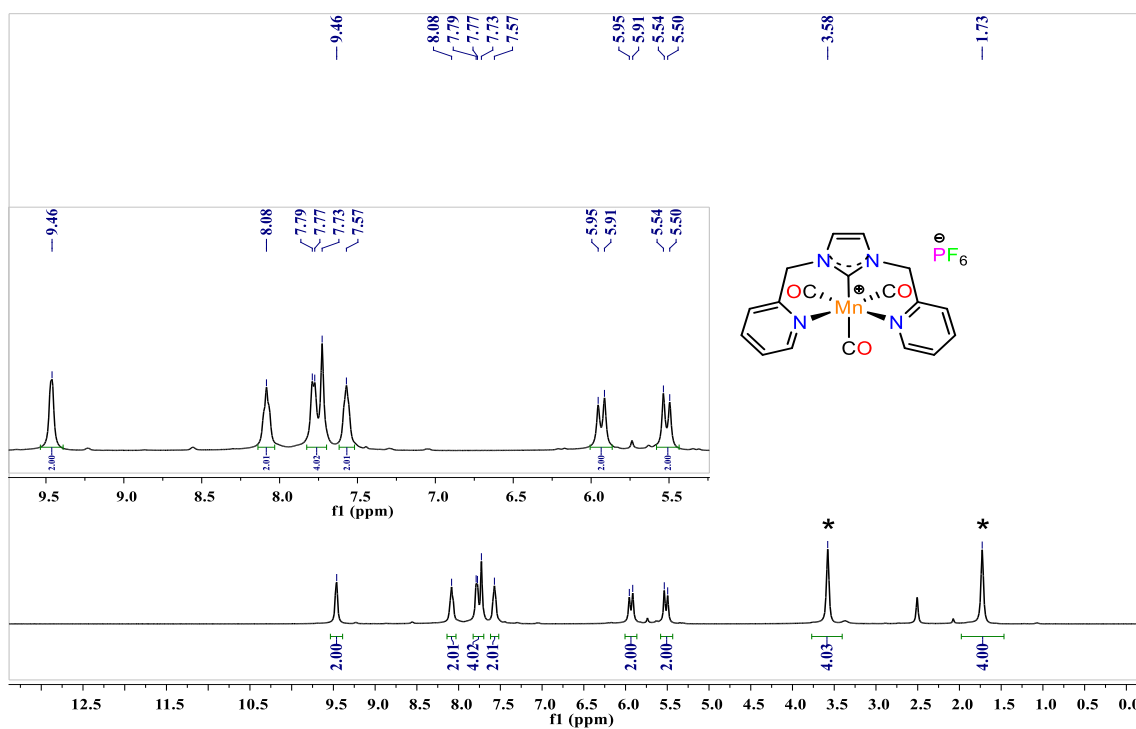


Figure 4.7.  $^1\text{H}$  NMR (400 MHz,  $\text{DMSO-d}_6$ ) of Complex 1 (\* indicates THF solvent peak).

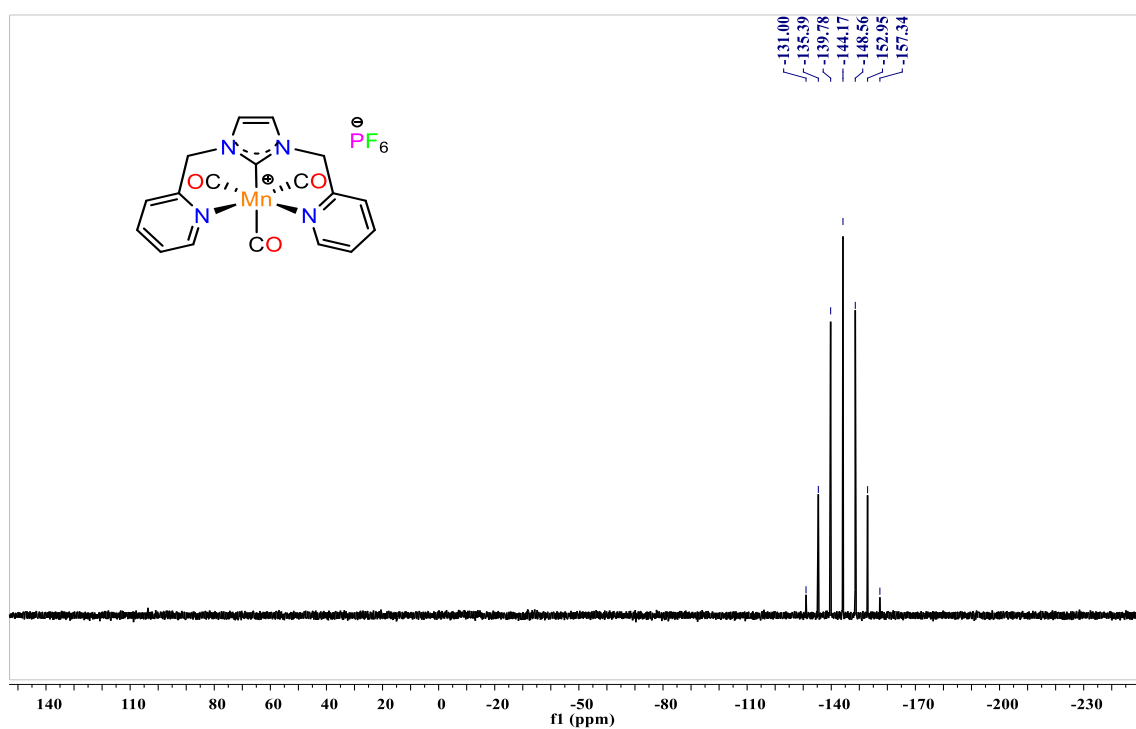
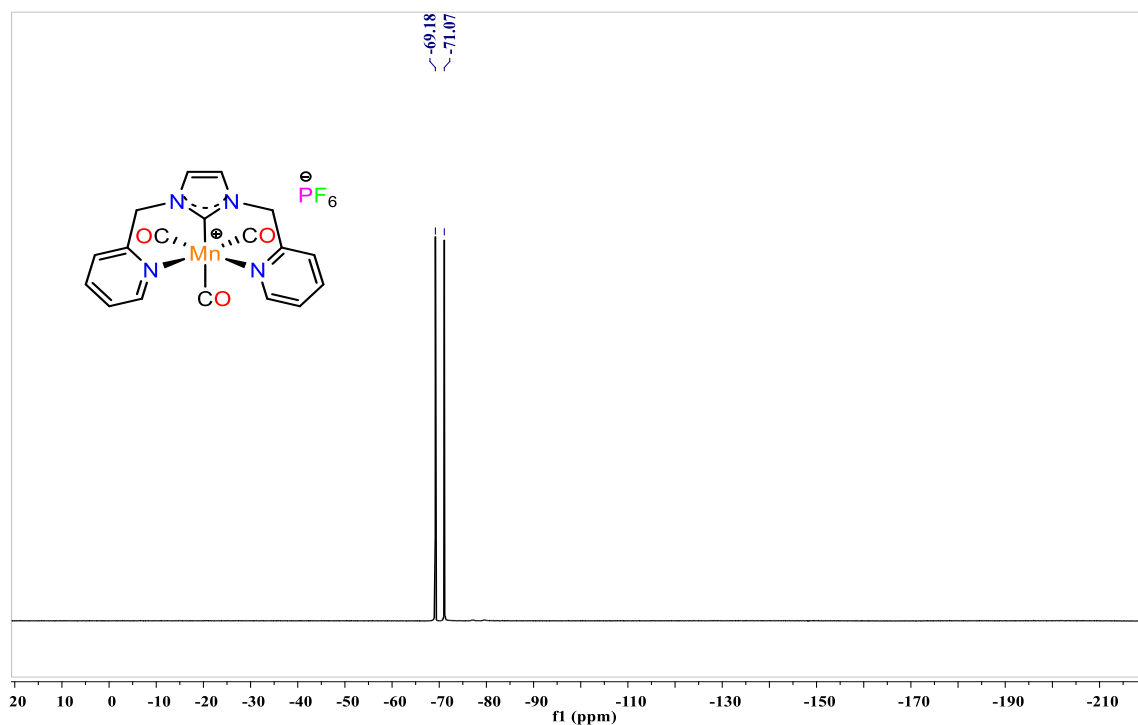
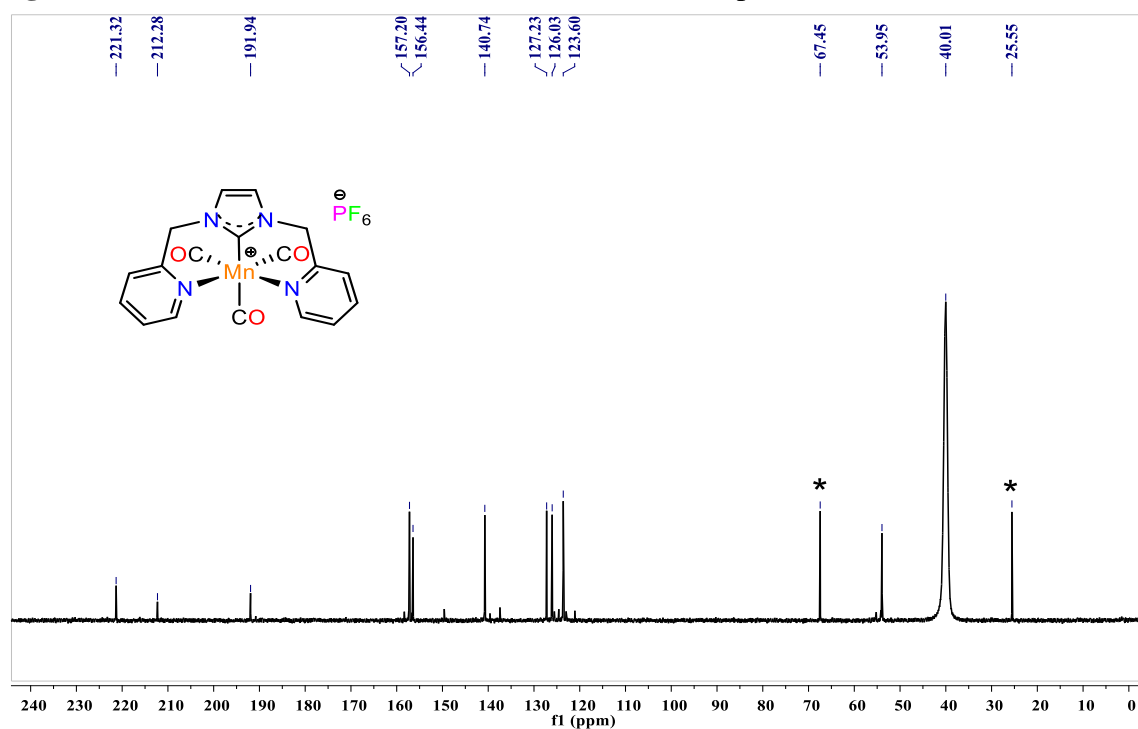


Figure 4.8.  $^{31}\text{P}\{^1\text{H}\}$  NMR (162 MHz,  $\text{DMSO-d}_6$ ) of Complex 1·THF.



**Figure 4.9.**  $^{19}\text{F}\{^1\text{H}\}$  NMR (377 MHz,  $\text{DMSO-d}_6$ ) of Complex **1**·THF.



**Figure 4.10.**  $^{13}\text{C}\{^1\text{H}\}$  NMR (101 MHz,  $\text{DMSO-d}_6$ ) of Complex **1** (\* indicates THF solvent peak).

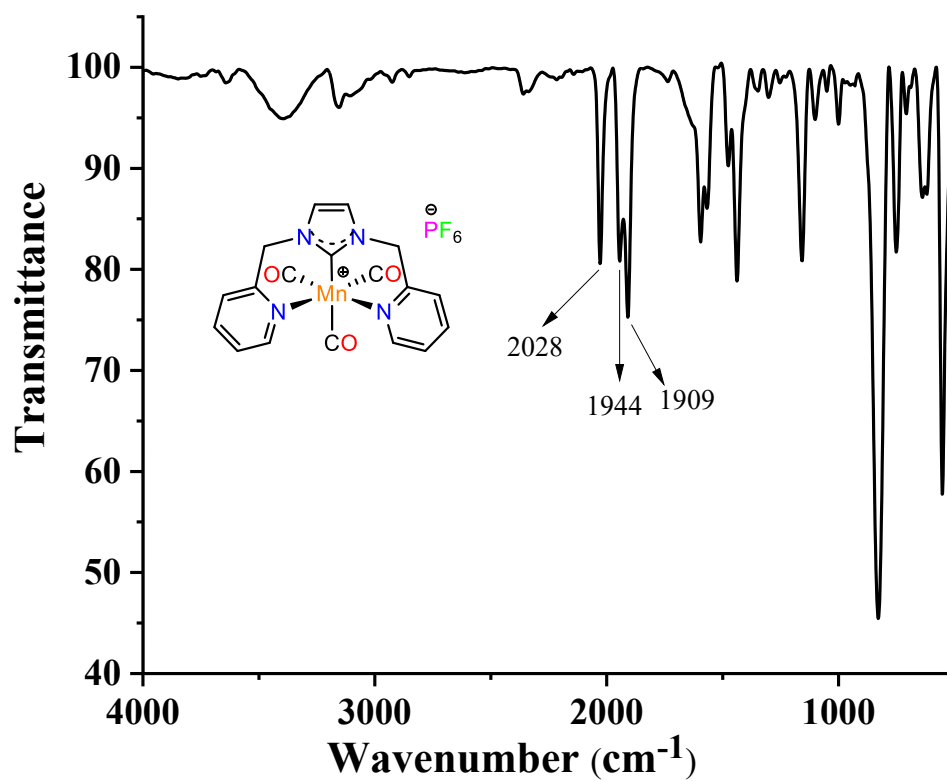
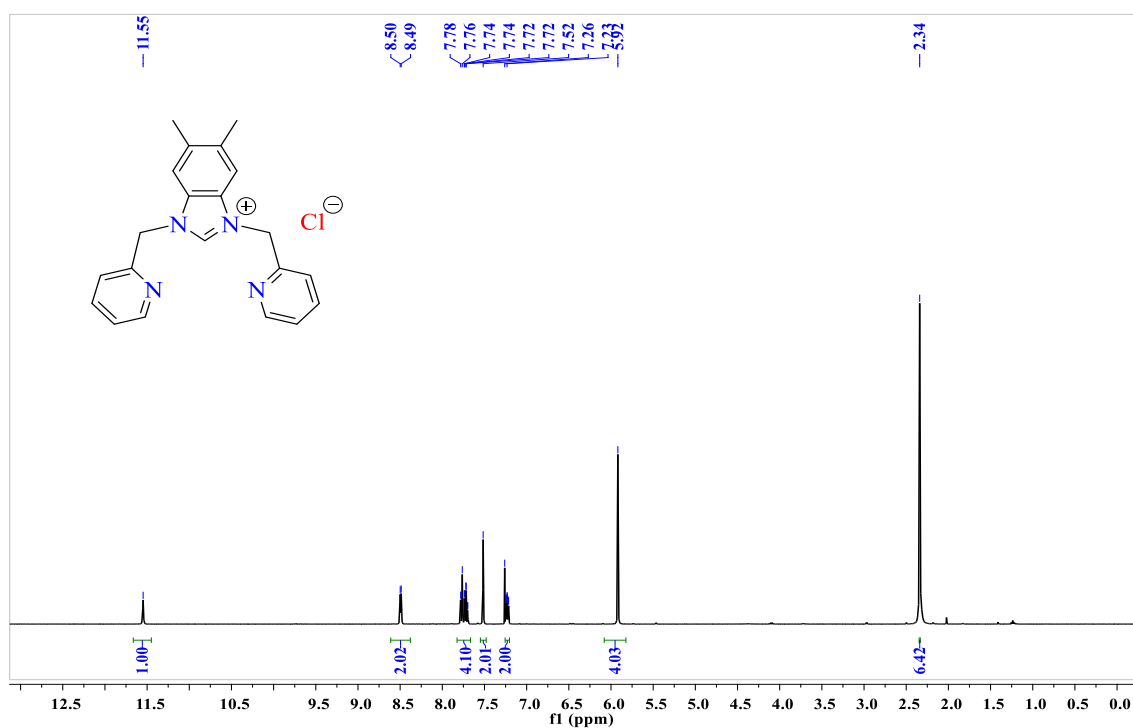
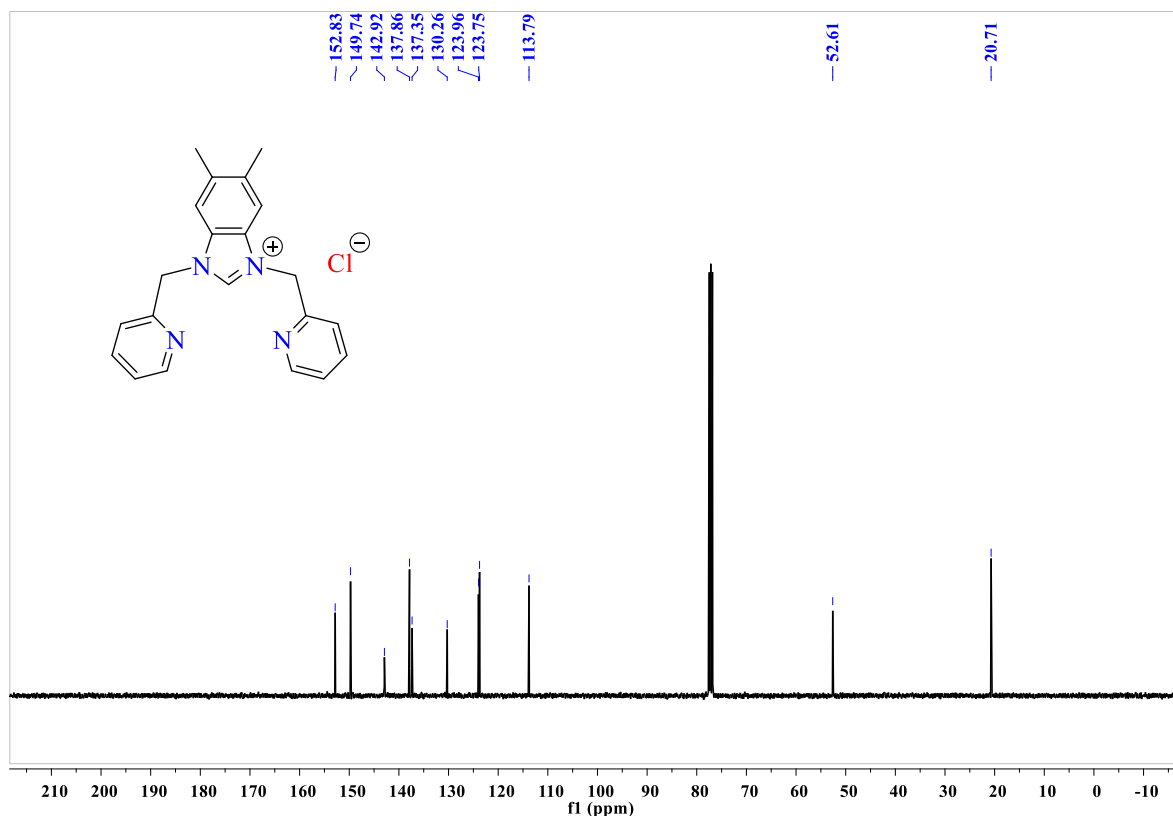


Figure 4.11. IR spectrum of Complex 1.



**Figure 4.12.**  $^1\text{H}$  NMR (400 MHz,  $\text{CDCl}_3$ ) of 5,6-dimethyl-1,3-bis(pyridin-2-ylmethyl)-1H-benzimidazole-3-mium chloride.



**Figure 4.13.**  $^{13}\text{C}\{^1\text{H}\}$  NMR (101 MHz,  $\text{CDCl}_3$ ) of 5,6-dimethyl-1,3-bis(pyridin-2-ylmethyl)-1H-benzimidazole-3-mium chloride.

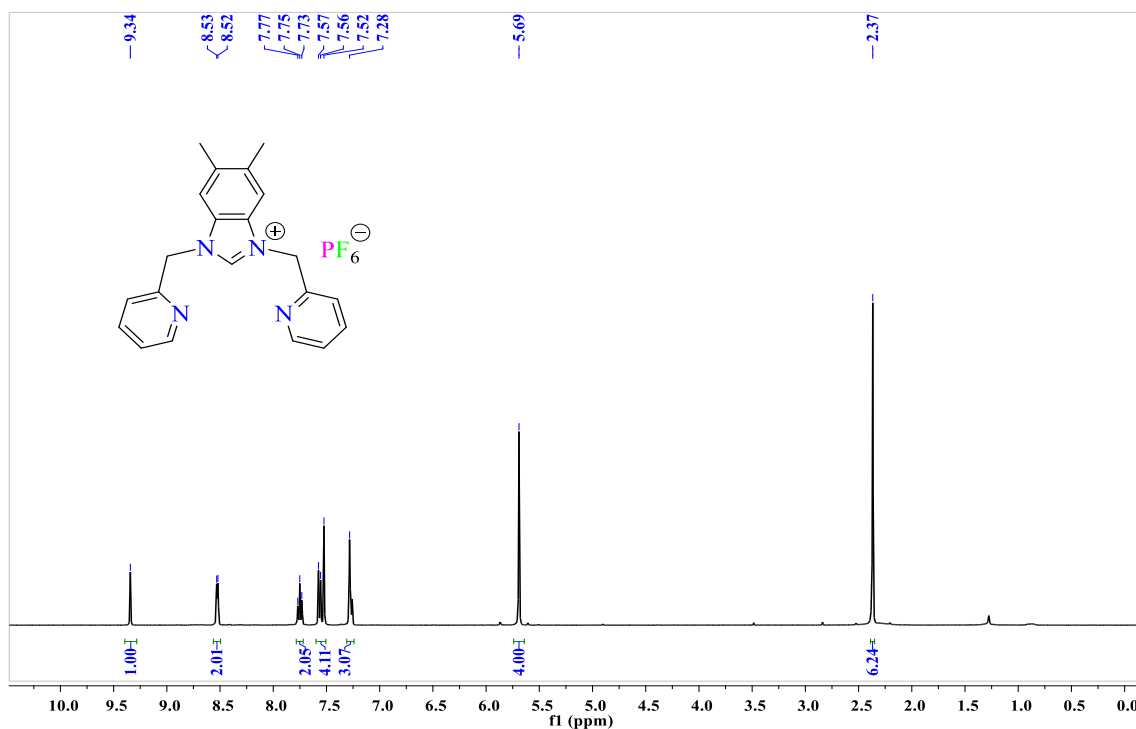


**Figure 4.14.**  $^1\text{H}$  NMR (400 MHz,  $\text{CDCl}_3$ ) of 5,6-dimethyl-1,3-bis(pyridin-2-ylmethyl)-1H-benzimidazole-3-mium hexafluorophosphate ( $\text{L}_2$ ).

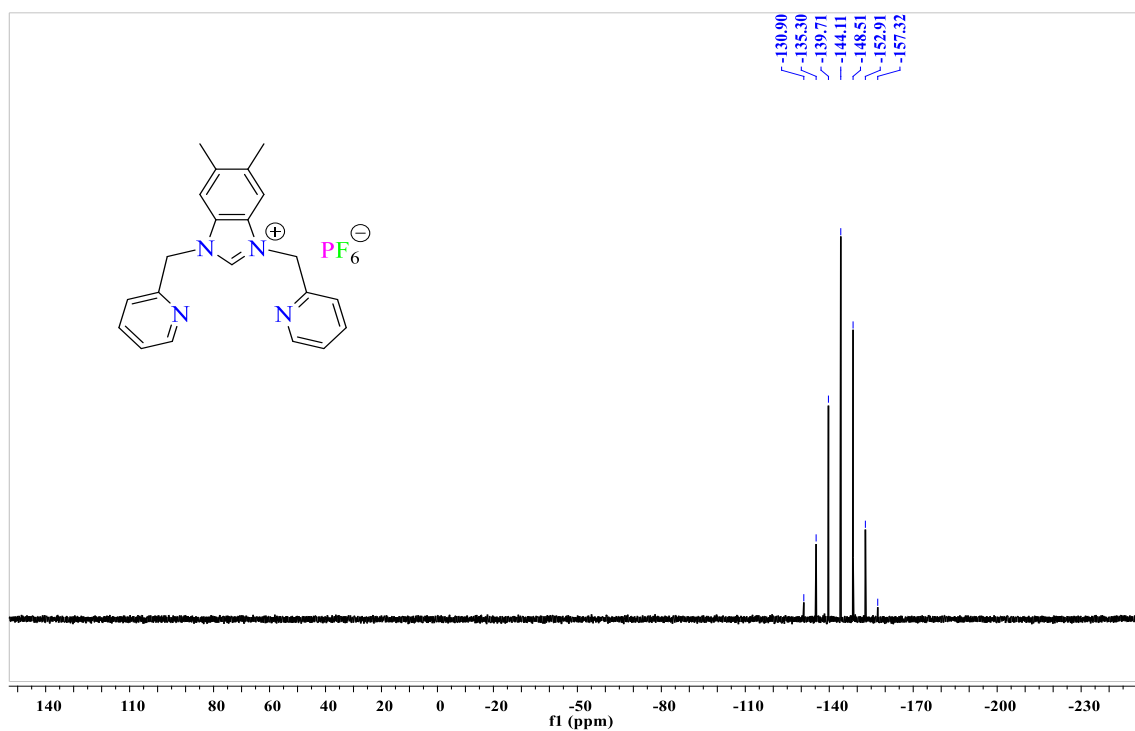


**Figure 4.15.**  $^{31}\text{P}\{^1\text{H}\}$  NMR (162 MHz,  $\text{CDCl}_3$ ) of 5,6-dimethyl-1,3-bis(pyridin-2-ylmethyl)-1H-benzimidazole-3-mium hexafluorophosphate ( $\text{L}_2$ ).

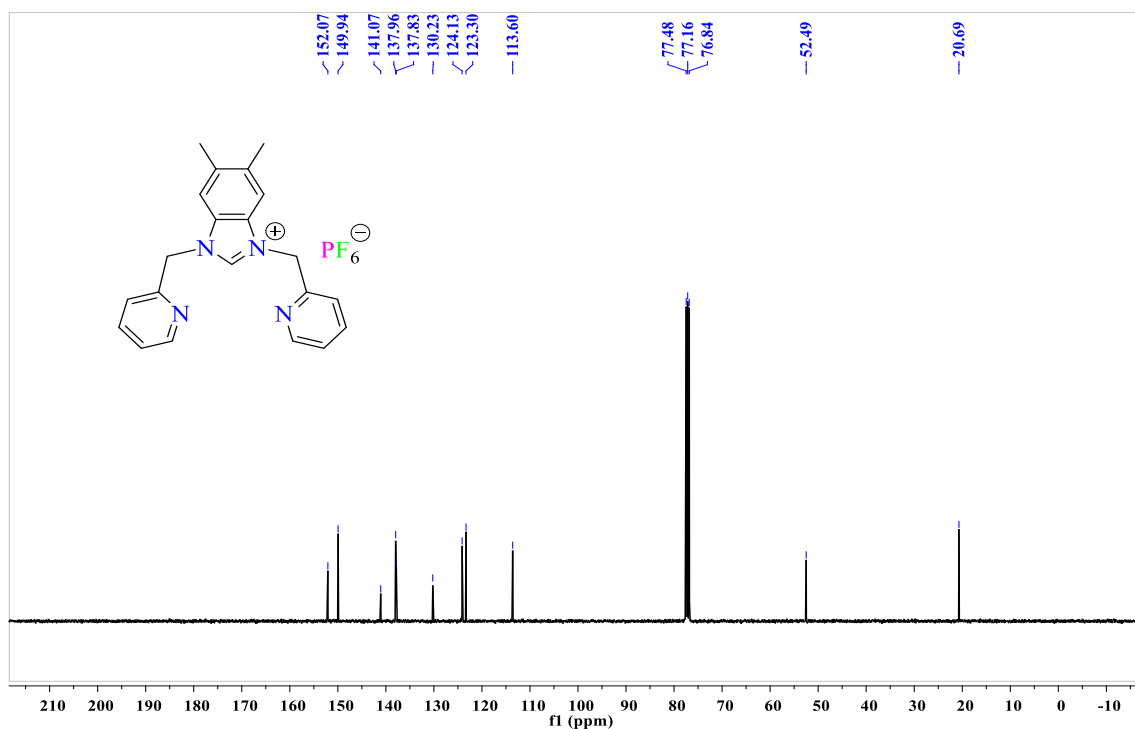


**Figure 4.16.**  $^{13}\text{C}\{^1\text{H}\}$  NMR (101 MHz,  $\text{CDCl}_3$ ) of 5,6-dimethyl-1,3-bis(pyridin-2-ylmethyl)-1H-benzimidazole-3-mium hexafluorophosphate ( $\text{L}_2$ ).

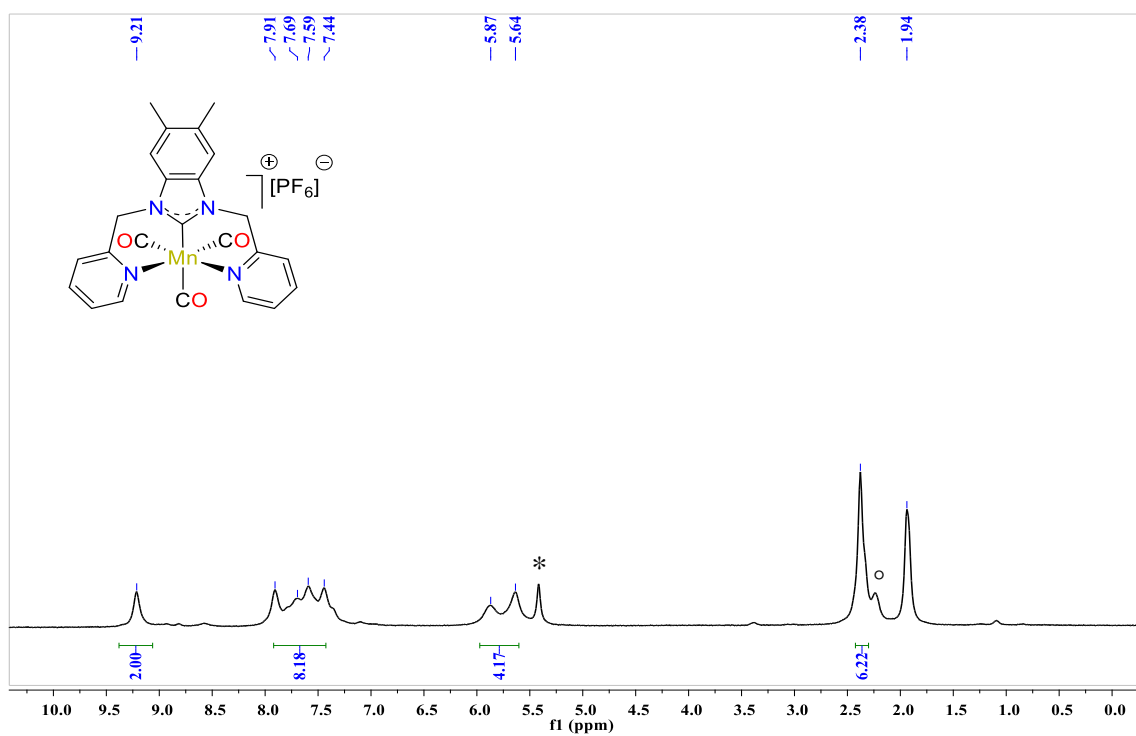


**Figure 4.17.**  $^1\text{H}$  NMR (400 MHz,  $\text{CD}_3\text{CN}$ ) of Complex **2** ( $^\circ$  indicates water and \* indicates DCM).

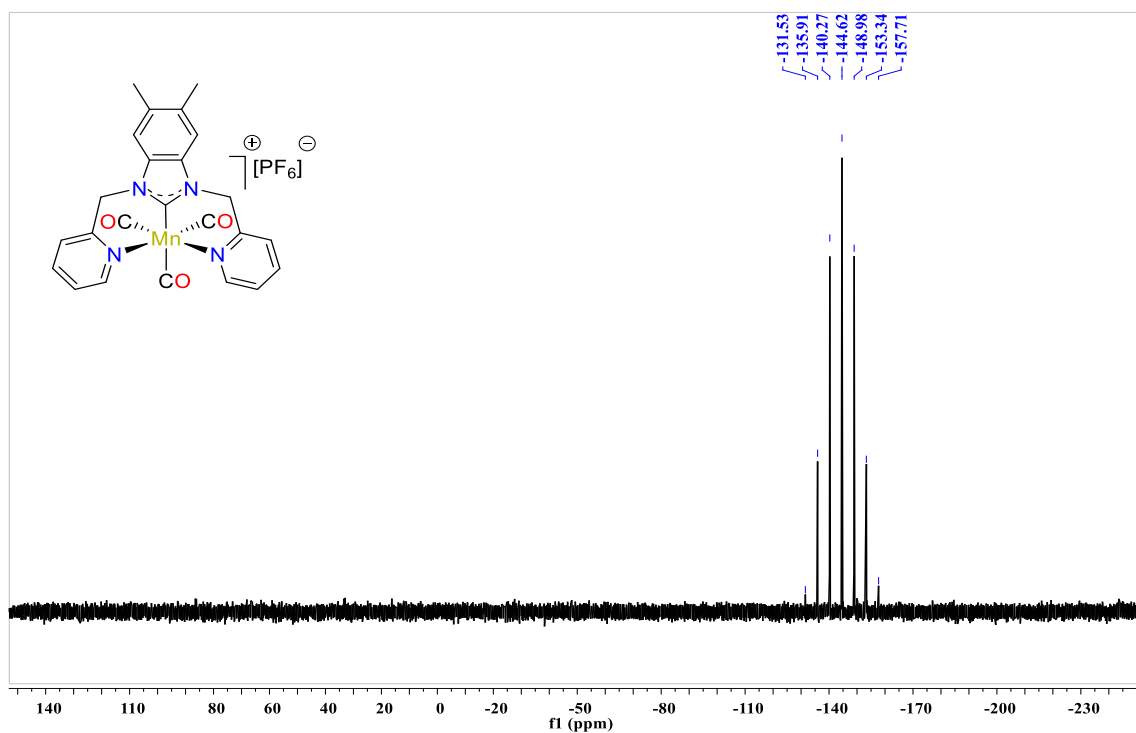


**Figure 4.18.**  $^{31}\text{P}\{^1\text{H}\}$  NMR (162 MHz,  $\text{DMSO-d}_6$ ) of Complex **2**.

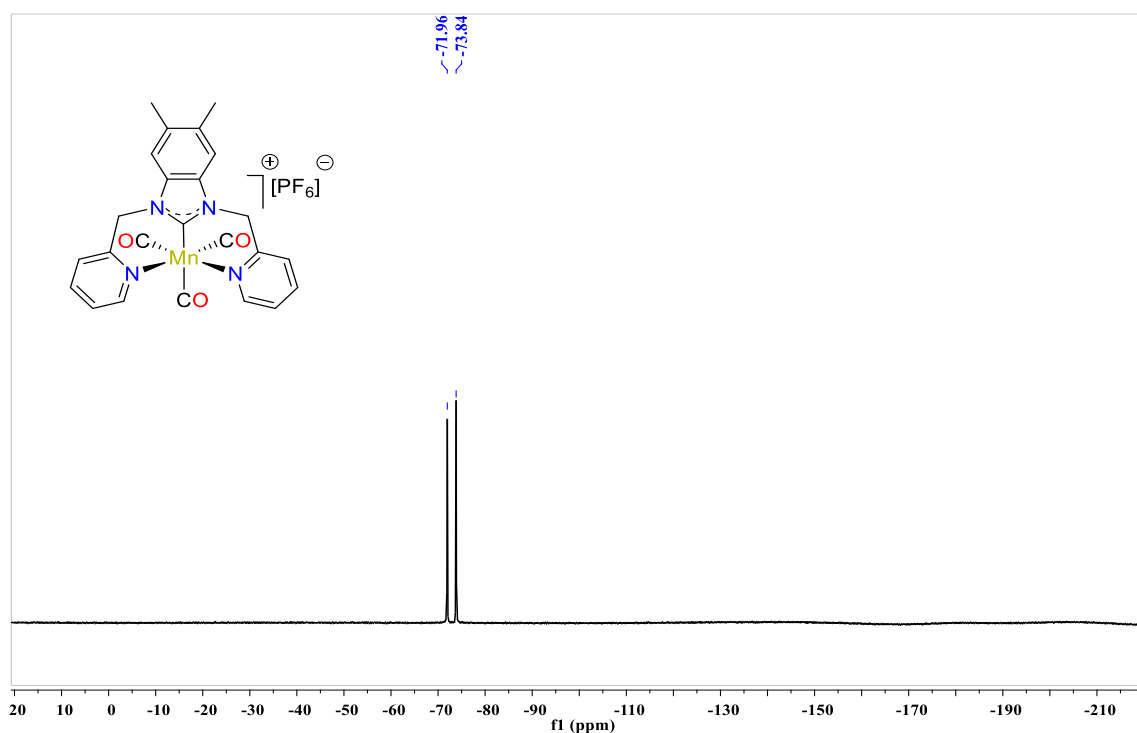


**Figure 4.19.** <sup>19</sup>F{<sup>1</sup>H} NMR (377 MHz, DMSO-d<sub>6</sub>) of Complex 2.

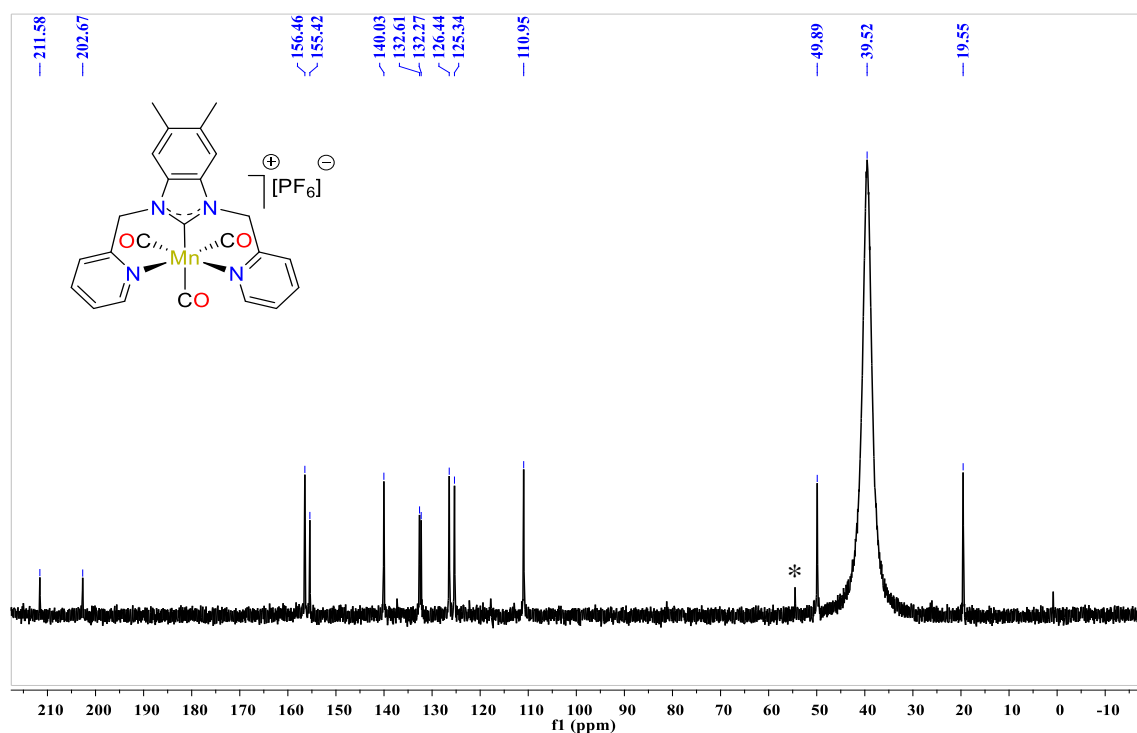


**Figure 4.20.** <sup>13</sup>C{<sup>1</sup>H} NMR (101 MHz, DMSO-d<sub>6</sub>) of Complex 2 (\* indicates DCM).

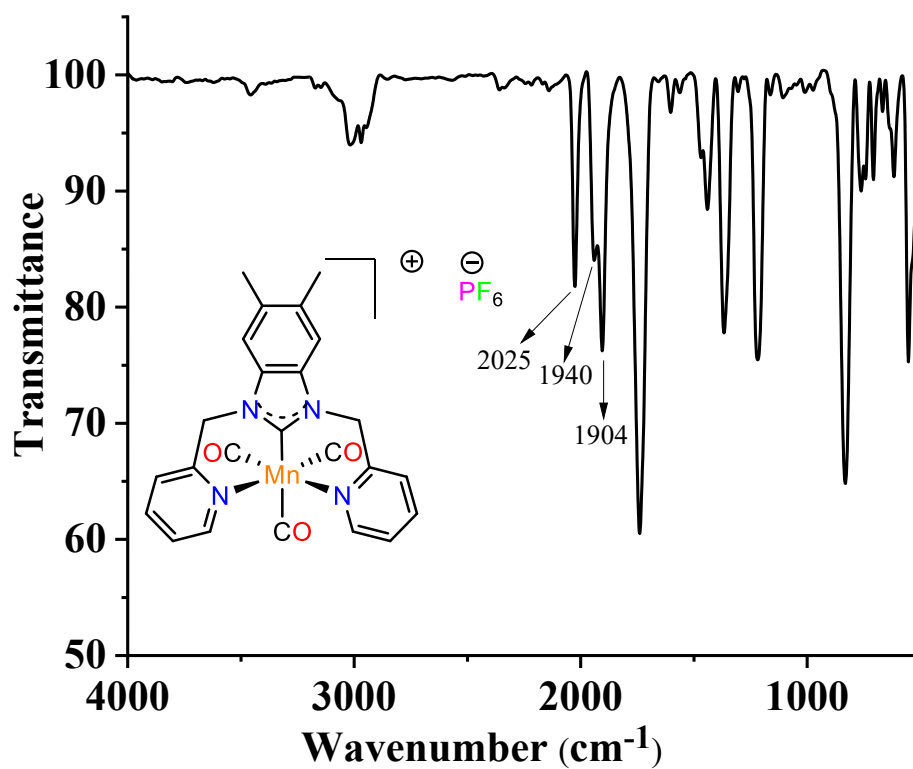


Figure 4.21. IR spectrum of Complex 2.

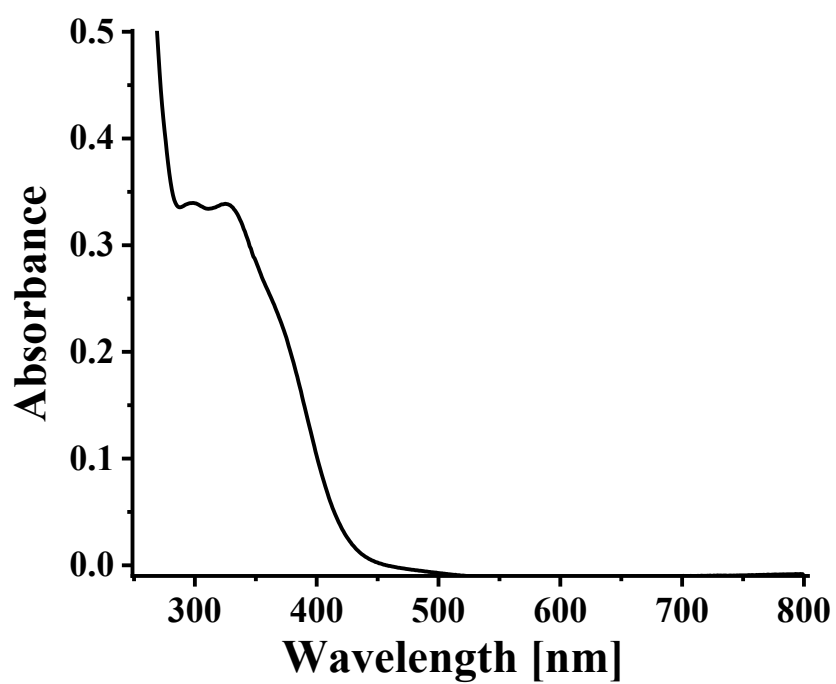
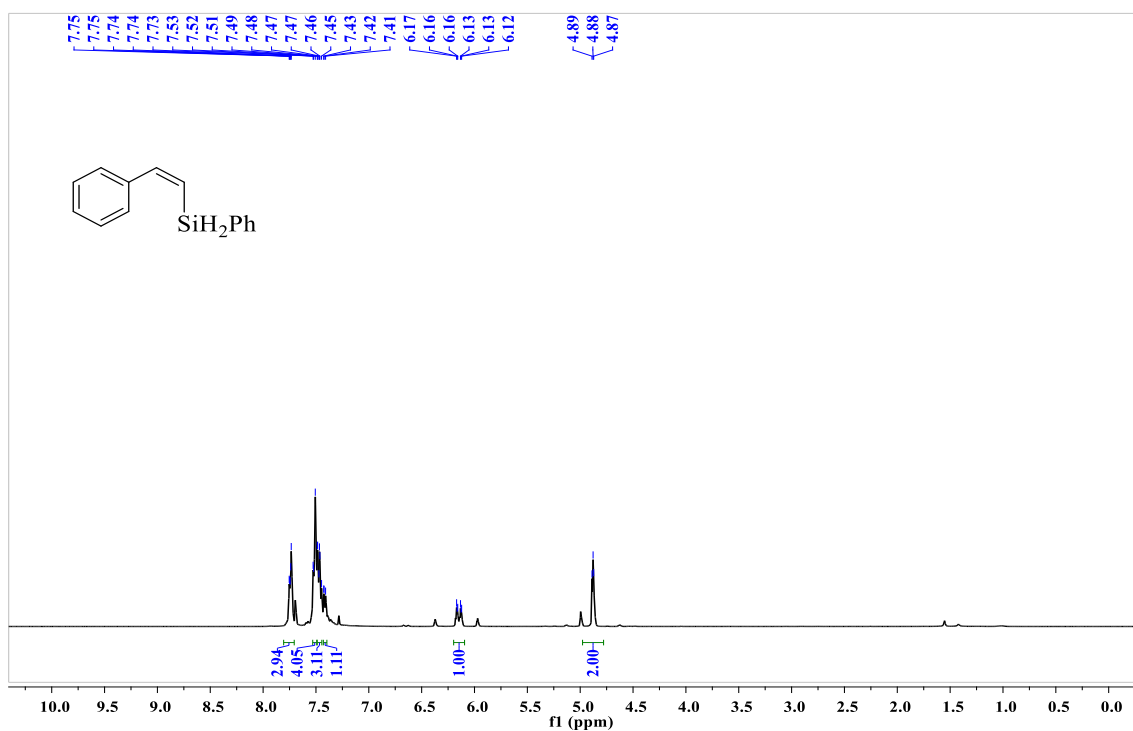
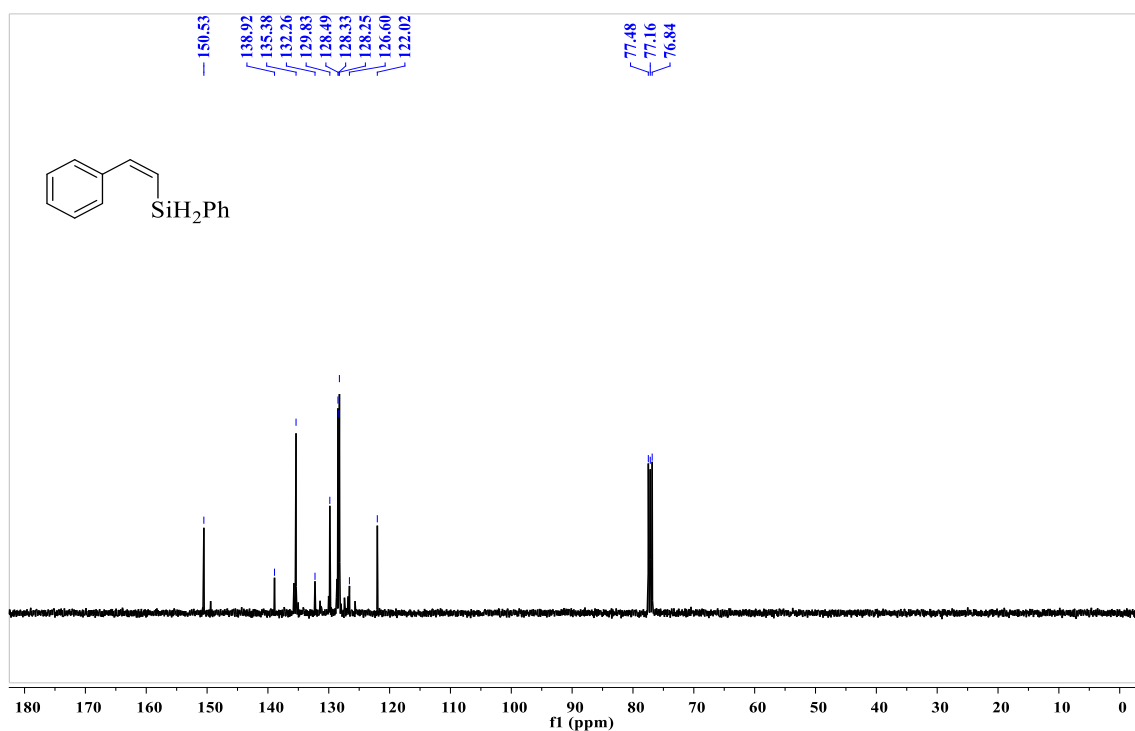


Figure 4.22. UV-Vis spectrum (MeCN,  $10^{-4}$  M) of complexes 1.



**Figure 4.23.** <sup>1</sup>H NMR (400 MHz) spectrum of (*Z*)-phenyl(styryl)silane (**P1a**) in CDCl<sub>3</sub> at r.t.



**Figure 4.24.** <sup>13</sup>C{<sup>1</sup>H} NMR (101 MHz) spectrum of (*Z*)-phenyl(styryl)silane (**P1a**) in CDCl<sub>3</sub> at r.t.

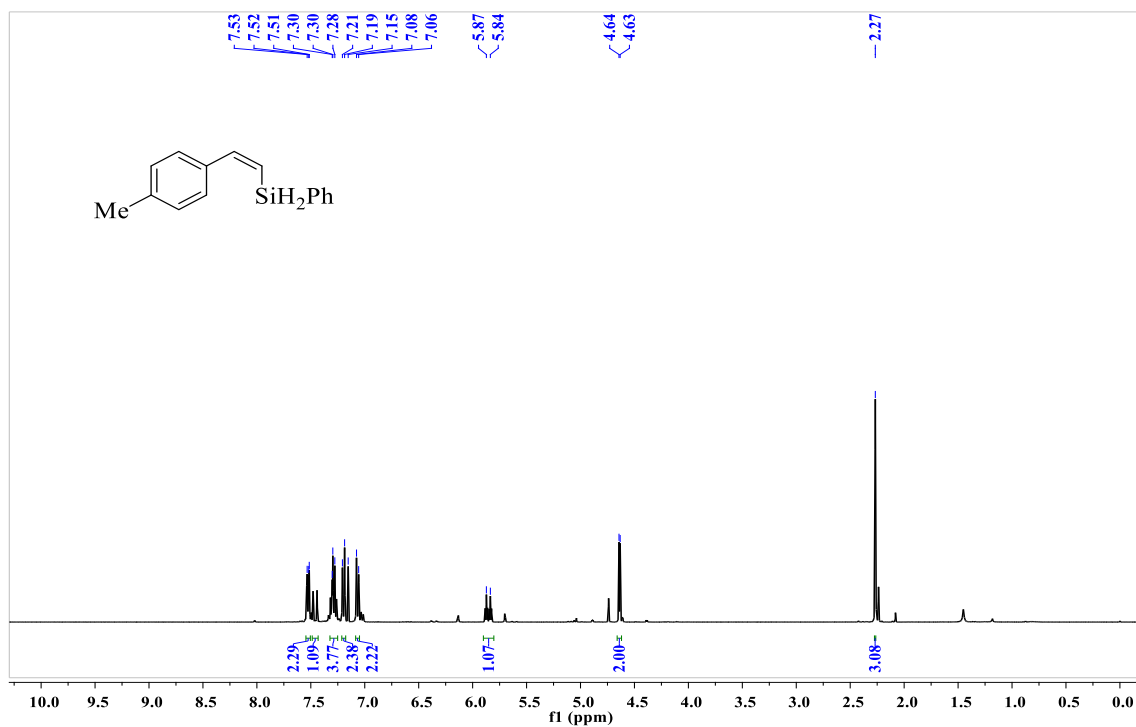


**Figure 4.25.** <sup>1</sup>H NMR (400 MHz) spectrum of (Z)-(4-methylstyryl)(phenyl)silane (**P<sub>2a</sub>**) in CDCl<sub>3</sub> at r.t.

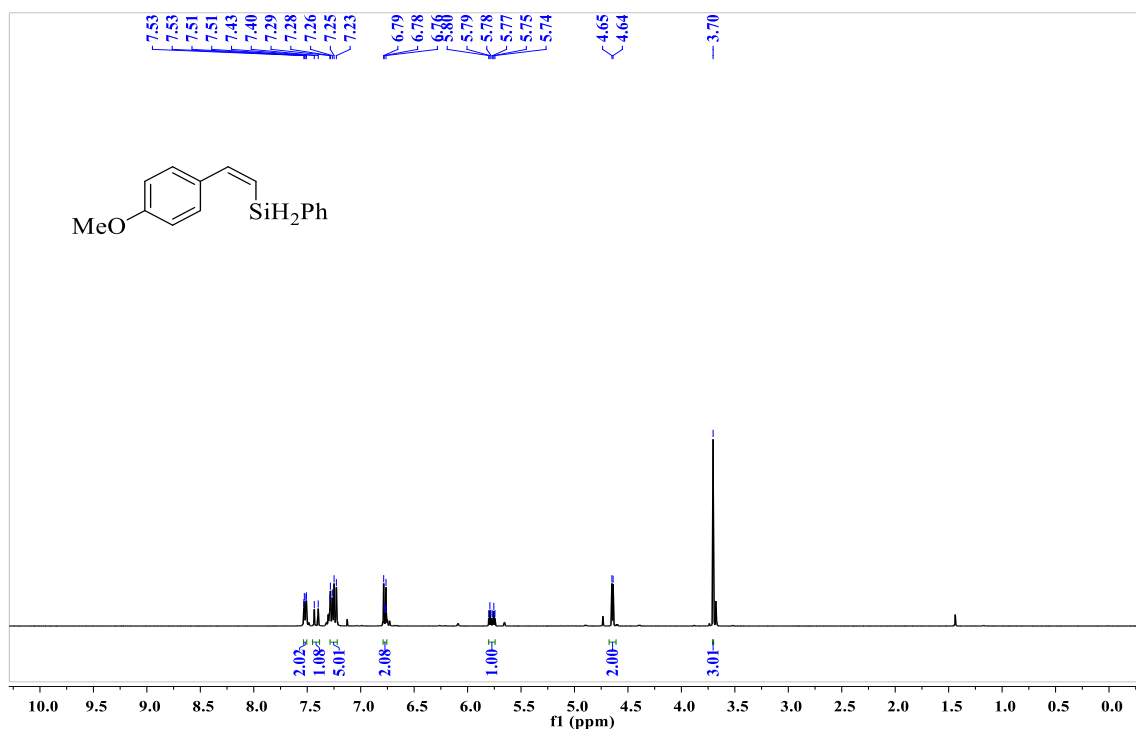


**Figure 4.26.** <sup>1</sup>H NMR (400 MHz) spectrum of (Z)-(4-methoxystyryl)(phenyl)silane (**P<sub>7a</sub>**) in CDCl<sub>3</sub> at r.t.

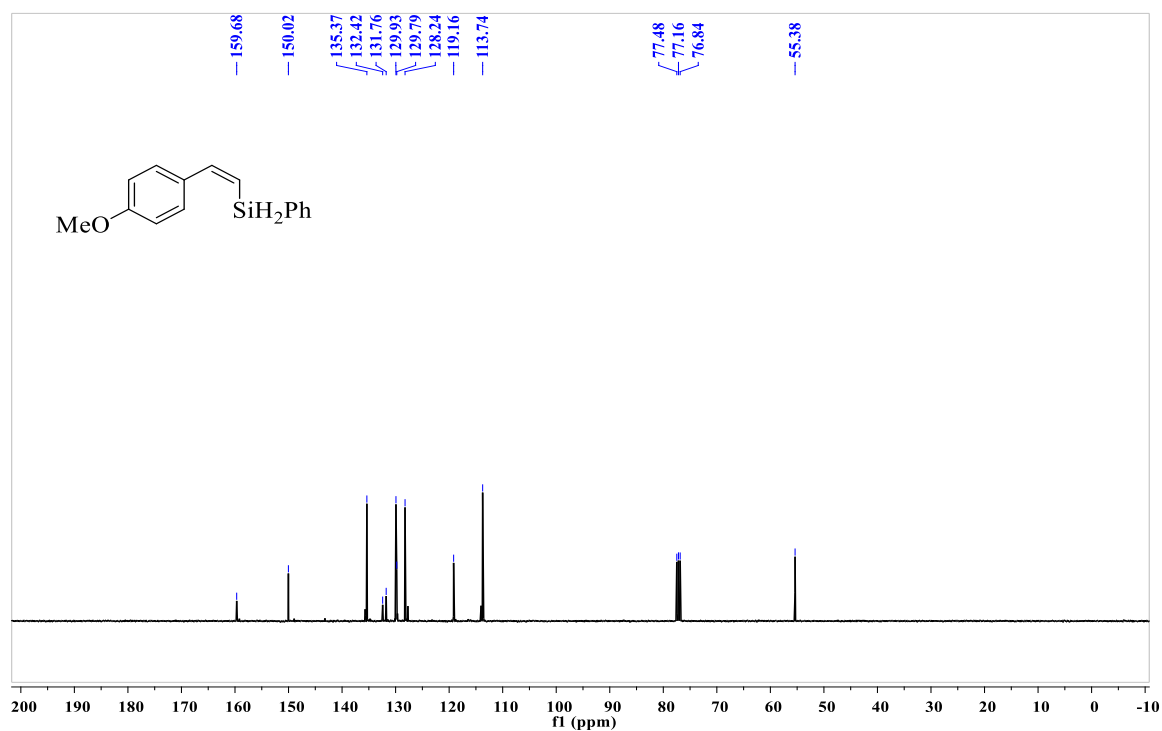


**Figure 4.27.**  $^{13}\text{C}\{^1\text{H}\}$  NMR (101 MHz) spectrum of (Z)-(4-methoxystyryl)(phenyl)silane (**P7a**) in  $\text{CDCl}_3$  at r.t.

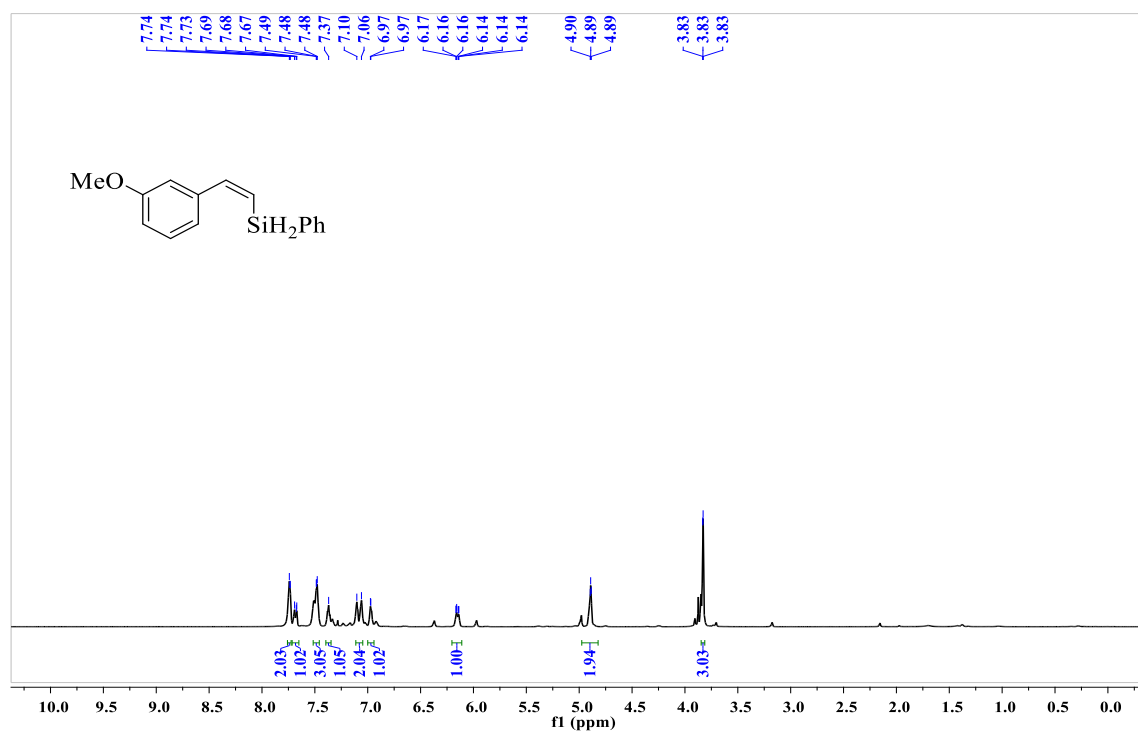


**Figure 4.28.**  $^1\text{H}$  NMR (400 MHz) spectrum of (Z)-(3-methoxystyryl)(phenyl)silane (**P8a**) in  $\text{CDCl}_3$  at r.t.

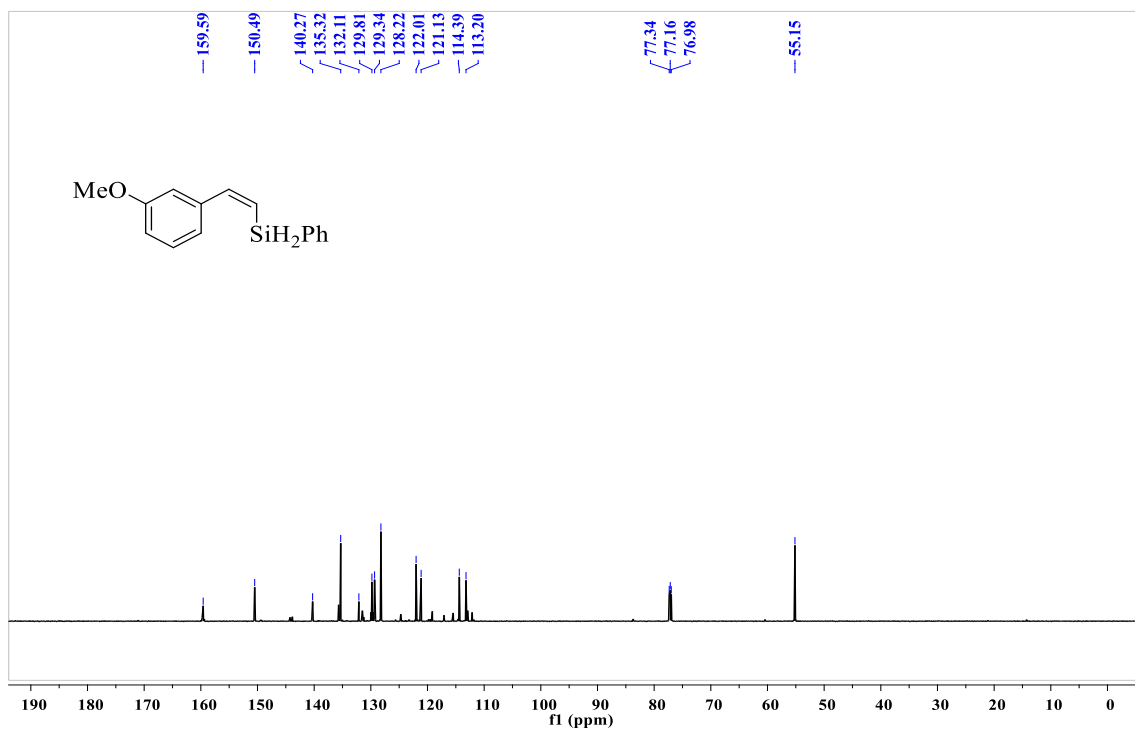


**Figure 4.29.**  $^{13}\text{C}\{^1\text{H}\}$  NMR (101 MHz) spectrum of (Z)-3-(3-methoxystyryl)(phenyl)silane (**P8a**) in CDCl<sub>3</sub> at r.t.

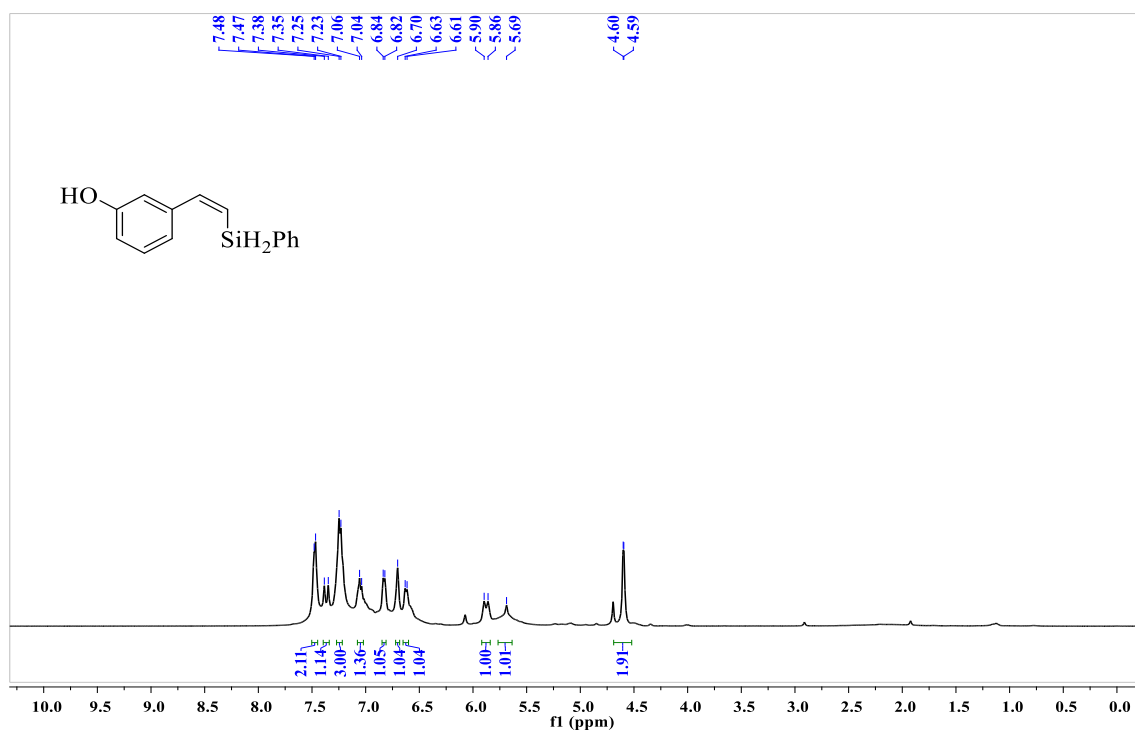


**Figure 4.30.**  $^1\text{H}$  NMR (400 MHz) spectrum of (Z)-3-(2-(phenylsilyl)vinyl)phenol (**P9a**) in CDCl<sub>3</sub> at r.t.

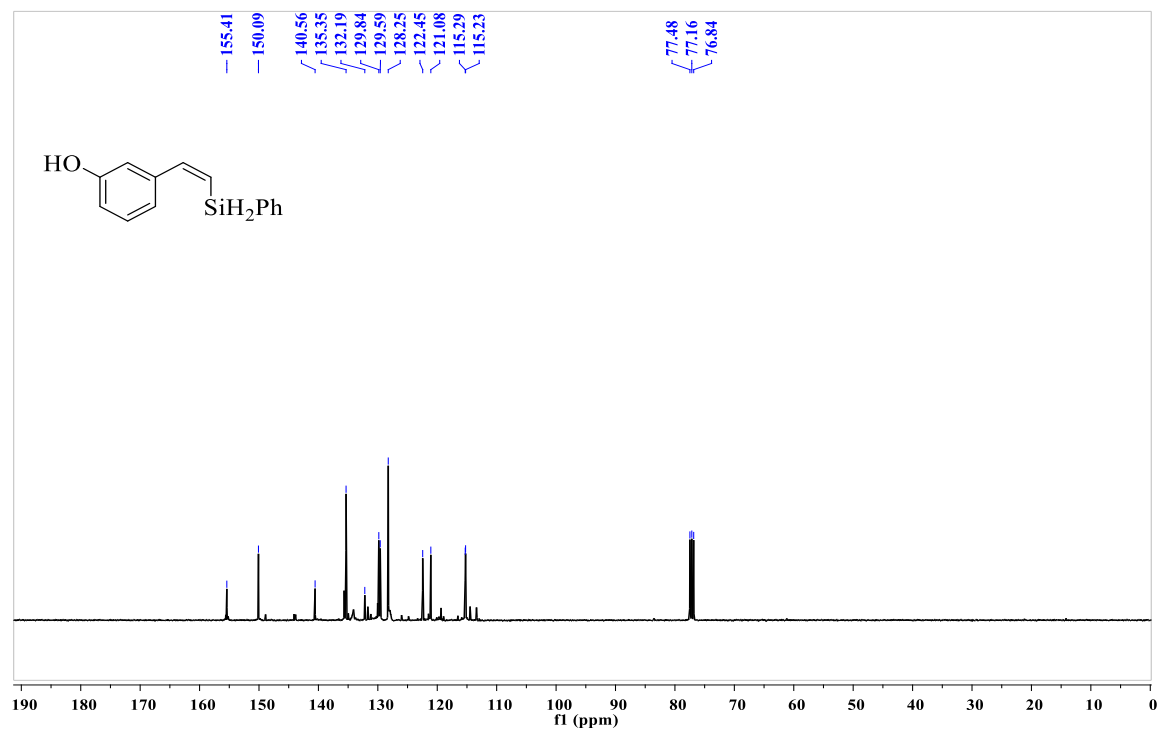


**Figure 4.31.**  $^{13}\text{C}\{^1\text{H}\}$  NMR (101 MHz) spectrum of (Z)-3-(2-(phenylsilyl)vinyl)phenol (P9a) in  $\text{CDCl}_3$  at r.t.

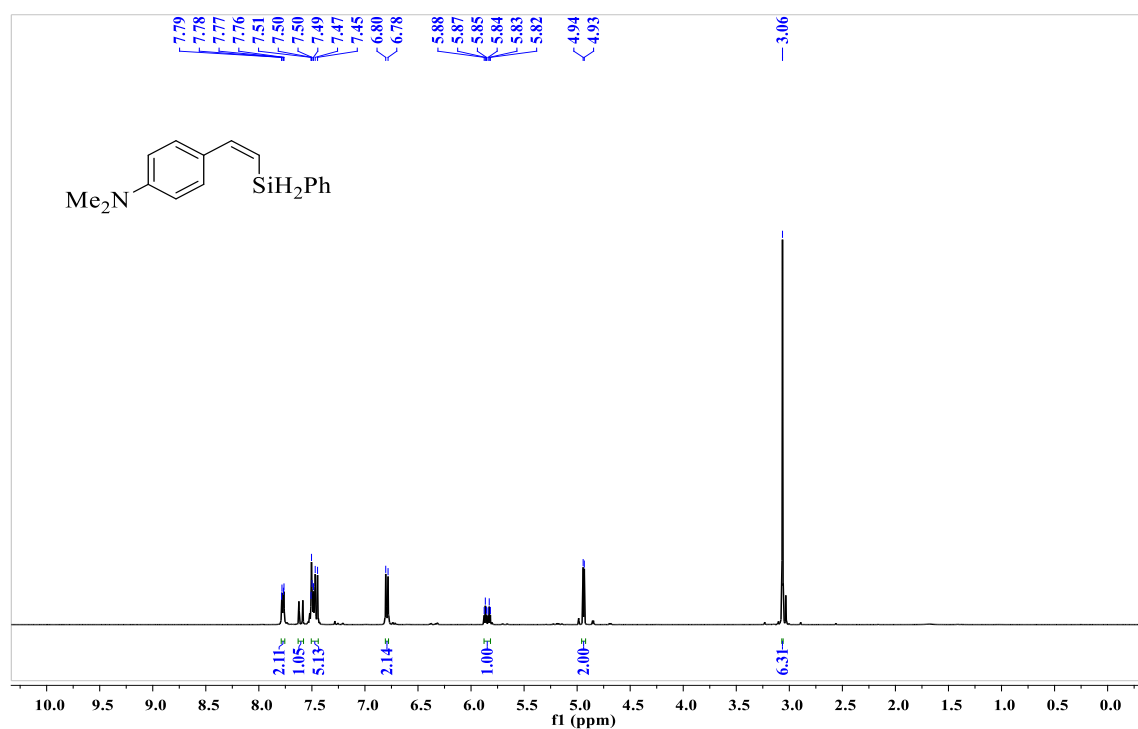


**Figure 4.32.**  $^1\text{H}$  NMR (400 MHz) spectrum of (Z)-N,N-dimethyl-4-(2-(phenylsilyl)vinyl)aniline (P10a) in  $\text{CDCl}_3$  at r.t.

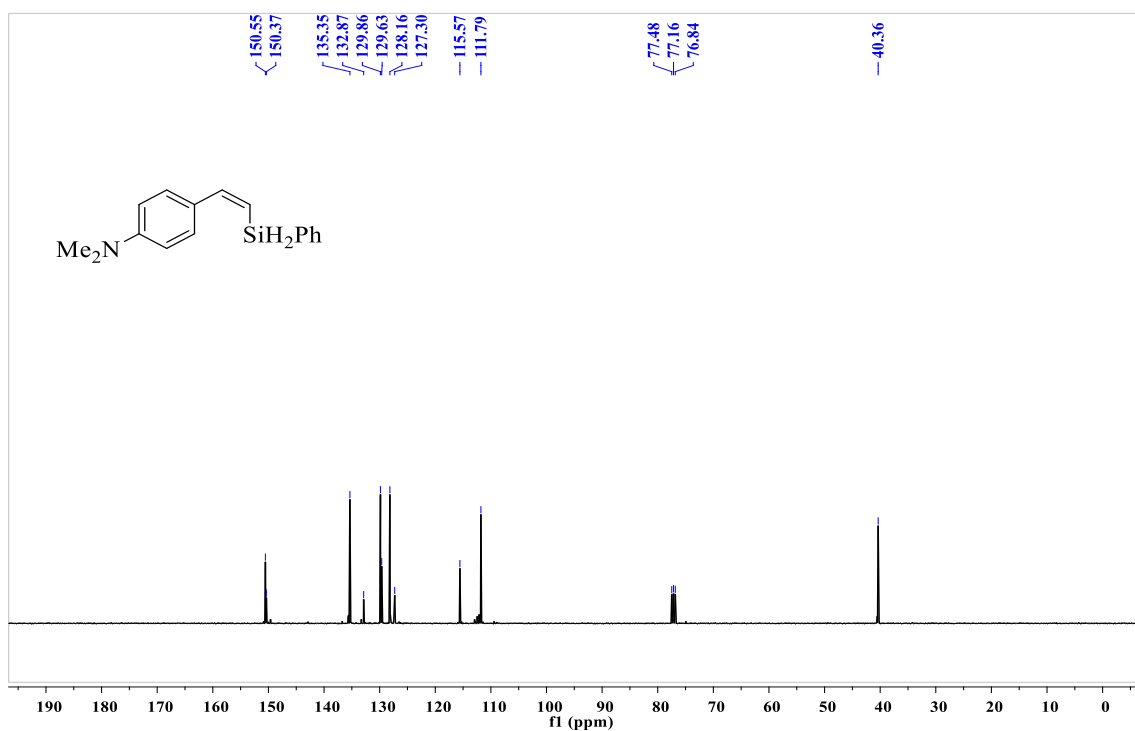


**Figure 4.33.**  $^{13}\text{C}\{^1\text{H}\}$  NMR (101 MHz) spectrum of (Z)-N,N-dimethyl-4-(2-(phenylsilyl)vinyl)aniline (**P10a**) in  $\text{CDCl}_3$  at r.t.

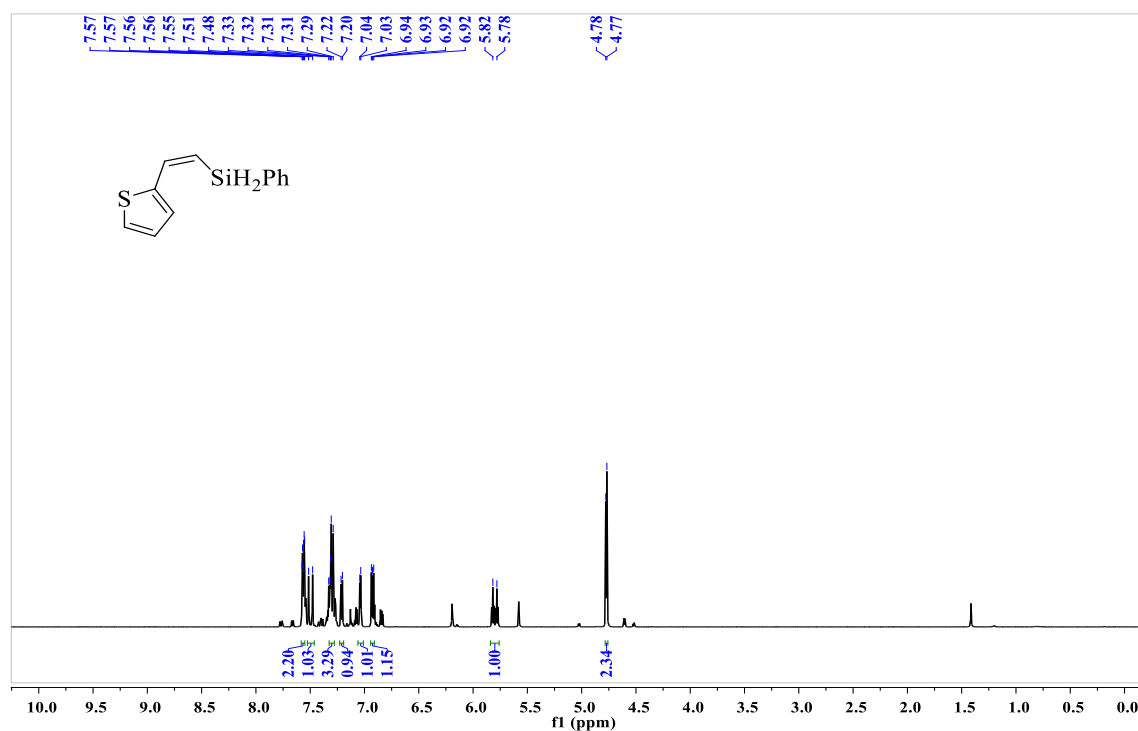


**Figure 4.34.**  $^1\text{H}$  NMR (400 MHz) spectrum of (Z)-phenyl(2-(thiophen-2-yl)vinyl)silane (**P20a**) in  $\text{CDCl}_3$  at r.t.

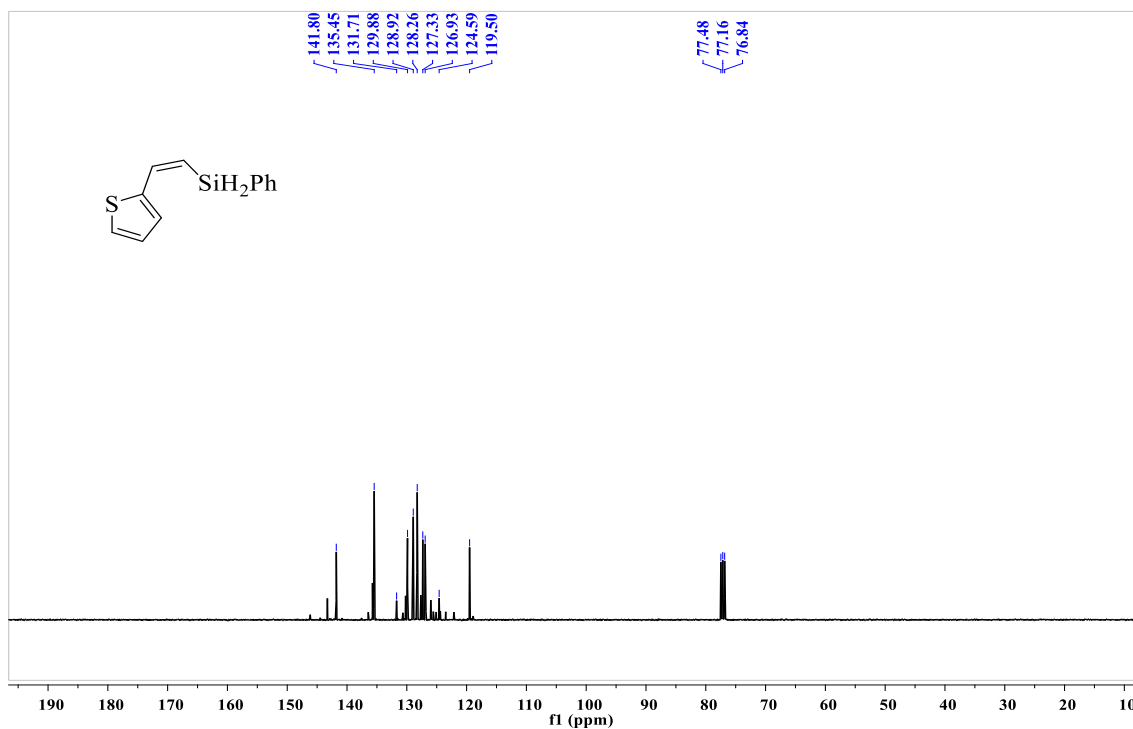


**Figure 4.35.**  $^{13}\text{C}\{^1\text{H}\}$  NMR (101 MHz) spectrum of (Z)-phenyl(2-(thiophen-2-yl)vinyl)silane (**P20a**) in  $\text{CDCl}_3$  at r.t.

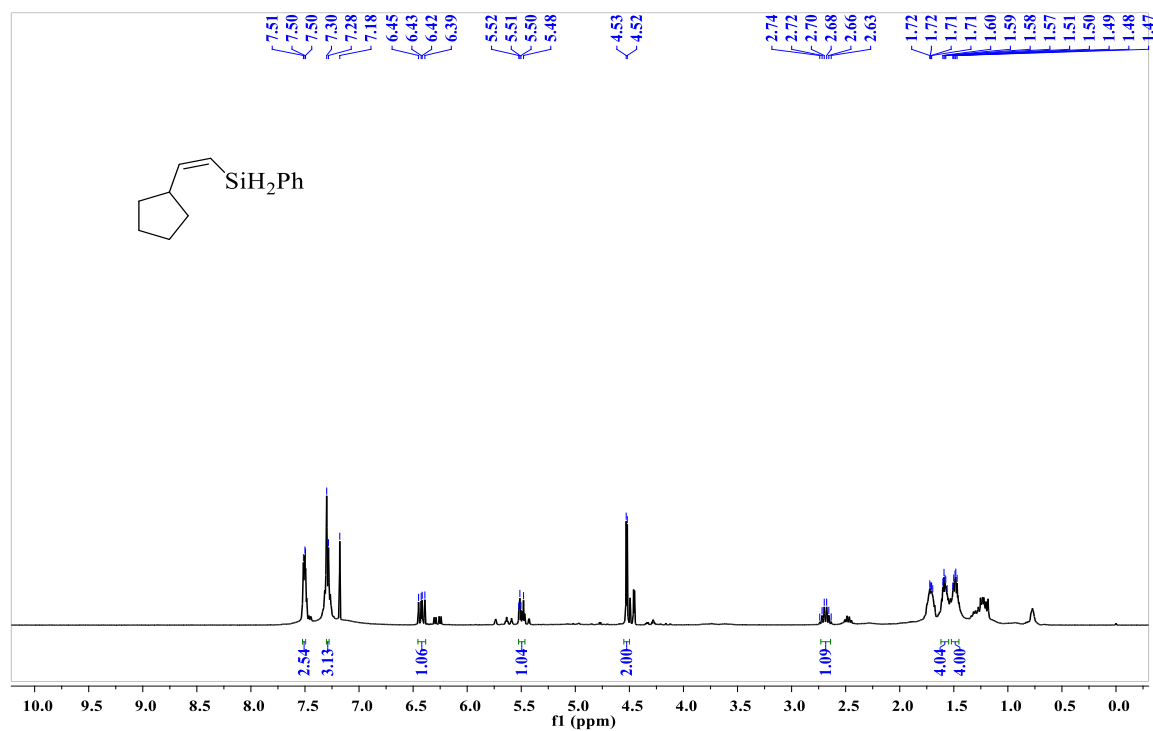


**Figure 4.35.**  $^1\text{H}$  NMR (400 MHz) spectrum of (Z)-(2-cyclopentylvinyl)(phenyl)silane (**P23a**) in  $\text{CDCl}_3$  at r.t.

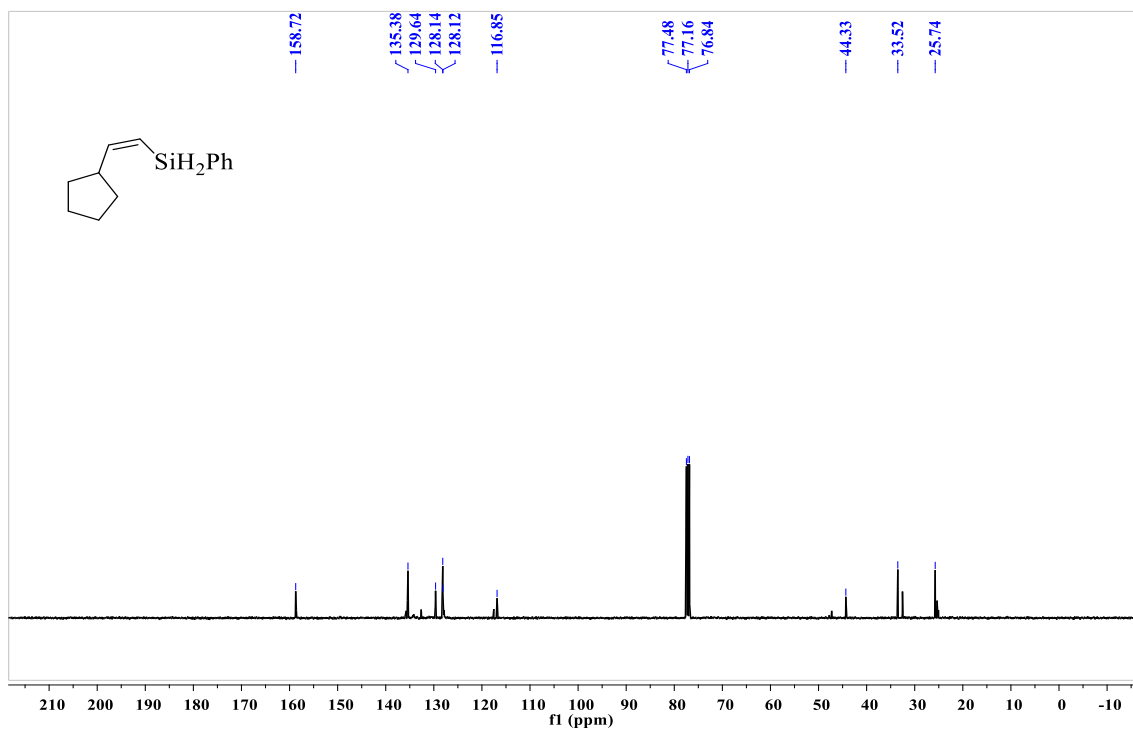


**Figure 4.37.**  $^{13}\text{C}\{^1\text{H}\}$  NMR (101 MHz) spectrum of (Z)-(2-cyclopentylvinyl)(phenyl)silane (**P23a**) in  $\text{CDCl}_3$  at r.t.

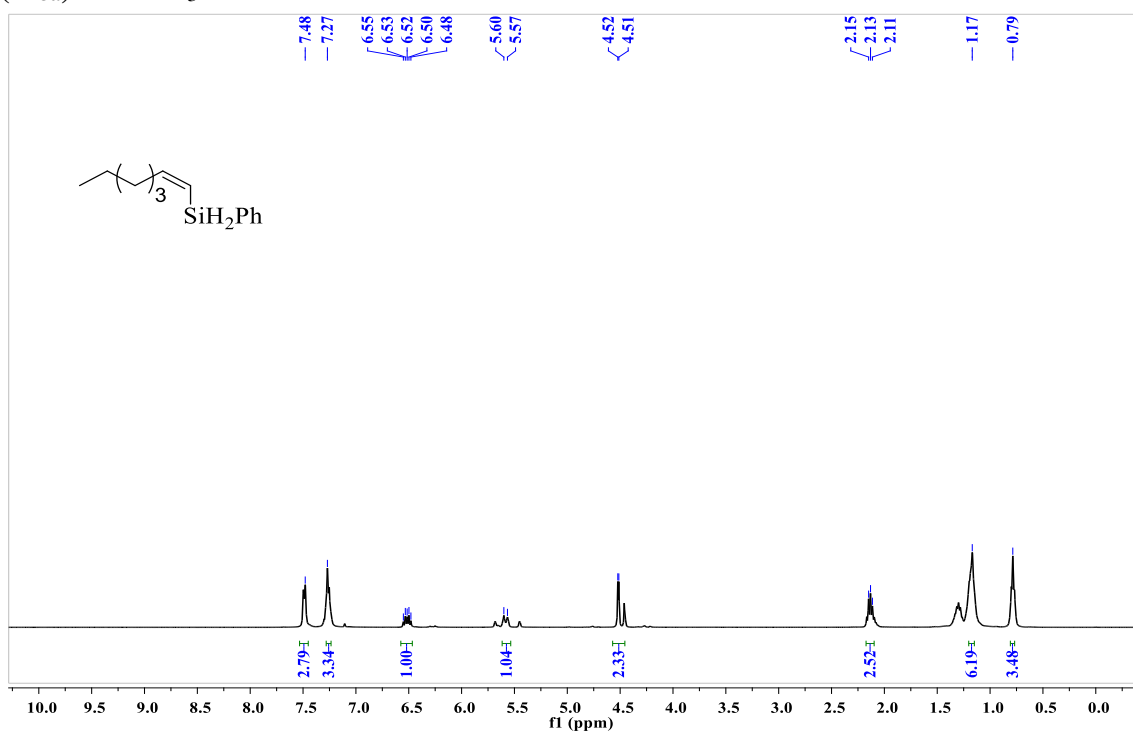


**Figure 4.38.**  $^1\text{H}$  NMR (400 MHz) spectrum of (Z)-hept-1-en-1-yl(phenyl)silane (**P25a**) in  $\text{CDCl}_3$  at r.t.

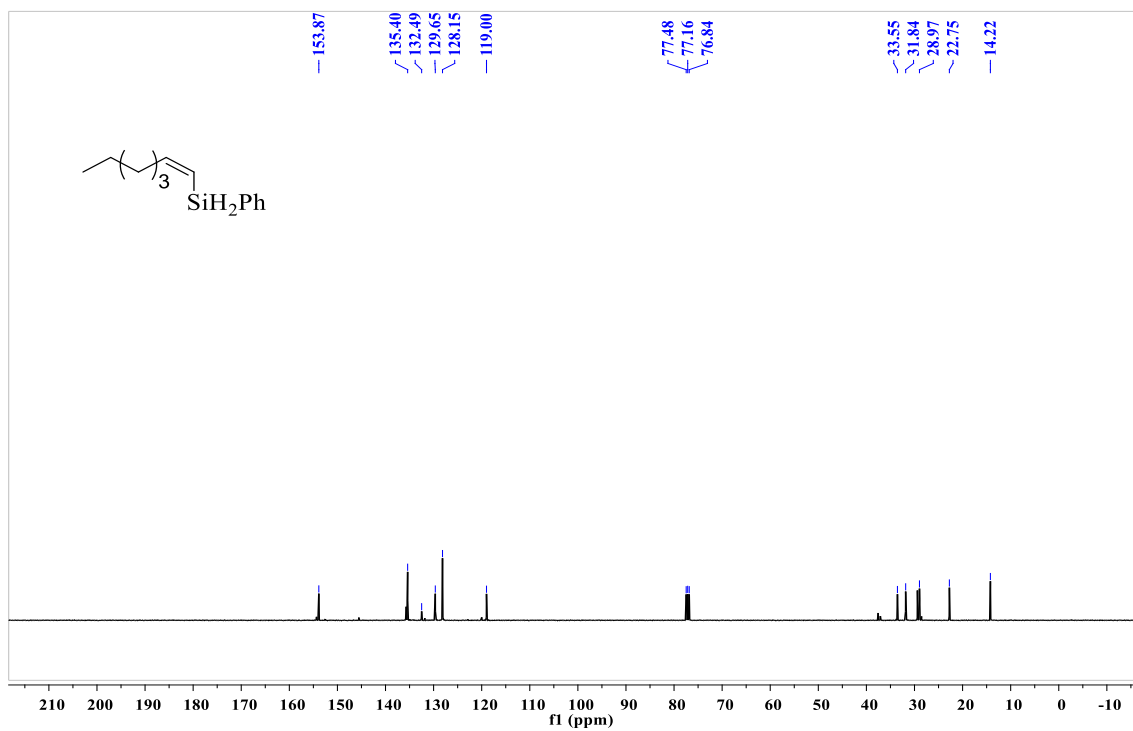


**Figure 4.39.**  $^{13}\text{C}\{^1\text{H}\}$  NMR (101 MHz) spectrum of (Z)-hept-1-en-1-yl(phenyl)silane (**P25a**) in  $\text{CDCl}_3$  at r.t.

## References

1. (a) Blumenkopf, T. A.; Overman, L. E. Vinylsilane- and Alkynylsilane-Terminated Cyclization Reactions. *Chem. Rev.* **1986**, *86*, 857-873. (b) Langkopf, E.; Schinzer, D. Uses of Silicon-Containing Compounds in the Synthesis of Natural Products. *Chem. Rev.* **1995**, *95*, 1375-1408. (c) Denmark, S. E.; Sweis, R. F. Eds. Palladium-Catalyzed Cross-Coupling Reactions of Organosilanols and Their Salts: Practical Alternatives to Boron- and Tin-Based Methods. *Acc. Chem. Res.* **2008**, *11*, 1486-1499. (d) Chan, T. H.; Fleming, I. Electrophilic Substitution of Organosilicon Compounds- Applications to Organic Synthesis. *Synthesis* **1979**, *1979*, 761-786. (e) Fleming, I.; Barbero, A.; Walter, D. Stereochemical Control in Organic Synthesis Using Silicon-Containing Compounds. *Chem. Rev.* **1997**, *97*, 2063-2192.
2. (a) Frohning, C. D.; Kohlpaintner, C. W. Hydroformylation (Oxo Synthesis. Roelen Reaction) In *Applied Homogeneous Catalysis with Organometallic Compounds*; Cornils, B., Herrmann, W. A., Eds.; VCH: Weinheim, Germany, 1996; Vol. 1; pp 29-104. (b) Marciniak, B.; Maciejewski, H.; Pietraszuk, C.; Pawluc, P. In *Hydrosilylation: A Comprehensive Review on Recent Advances*; Marciniak, B., Ed.; Springer: Berlin, 2009; Chapter 1. (c) Nakajima, Y.; S. Shimada. Hydrosilylation reaction of olefins: recent advances and perspectives. *RSC Adv.* **2015**, *5*, 20603-20616. (d) Sun, J.; Deng, L. Cobalt Complex-Catalyzed Hydrosilylation of Alkenes and Alkynes. *ACS Catal.* **2016**, *6*, 290-300.
3. Speier, J. L.; Webster, J. A.; Barnes, G. H. The Addition of Silicon Hydrides to Olefinic Double Bonds. Part II. The Use of Group VIII Metal Catalysts. *J. Am. Chem. Soc.*, **1957**, *79*, 974-979.
4. (a) Royo, B. Chapter Two – Recent advances in catalytic hydrosilylation of carbonyl groups mediated by well-defined first-row late transition metals. *Adv. Organomet. Chem.*

- 2019, 72, 59-102. (b) Díez-Gonzalez, S.; Nolan, S. P. Copper, Silver, and Gold Complexes in Hydrosilylation Reactions. *Acc. Chem. Res.* 2008, 41, 349–358. (c) Ojima, I.; Li, Z.; Zhu, J. Recent Advances in the Hydrosilylation and Related Reactions. In *The Chemistry of Organic Silicon Compounds*, 1998; pp. 1687. (d) Troegel, D.; Stohrer, J. Recent advances and actual challenges in late transition metal catalyzed hydrosilylation of olefins from an industrial point of view. *Coord. Chem. Rev.* 2011, 255, 1440-1459. (e) Díez-Gonzalez, S.; Nolan, S. P. Transition Metal-Catalyzed Hydrosilylation of Carbonyl Compounds and Imines. A Review. *Org. Prep. Proced. Int.* 2007, 39, 523-559.
5. (a) Kawasaki, Y.; Ishikawa, Y.; Igawa, K.; Tomooka, K. Directing Group-Controlled Hydrosilylation: Regioselective Functionalization of Alkyne. *J. Am. Chem. Soc.* 2011, 133, 20712-20715. (b) Rooke, D. A.; Ferreira, E. M. Platinum-Catalyzed Hydrosilylations of Internal Alkynes: Harnessing Substituent Effects to Achieve High Regioselectivity. *Angew. Chem., Int. Ed.* 2012, 124, 3279-3284. (c) Sumida, Y.; Kato, T.; Yoshida, S.; Hosoya, T. Palladium-Catalyzed Regio- and Stereoselective Hydrosilylation of Electron-Deficient Alkynes. *Org. Lett.* 2012, 14, 1552-1555. (d) Ding, S.; Song, L.-J.; Chung, L. W.; Zhang, X.; Sun, J.; Wu, Y.-D. Ligand-Controlled Remarkable Regio- and Stereodivergence in Intermolecular Hydrosilylation of Internal Alkynes: Experimental and Theoretical Studies. *J. Am. Chem. Soc.* 2013, 135, 13835-13842. (e) Ding, S.; Song, L.-J.; Wang, Y.; Zhang, X.; Chung, L. W.; Wu, Y.-D.; Sun, J. Highly Regio- and Stereoselective Hydrosilylation of Internal Thioalkynes under Mild Conditions. *Angew. Chem., Int. Ed.* 2015, 54, 5632-5635. (f) Zhao, X.; Yang, D.; Zhang, Y.; Wang, B.; Qu, J. Highly  $\beta$  (Z)-Selective Hydrosilylation of Terminal Alkynes Catalyzed by Thiolate-Bridged Dirhodium Complexes. *Org. Lett.* 2018, 20, 5357-5361.
6. (a) Aneetha, H., Wu, W., & Verkade, J. G. Stereo- and Regioselective Pt(DVDS)/P(*i*BuNCH<sub>2</sub>CH<sub>2</sub>)<sub>3</sub>N-Catalyzed Hydrosilylation of Terminal

Alkynes. *Organometallics* **2005**, *24*, 2590-2596. (b) De Bo, G.; Berthon-Gelloz, G.; Tinant, B.; Marko, I. E. Hydrosilylation of Alkynes Mediated by N-Heterocyclic Carbene Platinum (0) Complexes. *Organometallics* **2006**, *25*, 1881–1890. (c) Nakao, Y.; Imanaka, H.; Chen, J.; Yada, A.; Hiyama, T. Synthesis and cross-coupling reaction of alkenyl [(2-hydroxymethyl) phenyl] dimethylsilanes. *J. Organomet. Chem.* **2007**, *692*, 585–603. (d) Berthon-Gelloz, G.; Schumers, J.-M.; De Bo, G.; Marko, I. E. Highly  $\beta$ -(*E*)-Selective Hydrosilylation of Terminal and Internal Alkynes Catalyzed by a (IPr)Pt(diene) Complex. *J. Org. Chem.* **2008**, *73*, 4190–4197. (e) Hamze, A.; Provot, O.; Brion, J.-D.; Alami, M. Xphos ligand and platinum catalysts: A versatile catalyst for the synthesis of functionalized  $\beta$ -(*E*)-vinylsilanes from terminal alkynes. *J. Organomet. Chem.* **2008**, *693*, 2789–2797. (f) Blug, M.; Le Goff, X.-F.; Mezailles, N.; Le Floch, P. A 14-VE' Platinum(0) Phosphabarrelene Complex in the Hydrosilylation of Alkynes. *Organometallics* **2009**, *28*, 2360–2362. (g) Cano, R.; Yus, M.; Ramón, D. J. Impregnated Platinum on Magnetite as an Efficient, Fast, and Recyclable Catalyst for the Hydrosilylation of Alkynes. *ACS Catal.* **2012**, *2*, 1070–1078. (h) Igawa, K.; Yoshihiro, D.; Ichikawa, N.; Kokan, N.; Tomooka, K. Catalytic Enantioselective Synthesis of Alkenylhydrosilane. *Angew. Chem., Int. Ed.* **2012**, *51*, 12745–12748. (i) Dierick, S.; Vercruyse, E.; Berthon-Gelloz, G.; Marko, I. E. User-Friendly Platinum Catalysts for the Highly Stereoselective Hydrosilylation of Alkynes and Alkenes. *Chem. Eur. J.* **2015**, *21*, 17073–17078. (j) Takeuchi, R.; Nitta, S.; Watanabe, D. A Selective Synthesis of (*E*)-Vinylsilanes by Cationic Rhodium Complex Catalyzed Hydrosilylation of 1-Alkynes and Tandem Hydrosilylation/Isomerization Reaction of Propargylic Alcohols to  $\beta$ -Silyl Ketones. *J. Org. Chem.* **1995**, *60*, 3045–3051. (k) Munz, D.; Allolio, C.; Meyer, D.; Micksch, M.; Roessner, L.; Strassner, T. Oligoether substituted bis-NHC palladium and platinum complexes for aqueous Suzuki–Miyaura coupling and hydrosilylation. *J.*

- Organomet. Chem.* **2015**, *794*, 330–335. (l) Ortega-Moreno, L.; Peloso, R.; Maya, C.; Suarez, A.; Carmona, E. Platinum (0) olefin complexes of a bulky terphenylphosphine ligand. Synthetic, structural and reactivity studies. *Chem. Commun.* **2015**, *51*, 17008-17011.
7. (a) Cornils, B.; Herrmann, W. A.; Beller, M.; Paciello, R. *Applied Homogeneous Catalysis with Organometallic Compounds*, 3rd ed.; Wiley-VCH, 2017. (b) Zaranek, M.; Marciniak, B.; Pawluć, P. Ruthenium-catalysed hydrosilylation of carbon–carbon multiple bonds. *Org. Chem. Front.* **2016**, *3*, 1337-1344. (c) Chen, J.; Guo, J.; Lu, Z. Recent Advances in Hydrometallation of Alkenes and Alkynes via the First Row Transition Metal Catalysis. *Chin. J. Chem.* **2018**, *36*, 1075-1109. (d) Wen, H.; Liu, G.; Huang, Z. Recent advances in tridentate iron and cobalt complexes for alkene and alkyne hydrofunctionalizations. *Coord. Chem. Rev.* **2019**, *386*, 138-153. (e) Wei, D.; Darcel, C. Iron Catalysis in Reduction and Hydrometalation Reactions. *Chem. Rev.* **2019**, *119*, 2550-2610. (f) Gao, W.; Ding, S. Progress on Iridium-Catalyzed Hydrosilylation of Alkenes and Alkynes. *Synthesis* **2020**, *52*, 3549-3563. (g) Carreras, J., Caballero, A., & Pérez, P. J. Alkenyl Boronates: Synthesis and Applications. *Chem. Asian J.* **2019**, *14*, 329-343. (h) Du, X., Hou, W., Zhang, Y., & Huang, Z. Pincer cobalt complex-catalyzed Z-selective hydrosilylation of terminal alkynes. *Org. Chem. Front.* **2017**, *4*, 1517-1521. (i) Zhao, X.; Yang, D.; Zhang, Y.; Wang, B.; Qu, J. Highly  $\beta$  (Z)-Selective Hydrosilylation of Terminal Alkynes Catalyzed by Thiolate-Bridged Dirhodium Complexes. *Org. Lett.* **2018**, *20*, 5357-5361. (j) Puerta-Oteo, R., Munarriz, J., Polo, V., Jiménez, M. V., Pérez-Torrente, J. J. Carboxylate-Assisted  $\beta$ -(Z) Stereoselective Hydrosilylation of Terminal Alkynes Catalyzed by a Zwitterionic Bis-NHC Rhodium(III) Complex. *ACS Catal.* **2020**, *10*, 7367-7380. (k) Sánchez-Page, B., Munarriz, J., Jiménez, M.V., Pérez-Torrente, J.J., Blasco, J., Subias, G., Passarelli, V.

and Álvarez, P.  $\beta$ -(Z) Selectivity Control by Cyclometalated Rhodium(III)–Triazolylidene Homogeneous and Heterogeneous Terminal Alkyne Hydrosilylation Catalysts. *ACS Catal.* **2020**, *10*, 13334–13351. (l) Ohmura, T.; Yamamoto, Y.; Miyaura, N. Rhodium- or Iridium-Catalyzed *trans*-Hydroboration of Terminal Alkynes, Giving (Z)-1-Alkenylboron Compounds. *J. Am. Chem. Soc.* **2000**, *122*, 4990–4991. (m) Cid, J.; Carbó, J. J.; Fernández, E. Catalytic Non-Conventional *trans*-Hydroboration: A Theoretical and Experimental Perspective. *Chem. Eur. J.* **2012**, *18*, 1512–1521. (n) Gunanathan, C.; Hölscher, M.; Pan, F.; Leitner, W. Ruthenium Catalyzed Hydroboration of Terminal Alkynes to Z-Vinylboronates. *J. Am. Chem. Soc.* **2012**, *134*, 14349–14352. (o) Obligacion, J. V., Neely, J. M., Yazdani, A. N., Pappas, I., & Chirik, P. J. Cobalt Catalyzed Z-Selective Hydroboration of Terminal Alkynes and Elucidation of the Origin of Selectivity. *J. Am. Chem. Soc.* **2015**, *137*, 5855–5858. (p) Gorgas, N.; Alves, L. G.; Stöger, B.; Martins, A. M.; Veiros, L. F.; Kirchner, K. Stable, Yet Highly Reactive Nonclassical Iron(II) Polyhydride Pincer Complexes: Z-Selective Dimerization and Hydroboration of Terminal Alkynes. *J. Am. Chem. Soc.* **2017**, *139*, 8130–8133. (q) Gorgas, N.; Stöger, B.; Veiros, L. F.; Kirchner, K. Iron(II) Bis(acetylide) Complexes as Key Intermediates in the Catalytic Hydrofunctionalization of Terminal Alkynes. *ACS Catal.* **2018**, *8*, 7973–7982. (r) Garhwal, S.; Fridman, N.; de Ruiter, G. Z-Selective Alkyne Functionalization Catalyzed by a *trans*-Dihydride N-Heterocyclic Carbene (NHC) Iron Complex. *Inorg. Chem.* **2020**, *59*, 13817–13821. (s) Jang, W. J.; Lee, W. L.; Moon, J. H.; Lee, J. Y.; Yun, J. Copper-Catalyzed *trans*-Hydroboration of Terminal Aryl Alkynes: Stereodivergent Synthesis of Alkenylboron Compounds. *Org. Lett.* **2016**, *18*, 1390–1393. (t) Xu, S.; Haeffner, F.; Li, B.; Zakharov, L. N.; Liu, S. Y. Monobenzofused 1, 4-Azaborines: Synthesis, Characterization, and Discovery of a Unique Coordination Mode. *Angew. Chem. Int. Ed.* **2014**, *53*, 6795–6799. (u) Xu, S.; Zhang, Y.; Li, B.; Liu, S.

- Y. Site-Selective and Stereoselective *trans*-Hydroboration of 1,3-Enynes Catalyzed by 1,4-Azaborine-Based Phosphine–Pd Complex. *J. Am. Chem. Soc.* **2016**, *138*, 14566-14569. (v) Yang, Y.; Jiang, J.; Yu, H.; Shi, J. Mechanism and Origin of the Stereoselectivity in the Palladium-Catalyzed *trans* Hydroboration of Internal 1, 3-Enynes with an Azaborine-Based Phosphine Ligand. *Chem. Eur. J.* **2018**, *24*, 178-186.
8. (a) Pérez-Torrente, J. J.; Nguyen, D. H.; Jiménez, M. V.; Modrego, F. J.; Puerta-Oteo, R.; Gómez-Bautista, D.; Iglesias, M.; Oro, L. A. Hydrosilylation of Terminal Alkynes Catalyzed by a ONO-Pincer Iridium (III) Hydride Compound: Mechanistic Insights into the Hydrosilylation and Dehydrogenative Silylation Catalysis. *Organometallics* **2016**, *35*, 2410-2422. (b) Shimizu, R.; Fuchikami, T. Dehydrogenative Silylation of Terminal Alkynes by Iridium Catalyst. *Tetrahedron Lett.* **2000**, *41*, 907-910. (c) Jun, C.-H.; Crabtree, R. H. Dehydrogenative Silylation, Isomerization and the Control of Syn- vs. Anti-addition in the Hydrosilylation of Alkynes. *J. Organomet. Chem.* **1993**, *447*, 177-187.
9. (a) Esteruelas, M. A.; Herrero, J.; Oro, L. A. Exclusive Formation of *cis*-PhCH=CH(SiEt<sub>3</sub>) by Addition of HSiEt<sub>3</sub> to PhC=CH Catalyzed by RuHCl(CO)(P/Pr<sub>3</sub>)<sub>2</sub>. *Organometallics* **1993**, *12*, 2377-2379. (b) Katayama, H.; Taniguchi, K.; Kobayashi, M.; Sagawa, T.; Minami, T.; Ozawa, F. J. Ruthenium-catalyzed hydrosilylation of terminal alkynes: stereodivergent synthesis of (*E*)- and (*Z*)-alkenylsilanes. *Organomet. Chem.* **2002**, *645*, 192-200. (c) Aricó, C. S.; Cox, L. R. Regio- and stereoselective hydrosilylation of terminal alkynes using Grubbs' first-generation olefin-metathesis catalyst. *Org. Biomol. Chem.* **2004**, *2*, 2558-2562. (d) Maifeld, S. V.; Tran, M. N.; Lee, D. Hydrosilylation of alkynes catalyzed by ruthenium carbene complexes. *Tetrahedron Lett.* **2005**, *46*, 105-108. (e) Menozzi, C.; Dalko, P. I.; Cossy, J. Hydrosilylation of Terminal Alkynes with Alkylidene Ruthenium Complexes and Silanes. *J. Org. Chem.* **2005**, *70*, 10717-10719. (f) Nagao, M.; Asano, K.; Umeda, K.; Katayama, H.; Ozawa, F. Highly

- (Z)-Selective Hydrosilylation of Terminal Alkynes Catalyzed by a Diphosphinidene-cyclobutene-Coordinated Ruthenium Complex: Application to the Synthesis of (Z,Z)-Bis(2-bromoethenyl)arenes. *J. Org. Chem.* **2005**, *70*, 10511-10514.
- (g) Gao, R.; Pahls, D. R.; Cundari, T. R.; Yi, C. S. Experimental and Computational Studies of the Ruthenium-Catalyzed Hydrosilylation of Alkynes: Mechanistic Insights into the Regio- and Stereoselective Formation of Vinylsilanes. *Organometallics* **2014**, *33*, 6937-6944. (h) Na, Y.; Chang, S. Highly Stereoselective and Efficient Hydrosilylation of Terminal Alkynes Catalyzed by [RuCl<sub>2</sub>(p-cymene)]<sub>2</sub>. *Org. Lett.* **2000**, *2*, 1887-1889.
10. (a) Mori, A.; Takahisa, E.; Kajiro, H.; Hirabayashi, K.; Nishihara, Y.; Hiyama, T. RhCl(PPh<sub>3</sub>)<sub>3</sub>/NaI Catalyst System for Hydrosilylation of 1-Alkynes: Stereodivergent Syntheses of E- and Z-Alkenylsilanes with Heteroatom Substituents on Silicon. *Chem. Lett.* **1998**, *27*, 443-444. Puerta-Oteo, R., Munarriz, J., Polo, V., Jiménez, M. V., Pérez-Torrente, J. J. Carboxylate-Assisted β-(Z) Stereoselective Hydrosilylation of Terminal Alkynes Catalyzed by a Zwitterionic Bis-NHC Rhodium(III) Complex. *ACS Catal.* **2020**, *10*, 7367-7380 (b) Faller, J. W.; D'Allesio, D. G. Tunable Stereoselective Hydrosilylation of PhCCH Catalyzed by Cp\*Rh Complexes. *Organometallics* **2002**, *21*, 1743-1746. (c) Mori, A., Takahisa, E., Yamamura, Y., Kato, T., Mudalige, A.P., Kajiro, H., Hirabayashi, K., Nishihara, Y. and Hiyama, T. Stereodivergent Syntheses of (Z)- and (E)-Alkenylsilanes via Hydrosilylation of Terminal Alkynes Catalyzed by Rhodium(I) Iodide Complexes and Application to Silicon-Containing Polymer Syntheses. *Organometallics* **2004**, *23*, 1755-1765. (d) Jiménez, M. V.; Pérez-Torrente, J. J.; Bartolomé, M. I.; Gierz, V.; Lahoz, F. J.; Oro, L. A. Rhodium(I) Complexes with Hemilabile N-Heterocyclic Carbenes: Efficient Alkyne Hydrosilylation Catalysts. *Organometallics* **2008**, *27*, 224-234. (e) McBee, J. L.; Escalada, J.; Tilley, T. D. High Oxidation State Rhodium and Iridium Bis(silyl)dihydride Complexes Supported by a Chelating Pyridyl-Pyrrolide

- Ligand. *J. Am. Chem. Soc.* **2009**, *131*, 12703-12713. (f) Iglesias, M.; Pérez-Nicolás, M.; Miguel, P. J. S.; Polo, V.; Fernández-Alvarez, F. J.; Pérez-Torrente, J. J.; Oro, L. A. A synthon for a 14-electron Ir (III) species: catalyst for highly selective  $\beta$ -(Z) hydrosilylation of terminal alkynes. *Chem. Commun.* **2012**, *48*, 9480-9482 (g) Iglesias, M.; Sanz Miguel, P. J.; Polo, V.; Fernández-Alvarez, F. J.; Pérez-Torrente, J. J.; Oro, L. A. An Alternative Mechanistic Paradigm for the  $\beta$ -Z Hydrosilylation of Terminal Alkynes: The Role of Acetone as a Silane Shuttle. *Chem. – Eur.J.* **2013**, *19*, 17559-17566 (h) Ojima, I.; Clos, N.; Donovan, R. J.; Ingallina, P. Hydrosilylation of 1-Hexyne Catalyzed by Rhodium and Cobalt-Rhodium Mixed-Metal Complexes. Mechanism of Apparent Trans Addition. *Organometallics* **1990**, *9*, 3127-3133. (i) Zhao, X.; Yang, D.; Zhang, Y.; Wang, B.; Qu, J. Highly  $\beta$  (Z)-Selective Hydrosilylation of Terminal Alkynes Catalyzed by Thiolate-Bridged Dirhodium Complexes. *Org. Lett.* **2018**, *20*, 5357-5361.
11. (a) Jun, C. H.; Crabtree, R. H. Dehydrogenative silation, isomerization and the control of syn-vs. anti-addition in the hydrosilation of alkynes. *J. Organomet. Chem.* **1993**, *447*, 177-187. (b) Viciano, M.; Mas-Marzá, E.; Sanaú, M.; Peris, E. Synthesis and Reactivity of New Complexes of Rhodium and Iridium with Bis(dichloroimidazolyldiene) Ligands. Electronic and Catalytic Implications of the Introduction of the Chloro Substituents in the NHC Rings. *Organometallics* **2006**, *25*, 3063-3069. (c) Miyake, Y.; Isomura, E.; Iyoda, M. Selective hydrosilylation of 1-alkynes using iridium catalyst with biphosphinine ligand. *Chem. Lett.* **2006**, *35*, 836-837. (d) Sridevi, V. S.; Fan, W. Y.; Leong, W. K. Stereoselective Hydrosilylation of Terminal Alkynes Catalyzed by  $[\text{Cp}^*\text{IrCl}_2]_2$ : A Computational and Experimental Study. *Organometallics* **2007**, *26*, 1157-1160. (e) Zanardi, A.; Peris, E.; Mata, J. A. Alkenyl-functionalized NHC iridium-based catalysts for hydrosilylation. *New J. Chem.* **2008**, *32*, 120-126. (f) Pérez-Torrente, J.J.; Nguyen, D.H.; Jiménez, M.V.; Modrego, F.J.; Puerta-Oteo, R.; Gómez-Bautista, D.;

- Iglesias, M.; Oro, L.A. Hydrosilylation of Terminal Alkynes Catalyzed by a ONO-Pincer Iridium(III) Hydride Compound: Mechanistic Insights into the Hydrosilylation and Dehydrogenative Silylation Catalysis. *Organometallics* **2016**, *35*, 2410-2422. (g) Tanke, R. S.; Crabtree, R. H. Unusual Activity and Selectivity in Alkyne Hydrosilylation with an Iridium Catalyst Stabilized by an  $\sigma$ -Donor Ligand. *J. Am. Chem. Soc.* **1990**, *112*, 7984-7989.
12. (a) Ibrahim, A. D.; Entsminger, S. W.; Zhu, L. Y.; Fout, A. R. A Highly Chemoselective Cobalt Catalyst for the Hydrosilylation of Alkenes using Tertiary Silanes and Hydrosiloxanes. *ACS Catal.* **2016**, *6*, 3589–3593. (b) Noda, D.; Tahara, A.; Sunada, Y.; Nagashima, H. Non-Precious-Metal Catalytic Systems Involving Iron or Cobalt Carboxylates and Alkyl Isocyanides for Hydrosilylation of Alkenes with Hydrosiloxanes. *J. Am. Chem. Soc.* **2016**, *138*, 2480–2483. (c) Gao, Y. F.; Wang, L. J.; Deng, L. Distinct Catalytic Performance of Cobalt(I)-NHC Complexes in Promoting the Reaction of Alkene with Diphenylsilane: Selective 2,1 Hydrosilylation, 1,2-Hydrosilylation, and Hydrogenation of Alkene. *ACS Catal.* **2018**, *8*, 9637–9646. (d) Liu, Y.; Deng, L. Mode of Activation of Cobalt(II) Amides for Catalytic Hydrosilylation of Alkenes with Tertiary Silanes. *J. Am. Chem. Soc.* **2017**, *139*, 1798–1801. (e) Bocian, A.; Skrodzki, M.; Kubicki, M.; Gorczyński, A.; Pawluć, P.; Patroniak, V. The effect of Schiff base ligands on the structure and catalytic activity of cobalt complexes in hydrosilylation of olefins. *Appl. Catal., A*. **2020**, *602*, 117665. (f) Ito, T.; Sunada, Y. A Cobalt-Containing Polysilane as an Effective Solid-State Catalyst for the Hydrosilylation of Alkenes. *Org. Process Res. Dev.* **2023**. DOI: 10.1021/acs.oprd.2c00279. (g) Peng, D.; Zhang, Y.; Du, X.; Zhang, L.; Leng, X.; Walter, M. D.; Huang, Z. Phosphinite-Iminopyridine Iron Catalysts for Chemoselective Alkene Hydrosilylation. *J. Am. Chem. Soc.* **2013**, *135*, 19154–19166. (h) Hu, M.-Y.; He, Q.; Fan, S.-J.; Wang, Z.-C.; Liu, L.-

- Y.; Mu, Y.-J.; Peng, Q.; Zhu, S.-F. Ligands with 1,10-phenanthroline scaffold for highly regioselective iron-catalyzed alkene hydrosilylation. *Nat. Commun.* **2018**, *9*, 221.
13. Wang, C.; Teo, W. J.; Ge, S. Access to stereodefined (*Z*)-allylsilanes and (*Z*)-allylic alcohols via cobalt-catalyzed regioselective hydrosilylation of allenes. *Nat. Commun.* **2017**, *8*, 2258.
14. (a) Sang, H. L.; Yu, S.; Ge, S. Cobalt-catalyzed regioselective stereoconvergent Markovnikov 1,2-hydrosilylation of conjugated dienes. *Chem. Sci.* **2018**, *9*, 973–978. (b) Wen, H.; Wang, K.; Zhang, Y.; Liu, G.; Huang, Z. Cobalt-Catalyzed Regio- and Enantioselective Markovnikov 1,2-Hydrosilylation of Conjugated Dienes. *ACS Catal.* **2019**, *9*, 1612–1618. (c) Sun, W.; Li, M.-P.; Li, L.-J.; Huang, Q.; Hu, M.-Y.; Zhu, S.-F. Phenanthroline-imine ligands for iron-catalyzed alkene hydrosilylation. *Chem. Sci.* **2022**, *13*, 2721–2728.
15. (a) Bart, S. C.; Lobkovsky, E.; Chirik, P. J. Preparation and Molecular and Electronic Structures of Iron(0) Dinitrogen and Silane Complexes and Their Application to Catalytic Hydrogenation and Hydrosilation. *J. Am. Chem. Soc.* **2004**, *126*, 13794-13807. (b) Belger, C.; Plietker, B. Aryl–aryl interactions as directing motifs in the stereodivergent iron-catalyzed hydrosilylation of internal alkynes. *Chem. Commun.* **2012**, *48*, 5419-5421. (c) Greenhalgh, M. D.; Frank, D. J.; Thomas, S. P. Iron-Catalysed Chemo-, Regio-, and Stereoselective Hydrosilylation of Alkenes and Alkynes using a Bench-Stable Iron (II) Pre-Catalyst. *Adv. Synth. Catal.* **2014**, *356*, 584-590. (d) Challinor, A. J.; Calin, M.; Nichol, G. S.; Carter, N. B.; Thomas, S. P. Amine-Activated Iron Catalysis: Air- and Moisture-Stable Alkene and Alkyne Hydrofunctionalization. *Adv. Synth. Catal.* **2016**, *358*, 2404-2409. (e) Garhwal, S.; Fridman, N.; de Ruiter, G. *Z*-Selective Alkyne Functionalization Catalyzed by a *trans*-Dihydride N-Heterocyclic Carbene (NHC) Iron Complex. *Inorg. Chem.* **2020**, *59*, 13817-13821. (f) Hu, M.-Y.; He, P.; Qiao, T.-Z.; Sun,

- W.; Li, W.-T.; Lian, J.; Li, J.-H.; Zhu, S.-F. Iron-Catalyzed Regiodivergent Alkyne Hydrosilylation. *J. Am. Chem. Soc.* **2020**, *142*, 16894–16902. (g) Guo, Z.; Wen, H.; Liu, G.; Huang, Z. Iron-Catalyzed Regio- and Stereoselective Hydrosilylation of 1,3-Enynes to Access 1,3-Dienylsilanes. *Org. Lett.* **2021**, *23*, 2375–2379. (h) Hu, M.-Y.; Lian, J.; Sun, W.; Qiao, T.-Z.; Zhu, S.-F. Iron-Catalyzed Dihydrosilylation of Alkynes: Efficient Access to Geminal Bis(silanes). *J. Am. Chem. Soc.* **2019**, *141*, 4579–4583.
16. (a) Bartik, T.; Nagy, G.; Kvintovics, P.; Happ, B. Steuerung Der Nickel(O)-Katalysierten Hydrosilylierung von Phenylacetylen Mit Phosphorliganden. *J. Organomet. Chem.* **1993**, *453*, 29-32. (b) Tillack, A.; Pulst, S.; Baumann, W.; Baudisch, H.; Kortus, K.; Rosenthal, U. Hydrosilylation of symmetrically substituted alkynes and butadienes with  $L_2Ni(0)$  butadiene complexes [L =  $Ph_3P$ , (o-Tol-O) $_3P$ ] as catalysts. *J. Organomet. Chem.* **1997**, *532*, 117-123. (c) Chaulagain, M. R.; Mahandru, G. M.; Montgomery, J. Alkyne hydrosilylation catalyzed by nickel complexes of N-heterocyclic carbenes. *Tetrahedron* **2006**, *62*, 7560-7566. (d) Berding, J.; van Paridon, J. A.; van Rixel, V. H.; Bouwman, E.  $[NiX_2(NHC)_2]$  Complexes in the Hydrosilylation of Internal Alkynes. *Eur. J. Inorg. Chem.* **2011**, *2011*, 2450-2458.
17. (a) Garcia-Rubia, A.; Romero-Revilla, J. A.; Mauleon, P.; Gomez Arrayas, R.; Carretero, J. C. Cu-Catalyzed Silylation of Alkynes: A Traceless 2-Pyridylsulfonyl Controller Allows Access to Either Regioisomer on Demand. *J. Am. Chem. Soc.* **2015**, *137*, 6857–6865. (b) Wang, Z.-L.; Zhang, F.-L.; Xu, J.-L.; Shan, C.-C.; Zhao, M.; Xu, Y.-H. Copper-Catalyzed Anti-Markovnikov Hydrosilylation of Terminal Alkynes. *Org. Lett.* **2020**, *22*, 7735–7742. (c) Zhou, H.; Zhang, Q.-Y.; Lu, X.-B. Synthesis and catalytic application of N-heterocyclic carbene copper complex functionalized conjugated microporous polymer. *RSC Adv.* **2016**, *6*, 44995–45000.

18. (a) Skrodzki, M.; Patroniak, V.; Pawluc, P. Schiff Base Cobalt(II) Complex-Catalyzed Highly Markovnikov-Selective Hydrosilylation of Alkynes. *Org. Lett.* **2021**, *23*, 663–667. (b) Wang, D.; Lai, Y.; Wang, P.; Leng, X.; Xiao, J.; Deng, L. Markovnikov Hydrosilylation of Alkynes with Tertiary Silanes Catalyzed by Dinuclear Cobalt Carbonyl Complexes with NHC Ligation. *J. Am. Chem. Soc.* **2021**, *143*, 12847–12856. (c) Skrodzki, M.; Garrido, V. O.; Csáky, A. G.; Pawluć, P. Searching for highly active cobalt catalysts bearing Schiff base ligands for Markovnikov-selective hydrosilylation of alkynes with tertiary silanes. *J. Catal.*, **2022**, *411*, 116–121. (d) Wen, H.; Wan, X.; Huang, Z. Asymmetric Synthesis of Silicon-Stereogenic Vinylhydrosilanes by Cobalt-Catalyzed Regio- and Enantioselective Alkyne Hydrosilylation with Dihydrosilanes. *Angew. Chem., Int. Ed.* **2018**, *57*, 6319–6323.
19. (a) Teo, W. J.; Wang, C.; Tan, Y. W.; Ge, S. Cobalt-Catalyzed Z-Selective Hydrosilylation of Terminal Alkynes. *Angew. Chem., Int. Ed.* **2017**, *56*, 4328–4332. (b) Du, X.; Hou, W.; Zhang, Y.; Huang, Z. Pincer cobalt complex-catalyzed Z-selective hydrosilylation of terminal alkynes. *Org. Chem. Front.* **2017**, *4*, 1517–1521.
20. (a) Bai, W.; Sun, J.; Wang, D.; Bai, S.-D.; Deng, L. Low-coordinate cobalt(0) N-heterocyclic carbene complexes as catalysts for hydrosilylation of alkynes. *Appl. Organomet. Chem.* **2022**, *36*, e6694. (b) Sang, H. L.; Hu, Y.; Ge, S. Cobalt-Catalyzed Regio- and Stereoselective Hydrosilylation of 1,3-Diynes To Access Silyl-Functionalized 1,3-Enynes. *Org. Lett.* **2019**, *21*, 5234–5237. (c) Wu, C. Z.; Teo, W. J.; Ge, S. Z. Cobalt-Catalyzed (E)-Selective anti-Markovnikov Hydrosilylation of Terminal Alkynes. *ACS Catal.* **2018**, *8*, 5896–5900.
21. (a) Banach, Ł.; Brykczyńska, D.; Gorczyński, A.; Wyrzykiewicz, B.; Skrodzki, M.; Pawluć, P. Markovnikov-selective double hydrosilylation of challenging terminal aryl

- alkynes under cobalt and iron catalysis. *Chem Comm.* **2022**, 58, 13763–13763. (b) Cheng, Z.; Li, M.; Zhang, X.-Y.; Sun, Y.; Yu, Q.-L.; Zhang, X.-H.; Lu, Z. Cobalt-Catalyzed Regiodivergent Double Hydrosilylation of Arylacetylenes. *Angew. Chem., Int. Ed.* **2023**, 62, e202215029.
22. (a) Cheng, Z.; Guo, J.; Sun, Y.; Zheng, Y.; Zhou, Z.; Lu, Z. Regio-controllable Cobalt-Catalyzed Sequential Hydrosilylation/Hydroboration of Arylacetylenes. *Angew. Chem., Int. Ed.* **2021**, 60, 22454–22460. (b) Sun, Y.; Guo, J.; Shen, X.; Lu, Z. Ligand relay catalysis for cobalt-catalyzed sequential hydrosilylation and hydrohydrazidation of terminal alkynes. *Nat. Commun.* **2022**, 13, 650. (c) Zuo, Z.; Yang, J.; Huang, Z. Cobalt-Catalyzed Alkyne Hydrosilylation and Sequential Vinylsilane Hydroboration with Markovnikov Selectivity. *Angew. Chem., Int. Ed.* **2016**, 55, 10839–10843.
23. (a) Yang, X.; Wang, C. Manganese-Catalyzed Hydrosilylation Reactions. *Chem. Asian J.* **2018**, 13, 2307. (b) Das, K.; Waiba, S.; Jana, A.; Maji, B. Manganese-catalyzed hydrogenation, dehydrogenation, and hydroelementation reactions. *Chem. Soc. Rev.* **2022**, 51, 4386. (c) Gulyaeva, E. S.; Osipova, E. S.; Buhaibeh, R.; Canac, Y.; Sortais, J.-B.; Valyaev, D. A. Towards ligand simplification in manganese-catalyzed hydrogenation and hydrosilylation processes. *Coord. Chem. Rev.* **2022**, 458, 214421. (d) Schlichter, P.; Werlé, C. The Rise of Manganese-Catalyzed Reduction Reactions. *Synthesis* **2022**, 54, 517.
24. (a) Ma, X.; Zuo, Z.; Liu, G.; Huang, Z. Manganese-Catalyzed Asymmetric Hydrosilylation of Aryl Ketones. *ACS omega* **2017**, 2, 4688-4692. (b) Trovitch, R. J. The Emergence of Manganese-Based Carbonyl Hydrosilylation Catalysts. *Acc. Chem. Res.* **2017**, 50, 2842-2852. (c) Valyaev, D. A.; Wei, D.; Elangovan, S.; Cavailles, M.; Dorcet, V.; Sortais, J.-B.; Darcel, C.; Lugan, N. Half-Sandwich Manganese Complexes Bearing Cp Tethered *N*-Heterocyclic Carbene Ligands: Synthesis and Mechanistic Insights into

the Catalytic Ketone Hydrosilylation. *Organometallics* **2016**, *35*, 4090-4098. (d) Trovitch, R. J. Comparing Well-Defined Manganese, Iron, Cobalt, and Nickel Ketone Hydrosilylation Catalysts. *Synlett* **2014**, *25*, 1638-1642. (e) Zheng, J.; Elangovan, S.; Valyaev, D. A.; Brousses, R.; Cesar, V.; Sortais, J. B.; Darcel, C.; Lugan, N.; Lavigne, G. Hydrosilylation of Aldehydes and Ketones Catalyzed by Half-Sandwich Manganese (I) N-Heterocyclic Carbene Complexes. *Adv. Synth. Catal.* **2014**, *356*, 1093-1097. (f) Chidara, V. K.; Du, G. An Efficient Catalyst Based on Manganese Salen for Hydrosilylation of Carbonyl Compounds. *Organometallics* **2013**, *32*, 5034-5037. (g) Riener, K.; Högerl, M. P.; Gigler, P.; Kühn, F. E. Rhodium-Catalyzed Hydrosilylation of Ketones: Catalyst Development and Mechanistic Insights. *ACS Catal.* **2012**, *2*, 613-621. (h) Ghosh, C.; Mukhopadhyay, T. K.; Flores, M.; Groy, T. L.; Trovitch, R. J. A Pentacoordinate Mn(II) Precatalyst That Exhibits Notable Aldehyde and Ketone Hydrosilylation Turnover Frequencies. *Inorg. Chem.* **2015**, *54*, 10398-10406. (i) Son, S. U.; Paik, S.-J.; Chung, Y. K. Hydrosilylation of ketones catalyzed by tricarbonyl (naphthalene) manganese cation. *J. Mol. Catal. A: Chem.* **2000**, *151*, 87-90. (j) Son, S. U.; Paik, S.-J.; Lee, I. S.; Lee, Y.-A.; Chung, Y. K.; Seok, W. K.; Lee, H. N. Chemistry of [(1H-hydronaphthalene) Mn(CO)<sub>3</sub>]: The Role of Ring-Slippage in Substitution, Catalytic Hydrosilylation, and Molecular Crystal Structure of [(η<sup>3</sup>-C<sub>10</sub>H<sub>9</sub>)Mn(CO)<sub>3</sub>P(OMe)<sub>3</sub>]. *Organometallics* **1999**, *18*, 4114-4118. (k) DiBiase, M.; Gregg, B. T.; Cutler, A. R. Manganese Carbonyl Complexes as Catalysts for the Hydrosilylation of Ketones: Comparison with RhCl(PPh<sub>3</sub>)<sub>3</sub>. *Organometallics* **1996**, *15*, 2764-2769. (l) Saito, K.; Ito, T.; Arata, S.; Sunada, Y. Four-Coordinated Manganese (II) Disilyl Complexes for the Hydrosilylation of Aldehydes and Ketones with 1,1,3,3-Tetramethyldisiloxane. *ChemCatChem* **2021**, *13*, 1152-1156.

25. (a) Zheng, J.; Chevance, S.; Darcel, C.; Sortais, J.-B. Selective reduction of carboxylic acids to aldehydes through manganese catalysed hydrosilylation. *Chem. Commun.* **2013**, 49, 10010-10012. (b) Antico, E.; Schlichter, P.; Werlé, C.; Leitner, W. Reduction of Carboxylic Acids to Alcohols via Manganese(I) Catalyzed Hydrosilylation. *JACS Au* **2021**, 1, 742-749.
26. (a) Behera, R. R.; Ghosh, R.; Panda, S.; Khamari, S.; Bagh, B. Hydrosilylation of Esters Catalyzed by Bisphosphine Manganese (I) Complex: Selective Transformation of Esters to Alcohols. *Org. Lett.* **2020**, 22, 3642-3648. (b) Mukhopadhyay, T. K.; Ghosh, C.; Flores, M.; Groy, T. L.; Trovitch, R. J. Hydrosilylation of Aldehydes and Formates Using a Dimeric Manganese Precatalyst. *Organometallics* **2017**, 36, 3477-3483. (c) Mukhopadhyay, T. K.; Rock, C. L.; Hong, M.; Ashley, D. C.; Groy, T. L.; Baik, M.-H.; Trovitch, R. J. Mechanistic Investigation of Bis(imino)pyridine Manganese Catalyzed Carbonyl and Carboxylate Hydrosilylation. *J. Am. Chem. Soc.* **2017**, 139, 4901-4915.
27. Das, H. S.; Das, S.; Dey, K.; Singh, B.; Haridasan, R. K.; Das, A.; Ahmed, J.; Mandal, S. K. Primary amides to amines or nitriles: a dual role by a single catalyst. *Chem. Commun.* **2019**, 55, 11868-11871.
28. Ganguli, K.; Mandal, A.; Sarkar, B.; Kundu, S. Benzimidazole fragment containing Mn-complex catalyzed hydrosilylation of ketones and nitriles. *Tetrahedron* **2020**, 76, 131439.
29. (a) Mukhopadhyay, T. K.; Flores, M.; Groy, T. L.; Trovitch, R. J. A  $\beta$ -diketiminato manganese catalyst for alkene hydrosilylation: substrate scope, silicone preparation, and mechanistic insight. *Chem. Sci.* **2018**, 9, 7673-7680. (b) Carney, J. R.; Dillon, B. R.; Campbell, L.; Thomas, S. P. Manganese-Catalyzed Hydrofunctionalization of Alkenes. *Angew. Chem., Int. Ed.* **2018**, 57, 10620-10624. (c) Yang, X.; Wang, C. Diverse Fates of  $\beta$ -Silyl Radical under Manganese Catalysis: Hydrosilylation and Dehydrogenative Silylation of Alkenes. *Chin. J. Chem.* **2018**, 36, 1047-1051. (d) Dong, J.; Yuan, X.-A.;

- Yan, Z.; Mu, L.; Ma, J.; Zhu, C.; Xie, J. Manganese-catalysed divergent silylation of alkenes. *Nat. Chem.* **2021**, *13*, 182-190.
30. Behera, R. R.; Panda, S.; Ghosh, R.; Kumar, A. A.; Bagh, B. Manganese-Catalyzed Chemoselective Hydrosilylation of Nitroarenes: Sustainable Route to Aromatic Amines. *Org. Lett.* **2022**, *24*, 9179–9183.
31. (a) Yang, X.; Wang, C. Dichotomy of Manganese Catalysis via Organometallic or Radical Mechanism: Stereodivergent Hydrosilylation of Alkynes. *Angew. Chem., Int. Ed.* **2018**, *57*, 923-928. (b) Liang, H.; Ji, Y.-X.; Wang, R.-H.; Zhang, Z.-H.; Zhang, B. Visible-Light-Initiated Manganese-Catalyzed E-Selective Hydrosilylation and Hydrogermylation of Alkynes. *Org. Lett.* **2019**, *21*, 2750-2754.
32. Li, Q.; Huo, S.; Meng, L.; Li, X. Mechanism and origin of the stereoselectivity of manganese-catalyzed hydrosilylation of alkynes: a DFT study. *Catal. Sci. Technol.* **2022**, *8*, 2649-2658.
33. (a) Sau, S. C.; Hota, P. K.; Mandal, S. K.; Soleilhavoup, M.; Bertrand, G. Stable abnormal N-heterocyclic carbenes and their applications. *Chem. Soc. Rev.* **2020**, *49*, 1233–1252. (b) Vivancos, Á.; Segarra, C.; Albrecht, M. Mesoionic and Related Less Heteroatom-Stabilized N-Heterocyclic Carbene Complexes: Synthesis, Catalysis, and Other Applications. *Chem. Rev.* **2018**, *118*, 9493–9586. (c) Huynh, H. V. Electronic Properties of N-Heterocyclic Carbenes and Their Experimental Determination. *Chem. Rev.* **2018**, *118*, 9457–9492. (d) Hopkinson, M. N.; Richter, C.; Schedler, M.; Glorius, F. An overview of N-heterocyclic carbenes. *Nature* **2014**, *510*, 485–496. (e) Mathew, P.; Neels, A.; Albrecht, M. 1,2,3-Triazolylidenes as Versatile Abnormal Carbene Ligands for Late Transition Metals. *J. Am. Chem. Soc.* **2008**, *130*, 13534–13535.

34. Mutoh, Y.; Yamamoto, K.; Mohara, Y.; Saito, S. (*Z*)-Selective Hydrosilylation and Hydroboration of Terminal Alkynes Enabled by Ruthenium Complexes with an N-Heterocyclic Carbene Ligand. *Chem. Rec.* **2021**, *21*, 1–14.
35. (a) Panyam, P. K.; Atwi, B.; Ziegler, F.; Frey, W.; Nowakowski, M.; Bauer, M., & Buchmeiser, M. R. Rh(I)/(III)-N-Heterocyclic Carbene Complexes: Effect of Steric Confinement Upon Immobilization on Regio- and Stereoselectivity in the Hydrosilylation of Alkynes. *Chem. - Eur. J.* **2021**, *68*, 17220-17229. (b) Puerta-Oteo, R.; Munarriz, J.; Polo, V.; Jimenez, M. V.; Pe´ rez-Torrente, J. J.´ Carboxylate-Assisted β-(*Z*) Stereoselective Hydrosilylation of Terminal Alkynes Catalyzed by a Zwitterionic Bis-NHC Rhodium(III) Complex. *ACS Catal.* **2020**, *10*, 7367-7380. (c) Tyagi, A.; Yadav, S.; Daw, P.; Ravi, C.; Bera, J. K. A Rh(I) complex with an annulated N-heterocyclic carbene ligand for *E*-selective alkyne hydrosilylation. *Polyhedron* **2019**, *172*, 167–174. (d) Morales-Cerón, J. P.; Lara, P.; López-Serrano, J.; Santos, L. L.; Salazar, V.; Álvarez, E.; Suárez, A. Rhodium(I) Complexes with Ligands Based on N-Heterocyclic Carbene and Hemilabile Pyridine Donors as Highly *E* Stereoselective Alkyne Hydrosilylation Catalysts. *Organometallics* **2017**, *36*, 2460–2469. (e) Cassani, M. C.; Brucka, M. A.; Femoni, C.; Mancinelli, M.; Mazzanti, A.; Mazzoni, R.; Solinas, G. N-Heterocyclic Carbene Rhodium(I) Complexes Containing an Axis of Chirality: Dynamics and Catalysis. *New J. Chem.* **2014**, *38*, 1768–1779. (f) Busetto, L.; Cassani, M. C.; Femoni, C.; Mancinelli, M.; Mazzanti, A.; Mazzoni, R.; Solinas, G. N-Heterocyclic Carbene-Amide Rhodium-(I) Complexes: Structures, Dynamics, and Catalysis. *Organometallics* **2011**, *30*, 5258–5272.
36. (a) Karataş, M. O.; Alicı, B.; Passarelli, V.; Özdemir, I.; Pérez-Torrente, J. J.; Castarlenas, R. Iridium(I) complexes bearing hemilabile coumarin-functionalised N-heterocyclic carbene ligands with application as alkyne hydrosilylation catalysts. *Dalton Trans.* **2021**,

- 32, 11206-11215. (b) Lee, J.; Yoo, C.; Kwak, J.; Kim, M. N-Heterocyclic Carbene (NHC) Complexes of Rhodium and Iridium. In *Comprehensive Organometallic Chemistry IV*; Elsevier, 2022; pp 1–54. (c) Mancano, G.; Page, M. J.; Bhadbhade, M.; Messerle, B. A. Hemilabile and Bimetallic Coordination in Rh and Ir Complexes of NCN Pincer Ligands. *Inorg. Chem.* **2014**, *53*, 10159–10170. (d) Mas-Marzá, E.; Sanaú, M.; Peris, E. Coordination Versatility of Pyridine-Functionalized N-Heterocyclic Carbenes: A Detailed Study of the Different Activation Procedures. Characterization of New Rh and Ir Compounds and Study of Their Catalytic Activity. *Inorg. Chem.* **2005**, *44*, 9961-9967.
37. Lewis, L.N., Sy, K.G., Bryant Jr, G.L. and Donahue, P.E. Platinum-Catalyzed Hydrosilylation of Alkynes. *Organometallics* **1991**, *10*, 3750-3759.
38. (a) Wang, F. J.; Liu, L. J.; Wang, W. F.; Li, S. K.; Shi, M. Chiral NHC–metal-based asymmetric catalysis. *Coord. Chem. Rev.* **2012**, *256*, 804–853. (b) Glorius, F. N-Heterocyclic Carbenes in Transition Metal Catalysis, 1st ed.; Springer: Berlin, 2007. (c) Bera, S. S.; Szostak, M. Cobalt-NHC (NHC=N-Heterocyclic Carbene) Complexes in Catalysis. *ACS Catal.* **2022**, *12*, 3111–3137.
39. (a) Yang, W.; Chernyshov, I. Y.; van Schendel, R. K. A.; Weber, M.; Müller, C.; Filonenko, G. A.; Pidko, E. A. Robust and efficient hydrogenation of carbonyl compounds by mixed donor Mn(I) pincer complexes. *Nat. Commun.* **2021**, *12*, No. 12. (b) Elangovan, S.; Garbe, M.; Jiao, H.; Spannenberg, A.; Junge, K.; Beller, M. Hydrogenation of Esters to Alcohols Catalyzed by Defined Manganese Pincer Complexes. *Angew. Chem., Int. Ed.* **2016**, *49*, 15364–15368.
40. (a) Mourão, H.; Gomes, C. S.; Realista, S.; Royo, B. Visible light-induced catalytic hydrosilylation of ketones mediated by manganese NHC complexes. *Appl. Organomet. Chem.* **2022**, e6846. (b) Karataş, M. O.; Alıcı, B.; Passarelli, V.; Özdemir, I.; Pérez-Torrente, J. J.; Castarlenas, R. Iridium (I) complexes bearing hemilabile coumarin-

- functionalised N-heterocyclic carbene ligands with application as alkyne hydrosilylation catalysts. *Dalton Trans.* **2021**, *50*, 11206-11215.
41. (a) Straus, D. A.; Zhang, C.; Tilley, T. D. Trityl tetraphenylborate as a reagent in organometallic chemistry. *J. Organomet. Chem.* **1989**, *369*, C13–C17. (b) Bahr, S. R.; Boudjouk, P. Trityl Tetrakis(3,5-bis(trifluoromethyl)phenyl)- borate: A New Hydride Abstraction Reagent. *J. Org. Chem.* **1992**, *57*, 5545-5547. (c) Carney, J. R.; Dillon, B. R.; Campbell, L.; Thomas, S. P. Manganese-Catalyzed Hydrofunctionalization of Alkenes. *Angew. Chem., Int. Ed.* **2018**, *57*, 10620-10624.
42. Zong, Z.; Yu, Q.; Sun, N.; Hu, B.; Shen, Z.; Hu, X.; Jin, L. Bidentate Geometry Constrained Iminopyridyl Ligands in Cobalt Catalysis: Highly Markovnikov-Selective Hydrosilylation of Alkynes. *Org. Lett.* **2019**, *21*, 5767–5772.
43. Rad'kova, N. Y.; Kovyлина, T. A.; Cherkasov, A. V.; Lyssenko, K. A.; Ob'edkov, A. M.; Trifonov, A. A. Coordination Features of the 1, 3, 5-Triazapentadienyl Ligand in Alkyl Complexes of Rare-Earth Metals. *Eur. J. Inorg. Chem.*, **2021**, *24*, 2390-2400.
44. Manna, A.; Dinda, T. K.; Ghosh, nS.; Mal, P. CsPbBr<sub>3</sub> in the Activation of the C–Br Bond of CBrX<sub>3</sub> (X = Cl, Br) under Sunlight. *Chem. Mater.* **2023**, *35*, 628–637. (b) Bhanja, R.; Bera, S. K.; Mal, P. Regioselective Synthesis of Phenanthridine-Fused Quinazolinones using a 9-Mesityl-10-Methylacridinium Perchlorate Photocatalyst. *Chem. Commun.* **2023**, *59*, 4455–4458.

## SUMMARY

This thesis emphasizes on the synthesis, characterization applications of simple xanthphos, NNO based pincer and N-heterocyclic carbene based NCN pincer ligated manganese complexes, which catalyzed the hydrosilylation of esters, nitroarenes and terminal alkynes to provide corresponding alcohols, aromatic amines and vinylsilanes respectively. These complexes were characterized by FTIR,  $^1\text{H}$  NMR,  $^{13}\text{C}\{^1\text{H}\}$  NMR, ESI-mass spectra, CHN analyses and single crystal X-ray diffraction analyses.

The xanthphos based manganese catalyst is much more active and selective for the reduction of esters to alcohols. The reduction of esters for the production of alcohols is an extremely important process for the chemical industry. The substrate scope includes various aromatic, aliphatic, and cyclic esters. Interestingly, challenging aliphatic fatty esters also exhibited similar reduction and resulted in corresponding fatty alcohols. Furthermore, the catalytic system is also applicable to important substrates relevant to renewable chemistry and recycling of plastic waste.

Catalytic hydrosilylation reactions by manganese-based NNO pincer catalyst are developed using nitroarenes with silane to afford aromatic amines in good to excellent yields. Manganese catalyst (1 mol %), Na/Hg (2 mol %) and phenylsilane (2 eq.) under solvent-free conditions are sufficient for efficient hydrosilylation reactions of nitroarenes. Various aryl and heteroaryl nitro compounds are catalytically reduced to provide the selective corresponding amine products. The potential utility of the present catalytic protocol was demonstrated by the preparation of commercial drug molecules. Further, based on previous reports and supported by experimental evidence, we propose a catalytic path that involves reduction of manganese(II) to manganese(0) followed by oxidative addition of the silane. Mechanistic studies allowed inferring all of the intermediates involved. It is generally accepted that oxidative addition of the Si-H bond yields a manganese-hydride species as a key intermediate in the catalytic path,

and its highly hydridic nature is favorable for nitro reduction. different nature of the ligand environment allows all of the manganese intermediates to play an important role in these catalytic hydrosilylation reactions.

A simple protocol of manganese catalyzed hydrosilylation of terminal alkynes using phenylsilanes have been reported. The reactions proceeded well with a low loading of catalyst (1 mol %). Various aryl, heteroaryl and aliphatic terminal alkynes are catalytically silylated with good regioselectivity (anti-Markovnikov addition) and stereoselectivity ( $\beta$ -(*Z*)-product). Several control experiments suggest an organometallic mechanism is in action and an in situ generated manganese(I)-silyl intermediate acts as an active catalyst. The steric hindrance provided by NCN pincer ligand might play a crucial role for Ojima-Crabtree type rearrangement to give (*Z*)-vinylsilane as final product. A bulkier NCN pincer ligand was utilized to form another manganese(I) carbonyl complex. we failed to utilize complex 2 for the stereoselective hydrosilylation of alkynes due to very poor solubility (or insolubility) of complex 2 in organic solvents. Further modification of ligand frameworks is presently undergoing to achieve better selectivity for alkyne hydrosilylation.